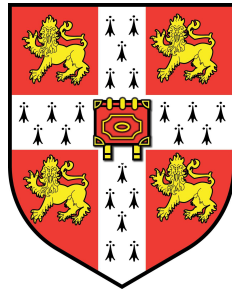# Deep ocean clay crusts: behaviour and biological origin

Matthew Yih-Han Kuo

King's College

University of Cambridge

A dissertation submitted for the degree of

Doctor of Philosophy

February 2011

To Kirsty, Mum, Dad and Ivana

"...observe the small facts upon which large inferences may depend."
- Sherlock Holmes, The Science of Deduction, Sir Arthur Conan Doyle

Acknowledgements

I would like to thank my PhD supervisor, Professor Malcolm Bolton for his tremendous interest, support and encouragement, and for the wonderful opportunity to undertake such an interesting and exciting project. It has been an honour to have completed this thesis under his guidance.

I would like to thank my PhD adviser, Professor Kenichi Soga for his helpful advice and suggestions for research directions, and for his ongoing interest and encouragement in this research.

I would like to thank Mr Andy Hill and BP Exploration for their assistance in providing core samples for the use in this thesis. Without these samples, the discoveries made in this work would not have been possible.

I would like to express particular thanks to Dr Diane Lister of the McDonald Institute of Archaeological Research for her assistance and patience in helping me learn more about microbiology. She gave me countless hours of advice, guidance and encouragement during my first year of research.

I would equally like to express particular thanks to Dr Ellen Nisbet of the Department of Biochemistry, University of South Australia for her thoughtful insight into possible directions for my research. She too gave me hours of assistance and guidance.

To my parents, for their endless love and care, and their support and encouragement of my ongoing studies.

To my wonderful and brilliant wife and best friend, Kirsty. I thank for her endless patience, love and understanding as I wrote this thesis. She has been ever supportive and encouraging of my work.

To God, my Lord and Saviour, I write this thesis for His glory, and through His strength alone.

I declare that, except for commonly understood and accepted ideas or where specific reference has been made to the work of others, this thesis is the result of my own work and includes nothing which is the outcome of work done in collaboration. This thesis is approximately 65,000 words in length and contains 149 figures.

Abstract

In water depths of 500m to greater than 2,000m, off the West coast of Africa, sediments comprise very soft clays with extremely high water contents and plasticity. In situ CPT and T-bar testing in these areas have identified 'crusts' with undrained shear strengths of up to 15kPa at 0.5m depth, before the strength reduces by an order of magnitude to normally consolidated strengths by 2m depth. This thesis presents an investigation into the behaviour and origin of these crusts.

Mini ball-penetrometer tests on natural cores confirm the crustal strength, and indicate a sensitivity of 3 within the crust. However, pipeline interface tests using the Cam-shear device demonstrate a significant variability in the measured interface friction coefficient. Particularly low strengths are observed when shearing in an undrained manner on a rough interface. These results are attributed to the heterogeneity of natural samples, and demonstrate the need to better understand the origin of the crust material in relation to interface micro-mechanics.

A microbiological investigation of crust material by extracting bacteria DNA from clay samples is described, and identifies the presence of the bacterium, *Marinobacter aquaeolei*. This bacterium is then used to inoculate sterile samples to determine its ability to produce crustal strength. Through this work, it is concluded that *M. aquaeolei* is unable to create crustal strength, although extracelluar polysaccharides produced by this bacterium will influence the permeability of sediments through the clogging of voids. It is therefore also concluded that future geotechnical investigation into marine sediments should consider the presence of bacteria and their ability to influence the soil properties.

Wet sieving of crust material shows that the crust comprises a mixture of burrowing invertebrate faecal pellets and clay. Pellets are found to represent 20% to over 55% of the crust material by dry mass. Individual pellets are shown to exhibit unconfined compressive strengths of between 5kPa and 50kPa, thus demonstrating their strength and robustness. Consolidation behaviour is governed by the percentage of pellets in natural samples. Based on their location, abundance and strength, it is concluded that the origin of crustal strength lies with the presence of burrowing invertebrate faecal pellets. When sheared on rough pipeline interfaces, however, pellets are observed to crush, expelling void-filling fragments that may generate positive excess pore pressures. Smeared clay produced when shearing natural samples obstructs the dissipation of pore pressures, which may encourage hydroplaning, and explain the observation of very low interface friction coefficients. It is therefore suggested that smooth pipelines offer more sliding resistance by minimising the risk of pellet crushing. This thesis proposes that wet sieving of core samples should be undertaken during the site investigations for future deep-water, hot-oil pipeline installations to provide design information on both the consolidation and strength behaviour of natural sediments.

Contents

Nomenclature

C	pore water solute concentration
C_0	sediment water solute concentration
c'	cohesion intercept produced by cementation at a sheared interface
c_c	compression index, defined as the slope of the $v - \sigma'_v$ relationship once past σ'_c
c_c*	intrinsic compression index
c_s	swelling index, defined as the slope of the unload-reload, $v - \sigma'_v$ relationship
c_v	coefficient of consolidation
d	drainage distance used to determine the c_v in a 1-D compression test
d_{pellet}	diameter of faecal pellet
d_0	depth of soil
D	diameter of the bar of a T-bar or the ball of a ball penetrometer
e	specific volume; the ratio of the volume of voids to the volume of solids
e_0	initial specific volume
$e_{100}*$	intrinsic specific volume at σ'_v=100kPa
$e_{1000}*$	intrinsic specific volume at σ'_v=1000kPa
F_0	platten force at failure
E'_v	tangential one-dimensional stiffness
I_v	normalised voids ratio
k	one-dimensional permeability in the vertical direction
L	length of the bar of a T-bar
LL	liquid limit
N_b	bar factor for a T-bar penetrometer
N_{ball}	ball factor for a ball penetrometer
N_k	cone factor of a cone penetrometer
P	force applied to a T-bar penetrometer
R	radius of sphere
R_v	ratio of the current settlement to the ultimate settlement under one-dimensional compression
s	suction pressure of pellet crusher
S_t	soil sensitivity defined as the ratio of the peak strength to the residual strength $\frac{s_{u,max}}{s_{u,res}}$
s_u	undrained shear strength
t	time
T_v	dimensionless time factor
v	specific volume

Greek Symbols

α	adhesion factor $\tau/\tau*$
α_b	bioirrigation by burrowing invertebrates
α_{bar}	adhesion factor for the bar of a T-bar penetrometer
γ'	submerged (or effective) soil unit weight
ϕ'	effective friction angle

CONTENTS

ϕ_{pellet}	diameter of a faecal pellet
κ	slope of the unloading-reloading line
λ	slope of the normal compression line
λ_{min}	minimum pipeline interface roughness wavelength
Λ	ratio describing the relative slopes of the normal compression and unloading-reloading lines
μ	pipe-soil interface friction coefficient, τ/σ
μ'	effective pipe-soil interface friction coefficient, τ/σ'
$\mu*$	internal soil-soil coefficient of friction
ψ	soil porosity
ρ	current settlement of an one-dimensional compression test
σ	vertical total stress
σ'	vertical effective stress
σ'_0	initial vertical effective stress
σ_c	unconfined compressive strength
σ'_c	vertical effective preconsolidation stress
σ_t	tensile stress at failure
τ	interface shear strength developed during axial sliding
$\tau*$	shear strength available in soil just outside the interface zone

Subscripts

LB	lower bound
max	maximum value
$mean$	arithmetic mean
min	minimum value
nc	normally consolidated
$peak$	maximum value
res	residual value
UB	upper bound

Abbreviations

BSA	bovine serum albumin
$dH2O$	distilled water
$dNTP$	deoxyribonucleotide triphosphate
DOM	discrete organic matter
EPS	extracellular polysaccharide substance
FF	formation factor
ICL	intrinsic compression line
NCL	normally consolidated line
OCR	overconsolidation ratio $\frac{\sigma_{v,max}}{\sigma_v}$
OMZ	oxygen minimum zone
PCR	polymerase chain reaction
SCL	sedimentation compression line
SMT	sulphate-methane transition
SRR	sulphate reduction rate
Taq	thermostable DNA polymerase
TEM	transmission electron microscopy
TEP	transparent exopolymer particles
TOC	total organic carbon

List of Figures

List of Tables

Chapter 1

Introduction

The offshore oil and gas industry is under greater scrutiny than ever before. Resource exploration continues to be pushed to the limits due to the depths of water in which resources are found and, therefore, so is the technology required for economical extraction. Hot-oil pipelines laid on the seabed undergo hundreds of thermally-induced shearing cycles, potentially degrading the strength of the seabed.

The year 2010 will be remembered by the oil and gas industry and the general public alike, for the catastrophic collapse of the BP Macondo, deep-water drilling platform in the Gulf of Mexico. This collapse resulted in multiple fatalities, and significant environmental impact due to the uncontrolled flow of unprocessed oil into the Gulf of Mexico. Though the oil and gas industry considers itself a leader in health and safety and the environment, this event served as a reminder that significant challenges will continue to face the deep-water oil and gas sector in the coming decades.

Ultra deepwater installations currently extract oil in water depths of greater than 2,000m, representing environments that require state-of-the-art engineering at the boundary of technological advancement. To facilitate the successful extraction of resources, geotechnical designs for sub-sea structures such as pipelines, shallow and deep foundations and anchors, are required. Sub-sea pipelines installed on the seabed are designed to transport hot oil from well heads to deepwater risers over a distance of hundreds of metres to tens of kilometres. These pipelines are laid cold at 4℃, but oil emerges from wells at temperatures over 160℃ in order to maintain a suitable flow rate and prevent clogging due to the formation of hydrates. This dramatic change in temperature causes the pipelines to expand axially and buckle laterally. Hot oil typically flows for a period of weeks before the line shuts for maintenance and cools. This causes the pipe to return to its original position. During their lifetime, pipelines may be subject to hundreds of thermal cycles, typically moving between five and twenty pipe diameters (White and Cheuk, 2008), equivalent to many metres on each occasion (Bruton et al., 2007). Excessive movement of the pipeline may result in loss of pipeline integrity and

ultimately, failure. To prevent this, designers require knowledge of the resistance to pipeline relative movement provided by the soil, both in the short and long term. This resistance is quantified using the peak and residual soil and soil-interface shear strengths.

Hot oil pipelines installed in locations of relatively shallow water (less than 100m) are trenched into the seabed sediments to minimise the risk of being damaged by shipping trawlers, or being ruptured by iceberg gauging. The backfill material used to cover the pipeline provides thermal insulation and some resistance to pipeline buckling. However, over the lifetime of the pipeline, progressive vertical movements caused by the thermal cycles may cause the pipeline to ratchet itself back to the seabed surface. In these situations, an understanding of how the backfill material behaves as an engineering fill is therefore required.

Deepwater pipeline installations (greater than 1,000m) however, do not require trenching, as there is minimal risk of damage from trawlers or icebergs. The seabed at these water depths usually comprises very soft, normally consolidated clays with very high water content and soil plasticities. In these environments, the preferred method of installation is to allow the pipeline to embed into the sediment under self weight. It has been shown by Westgate et al. (2010), that a large amount of remoulding and entrainment of free water occurs as pipelines are laid, due to the transmitting of ship movements via the catenary length of pipeline to the seabed. Typical pipe diameters are between 0.5m and 0.9m and initial pipe embedment may range between 0.3 and 0.6 pipe diameters, depending on the undrained shear strength of the clay and the the vertical cyclic loading experienced by the pipe during installation. The resulting embedment depths therefore range from 0.2m to 0.5m. The absence of pipe trenching and soil cover, permits only minimal resistance to axial and lateral pipeline deformations during thermal cycling. A typical example of buckling caused by thermal cycling is shown in Figure 1.1, where it can be seen that the maximum pipeline lateral displacement is of the order of several pipeline diameters.
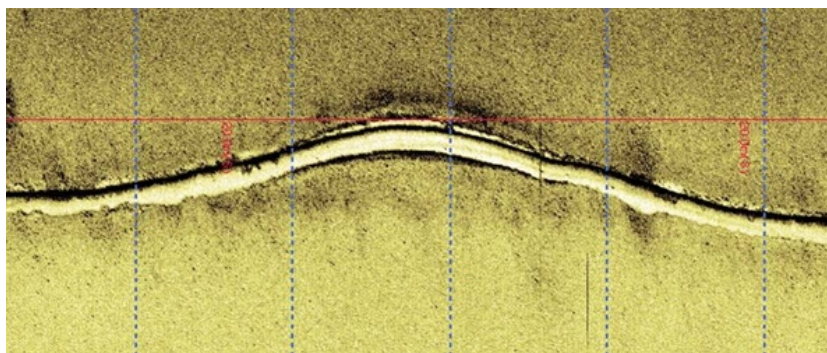
Fig. 1.1 Example of pipeline bucking on the seabed, showing displacement of several pipe diameters, modified after Bruton et al. (2008).

1.1 The Interaction Between Biology and Geomechanics

Biological processes influence the physical and chemical properties of deposited and depositing sediments. These processes range from the penetration of plant roots into terrestrial soil to the penetration of invertebrates into subsea sediments, and may include the more subtle effects of bacterial activity within porespaces, and the less subtle burrows produced by vertebrates. Physical and chemical properties of the soil that may be influenced by biological processes include in situ water content, stiffness, strength, permeability and porosity, gas content, and ion concentration. In favourable environmental conditions, biological activity may also be a source of methane production and precipitate formation.

Geomechanics may be broadly described as the study of the mechanical behaviour of soil and rock, and their engineering for man-made structures. Historically, the geomechanics field has tended to ignore biological processes. It is difficult to relate these two separate fields of research, and there is currently an incomplete understanding of how biological processes affect soil properties. It is likely that in many geomechanical situations, the influence of biological processes is insignificant when considered against other mechanical factors. Furthermore, factors of safety used in engineering design will tend to compensate for any errors introduced by variations in soil strength or stiffness that may be generated by biological processes.

As the field of geomechanics continues to develop, interest is now turning to interdisciplinary studies with the aim of improving the current understanding of geotechnical issues. Man-made structures will continue to impact on the natural soil environment through the construction of foundations, tunnels and pipelines. Consequently, higher priority needs to be given to the integration of geomechanics and biology in order to minimise any negative impacts on both the environment and the engineered structure, which may result from a lack of understanding of biological processes.

Two examples of biological processes that impact directly on the soil or man-made structures include: 'bio-clogging'; the growth of microbes within water pipes that results in a loss of functionality of the system, and the alteration of soil permeability caused by burrowing invertebrates mixing the original soil fabric. On-going research topics in this field include the utilisation of bacteria to aid in the recovery of oil; the use of bio-clogging to generate 'self-healing' soils, particularly in underground infrastructure where maintenance is expensive and difficult to implement (e.g. Soga, 2007); and the creation of biologically enhanced, cemented soils. The current understanding of how biological processes may influence the strength and stiffness of soil in the natural environment, particularly in the deep oceans, however, remains limited. This has in part, resulted in vague concepts such as "bioturbation" being used by engineers.

When a foundation sited on clayey soils is found to be unable to support the required design

3

loads, modification to the construction sequence and the foundation design will generally be undertaken. In such a situation, the geotechnical practitioner can address the problem of the unsuitable soil using a number of plausible solutions. These include soil strengthening by reinforcement, such as by installation of stone columns or anchors; prior surcharging to promote controlled consolidation and thus increased soil strength; and bridging the problematic soil by the use of piles. The clay's shear strength or stiffness is rarely considered to be a function of the biological activity that may be present within the soil. Indeed, the possible variation in strength or stiffness may only be of the order of a few kilopascals, if that. Deep marine environments that naturally exhibit low sediment strengths, however, may represent a situation where biological activity has a more significant influence on sediment strength and stiffness. Without further developments in the joint fields of biology and geomechanics, the geotechnical design of foundations and structures including hot-oil pipelines, will continue without consideration of the effect of biological processes on soil properties.

1.2 Focus of the Research and Thesis Outline

This thesis proposes to consider the behaviour of deep ocean West African clays that have been found to exhibit anomalously high undrained shear strengths at shallow sediment depths. These 'crusts' are the founding material for installed hot-oil pipelines and, therefore, there is particular interest in understanding and predicting the soil-pipeline behaviour. It is proposed that an academic inquiry into the origins of these materials may provide a framework in which the soil-pipeline interaction behaviour can be interpreted. As the crust strength is only of the order of a few kilopascals, biological activity may have an influence on both the natural strength and subsequent interaction behaviour with installed pipelines. It is this interaction that this thesis proposes to investigate through the laboratory testing of natural core samples and by employing a scientific approach to the analysis of crust material. The subtle interplay between thermal cycling and biological processes may make a significant difference to pipeline longevity and performance. It is upon this scenario that this thesis is formulated, with the aim of better understanding the interplay between the biological sciences and geotechnical engineering. An outline of the thesis is shown in Figure 1.2.

In Chapter 2, a review of the literature concerning the current knowledge on West African clays, including geotechnical properties and in situ and laboratory testing of core material is presented. This chapter concludes with a summary of the key aims of research, based on the gaps in understanding as evidenced from the literature review.

Chapter 3 presents the laboratory testing of natural core samples of West African clay crusts, including a consideration of the geotechnical properties and Cam-shear testing to determine soil-pipeline interface behaviour. The chapter also presents the design and use of a

mini ball penetrometer, for laboratory testing of natural cores. This device is used to undertake measurements of soil strength within core material and to provide an understanding of the soil's strength degradation behaviour and sensitivity. This chapter concludes with a summary of the key test results, which clearly indicate that a better understanding of the origin for the soil's remarkable strength is required.

Chapter 4 outlines the viable hypotheses for the crust's origin based on the review of the relevant literature. Discussion is provided for each hypothesis to either discount its validity, or to suggest that further research into their possible role in crust formation is required. Based on the conclusions of this chapter, the following two chapters (Chapters 5 and 6) investigate the influence of bacteria and burrowing invertebrates on sediment strength, respectively.

Chapter 7 provides a discussion of the key results and presents links between the conclusions of the preceding chapters of this thesis.

The thesis concludes with Chapter 8, which provides the final conclusions and recommendations for future research into this topic, based on the understanding gained by the author from the completion of this thesis.
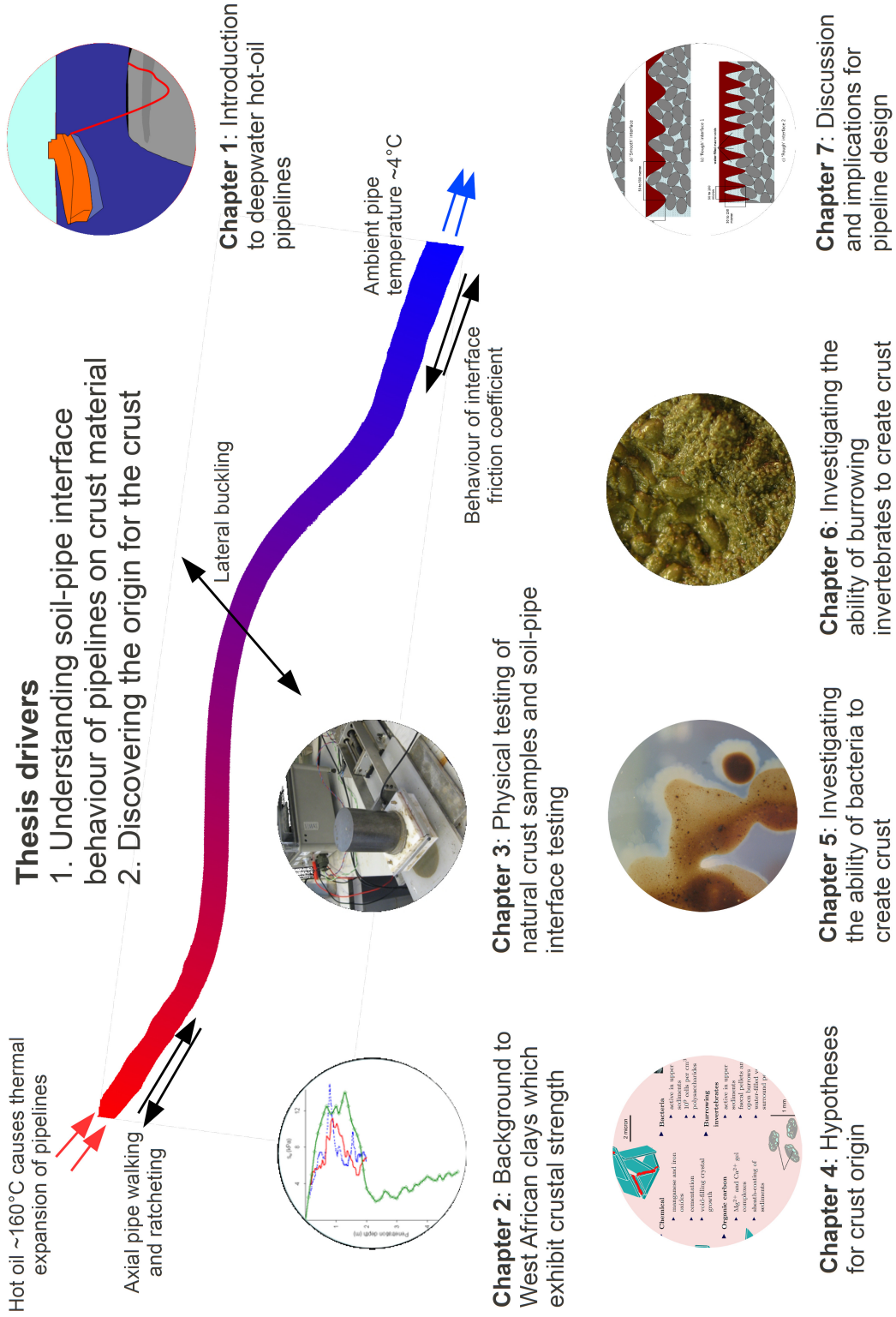
Fig. 1.2 Graphical summary of this thesis, outlining the main chapters.

Chapter 2

West African Clays

As the oil and gas industry continues to expand its offshore exploration, and the knowledge and technology for resource recovery improves, deposits located beneath deep water (greater than 1,000m) become viable for exploitation. This, however, results in an exponential increase in investigation costs relating to the need for specific, detailed information of the soil properties along pipeline routes. Investigations may include measurement of the in situ undrained shear strength using cone penetration (CPT) and T-bar tests; laboratory soil-pipe interface shear testing of samples and the consulting of prior records. This thesis focuses on Blocks 18 and 31, which are operated by BP Exploration and located off the west coast of Africa, as shown in Figure 2.1.
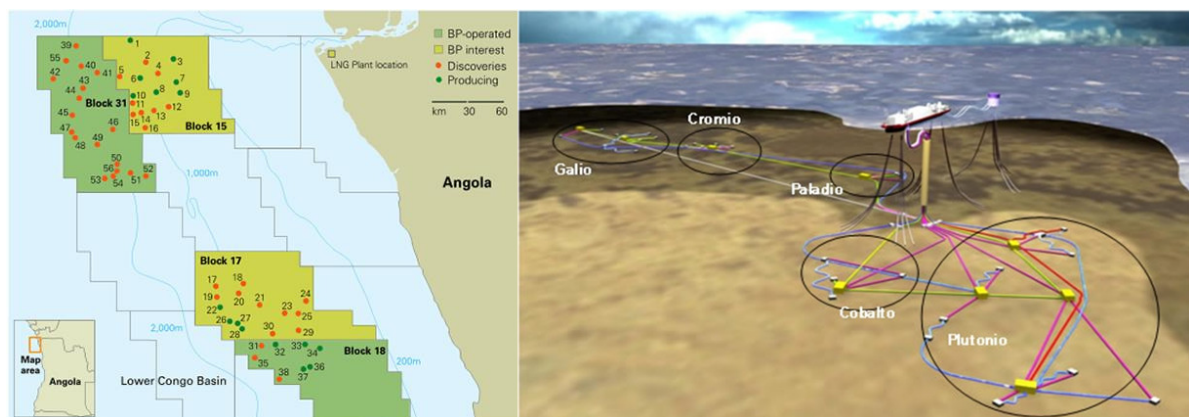
Fig. 2.1 Location of offshore sites Block 18 and 31, off the west coast of Africa (left) (Newswires, accessed 12 October 2010); and a schematic diagram of the Block 18 infrastructure (right) (Offshore-technology, accessed 26 August 2010).

The oil reserves located in Block 18 were discovered in water depths of 1,200 to 1,500 metres between 1999 and 2003, and comprise six fields: Platina, Plutonio, Galio, Paladio, Cromio and Cobalto (Offshore-technology, accessed 26 August 2010). Production commenced in 2007, and an estimated 750 million barrels of recoverable oil has been identified. All forty-three subsea

wells, including twenty production, twenty water injection and three gas injection wells are *"tied back to a single spread-moored FPSO facility to process produced fluids and export crude"* (Offshore-technology, accessed 26 August 2010).

In Block 31, oil reserves continue to be discovered, with the most recent discovery (the nineteenth) being reported in October 2009 (BPExploration, accessed 19 December 2009). This block covers an area of over 5,000 square kilometres and is situated in water depths of between 1,500m and 2,500m.

This chapter presents a literature review of the sediments found in Blocks 18 and 31, and the surrounding area, with the key areas of interest including: in situ soil strength characterisation; laboratory soil characterisation; and soil-pipeline interaction.

2.1 Soil Characterisation

The sediments encountered within Block 18 are predominately pelagic clays, which are influenced by the Benguela Upwelling, associated with the Walvis Ridge to the south (Pufahl et al., 1998). This results in a relatively high organic matter content of between 2% and 6% as identified by Thomas et al. (2005) and confirmed by Puech et al. (2010). Block 31 is situated a similar distance from the coastline to Block 18, however it is directly in line with the mouth of the Congo River. The sediments are therefore more strongly influenced by material of a terrestrial origin.

Laboratory test results presented by Puech et al. (2005) demonstrate that West African clay samples taken from within the top two metres exhibit very high water contents, generally between 150% and 250% and very high plasticity, typically between 70 and 120, but increasing to 150 near the seabed. These results are shown in Figures 2.2 and 2.3, respectively. These water content and plasticity values are very high compared to other offshore locations such as the Gulf of Mexico where water content and plasticity indices may range from 50% to 125% (Yun et al., 2006) and 30 to 70 (Puech et al., 2010), respectively. Carbonate content is observed by Puech et al. (2005) to range generally between 5% and 15% of the total soil weight, and is predominantly in the form of crushed shells less than 30μm. More recent work undertaken by Puech et al. (2010) suggests that the carbonate content may be as high as 23% in some areas. Particle size distributions completed by Thomas et al. (2005) suggest that, generally, 95% of the sediment material is smaller than 40μm, determined with a clay content of between 40% and 80%, with the dominant clay minerals identified by X-ray defraction as smectites, with a smaller percentage of kaolinites. A more recent study by Thomas et al. (2007), however, suggests a smaller amount of smectites and a dominance of kaolinites. Scanning and transmission electron microscopy undertaken by Thomas et al. (2005), showed an open, flocculated structure with clay aggregates, as seen in Figure 2.4. Puech et al. (2010) reviews

the techniques used to obtain particle size distributions and comments on the importance of result interpretation taking into account the method employed for the test. They show that using a laser granulometer, which is known to overestimate the coarser grain sizes, as discussed by Puech et al. (2010), the percentage passing 2μm is between 20% and 30%. Difficulty with breaking down the inherent structure of these clays, as indicated by Figure 2.4, may also influence the particle size distribution results.
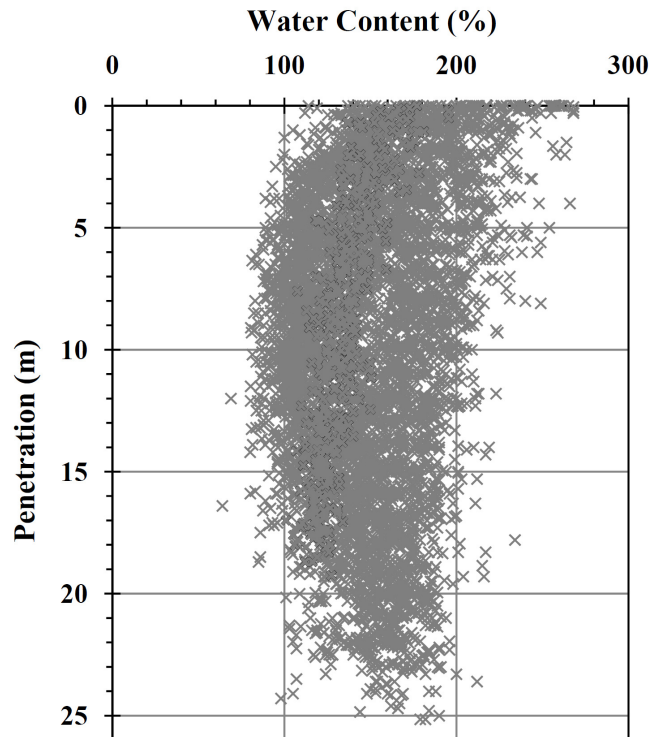
Fig. 2.2 Water content of West African clays plotted against penetration depth, modified after Puech et al. (2010).

2.2 Undrained Shear Strength

A significant number of in situ undrained shear strength tests have been undertaken using vane shears, cone penetration tests (CPTs) and T-bar testing. The results of CPT and T-bar testing in West African sediments in water depths ranging between 500m and 2,000m indicate a 'crust' in the top metre of sediment, within which the clay is an order of magnitude stronger than would be expected for a virgin deposit. Measured undrained shear strengths rise to a maximum of 15kPa at 0.5m to 1m depth, as shown in Figures 2.5 and 2.6. Crustal material is typically observed to have a strength gradient of 24kPa/m when approaching the peak strength value. Below the crust, a sharp loss in strength is observed, exhibiting a comparable strength gradient to its rise. A strength profile approximating normally consolidated conditions is then
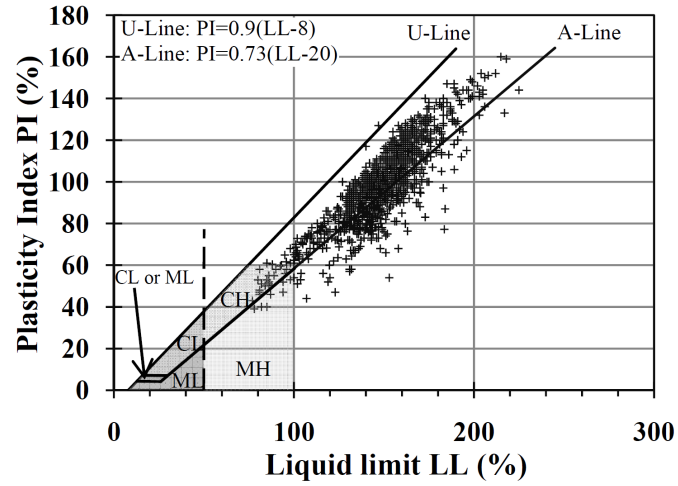
Fig. 2.3 Casagrande plasticity chart showing the high plasticity clays of the Gulf of Guinea, modified after Puech et al. (2010).
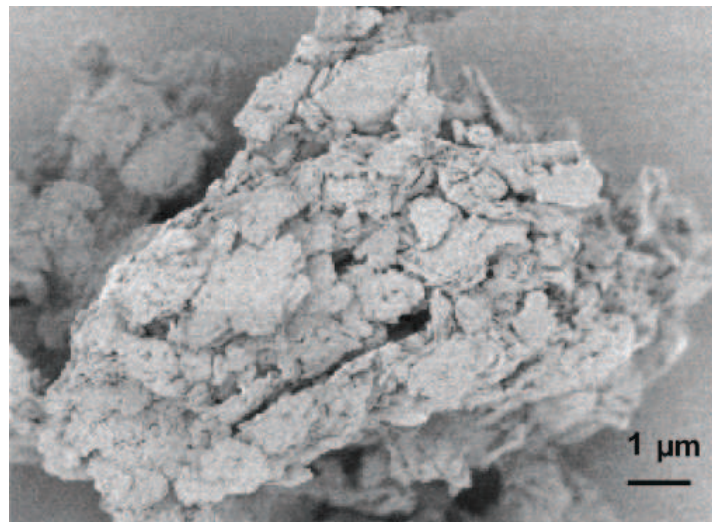
Fig. 2.4 Example of a scanning electron microscopy micrograph showing a clay aggregate, after Thomas et al. (2005).

apparent (Figure 2.5); characteristically demonstrating strength proportional to depth for the succeeding tens or hundreds of meters of apparently similar sediment. The assumed virgin consolidation line based on a submerged unit weight of $2.5\mathrm{kN/m^3}$ is shown on Figure 2.5 for comparison. The location of the crust at the clay surface suggests that the crust formation depends on some currently existing process that has a link to the shallow seabed. However, the sudden reduction of crust strength following modest sediment burial also suggests a certain vulnerability.

Though a significant amount of data is now available highlighting the phenomena of deep ocean clay crusts, no apparent correlation has previously been found between its presence and the constituents of the sediment determined in situ or in the laboratory (Puech et al., 2010).
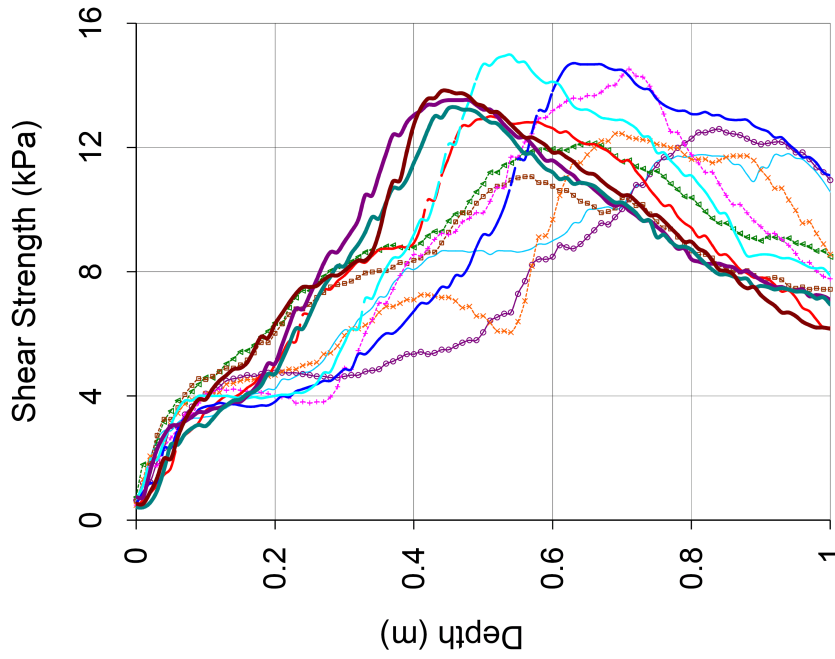
Fig. 2.6 T-bar profiles of undrained shear strength showing the presence of a 'crust' at 0.5m to 0.7m depth, with permission from BP Exploration.
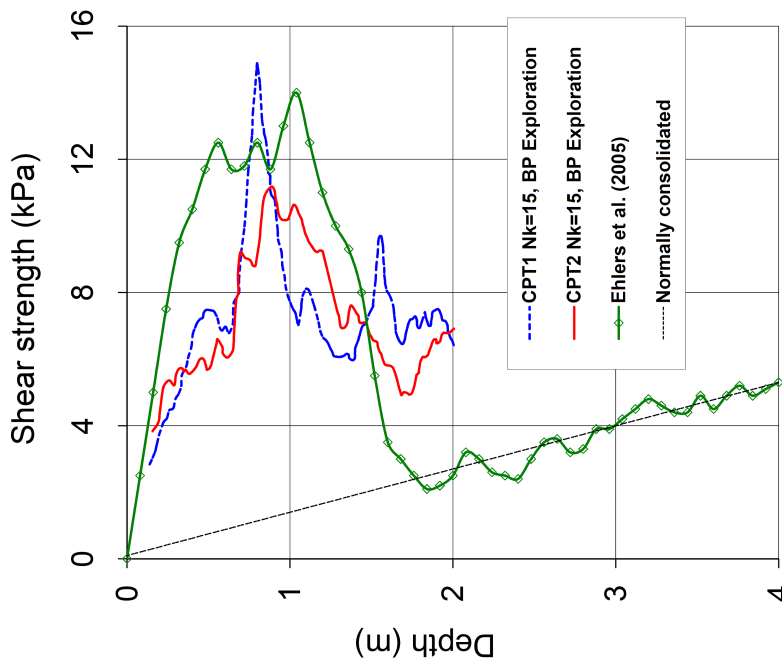
Fig. 2.5 CPT profiles of undrained shear strength showing presence of a 'crust' at 0.5m to 1.5m, modified after Ehlers et al. (2005) and with permission from BP Exploration. The virgin consolidation strength based on $\gamma' = 2.5 \mathrm{kN/m^3}$ is also shown.

2.3   Compressibility

De Gennaro et al. (2005) undertook one-dimensional compression tests using oedometers on samples of clays from the Gulf of Guinea, with water depths of 600m to 900m and 1,300m to 1,500m. Cores were 100mm in diameter and approximately 20m in length, and tested samples were taken from depth of between 2m and 20m. Samples were reconstituted at the liquid limit, w_L, to establish the intrinsic compression line (ICL). Results of normalised voids ratio, I_v plotted against the vertical effective stress, σ'_v, are shown in Figure 2.7 with oedometer tests on several natural clay samples. Estimated preconsolidation stresses, σ'_{v0} are denoted in this figure by the arrows. I_v is defined as

$$I_v = \frac{e_0 - e^*_{100}}{c^*_c}, \tag{2.1}$$

where e^*_{100} and c^*_c (defined as $e^*_{100} - e^*_{1000}$) are intrinsic constants of compressibility and may be determined for the particular sediment in question.

Following Burland (1990), the sedimentation compression line (SCL) was derived by measuring the void ratio at 100kPa (e^*_{100}) and the consolidation coefficient (c^*_c). The SCL for one of the sites is also shown on Figure 2.7. This figure also presents an extension of Burland (1990) by Cotecchia and Chandler (2000), who placed the SCL within a framework of strength sensitivity, S_t, defined as the ratio of undrained shear strength to the remoulded shear strength. It was found that a family of parallel SCLs existed, in which the SCL of Burland (1990) corresponds to $S_t \cong 5$.

De Gennaro et al. (2005) present results for depths greater than 2m to show that the West African clays display an SCL that mostly lies between the ICL and the SCL for $S_t=3$. De Gennaro et al. (2005) draw attention to a variance observed in the SCL at very low confining pressures, which correspond to very high water contents; and in particular, at approximately 0.5m depth where a sudden drop in water content occurs. They suggest that this may be associated with the sediment's deposition conditions, "*which are likely to depend on the enhanced chemical activity of the upper layers of the sediments*" (De Gennaro et al., 2005, p1066). They do not, however, discuss the nature of the enhanced chemical activity and why it might influence the sediment behaviour.

Hattab and Favre (2010) undertook further analysis of the soil compressibility of samples taken from the same location, but not specifically focusing on the crust material. It is suggested that the pseudo 'overconsolidation' found at some locations and observed in samples to a depth of about 6m, may be attributed to the presence of 'aggregates of clayey particles' or 'grains' that may be glued or cemented to other aggregates. The origins of the cementation is suggested as being physical-chemical in nature, which may be similar to the activity described by De Gennaro et al. (2005). The size of the clay 'grains' is not stated. Through the use of mercury
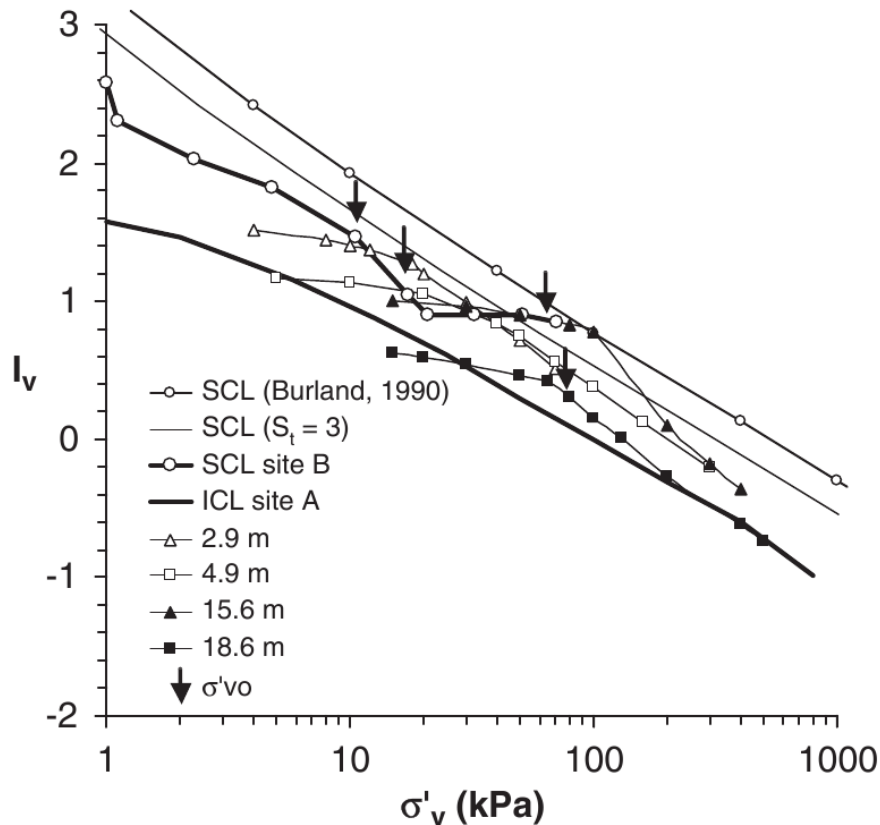
Fig. 2.7 Normalised oedometer results of natural core samples, including the sedimentation compression line (SCL), and lines corresponding to sensitivities, S_t of 3 and 5, modified after De Gennaro et al. (2005).

intrusion porosimetry analysis, Hattab and Favre (2010) show the presence of macro-pores of $\approx 1\mu m$ between aggregates of about $1\mu m$ diameter. During one dimensional compression to a vertical effective stress of 1MPa, the structure surrounding the macro-pores is shown to collapse, causing the pore size to decrease to about $0.2\mu m$ diameter, which is comparable to that obtained from a remoulded sample.

Though Hattab and Favre (2010) suggest these results show the presence of 'pseudo over-consolidation', the results do not explain why or how the sediment returns to strengths comparable to normally consolidated conditions by about 6m depth. At this depth, the in situ vertical effective stress is only approximately 15kPa (assuming a submerged unit weight, γ of 2.5kN/m^3) and therefore, presumably, mechanical crushing of the aggregates due to burial alone cannot explain the reduction in strength. No evidence of past slumping was observed in the areas that were investigated by Puech et al. (2005).

The results of the investigations presented by De Gennaro et al. (2005); Puech et al. (2005); Thomas et al. (2005); Hattab and Favre (2010) suggest the crust's presence may be independent of the depositional environment, as the crust is observed in a range of areas,

including sediments in the south west of the Gulf of Guinea, sediments influenced by the Congo River and sediments influenced by the Benguela Upwelling.

2.4   Interface Shear Behaviour

Bolton et al. (2007, 2009) undertook extensive interface shear testing using the Cam-shear device, which is described in Chapter 3, on fully reconstituted and reconsolidated samples of West African clays. These tests were undertaken in order to obtain high-quality soil-pipeline interface data for hot-oil pipeline designers. Test samples were thoroughly remoulded using a electric, drill-driven vane mixer prior to being placed under suction for 30 minutes to remove any entrained air within the sample. The samples were then reconsolidated to vertical effective stresses corresponding to undrained shear strengths measured using in situ T-bar testing, calculated using a modified version of the formulation by Skempton (1954) given as,

$$s_u = \left(\frac{s_{u,nc}}{\sigma'_{v0,nc}} \right) \gamma' d, \tag{2.2}$$

where s_u is the soil's undrained shear strength, $s_{u,nc}$ is the undrained shear strength of a normally consolidated soil, $\sigma'_{v0,nc}$ is the vertical effective stress experienced by a normally consolidated soil to produce $s_{u,nc}$, γ' is the effective unit weight of the soil, and d is the soil depth. Based on the Cam clay model for critical state soil mechanics, Wood (1990) proposed Equation 2.3, where the superscript Λ is defined as $\frac{\lambda - \kappa}{\lambda}$; a ratio that describes the relative slopes of the normal compression, λ and unloading-reloading, κ lines (Wood, 1990), and generally ranges 0.7 to 0.9. $\left(\frac{s_u}{\sigma_{v,0}} \right)_{nc}$ is the material constant which rises from about 0.2 to beyond 0.4 for clays of increasing plasticity, and OCR is the overconsolidation ratio, defined as the ratio of the maximum previous vertical effective stress to the current stress condition. Values of $\Lambda = 0.8$ and $\left(\frac{s_u}{\sigma_{v,0}} \right)_{nc} = 0.45$ were found by Bolton et al. (2007) to be appropriate based on previous work with these high plasticity West African clays.

$$\left(\frac{s_u}{\sigma'} \right) = \left(\frac{s_u}{\sigma'_{v,0}} \right)_{nc} OCR^{\Lambda} \tag{2.3}$$

The shear tests undertaken by Bolton et al. (2007, 2009) considered the speed of shearing, interface roughness, smeared or 'clean' interfaces and repeatability. These variables influence soil behaviour, and can be investigated using the Cam-shear apparatus.

Bolton et al. (2009) observed that the shear behaviour of reconstituted and reconsolidated West African clays could be appropriately analysed using the Cam clay model proposed by Schofield and Wroth (1968). The Cam clay model yield surface is represented by,

$$\frac{\tau^*_{max}}{\sigma'_0} = \mu^* ln\left(\frac{\sigma'_c}{\sigma'_0}\right), \tag{2.4}$$

where τ^*_{max} is the maximum soil shear strength; σ'_0 is the normal effective stress experienced by the soil; μ^* is the soil-soil shear strength divided by the applied normal stress; and σ'_c is the previous maximum effective stress experienced by the soil. Figure 2.8, modified after Bolton et al. (2009), shows a reasonably good fit of the Cam clay yield surface to the soil-soil results obtained at all shear rates tested (0.001mm/s, 0.05mm/s, 0.5mm/s). It is noted, however, that variability exists at all the vertical stress conditions tested. The particular yield surface shown is for data tested at 0.05mm/s.

The mechanisms causing this variability are currently poorly understood, and if explained, could allow greater confidence and economy in hot-oil pipeline design.
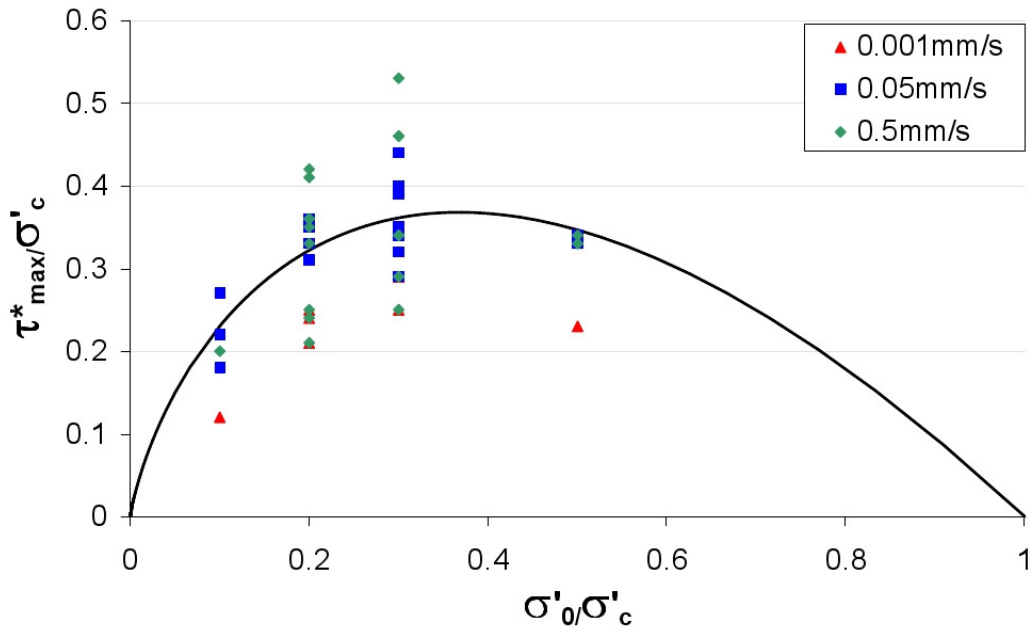
Fig. 2.8 Cam-shear data of remoulded, reconstituted West African clay plotted on normalised axes of shear strength and vertical effective stress, modified after Bolton et al. (2009).

2.5 Implication for Sub-Sea Pipelines

The origin of the crust is as yet unknown but it has significant implications for the design of pipelines that connect sub-sea well completions and risers. Pipelines generally self-embed up to about half their diameter, and therefore rest on the crust material. The dramatic reduction in strength with depth below the crust is of concern to pipeline designers as it is not currently known why the strength drops, nor whether hot pipelines will encourage strength loss with time.

2.6 Crusts in Marine Clays

No operational offshore installations that include sea-bed pipelines on marine clays in the North Sea or the Gulf of Mexico have yet encountered soil characteristics comparable to those observed in West African clays. Figure 2.9 presents an undrained shear strength design profile derived from CPTs undertaken in the Gulf of Mexico by Quiros and Little (2003); and CPT (Puech et al., 2005) and in situ T-bar (BP Exploration) profiles undertaken in West African clays. From this figure, it is observed that the strength profiles obtained from these two areas are significantly different, with the Gulf of Mexico design profile exhibiting no evidence for crustal strength. When compared with West African clays, the sediments of the Gulf of Mexico exhibit lower water contents and plasticities (Puech et al., 2005). This characteristic may have a negative influence on the generation of clay crusts in Gulf of Mexico sediments. In the North Sea, the absence of crusts is most likely due to stiff clays of high overconsolidation ratio of a geological origin dominating the strength characteristics.

There are, however, examples of crust-like material with strength profiles similar to those observed in West African sediments in locations not currently subject to oil and gas exploration. Their discoveries have not been driven by geotechnical design of shallow foundations, and in most cases, as discussed in Section 4.5.6, these sediments are not described as 'crusts'. A compilation of strength profiles from various locations are shown in Figure 2.10. Furthermore, Randolph et al. (2005) state that the occurrence of anomalously high strengths within 1 metre of the seabed is very common. This suggests that these crusts are more prevalent than mentioned in the published literature.

Fig. 2.10 Compilation of strength profiles from the literature, including Nova Scotia, the deep Pacific and the Peru Margin.

Fig. 2.9 Comparison of undrained strength profiles of clay sediments from the Gulf of Mexico and West Africa.

2.7 Concluding Comments and Objectives for Research

No previous literature has considered the possible significance of the presence of crusts in marine sediments. As the oil and gas industry continues to expand, the importance of understanding the mechanical behaviour of these crust materials in relation to pipeline installations increases. This thesis will therefore focus on utilising laboratory tests to obtain information on the behaviour of natural crust samples relevant to pipeline design.

This review of the existing literature on West African sediments highlights several key areas requiring further investigation. These are:

- an understanding of soil-pipeline interaction of natural crust samples at low vertical effective stresses;
- an explanation of the large variation in strengths;
- a better understanding of the natural clay's structure;
- an understanding of the relationship between the presence of the crust and the measured mechanical properties; and
- an understanding of the origin of the crust, and its implications for pipeline design.

The objective of this thesis is to address these five areas. This will be achieved through:

- Cam-shear testing of natural crust samples;
- a review of the literature on processes which may influence sediment strength; and
- observation of natural samples on a microscopic and macroscopic level.

These objectives are the subject of the following four chapters, beginning with the Cam-shear testing of natural cores in Chapter 3.

Chapter 3

Laboratory Testing of West African Clays

The design of hot-oil pipelines requires a knowledge of the soil's undrained shear strength, s_u, which governs embedment, and the soil-pipe interface friction coefficient, μ, which governs the resistance to axial displacements. These soil parameters are usually determined by in situ strength measurement and by collecting core samples for laboratory interface testing. The permeability of the soil is also of interest, as this dictates the length of time for consolidation, hence, how soon after pipe laying the interface strength will be developed. Furthermore, for a given rate of pipe movement, the permeability also governs whether the shearing behaviour is 'drained' or 'undrained'. In situ testing using cone penetrometer and T-bar testing (see Figure 2.6) indicate a relatively repeatable crustal strength over several hundreds of kilometres of investigated pipeline routes. The self-embedment of hot-pipelines locate the pipelines at the sediment depth approximately corresponding to peak in situ shear strength within the crust. Previous investigations into the mechanical behaviour of these sediments have focused on the testing of remoulded, reconsolidated material. This thesis considers the testing of natural core samples, and therefore represents an important contribution to the understanding of clay crusts. To confirm and extend in situ soil data, this chapter firstly outlines laboratory tests on natural cores identifying the bulk soil properties. Secondly, a series of interface tests of core samples undertaken using the Cam-shear device is presented and discussed. Thirdly, the design of a new mini ball penetrometer is outlined followed by the presentation of test results of remoulded and natural samples. The chapter concludes with a summary of the key results and observations.

3. LABORATORY TESTING OF WEST AFRICAN CLAYS

3.1 Bulk Soil Properties

BP Exploration has provided box core and STACOR samples from Blocks 18 and 31 for use in this research. The STACOR system patented by Fugro Ltd. (Fugro) is described in detail by Borel et al. (2002). This system allows the collection of high-quality piston core samples in water depths of over 1,500m, and can obtain continuous sediment cores of up to 20m in length as described by Puech et al. (2004). These samples were collected during site investigations undertaken by Fugro from 2003 to 2007 and represent material from between 1,000m and 1,500m water depth. Box cores samples are collected with a box corer with internal dimensions of approximately 0.5x0.5x0.5 metres. Once recovered on ship, mini T-bar tests were undertaken in the box core by BP Exploration. Core liners were then pushed into the box core sample to allow subsequent transportation with minimal sample disturbance. This method is considered to produce high-quality samples. Where possible, box cores were stored in a portable chest refrigerator at 4℃. STACOR samples were kept in a cool room at approximately 12℃. Box core sub-samples are 83mm in diameter whereas STACOR samples are 96mm in diameter.

3.1.1 Water Content and Liquid Limit

Water content measurements, shown in Figure 3.1 were taken from tested core samples at depths of 0m (seabed) to 2m, by oven drying samples according to the procedures set out in ASTM D2216. Measurements made at depths greater than 1.2m are located below the crust. It is observed that the water content values are extremely high; generally greater than 150%, and do not vary significantly throughout the sediment profile. This shows that the crust strength is largely independent of the water content. The water content may exceed 300% within the top 0.1m, which is the observed location of an 'unconsolidated ooze', comprising oxidated sediment. Liquid limits undertaken on samples using a fall cone apparatus according to ASTM D4318 are also shown in Figure 3.1, along with measurements undertaken by Fugro in 2009. As observed in previous studies, the liquid limits are very high, well above 150% within the crust material. Such results would usually be taken to indicate that the natural sediment is a highly flocculated clay.

3.1.2 Density and P-wave Velocity

To aid characterisation of the West African clays, four undisturbed core samples were subject to non-intrusive testing using a multi scan core logger (MSCL), shown in Figure 3.2. The MSCL determines pressure wave (P-wave) velocity, bulk density, magnetic susceptibility and porosity of samples. Depending on the rate of scanning used, the resolution level can be varied from decimetre to sub-millimetre scale. Calibration of the equipment was undertaken
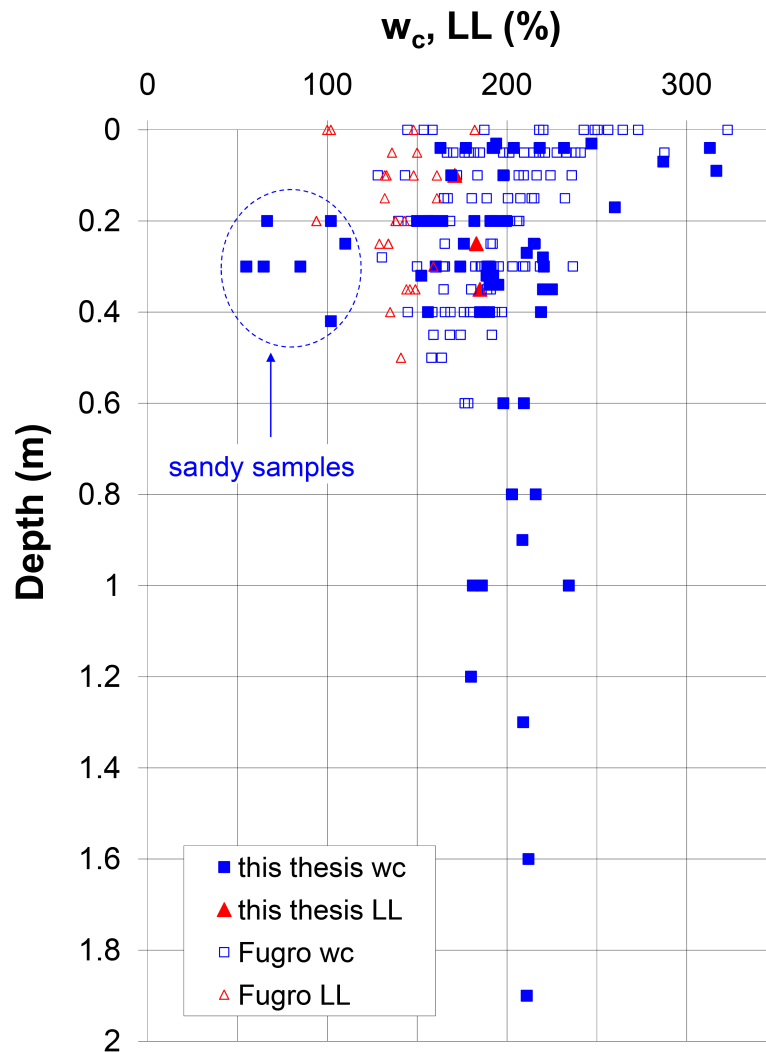
Fig. 3.1 Water content and liquid limit measurements taken from box and STACOR core samples confirming measurements by Fugro (also shown).

using a sample of core liner, which was scanned prior to the samples. This allowed the measurements to be corrected for the influence of the liner during scanning. Core samples were laid horizontally on the scanner bed behind a calibration core sample containing water. To correct for temperature variations during scanning, temperature measurements were taken throughout the testing period using a temperature probe inserted into the top of the core samples. Cores were scanned then split, photographed and geologically logged. The raw data obtained from the MSCL was processed with the corresponding calibration information using in-house software developed by the National Oceanography Centre, Southampton. The resulting data is shown in Figure 3.3. This figure shows the bulk properties determined from the MSCL, the undrained shear strength measured in situ by BP Exploration using CPTs and

mini T-bars, and photographs of split cores corresponding to the CPT samples.
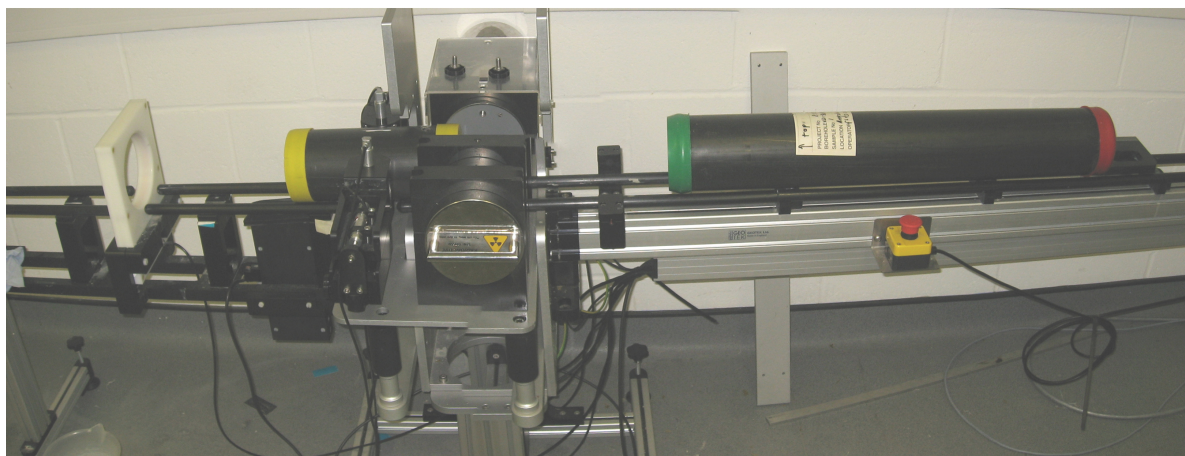
Fig. 3.2 Photograph of the multi scan core logger developed by the National Oceanography Centre, Southampton, to allow non-intrusive determination of bulk soil properties.
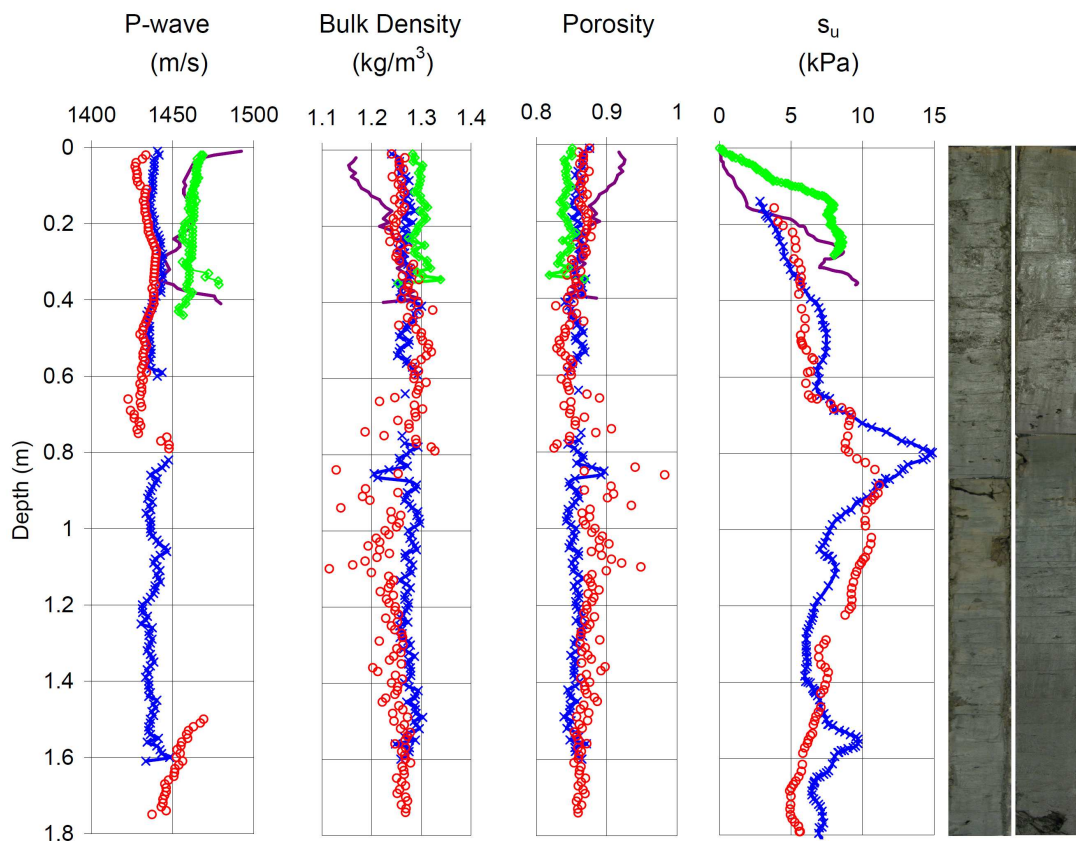
Fig. 3.3 Comparison of MSCL pressure wave velocity, bulk density and porosity to undrained shear strength profile determined from in situ CPT and on-ship mini T-bars for the four core samples, together with representative core photographs.

From Figure 3.3 it is observed that the P-wave velocity for the two longest core samples

drop below the typical P-wave velocity of sea water of about 1,450m/s, suggesting that the cores either contain a significant amount of 'free gas' based on discussion by Yun et al. (2006), or had partially desiccated causing the samples to pull away from the core liner, allowing air to enter the cavity. As expected with very high water contents, very low bulk density and correspondingly high porosity is measured for all samples, suggesting a very open structure. The figure also shows that there is limited correlation between the peak in undrained shear strength and the bulk soil properties. If the crustal strength was caused by a densification of material, large reductions in porosity with a correspondingly large increase in the bulk density and P-wave velocity would be expected; a trend that is not apparent in the results. A large amount of scatter is observed in bulk density and porosity between 0.6m and 1.2m for the two longest cores, which corresponds to the location of the peak crust strength. Core photographs indicate the presence of open burrows that would contribute to the observed variation in measured bulk properties.

The MSCL is a tool that can be used to obtain information on the bulk properties and conditions of samples while still in core liners, thus reducing the influence of core disturbance on measurements. It is, however, observed that due to the nature of the crust material, the bulk properties measured by the MSCL do not identify the presence of a crust. These observations demonstrate that the crust's structure is capable of supporting high undrained shear strengths whilst maintaining a consistently high water content and low bulk density. It is also noted that the MSCL's use is limited by the quality of core material scanned. It is possible that the core samples were disturbed within the core liner prior to scanning, which would increase the inaccuracy of the results.

3.1.3 Visual Examination of Cores

Figure 3.4 shows box core samples that were split using a thin nylon string after MSCL scanning. The surface was then scraped clean with a spatula before photographing. This figure shows that:

- the upper 0.05m to 0.1m exhibits minor oxidation resulting in a pale brown discolouration, corresponding with an 'unconsolidated ooze' material;
- the underlying core material is a relatively consistent grey colour, and comprises firmer clay;
- several 'pockets' of faecal pellets of between 0.5mm and 1.5mm diameter are observed in both cores from 0.1m to 0.3m depth; and
- numerous 'voids' of about 1mm to 1.5mm diameter are observed throughout the core samples, which may correspond to open invertebrate burrows. A large burrow of about 10mm diameter is observed at 0.4m depth in the left core.
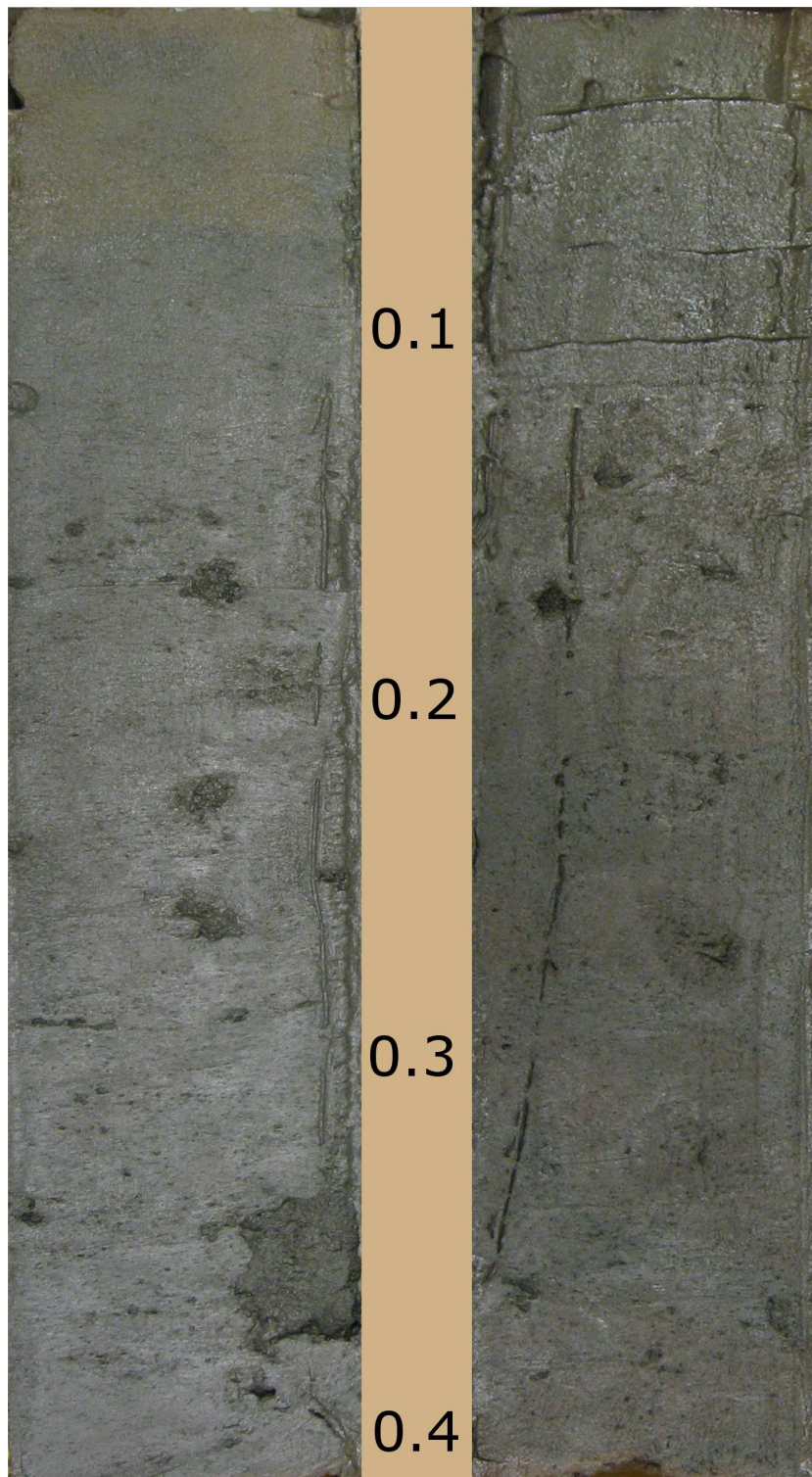
Fig. 3.4 Photographs of box cores after splitting.

A mini shear vane was used to measure the undrained shear strength of three of the split cores. Results are shown in Figure 3.5. The values presented in this figure are generally smaller than those measured in situ by BP Exploration using CPTs and T-bars, as well as mini T bar measurements undertaken on ship. This reduction may be due to disturbance caused by splitting the core prior to shearing. The splitting and logging of core samples shows that there is no correlation between the appearance of the sample and the undrained shear strength, which increases from 2kPa at about 0.05m depth to about 6kPa at 0.4m depth. This, together with the measurements obtained from the MSCL, suggests that the increase in strength is due to micro-scale variation rather than macro-scale influences. The presence of open burrows and randomly-located pockets of faecal pellets, however, are likely to contribute towards the variation observed in the MSCL data.
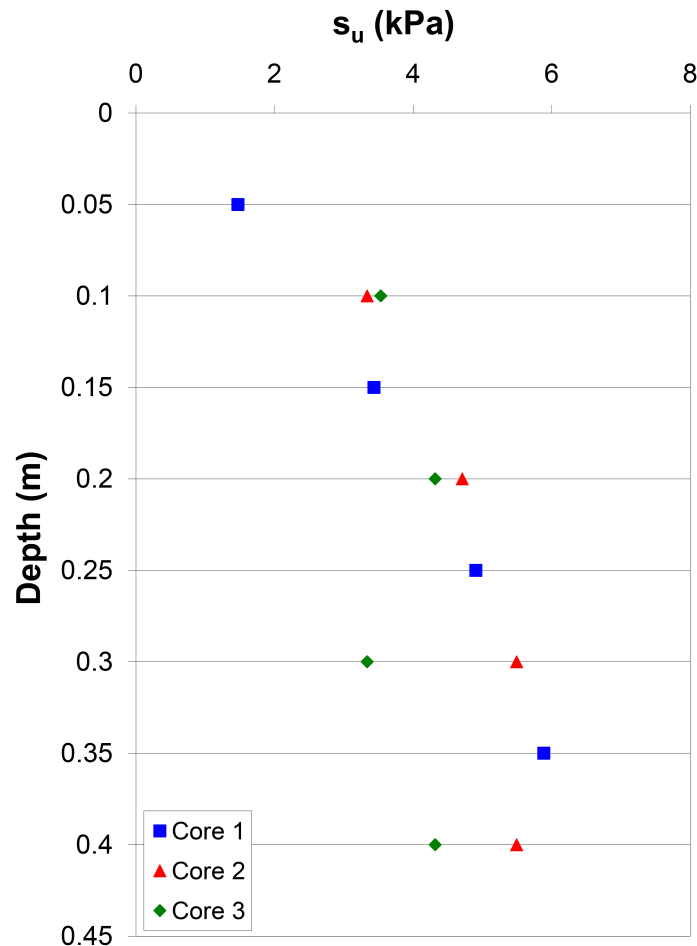
Fig. 3.5 Undrained shear strength of split core samples measured by testing cleaned, split surfaces using a mini vane shear.

3.1.4   Summary of Bulk Soil Properties

The results of tests presented in this section highlight the following key points:

- the structure of the natural sediment appears to have a significant influence on the crust strength, however, the nature of the structure is such, that material below the crust exhibits comparable mechanical properties;

- the water content values are high below the crust, which suggests that the soil at this depth is also highly structured. This structure, however, must be significantly different from that within the crust; and

- it is observed that the natural crust material is highly variable, as evidenced from viewing split core samples. It was therefore to be expected that some variation is also observed in the MSCL data.

3.2   Determination of Interface Shear Strength

Interface testing with clays has been undertaken by several authors using different types of shearing equipment. The literature is summarised in Table 3.1. Previous ring-shear testing of West African clays on rough and smooth interfaces by Puech et al. (2010) is presented in Figure 3.6 plotted with axes of the initial vertical effective stress, σ_0' and peak interface shear strength, τ_{max}. It should be noted, in the case of undrained or partially drained shear tests that the axes of Figure 3.6 do not record the actual effective stresses on the sliding interface. Excess pore pressures will cause the normal effective stress to change during rapid shearing. The friction coefficients determined from $\frac{\tau_{max}}{\sigma_0'}$ in this figure are therefore not true effective-stress friction coefficients. They are, however, of use to pipeline designers who are prepared to deduce σ_0' from the pipeline submerged self-weight and embedment, applicable to the service condition following the passage of sufficient time for soil consolidation after pipe-laying. This data includes tests undertaken at vertical effective stresses of between 20kPa and 60kPa, which is representative of in situ depths of between 7 and 23 metres. These stress levels are significantly higher than that experienced by the shallow sediments under pipeline stresses. Such stresses range from 2kPa to 6kPa, depending on pipe embedment depth. Nevertheless, it is observed that these samples demonstrate a large amount of variability at all tested stress levels, similar to the behaviour encountered by Bolton et al. (2009) using the Cam-shear device with a polytetrafluoroethylene (PTFE) shear box.

Puech et al. (2010) acknowledges that there is currently no known explanation for this variation. The shear strength of clays at the seabed/water interface generally varies from 0.5kPa to 5kPa, which is too small to be reliably measured with conventional shearing devices such as a ring shear or direct simple shear. This is mainly due to the design of these devices for

the testing of terrestrial sediments that generally experience higher effective stress levels than those in shallow marine sediments. The relatively large internal friction arising from the weight of the moving parts limits the achievable resolution of strength measurement. Furthermore, the ring shear and the tilt table (Table 3.1) are inherently unable to test natural samples due to the method of sample preparation. With the ring shear, the sample is subject to remoulding prior placement within the ring annulus. Attempts may be made to prepare an 'undisturbed' ring of natural sample, however, it is commonly accepted that the process of producing a ring will cause significant disruption to the sample's structure. Sample preparation for the tilt table apparatus involves fully remoulding the sample prior to spreading evenly over the table. A detailed description of the sample preparation procedure for the tilt table is given by Najjar et al. (2007). A key objective of this thesis is to investigate the interface shearing behaviour of natural crust material, and therefore, a device that is capable of testing natural cores is required.
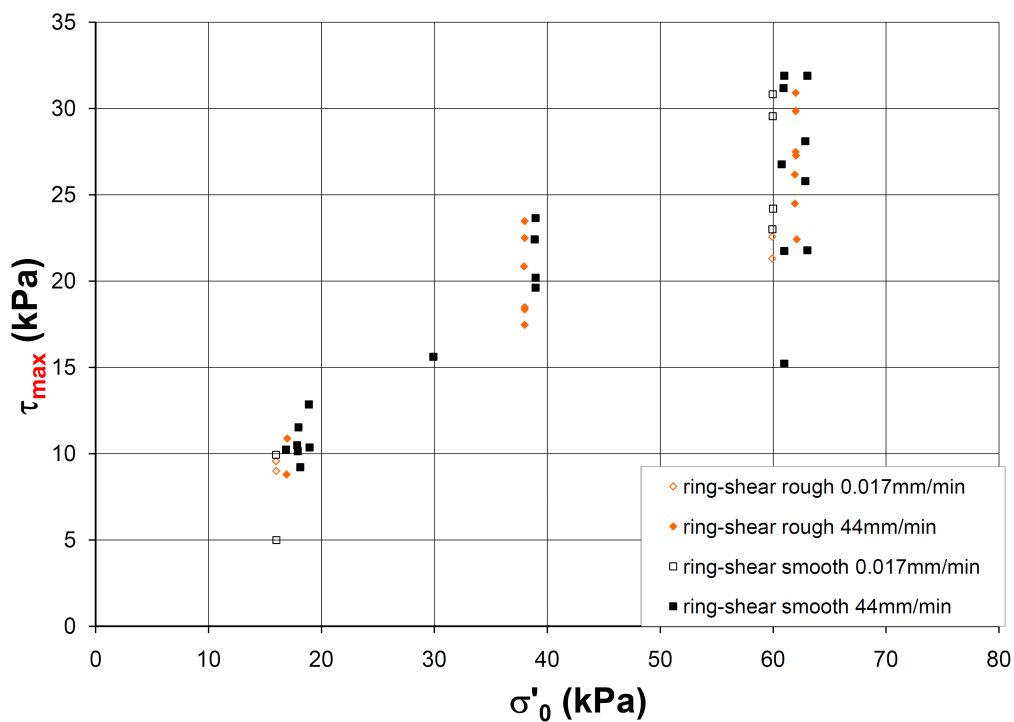
Fig. 3.6 Interface strength of remoulded West African clay measured by Puech et al. (2010) using a ring-shear apparatus and showing results of shearing at different rates.

Table 3.1 Comparison of existing interface shearing devices with selected references.

Shearing device	Sample condition	Interface	Stress level (kPa)	Reference	Comments / Limitations
	Remoulded	Rough & smooth	20 to 60	Puech et al. (2010)	- Only remoulded samples can be tested due to the nature of sample preparation
Ring shear	Remoulded	Rough (coarse sand blasting) & smooth (glass)	50 to 400	Lemos and Vaughan (2000)	- Apparatus internal friction limits the minimum achievable stress level
	Remoulded	Rough & smooth	10 to 50	Fugro (2007-2010)	- Samples can be tested endlessly to obtain residual strength values
Tilt table	Remoulded	Clay-smeared interface	5 to 30	Pedersen et al. (2003)	- Only remoulded samples can be tested due to nature of the sample preparation - The stress distribution on the interface varies depending on the angle of the table - Shearing displacement is limited to the size of table
	Remoulded	Rough & smooth	2.5 to 6	Bolton et al. (2007, 2009)	- Low friction PTFE split-plane shear box allows for testing at small stress levels - Both intact and remoulded samples can be sheared
Cam-shear	Intact	Rough & smooth	2 to 6	This thesis	- Both interface and soil strength (split-plane) can be measured - Shearing displacement is limited to the range of the actuator - Potential for entrainment of water at front 'lip' of the box

3.3   Cam-Shear Testing

The Cam-shear device is a simple shearing apparatus with negligible friction in the system, which allows test conditions to approximate the stress levels experienced by soils under pipelines.

The Cam-shear device was originally developed for the shearing of granulated bones at low stress levels (Bolton et al., 2007). The device was modified to allow the simulation of axial pipe-soil interaction behaviour through the dragging of a clay sample exhibiting low undrained shear strength over a flat sheet of pipe coating material such as polypropylene or polyethylene. The key advantages of the Cam-shear device are its simplicity and ease of modification to consider parameters governing interface shear behaviour, including shearing rates and pipeline stresses. The device is however, limited by its inability to match the magnitudes of pipe displacement that can occur in the field. A more detailed discussion of possible limitations is presented in Chapter 7.

The Cam-shear device comprises a split-plane shear box with an open base and an actuator, as shown in a schematic diagram (Figure 3.7) and in photographs of the whole device (Figure 3.8). The shear box consists of two 100x100mm pieces of polytetrafluoroethylene (PTFE), each 20mm thick, with a central circular bore of 75mm diameter to house the soil sample. This shear box was specifically made for the testing of new natural core samples that have a smaller diameter than the remoulded samples tested by Bolton et al. (2007, 2009). PTFE is used to minimise the inherent friction in the system since the weight of the sliding portion is only 0.530kg (equivalent to a normal stress on the shear plane of 0.66kPa) and the coefficient of friction between PTFE and smooth polypropylene is approximately 0.1 so the sliding friction of an empty box is equivalent to an inferred shear stress of approximately 0.1kPa over the test area. The interface shear strength of the soil is measured by dragging the shear box, containing the clay sample, over a flat sheet of interface material. Although simplified, this represents a pipeline coating interface moving above a sample of clay, as the Cam-shear arrangement also allows the consolidation of the sample against the interface material. The vertical effective stress at the interface is created by the self weight of the tested sample and the applied vertical load. At the soil-soil shear plane, the vertical effective stress is slightly smaller, being due to half the self weight of the tested sample and the applied pipeline load.

The internal shear strength of the clay sample can also be measured by removing the locking pins and splitting the shear box at its mid-depth. The bottom of the box is prevented from moving while the top is moved to impose shear failure in the soil. Normal stress corresponding to the pipe weight is applied by steel discs bearing on top of the soil sample. Drainage layers are inserted between the loading platen and the clay to allow water to escape during consolidation and shearing.
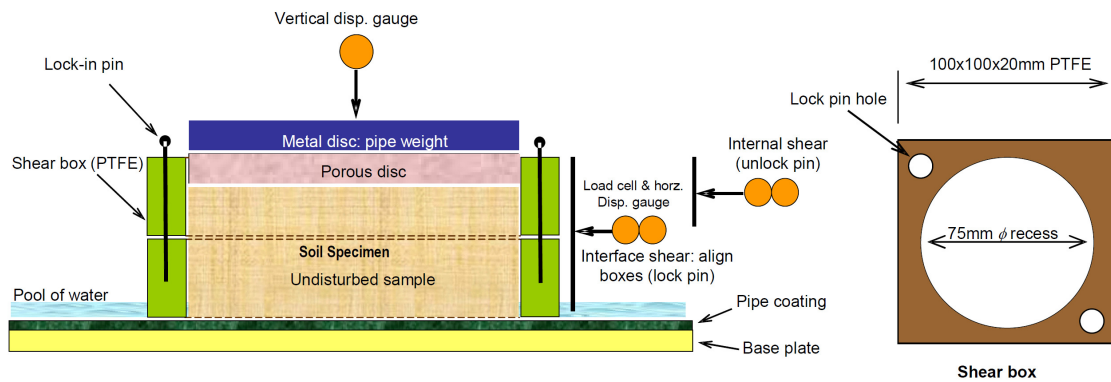
Fig. 3.7 Schematic diagram of the shear box showing the main features, modified after Bolton et al. (2007).

A linear push-pull device (actuator) is used to apply relative displacement between the stationary interface material and the moving clay sample in the shear box, and also to shear the clay sample after splitting the box. A 30V DC motor coupled with a tachometer drives the actuator through a lead screw, as seen in Figure 3.8. Both load-controlled and speed-controlled testing can be undertaken, though in the series of tests undertaken herein, only speed-controlled testing is used. The device was used by Bolton et al. (2009) to run tests at a wide range of speeds, and was proof tested from 5mm/s to 0.005mm/s. A total stroke length of 190mm can be achieved.
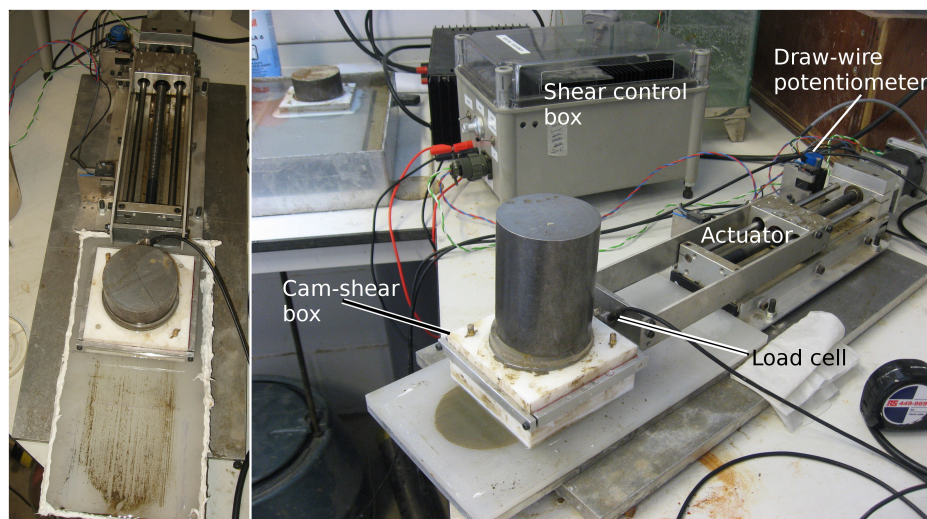
Fig. 3.8 Cam-shear set up showing actuator, load cell, draw-wire potentiometer, and shear control box.

The interface and internal soil strength are measured by a 50N load cell (Novatech Z250, push-pull type) coupling the shear box and the actuator. Associated horizontal displacement and the shearing rate is measured using a draw wire potentiometer mounted on the actuator.

A linear variable displacement transducer (LVDT) monitors the vertical displacement in the soil specimen during sample consolidation.

3.3.1 Comments on Pore-Pressure Measurements

Ideally, excess pore pressures would be measured during shearing, however, the options for locating the pore pressure transducers (PPTs) close to the soil-coating interface are limited to either:

- drilling or pushing the transducer from above through the soil sample and positioning its face in close proximity to the sheared interfaces (locations 1 through 3 in Figure 3.9); or
- embedding the transducer from below into the pipeline coating material (location 4).
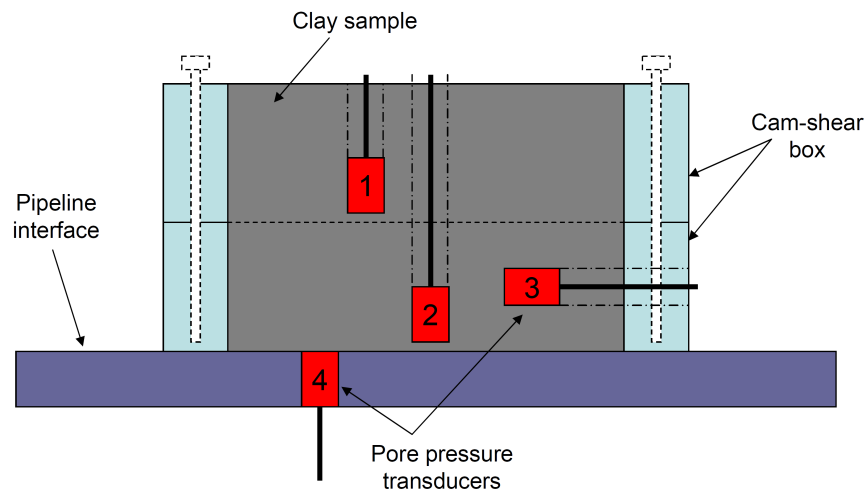
Fig. 3.9 Schematic diagram showing the possible locations of PPTs for Cam-shear testing to measure pore pressures during shearing.

Location 1 would only permit the measurement of pore pressure generation at the soil-soil interface, whereas location 2 would measure pressures at the pipeline interface. These locations have the inherent disadvantage of disturbing the natural state of the sample. Furthermore, there is risk that during consolidation, the final location of the transducer could encroach on and influence the sheared plane. Location 3 minimises the risk of disturbing shearing planes; however, this location risks not being close enough to the location of pore pressure generation. Location 4 allows the sample to remain intact, however, it introduces the philosophical problem of measuring the pore pressure generated by the soil shearing against the transducer's porous filter stone, not against the pipeline interface. Due to these concerns, and their associated difficulty in interpretation of the obtained data, it was decided that the shear tests would not involve pore pressure measurement.

3.3.2   Cam-Shear Sample Preparation

Core tube samples of undisturbed box cores collected from West Africa were used in Cam-shear testing. Core tube liners with an inner diameter of 83mm contained clay material representing seabed material from between 0.3m and 0.5m depth. Tube samples were sealed and protected using a polystyrene disk at the bottom; and with wax and a polystyrene disk at the top surface prior to capping and taping. Cores were stored upright and refrigerated during transportation from the collection site and once received, were stored upright at 4℃.

Sub-samples of about 55mm length were prepared by sawing through the acrylic core liners and then extruding the sample. Samples were then trimmed to 75mm diameter using a sharpened stainless-steel cutting ring and extruded vertically into the PTFE Cam-shear box (with split-plane locked together with brass pins) using an acrylic positioning guide. The stainless-steel cutting ring and the acrylic positioning guide shown in Figure 3.10 were specially designed for use with the current testing to allow minimal disturbance of natural samples. Once in the shear box, the clay surfaces were carefully trimmed flush with the box edge using cheese wire. The box, now containing the 40mm trimmed sample, was then placed on the surface of a wet pipeline coating interface.
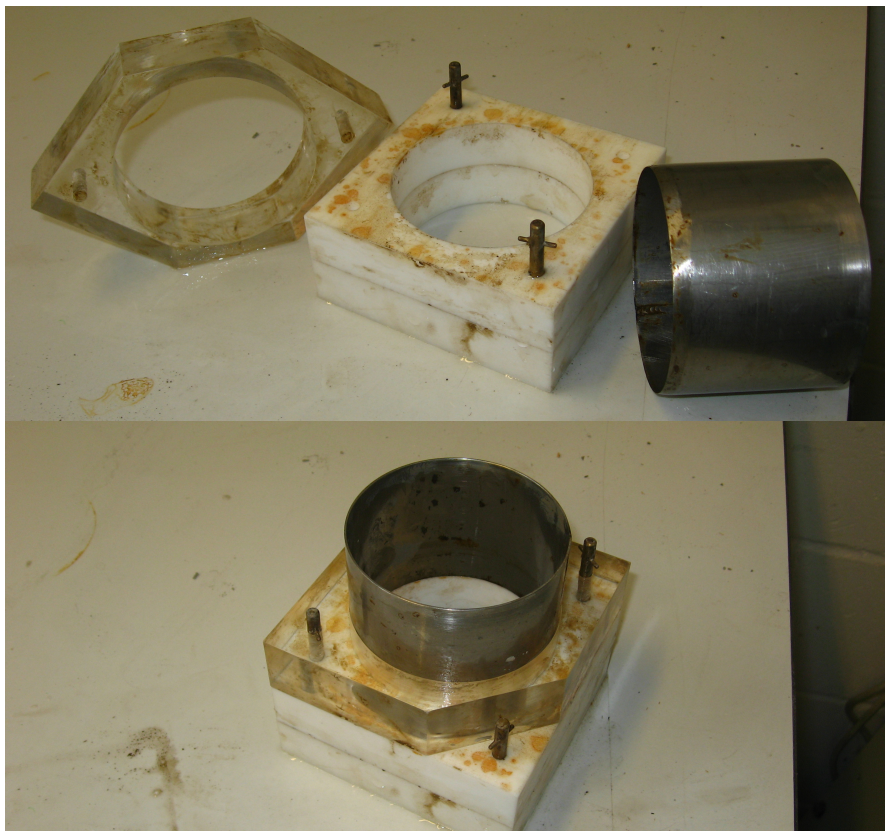
Fig. 3.10 Photographs showing sharpened stainless-steel cutting ring and acrylic positioning guide used to prepare 'undisturbed' samples of natural clay.

The shear box was then sealed to the interface material with a silicon sealant to permit only upward drainage during consolidation and prevent extrusion of clay through the bottom interface. A layer of filter paper, a porous-plastic disc and a PTFE drainage disc were placed between the loading mass and the clay sample. The sample was then allowed to consolidate under the specified pipe weight until at least 95% of primary consolidation had been achieved. Consolidation periods were typically between 1.5 and 2 days. Settlement was measured using an LVDT resting on the upper surface of the PTFE drainage disc and logged using a mobile data-logger using the commercial software, Dasylab. After consolidation, the silicon seal between the shear box and the interface material was carefully peeled off. The pipeline interface surface was kept submerged during shearing to prevent the sample from drying out and to produce a more representative testing environment.

3.3.3 Pipe Coating Interface Material

Pipe interface coating samples of two roughnesses were supplied by Fugro. The surface roughness of the coatings was characterised by a profilometer (Taylor Hobson Precision, Form Talysurf) that plots surface undulations at a suitably magnified scale by traversing a sensitive probe on the coating surface along the longitudinal pipe axis. The average surface roughness of the coating, expressed in this case by measuring the maximum vertical distance between a trough and crest of the surface undulations, was determined by visually analysing the roughness plots. Figure 3.11 shows the surface roughness plots of the two coatings which had measured roughnesses of 5μm and 100μm. These roughness values are considered to be representative of smooth and rough pipes.

3.3.4 Method of Testing Natural Samples

A pool of saline water was spread and maintained on the coating material so that the clay sample did not dry out during slow shearing. The shear box was dragged over the interface material to assess the interface resistance. To study rate effects, and to investigate the 'undrained' and 'drained' responses, tests were performed at shear rates of 0.005mm/s, 0.05mm/s and 0.5mm/s. Average shearing displacements were 50mm, which is considered to be sufficient displacement for the measurement of residual strengths based on Bolton et al. (2009). When the interface tests were completed, the corresponding shear strength of the same soil sample was assessed by splitting the shear box, and shearing at a rate of 0.05mm/s or 0.005mm/s. To quantify the effect of inherent friction in the system, an interface test was conducted with the empty shear box on the smooth and rough interfaces and these values were appropriately deducted from the clay sample test results.

Fig. 3.11 Roughness profiles for smooth (top) and rough (bottom) pipeline coating interfaces.

3.3.5   Presentation of Results

As discussed in Section 2.4, Bolton et al. (2007, 2009) used the Cam clay model to analyse shear behaviour with acceptable results. The Cam clay model was therefore used in this thesis to deduce the apparent pre-consolidation pressure, σ'_c by setting the values of the soil-soil critical state friction coefficient μ^* and the interface shear coefficient, α to those identified by Bolton et al. (2009). Bolton et al. (2009) found that μ^* of 0.6 and α of 0.8 adequately described the shearing behaviour of the remoulded and reconsolidated samples at the soil-soil and interface planes, respectively. The influence of 'natural structure' in the samples can therefore be accounted for in this thesis.

3.4   Cam-Shear Testing Results

A suite of 77 interface and soil-soil shear tests were undertaken at various shearing rates and pipeline stresses. The results of these tests are presented, analysed and discussed in this section. Vertical effective stresses of 2kPa, 4kPa, 5kPa and 6kPa, which are representative of hot-oil pipeline stresses were used to consolidate the samples prior to shearing. The testing schedule was designed to provide an understanding of the shearing behaviour of natural crust samples under different pipe stresses, shearing rates and pipeline coating roughnesses.

3.4.1   Soil-Soil Shearing

Twenty-one soil-soil tests were completed, representing samples taken from depths ranging between 0 and 0.4 metres. The measured peak shear strengths are summarised in Table 3.2. Typical soil-soil shear-displacement curves for samples sheared at 0.05mm/s are shown in Figure 3.12. From this figure, it is observed that the strength can either achieve an initial peak value before reducing by a factor of approximately 1.5, or the strength may remain relatively constant once it has been fully mobilised. Only peak strength values can be reliably determined from soil-soil shearing due to the influence of a reduced shearing area as the test progresses. Shearing displacements greater than 10mm are influenced by the PTFE shear box due to soil-PTFE shearing rather than soil-soil shearing, and therefore can not be treated as an accurate measurement of soil strength. A shearing displacement of 10mm is insufficient to achieve residual strength values; hence, only peak strengths are quoted in Table 3.2. Appendix B presents all Cam-shear test results from this phase of testing.

A summary of the peak strength results for soil-soil shearing is presented in Figure 3.13, together with upper bound and lower bound Cam clay yield surfaces calculated based on the high plasticity samples. As before, with Figure 3.6, plots such as Figure 3.13 represent the strength of the soil following consolidation at a normal stress, σ'_0, and shearing at various speeds. The data points will not generally indicate the state of effective stress *at failure* due to the creation of excess pore pressures.

From Figure 3.13, it is noted that by accepting μ*=0.6 based on Bolton et al. (2009), the apparent preconsolidation stress σ'^*_c is determined to range from a lower bound of 6kPa to an upper bound of 35kPa for the high plasticity clays, indicating a variability in 'apparent overconsolidation'. The soil's preconsolidation stress, σ'^*_c was calculated for each test result by using μ*=0.6 and fitting the Cam clay yield surface through the test point. An arithmetic mean of approximately $\sigma'^*_{c,mean}$=16kPa was found, as shown in Figure 3.13, which is comparable to σ'^*_c values used by Bolton et al. (2009) to prepare remoulded, reconsolidated samples. The soil-soil friction coefficient, μ*, ranges from 0.5 to 1.2, corresponding to apparent friction angles of 30° to 50°, with the highest values generated by shearing sandy samples, shown in
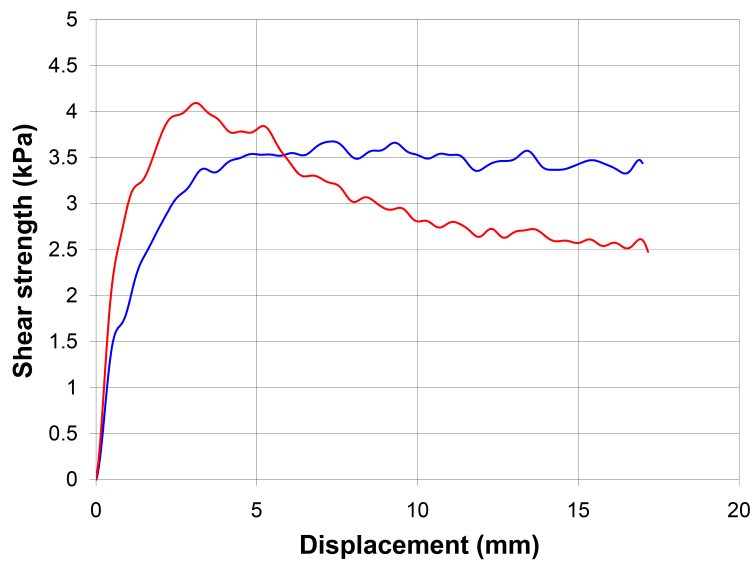
Fig. 3.12 Typical soil-soil strength results for natural West African clays tested with the Cam-shear device.
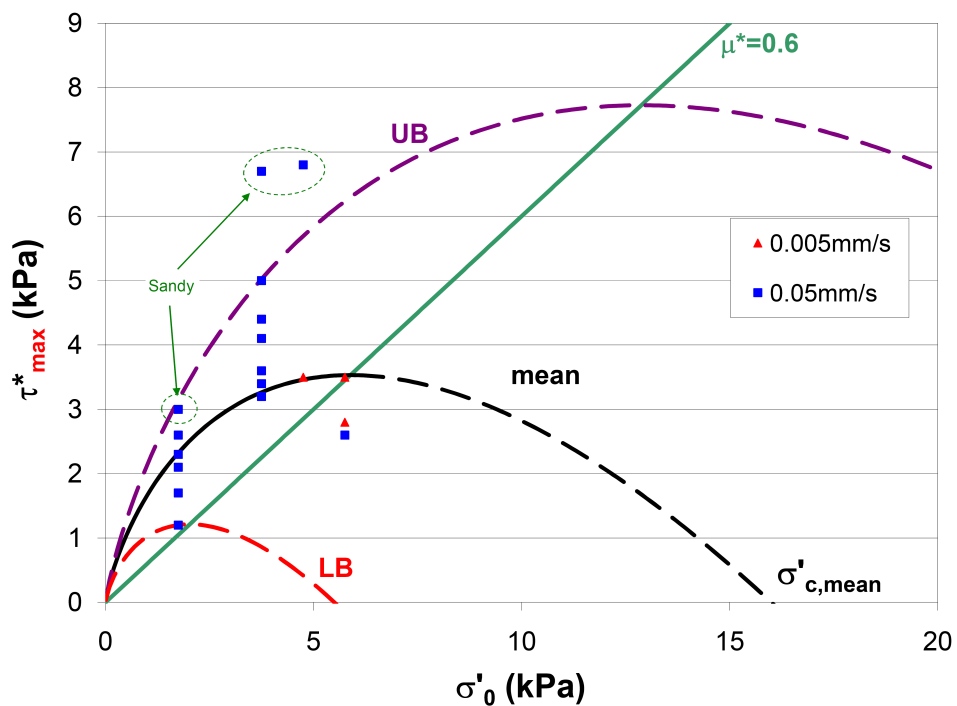
Fig. 3.13 Peak strength values for all soil-soil Cam-shear tests with upper bound and lower bound Cam clay yield surfaces calculated based on μ^*=0.6 following Bolton et al. (2009).

Table 3.2 Summary of Cam-shear peak soil-soil strength values for high plasticity and sandy clay samples.

Sample	Tested depth m	Normal stress kPa	Shear strength τ kPa	Apparent friction coefficient $\mu = \tau/\sigma'$	Apparent friction angle $\phi°$	Speed mm/s
A	0.02	2.1	2.1	1	45	0.05
A	0.18	4.1	3.4	0.83	40	0.05
A	0.32	6.1	3.2	0.52	28	0.005
B	0.02	2.1	2.1	1	45	0.05
B	0.18	4.1	3.4	0.83	40	0.05
C	0.02	2.1	1.3	0.62	32	0.05
C	0.18	4.1	3.6	0.88	41	0.05
C	0.3	6.1	3.8	0.61	32	0.005
D	0.02	2.1	2.6	1.24	51	0.05
D	0.28	5.1	3.5	0.69	34	0.005
E	0.02	2.1	1.3	0.62	32	0.05
E	0.18	4.1	3.6	0.88	41	0.05
E	0.3	6.1	3.8	0.61	32	0.005
F	0.02	2.1	2.6	1.24	51	0.05
F	0.28	5.1	3.5	0.69	34	0.005
G	0.07	2.1	1.7	0.81	39	0.05
G	0.18	4.1	5	1.22	51	0.05
G	0.3	6.1	2.6	0.43	23	0.05
H	0.08	2.1	2.3	1.1	48	0.05
H	0.18	4.1	4.4	1.07	47	0.05
I	0.18	4.1	3.2	0.78	38	0.05

Figure 3.14. It is observed in these sandy samples, that black, incompressible grains of between 1mm to 2mm diameter are present within a matrix of clay. The variability in strength that is observed in the remaining high plasticity clay data is attributed to the samples' natural structure, which is likely to be heterogeneous in nature.

Fig. 3.14 Cores exhibiting black sand grains, to which highest undrained shear strength measured and presented in Figure 3.13 is attributed.

It is noted that the use of Cam clay yield surfaces as a framework in which to present the Cam-shear data (from a direct shear apparatus) is unusual. Though usually drawn in $q - p'$ space appropriate to triaxial tests, the Cam clay yield surfaces are here drawn in $\tau - \sigma'$ space appropriate to direct simple shear (DSS) tests. The stress paths taken by the soil to reach their ultimate states are not known as pore pressures are not measured. Nevertheless, if the initial vertical effective stress, $\sigma'_{v,0}$, following vertical consolidation is known, and if it is accepted that within the yield surface the behaviour is elastic, then the yield strength, τ_y, can be determined (see top sketch of Figure 3.15; path 'A' to 'Y'), regardless of whether the test is undertaken in a drained or undrained manner. Once yielded, the soil will follow the idealised paths shown by 'Y-D' for drained shearing or 'Y-U' for undrained shearing (at constant volume). In any case, the predicted maximum shear strength, τ_{max}, developed in a DSS test starting on the "dry" side of the critical state line (i.e. $\sigma'_0 < \frac{\sigma'_c}{2.7}$) will be the yield stress, τ_y, or perhaps slightly higher in an undrained test. So there is some theoretical underpinning for the use in Figure 3.13 of a diagram of soil strength τ^*_{max} versus $\sigma'_0 << \sigma'_c$.
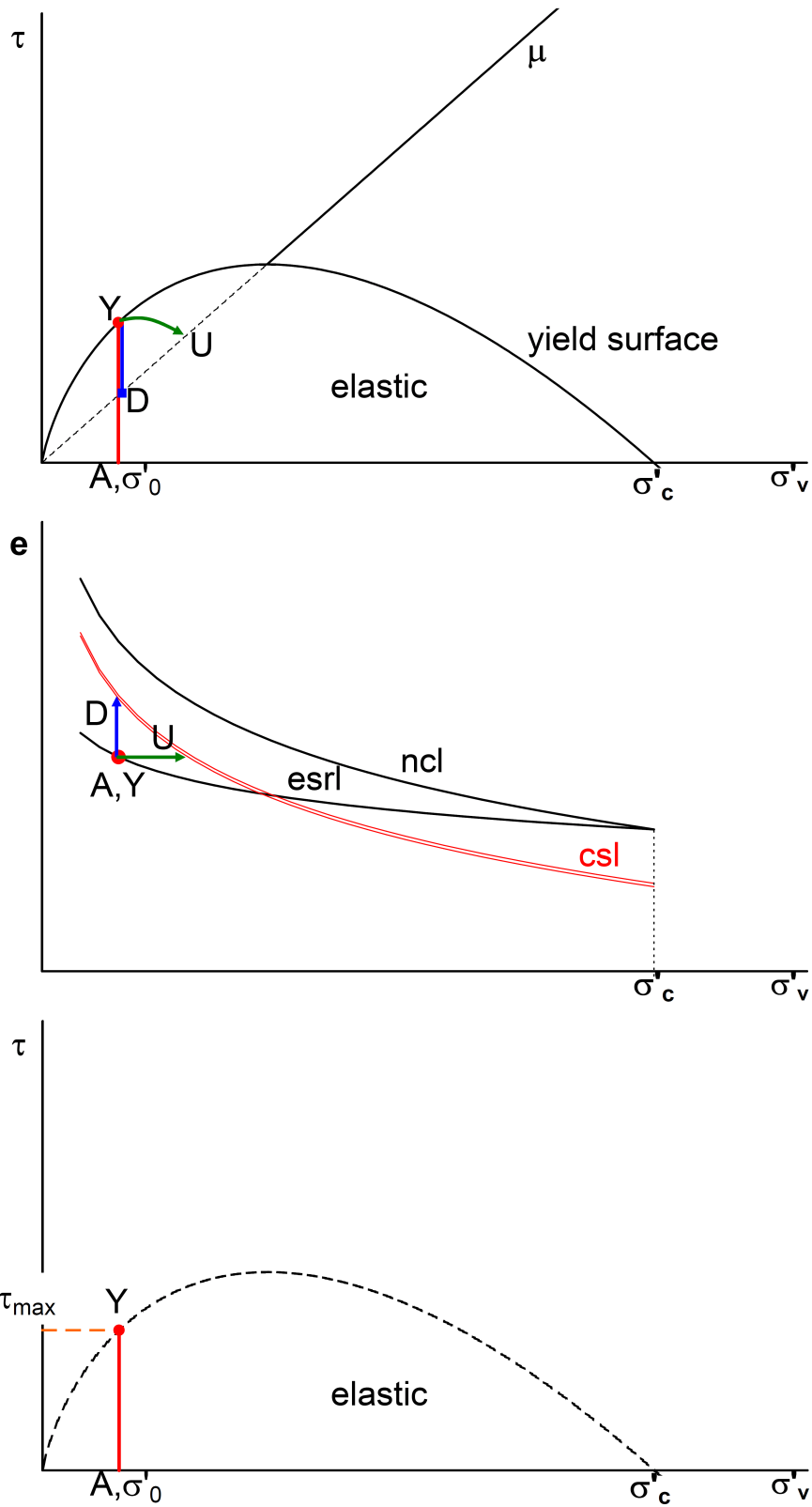
Fig. 3.15 Schematic diagram showing the definition of peak shear strength values obtained from the Cam-shear apparatus using the Cam clay model.

3.4.2   Interface Shearing

Interface Cam-shear tests were undertaken at three shear rates of 0.05mm/s, 0.5mm/s and 0.005mm/s, and for approximately 50mm displacement each. A pause of 30 minutes was permitted between each change of shear rate, as shown in Figure 3.16, which shows the testing procedure used for interface tests.
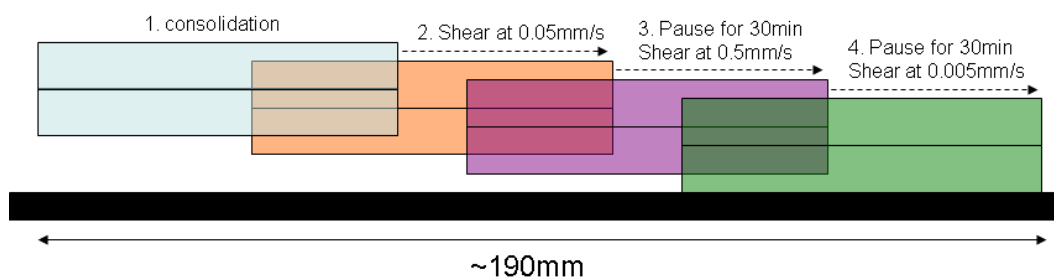
Fig. 3.16 Schematic diagram outlining the procedure for interface Cam-shear tests.

Following Bolton et al. (2007), an alpha scaling factor, α of 0.8 was applied to μ^*, resulting in μ=0.48 for interface shearing. Figure 3.17 shows the derivation of these parameters, as well as the calculated upper bound Cam clay yield surface for interface tests, which was found to exhibit $\sigma'_{c,UB}=\sigma'^*_{c,mean}$, that is, the mean preconsolidation stress for soil-soil shearing shown in Figure 3.13.

Figure 3.18 shows typical shear-displacement profiles for interface shearing. All interface shearing data is presented in Appendix B. Shearing rates of 0.5mm/s and 0.05mm/s tend to demonstrate a distinct initial peak in strength before reducing by a factor of between 1.2 and 4. Strengths may then either remain constant or gradually increase with displacement. Tests undertaken at 0.005mm/s tend not to produce a distinct peak in strength at small displacements and generally exhibited a constant strength value for the duration of the shearing.
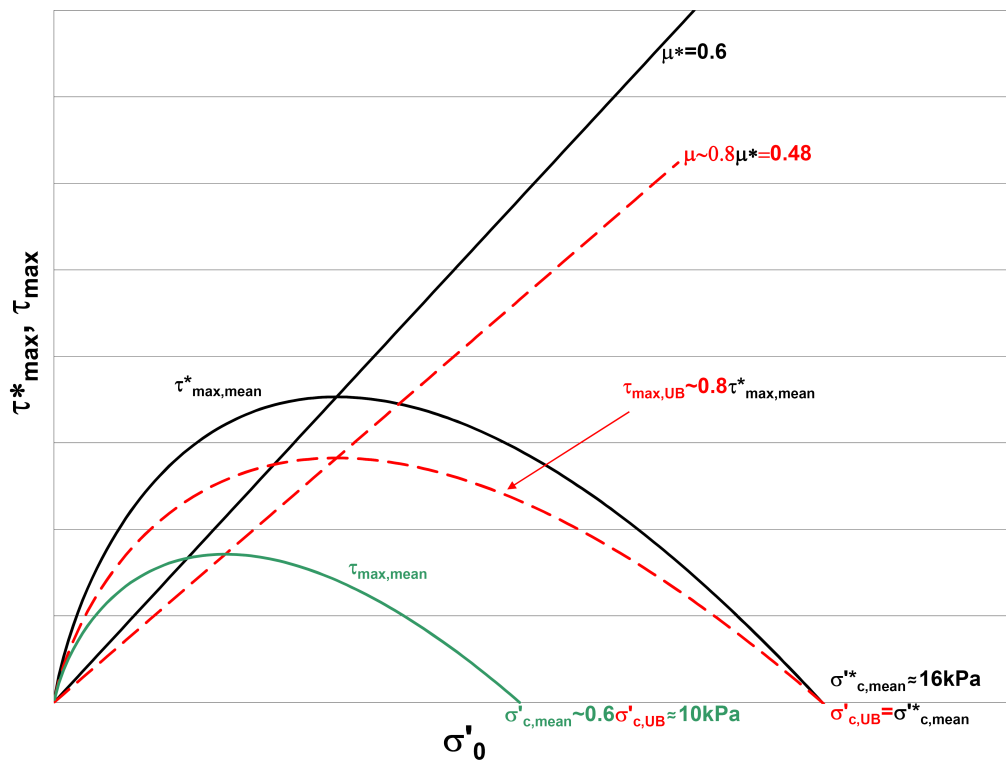
Fig. 3.17 Schematic diagram illustrating the derivation of Cam-shear parameters for interface shearing.
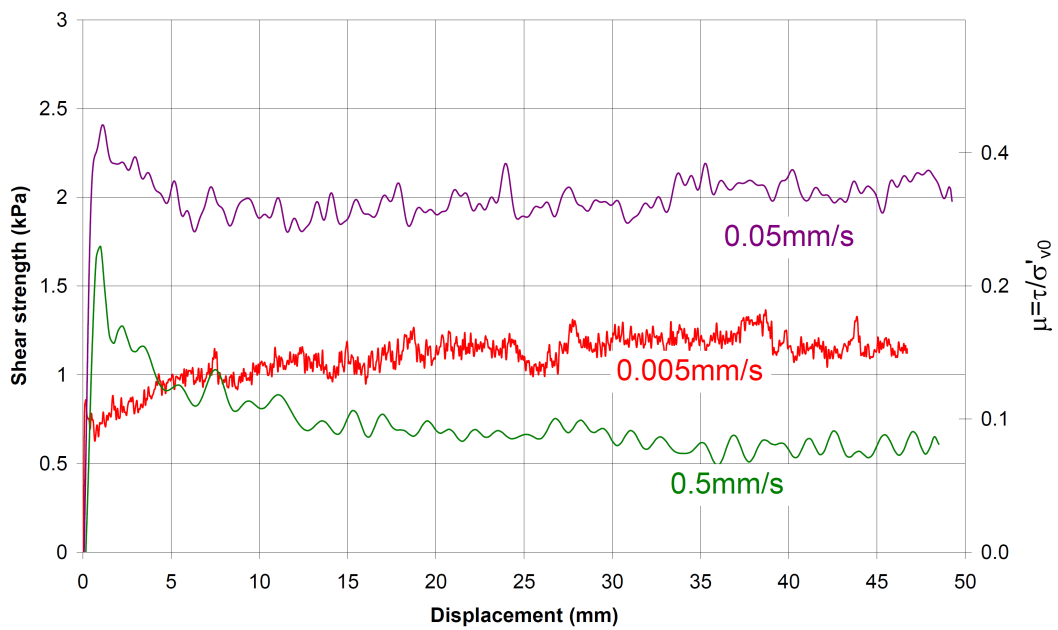
Fig. 3.18 Typical strength profiles for Cam-shear interface testing rates of 0.5mm/s, 0.05mm/s and 0.005mm/s.

3. LABORATORY TESTING OF WEST AFRICAN CLAYS

3.4.2.1 Peak Strength

The peak values of soil-pipeline interface shearing on rough and smooth coatings are summarised in Figures 3.19 and 3.20, respectively. From Figure 3.19, it is observed that significant variation is apparent across all vertical effective stresses. At σ'_v=2kPa, and shearing at an undrained rate of 0.5mm/s, the peak strength may be as low as zero. The lower-bound values for σ'_v=4kPa and 6kPa, though higher than at 2kPa, are still unexpectedly low. From this figure, it can be concluded that the shear rate does not appear to influence the measured strength, though there is a suggestion that on average, slower shearing may produce consistently higher strength values. An upper bound Cam clay yield surface described using μ=0.48 and σ'_c=16kPa is found to be reasonably appropriate for the test data.
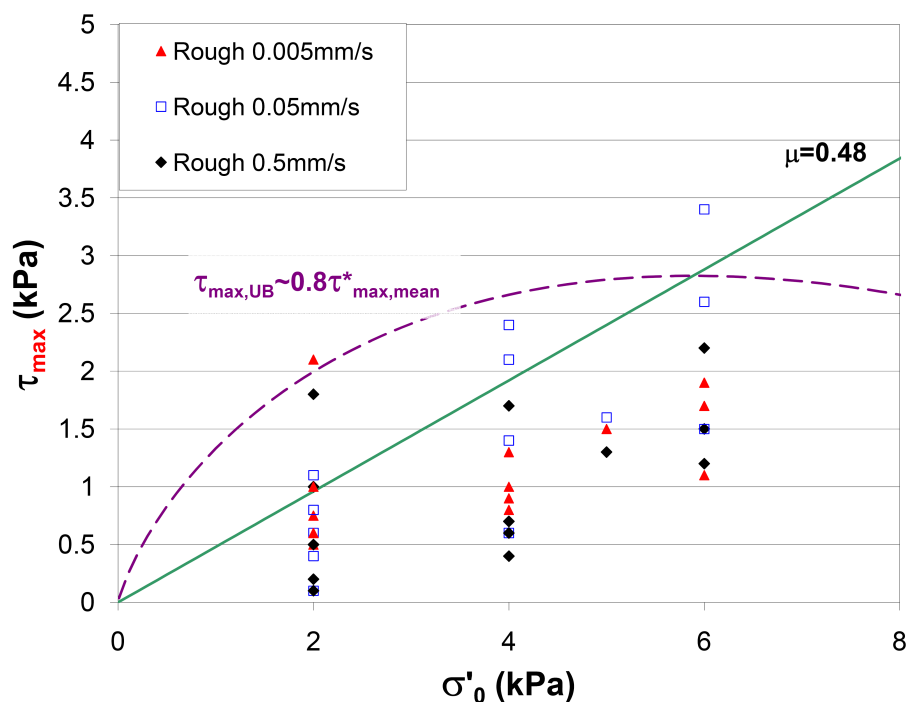
Fig. 3.19 Peak strength values obtained from Cam-shear testing on a 'rough' interface.

Figure 3.20 presents a comparison of the peak strength results from tests undertaken on a smooth interface and the results from the rough interface tests. It is observed that though only nine tests were completed; three at each shearing rate, the results suggest that the rate does not have a significant influence on the resulting shear strength. In contrast to the results from shearing on the rough interface, the smooth interfaces do not produce unexpectedly low strengths. At a vertical effective stress of 2kPa, it is shown that the shear strength values
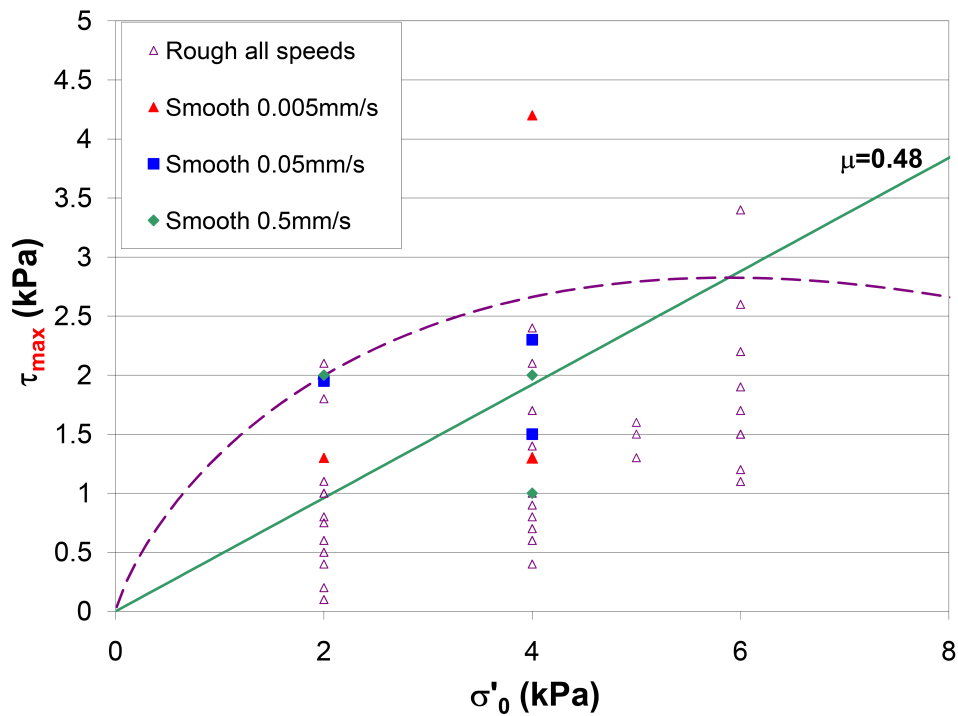
Fig. 3.20 Peak strength values obtained from Cam-shear testing on a 'smooth' interface.

obtained on the smooth interface predominantly result in higher friction values than those obtained on the rough interface. As a general observation, the data suggests that a smooth interface behaves in a more frictional manner than a rough interface. The Cam clay yield surface described using $\mu=0.48$ and $\sigma'_c=16$kPa is found to be a reasonable upper bound for the smooth interface test data.

3.4.2.2 Residual Strength

Residual strengths could not be determined for soil-soil tests due to the limited length of shearing at the shear-box split-plane. However, rough and smooth interface residual strength measurements were undertaken after 40mm to 60mm shearing distance, and are shown in Figures 3.21 and 3.22, respectively. From these figures, it is again observed that a significant variation in strength is measured across all vertical effective stresses tested. Whereas extremely low values of peak strength for the rough interface were seen only for the smallest initial confining stress of $\sigma'_v=2$kPa, the "undrained" strength while shearing at 0.5mm/s could produce residual values approximating zero for all effective stresses tested. A comparison between 0.5mm/s and 0.005mm/s test results also suggest that the shearing rate has a more

pronounced influence on friction values after large shearing distances. It is observed that slow shearing tends to produce higher strengths than the fastest shear tests, which gave a residual friction coefficient below $\mu=0.25$. As for the peak strengths of Figure 3.20, Figure 3.22 shows that smooth interfaces consistently produce higher residual friction values compared to rough interfaces. These results suggest that the rough interface can disrupt the fabric or structure of the soil, thereby generating positive excess pore pressures at the interface, which leads to an almost total loss of shear strength.
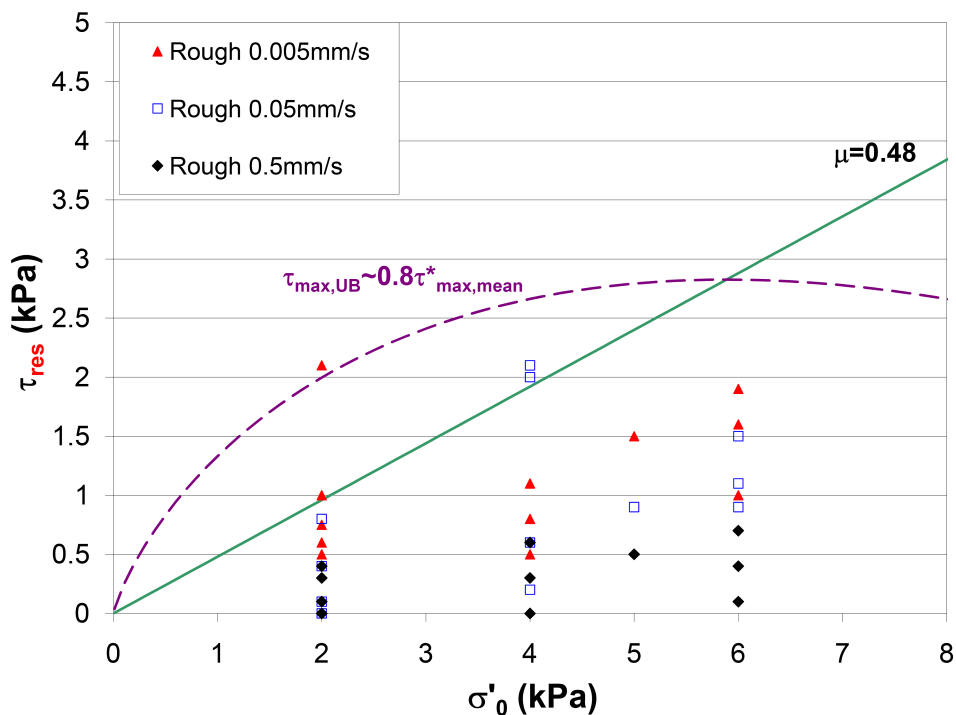
Fig. 3.21 Cam-shear test residual strength values for a rough interface at shearing speeds of 0.5mm/s, 0.05mm/s and 0.005mm/s.

Figure 3.23 presents the variation with depth of the equivalent preconsolidation pressure of soil-soil and interface tests; σ'^*_c and σ'_c, respectively, and deduced by separately fitting a Cam clay yield surface through each point. This associates the variation in observed strength with variation in soil structure represented by the parameter σ'_c. Shearing on an interface disrupts the fabric or structure of the material and somehow results in $\sigma'_{c,mean}$ being lower than $\sigma'^*_{c,mean}$. These values, nevertheless, far exceed the vertical effective stress present at the depth of the samples that were taken. Although the sediment appears to have been free of any previous overconsolidation loading cycle, it has behaved rather as though it had been overconsolidated, albeit, rather haphazardly.

46
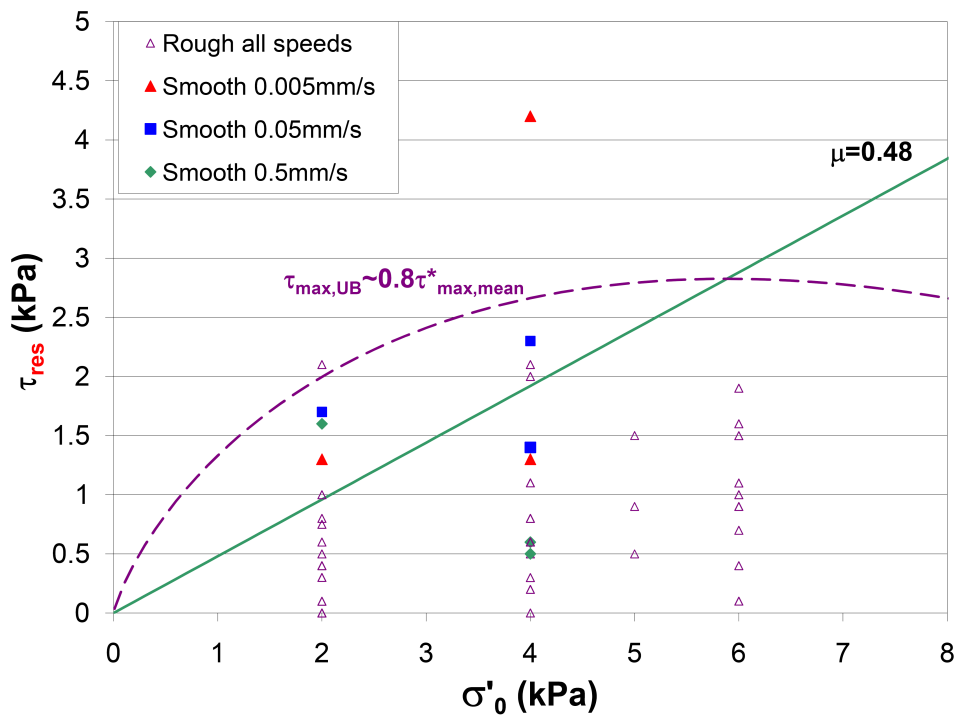
Fig. 3.22 Cam-shear test residual strength values for a smooth interface at shearing speeds of 0.5mm/s, 0.05mm/s and 0.005mm/s, compared to values obtained for a rough interface.
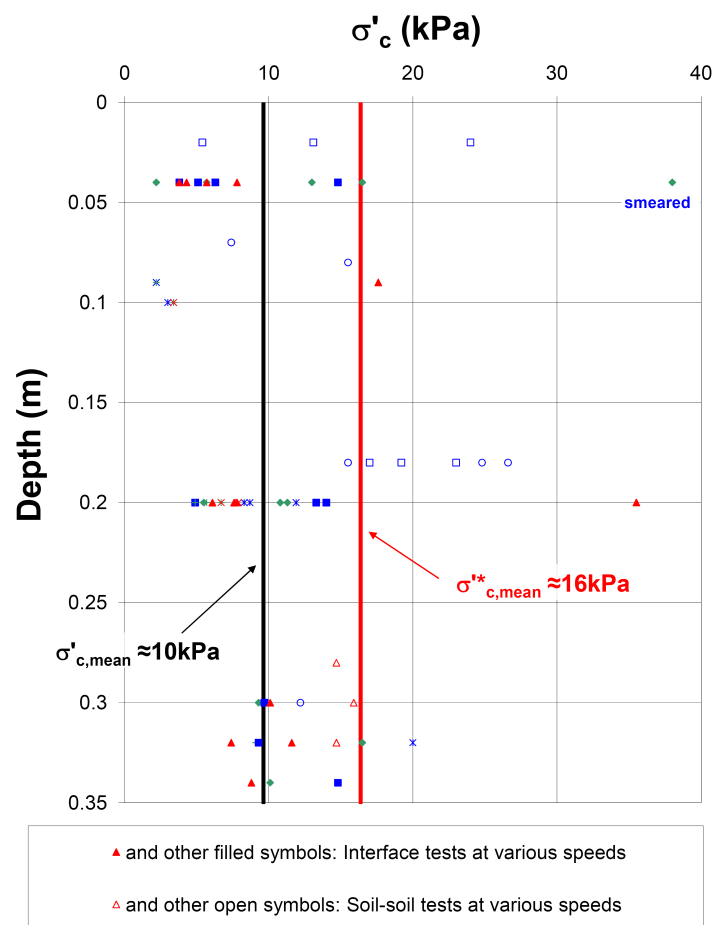
Fig. 3.23 Variation of σ'^*_c and σ'_c with depth as determined from peak strength values.

3.4.3 Discussion

It has been found that the tested natural samples generally exhibit a lower strength than remoulded, reconsolidated samples tested by Bolton et al. (2009), who found that the interface shear coefficient, α, was 0.8. It has been shown in Figures 3.19 and 3.20 that the upper bound interface strengths may be approximated by applying α=0.8 to the *mean* of the soil-soil shear tests. When intact samples are tested, it is usually expected that the natural structure will show an increase in strength. It is demonstrated here, that when shearing on interfaces, the opposite behaviour can occur.

Interface testing has highlighted other unexpected shear behaviour, which is of importance to pipeline designers. Firstly, a significantly large variation in friction values has been found for all vertical effective stresses in the range of interest. At 2kPa, μ_{peak} may lie anywhere

between 0 and 1 for a rough interface. A similar range of values is observed for 4kPa and 6kPa tests, offset upwards by about 0.5kPa per 2kPa increase in applied vertical effective stress, as seen in Figure 3.13. This variation in strength is not wholly unexpected, as results presented by Bolton et al. (2007), show similar variation in reconstituted samples sheared on a pipeline interface. The mechanisms behind Bolton et al. (2007)'s observations are not well understood, as sediment structure is not expected to greatly influence the strength of remoulded samples.

Secondly, peak interface friction on rough interfaces may be as small as zero at σ'_v=2kPa. Residual friction for tests sheared at 0.5mm/s and at all vertical effective stresses tested may also approximate zero. Again, previous testing of reconstituted samples by Bolton et al. (2007) showed that some tests could produce very low residual strengths, though this was not observed for peak strengths. This behaviour may be explained by the generation of positive excess pore pressures at the soil-coating interface that causes a phenomenon similar to 'hydroplaning'. The mechanism generating the excess pore pressures, however, is not well understood. Presumably the presence of a 'collapsible structure' is one possible means of producing this phenomenon, and this therefore indicates that a better understanding of the natural sediment's fabric is required.

Peak strength results for a rough interface shown in Figure 3.19 demonstrate that shearing the natural samples at 0.005mm/s may occasionally produce strengths that are even smaller than those obtained from the 0.5mm/s and 0.05mm/s tests. Bolton et al. (2009), in contrast, demonstrated for reconstituted material that strength was rate dependent, and that shearing at 0.005mm/s was capable of producing a drained response, with consistently higher strengths than undrained shearing. The results in the current series of tests on natural samples suggest firstly, that variability in natural structure is rather greater than in reconstituted soil structure, and secondly, that positive excess pore pressures may still be generated at the very slow shearing rate of 0.005mm/s. An even slower shear speed of 0.0005mm/s may therefore be required to obtain truly 'drained' shear conditions.

Figure 3.24 presents the current test data plotted with existing ring-shear data obtained by Puech et al. (2010). It is observed that similar interface phenomena exist for both sets of data and, as commented by Puech et al. (2010), there is a significant variation in strength that may be measured at each stress level, which may mask any influence of the shearing rate on the measured strength.

The observations made from this series of Cam-shear results have a common theme: the importance of understanding the influence of structure on mechanical behaviour during shearing. It is hypothesised that the structure of the natural soil should provide an explanation for the presence of crustal strength, the variation in measured shear strength, and the quasi-hydroplaning, which can generate extremely low shear strength values.
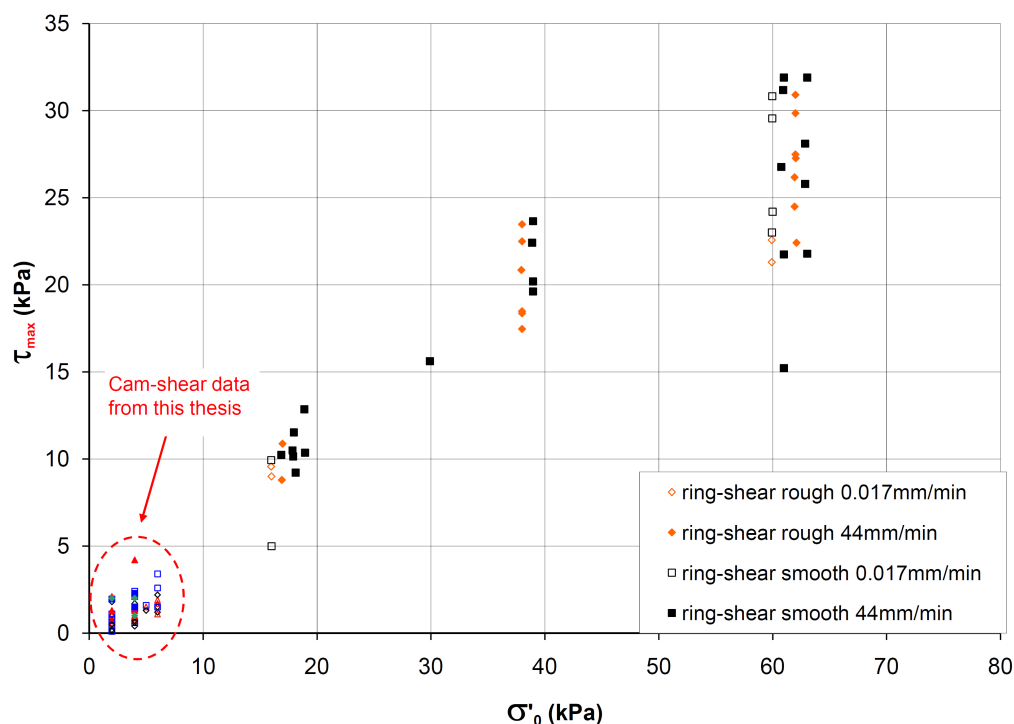
Fig. 3.24 Comparison of Cam-shear soil-soil test results from this thesis to ring-shear test results obtained by Puech et al. (2010) showing variation in measured strength and its independence of shearing speed.

3.5 Mini Full-Flow Penetrometer Testing

To undertake laboratory testing of natural core samples for comparison with in situ (T-bar and CPT) and ship-based (mini T-bar) testing, a new laboratory penetrometer was required. It needed to be small enough to penetrate into intact core samples without the concern of results being influenced by boundary effects. To achieve acceptable resolution in a small penetrometer device, a mini full-flow penetrometer was designed and manufactured. The considered penetrometer shapes were a 'T-bar' and a 'ball' to allow for sufficiently high area ratios, defined as the maximum cross-sectional area of the 'T' or 'ball' compared with the cross-sectional area of shaft alone, which is considered equivalent to pushing a cone into the soil (Yafrate et al., 2007).

This section details the process of choosing and designing a new mini full-flow penetrometer, based on the requirements of high strength resolution and small device size.

3.5.1 Mini T-bar Penetrometer

T-bars are commonly used in offshore in situ site investigations due to their ability to resolve strength in soft clayey soils. In miniature versions, an advantage of using T-bar penetrometers

is that the shaft directly behind the 'T' can be strain-gauged, eliminating the need to correct readings for soil resistance acting along the length of the shaft. This shaft friction may otherwise be a significant value when measuring very small forces on the device. Randolph and Houlsby (1984) derive the plasticity solution for the *"limiting pressure acting on a cylinder (bar) moving laterally through cohesive soil"* (Stewart and Randolph, 1991, p532), which is given by

$$\frac{P}{s_u D} = N_b, \tag{3.1}$$

where P is the force per unit length acting on the bar; D is the diameter of the bar; s_u is the undrained shear strength of the soil; and N_b is the bar factor.

The deformation of the soil around the bar as it penetrates the material is assumed to be symmetrical about the plane perpendicular to the vertical axis for Equation 3.1 to hold. It follows then, that unlike for CPTs, no correction for overburden pressure is required. Furthermore, this solution is representative of an infinitely long cylindrical bar. The bar factor, N_b is chosen based on the bar's roughness, which is dependent on its adhesion factor, α. Stewart and Randolph (1991) present upper bound and lower bound values for the relationship between α and N_b.

Following Stewart and Randolph (1991), the average value of 10.5 has been shown to be an acceptable value for N_b. This value also resulted in acceptable s_u values in very soft deltaic clays of less than 5kPa strength (Newson et al., 2004) and very soft peaty Dutch clays (Oung et al., ?).

To reduce T-bar end friction, Stewart and Randolph (1994) suggest that the bar's ends be machined smooth. Newson et al. (2004) suggests bar lengths of 4 to 5 times the bar diameter should be used to limit instabilities and any possible variation in resistance, which could cause bending moments in the vertical shaft behind the bar. This is of greater concern for bars with large aspect ratios.

Based on the literature, the current research initially proposed to manufacture mini T-bars of length L=25mm and diameter D=5mm, with a hollow shaft of 5mm, tapered to 3.5mm outer diameter toward the junction with the bar. A Wheatstone bridge would be attached to measure strains with inherent temperature compensation. Two gauges would be attached to the T-bar shaft and two would be left unstrained and covered with epoxy to a total outer diameter of 4.5mm.

When completing the calculations for the thickness of shaft to be strain-gauged it was found that the required thickness of the shaft would not be sufficient to withstand the applied force during testing, and increasing the size of the bar would create significant boundary effects when testing within cores. A ball penetrometer of diameter comparable to the T-bar length of

25mm, however, would produce a larger area ratio for the same diameter shaft. Thus, a more sensitive ball device would be possible with a larger diameter shaft.

3.5.2 Mini Ball Penetrometer

Based on Yafrate et al. (2007), an area ratio of 10 was chosen to maximise the resistance output obtained from the penetrometer, whilst maintaining an appropriate size. To facilitate this ratio, the shaft diameter could not be reduced sufficiently to allow for strain-gauging, as was the case with the T-bar design. The options for force measurement were therefore:

- attach a load cell to the top of the shaft; or
- design a force measurement system internal to the ball; an option which was not available with the T-bar.

A practical difficulty with a top-located load cell attached to a thin penetrometer shaft is the likelihood of large bending moments caused by slight deflections from the vertical during pushing/pulling, which would affect the readings. Furthermore, resistance caused by soil on the shaft would be significant, causing difficulties in interpreting the force on the ball alone. Due to these factors, a design with the load cell at the top of the shaft was excluded.

The remaining option was to create a load measurement device within the ball itself and to eliminate the need for correction of shaft friction. The initial design comprised a copper-beryllium, strain-gauged disc, similar to a diaphragm, located at the mid-section of a hollow Delrin ball to which the push-rod was attached. During pushing/pulling, the slight deformation of the disc was measured by the strain gauges that were calibrated with an applied load. During calibration, however, it was observed that the disc deformed in a non-linear fashion which was unacceptable for the device. A new design comprising a strain-gauged Dural ring was therefore developed, and is shown in Figure 3.25. Calculations (see Appendix C) showed that a 16mm diameter ring with wall thickness of 1mm and 8mm height would generate strains of the appropriate magnitude during testing.

To prevent ingress of mud and water into the ball and to prevent measurement of sleeve friction, a series of three inter-sleeved tubes were devised to push and pull the ball through the samples. The outermost shaft serves as protection from soil-shaft friction. This shaft is mechanically connected to the actuator driving the ball into and out of the soil and terminates 1mm from the ball. The centre shaft connects directly to the ball's shell and serves as a 'tube seal' for the inner shaft, preventing ingress of water and mud. The innermost shaft connects to the internally mounted, strain-gauged Dural ring. The ball is driven into the soil by a mechanical connection at the top of the innermost shaft. Figure 3.26 presents a technical drawing of the ball's internal 'proving-ring' load cell and the three-shaft arrangement used to exclude the measurement of shaft friction during testing. Appendix C presents further

Fig. 3.25 Photographs of the strain-gauged, 1mm thick Dural ring inside the mini ball penetrometer, showing the location of the four strain gauges, and the wires passing through the central push-rod.

details of the ball's design. The design of this ball penetrometer represents a novel method of excluding the shaft friction from measurements which would have otherwise had a large influence on the results.

Based on Yafrate and DeJong (2005, 2007), a N_b value of 10.5 has been used for the mini ball penetrometer. This average value is considered to be acceptable for materials with moderate sensitivity, however, it is considered common practice that laboratory tests be used to perform a calibration of full flow penetrometers. Calibration using fall-cone tests of natural soils is detailed in Chapter 6.

3.5.3   Testing of Remoulded Samples

Initial testing with the mini ball penetrometer was undertaken on 0.3m diameter, 0.40m high cylindrical containers of remoulded, consolidated West African clay. Samples were consolidated from a slurry under a nominal 1.4kPa stress for 30 days, allowing drainage through filter paper at the top and bottom of the containers. The initial water content prior to consolidation was approximately 300%. The purpose of these tests was to consider the rate of testing for natural core samples and provide a comparison of the sensitivity and degradation behaviour of remoulded and natural West African clays. A 2D actuator was used to position and drive the penetrometer into the samples. Tests were undertaken at penetration rates of 0.5mm/s,
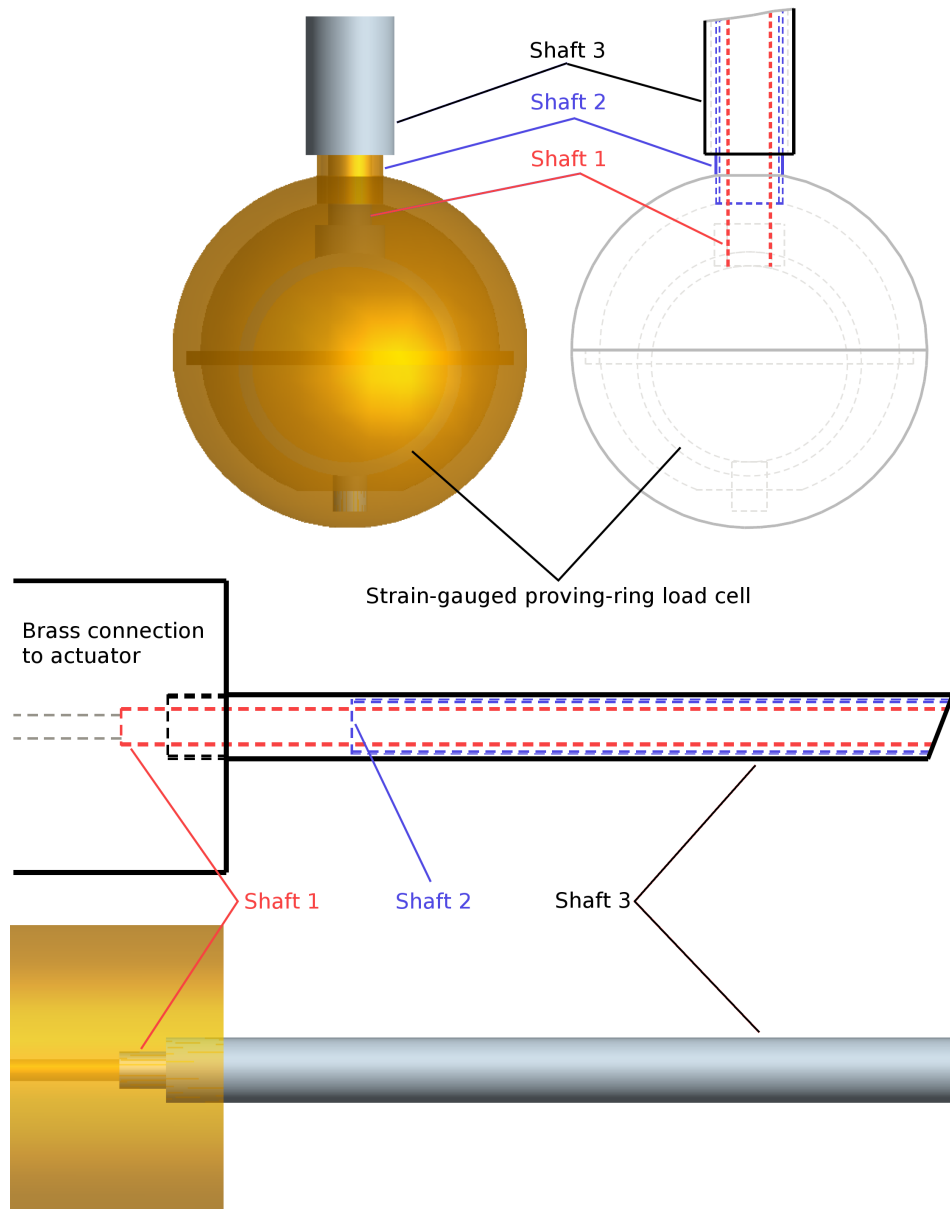
Fig. 3.26 Drawings of mini ball penetrometer design showing the internal proving-ring load cell and arrangement of the three-shaft design used to prevent measurement of sleeve friction.

5mm/s and 25mm/s, with the undrained shear strength profiles shown in Figure 3.27. This figure shows that the tests undertaken at 5mm/s and 25mm/s produce almost identical profiles, whereas the 'slow' test undertaken at 0.5mm/s produces a significantly lower strength. Two cyclic tests were undertaken during the 5mm/s test, with a pause of 20 seconds prior to the first cyclic test. This pause appears to have caused softening in the underlying clay during the initial penetration, resulting in a slightly lower strength being measured for the 5mm/s test compared to the 25mm/s test at a penetration depth of 150mm.
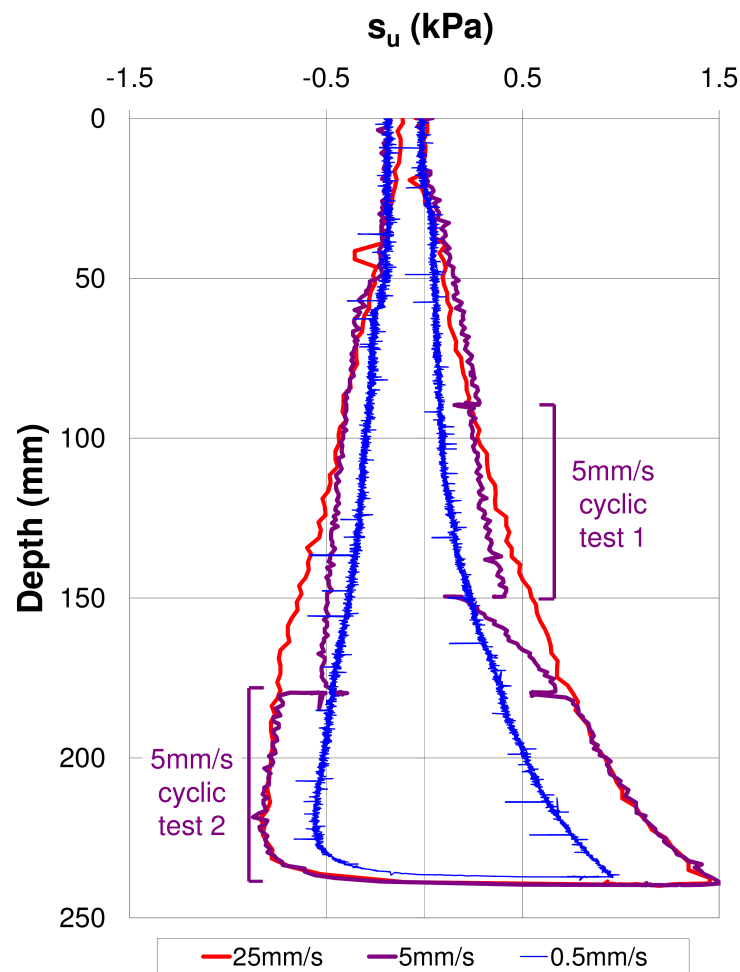
Fig. 3.27 Variation of strength determined using the mini ball penetrometer at penetration and extraction rates of 0.5mm/s, 5mm/s and 25mm/s in West African clay slurry.

Figure 3.28 presents the results of two 60mm-stroke cyclic tests undertaken at a rate of 5mm/s. The commencement depths of the cycles were 90mm and 180mm. Pauses between penetration and extraction for each cycle were about 10 seconds. Reference depths to consider

the degradation of strength with number of cycles were taken at the mid-depths of each test, as seen in Figure 3.28. These correspond to depths of 120mm and 210mm and are presented in Figure 3.29 as curves normalised with respect to the strength of the first penetration or extraction. These results demonstrate that at both test depths, the strength drops to 60% of the 'intact' strength with the first cycle.
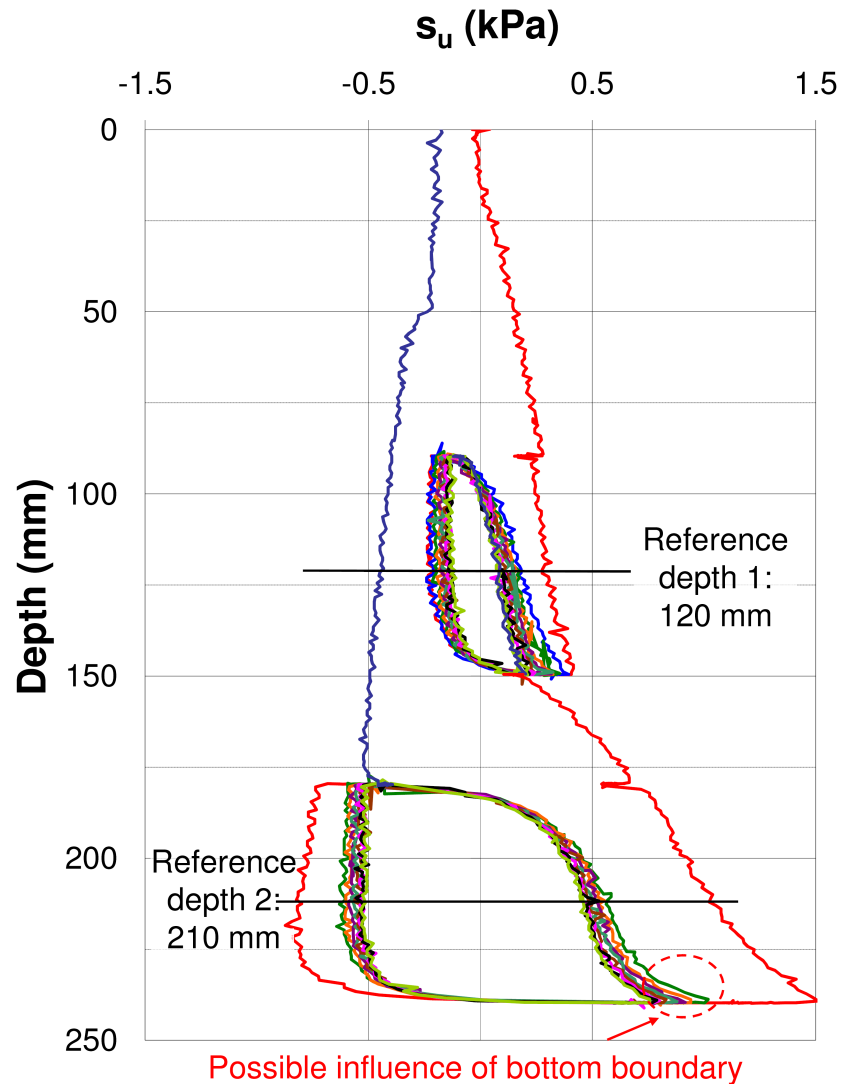
Fig. 3.28 Mini ball penetrometer test at penetration and extraction rates of 5mm/s, with cyclic tests undertaken at depths of 120mm and 210mm.

Strength continues to decrease to about 30% for the shallow test and about 42% for the deep test. However, it is noted that the profiles suggest that after 9 cycles, the 'fully remoulded' state had not yet been reached. The extraction profiles have similar degradation gradients

to those for ball penetration, however, due to the initial disturbance of the intact soil with the first push, the loss of strength with the first extraction cycle is smaller than the loss of strength with the first penetration cycle. The final extraction of the ball penetrometer shown in Figure 3.28 registers a larger strength than the first extraction of the first cyclic test. This discrepancy in measurement may be due to remoulded material remaining on the top of the ball as it was extracted.

Figures 3.27 and 3.28 suggest that the process of cycling influences the surrounding material by approximately one ball diameter. This is based on the observation that the first cyclic test ended at 150mm, however, the soil strength measured by the ball only recovers to the strength profile of the continuous 25mm/s test at a depth of about 175mm. Yafrate and DeJong (2005); Randolph (2004) indicate that remoulding occurs within 1 to 2 ball diameters. The remoulded zone around a ball penetrometer is therefore approximately 2.5 ball diameters which is of a similar magnitude to that found in this study.
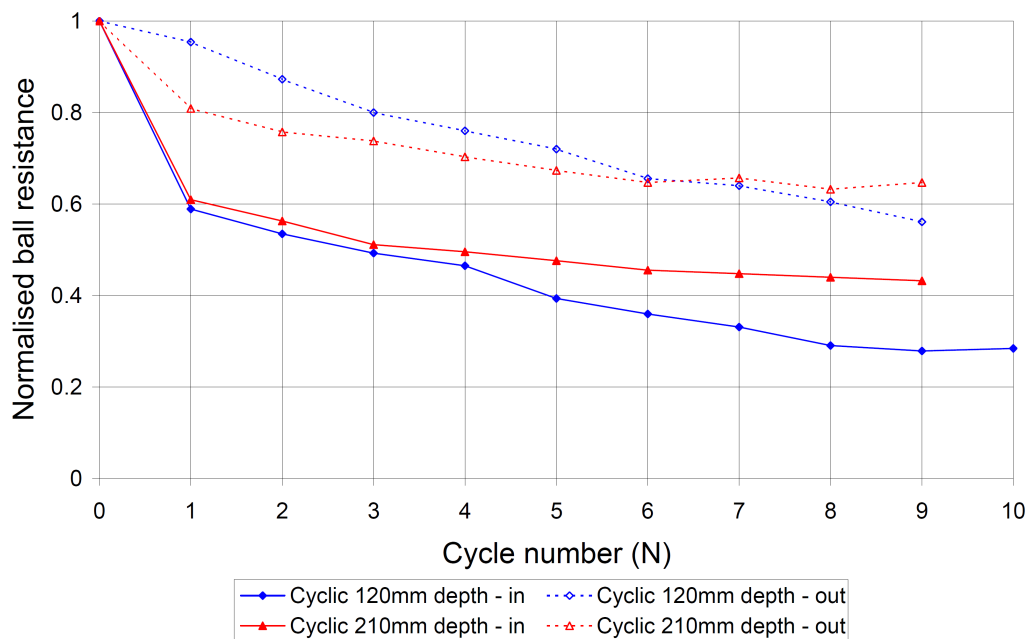
Fig. 3.29 Normalised ball resistance degradation curves of 5mm/s cyclic tests undertaken in clay slurry at depths of 120mm and 210mm.

3.5.4 Mini Ball Penetrometer Testing of Natural Cores

The mini-ball penetrometer was used to measure the undrained shear strength of box-core tube samples containing crust material in order to confirm the crust strength observed in laboratory cores, and to obtain a comparison with in situ measured strengths. Two natural cores were tested at a penetration rate of 20mm/s, which is the standard penetration rate for the CPT,

and which is considered acceptable for full-flow testing (Yafrate and DeJong, 2007). Arasu (2010) considered penetration rate effects with a T-bar in high plasticity marine clays similar to the soils considered in this thesis, but in a reconstituted state. A rate of 20mm/s implies undrained soil behaviour. Figure 3.27 indicates that 20mm/s sits within the region where the soil strength is relatively unaffected by rate effects based on the comparable strength profiles of the tests at 5mm/s and 25mm/s. The remoulded strength was obtained by cycling the ball 10 times over the depth of the core sample. No free water was available at the top of the core and therefore remoulding was achieved at constant overall water content. The peak undrained strength is shown in Figure 3.30 with a comparison to strength profiles from mini T-bar tests undertaken on the ship deck. The corresponding soil sensitivity, determined as the ratio of the first push and the tenth push, is shown in Figure 3.31.

Figure 3.30 shows that the ball penetrometer confirms the presence of crustal strength in cores 'A' and 'B', but measured strengths are higher than those obtained from on-deck measurements taken in the box core immediately after sample recovery. This discrepancy may be due to positive excess pore pressures which were generated during the process of sampling and raising the sample to the ship deck, and which had not had sufficient time to dissipate before testing with the mini T-bar. In that case, the higher laboratory measurements would be indicative of consolidation due to initial sampling disturbance.

Figures 3.32 and 3.33 present cyclic tests for the natural cores. The corresponding strength degradation curves with increasing number of cycles are presented in Figure 3.34 as normalised ball/T-bar resistance and absolute soil strength with an example curve from an in situ T-bar test. Also shown in this figure are the values for all available in situ T-bar data at 10 cycles. Though in situ T-bar information has been provided by BP Exploration, analysis and interpretation of the results as presented in this thesis has been undertaken by the author. A reference penetration depth of 300mm has been used for comparison purposes for cores A and B, and for in situ T-bar data. Figure 3.34 indicates that the strength degradation behaviour for in situ material and core samples are similar, with 9 or 10 penetrometer cycles resulting in values ranging between 20% and 40% of the intact strength.
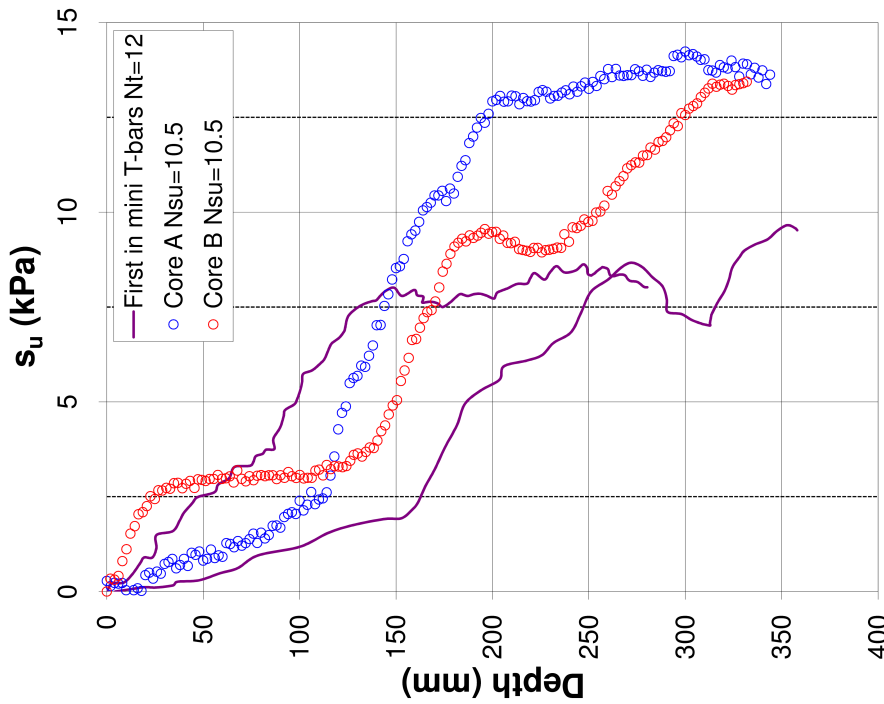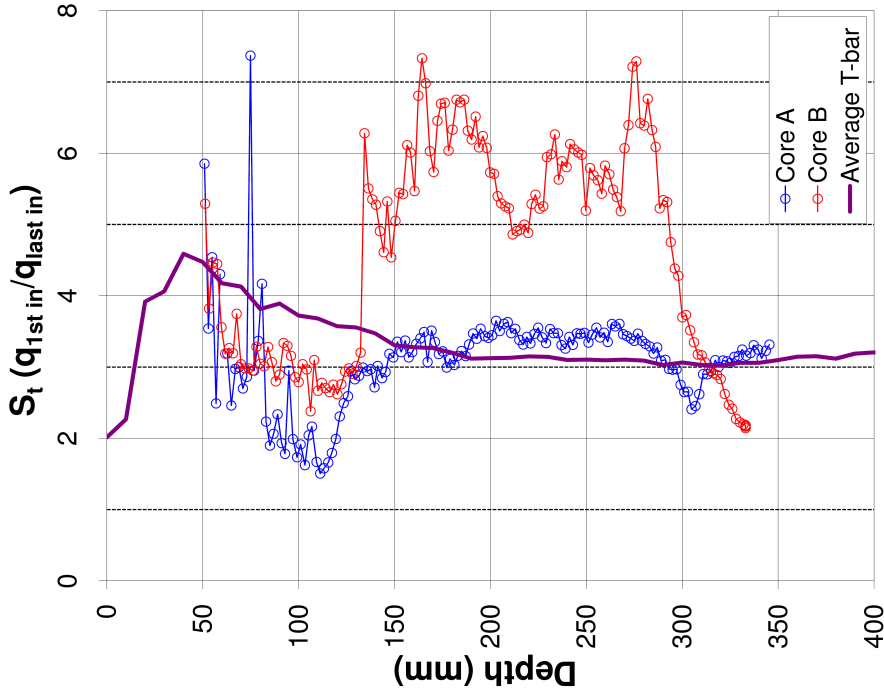
Fig. 3.31 Comparison of soil sensitivity based on mini-ball (laboratory cores) and mini T-bar (box core on ship) penetrometers.

Fig. 3.30 Comparison of undrained shear strengths determined using the mini ball (laboratory cores) and T-bar (box core on ship) penetrometers.

59
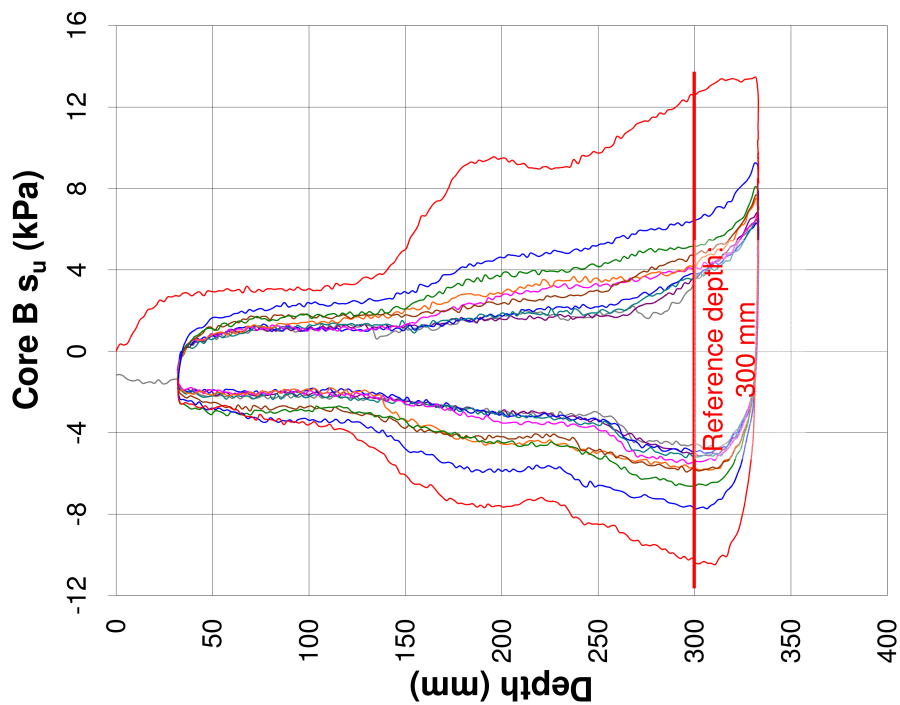
Fig. 3.33 Cyclic test for 'Core B' over 10 cycles, note reference depth for strength degradation analysis (see Figure 3.34).
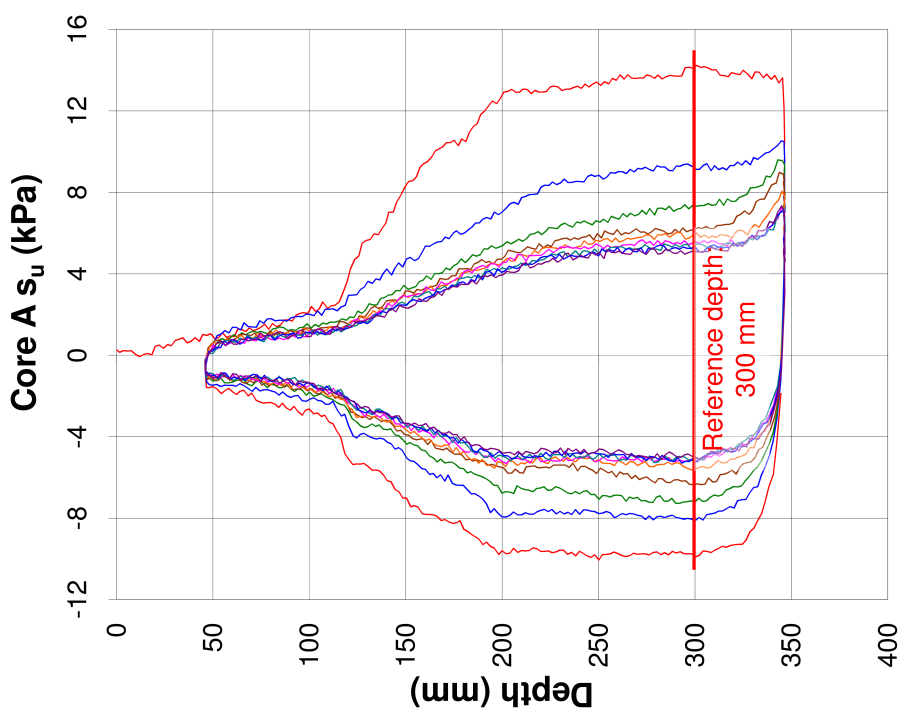
Fig. 3.32 Cyclic test for 'Core A' over 10 cycles, note reference depth for strength degradation (see Figure 3.34).
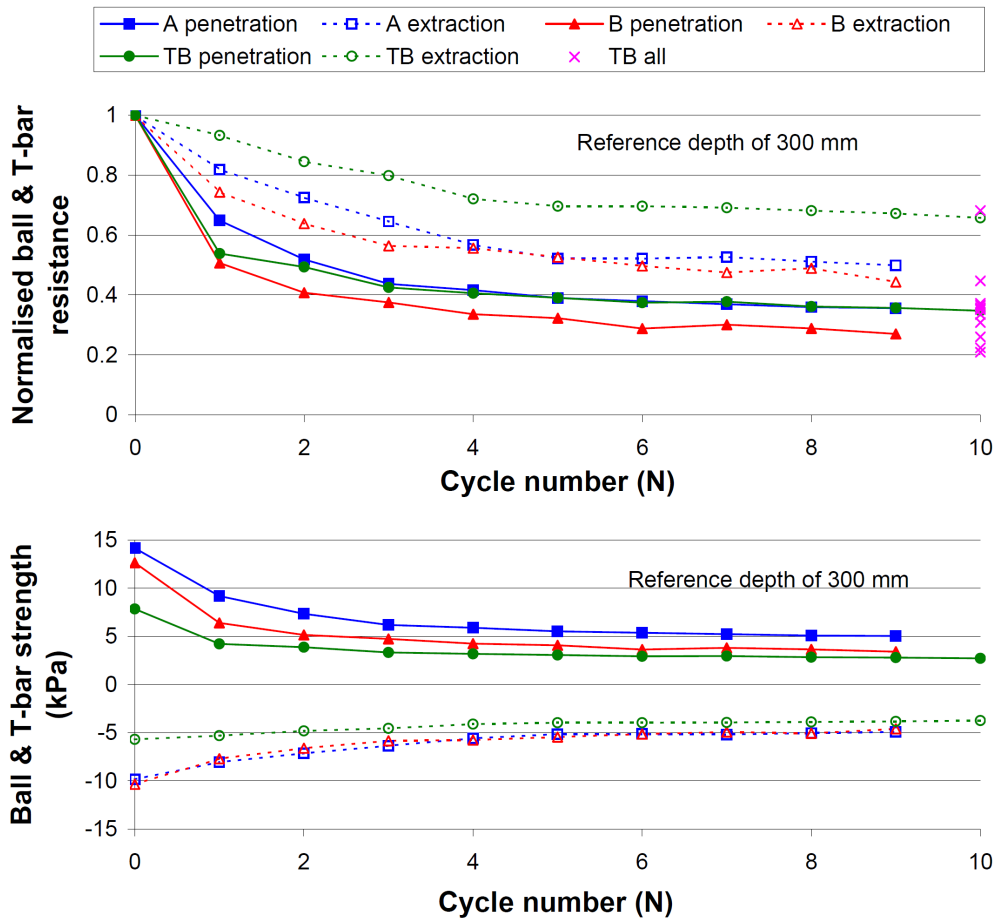
Fig. 3.34 Degradation of mini-ball and T-bar strength and normalised values plotted against cycle number for the reference depths shown in Figures 3.32 and 3.33.

The method generally accepted for soil sensitivity (S_t) determination with full flow penetrometers, is calculation of the ratio of the first penetration resistance to the final penetration resistance, at which the strength degradation should remain relatively constant. Based on the inverse of values obtained in Figure 3.34 at 9 and 10 cycles, a sensitivity of 3 is suggested. It is noted, however, that the degradation curves may still be decaying based on the data presented in this figure. However, Figure 3.31 presented the variation in sensitivity for cores A and B, suggesting that the value may range from about 3 to 6 within the crust material at depths greater than 0.15m. Average in situ T-bar tests also suggested that a sensitivity value of about 3 is typical for these sediments. During testing of core B, which produced a sensitivity of about 6, it was observed that a 'core' of soil remained on the ball after the first penetration-extraction cycle. This material was lifted beyond the core's surface. Figure 3.35 shows examples of mini-ball penetration of natural cores before, during and after testing. The material remained on the ball during subsequent cycles, suggesting that a 'full-flow' mechanism was unlikely to exist. Ten cycles of the ball may have only resulted in remoulding of material

61

located in a cylinder of one ball diameter, leaving a void beneath the ball during extraction. It is suggested that the resulting resistance would indicate a disproportionately larger reduction in strength during cycling and therefore a larger sensitivity value. This mechanism is not uncommon when testing in shallow sediment depths, as reported by White et al. (2010) who suggest a method for correcting for these effects. In practice, the full-flow mechanism can be 'induced' by preventing the shallow soil surrounding the penetrometer from heaving during testing. Alternatively, penetration-extraction cycles may be undertaken at a greater depth where the unwanted plug of material does not form. Based on these observations, a sensitivity value of 6 is considered to be an overestimate. An acceptable value of soil sensitivity within the crust is therefore taken to be 3.

A value of 3 indicates that the soil is only moderately sensitive. After 10 cycles, the soil's undrained shear strength may still be between 3kPa and 5kPa as demonstrated by core A in Figure 3.34. This strength range for a 'remoulded' soil is still higher than that expected for a 'normally consolidated' soil of similar depth. Based on Skempton (1954) given as Equation 2.2, at 0.5m depth an undrained shear strength of only about 0.6kPa is expected in these high plasticity sediments. A comparison of the degradation curves for the remoulded, reconsolidated samples and the natural cores (Figures 3.29 and 3.34, respectively) indicates similar behaviour under cyclic testing. Degradation curves follow similar trends and the final normalised resistances are comparable.
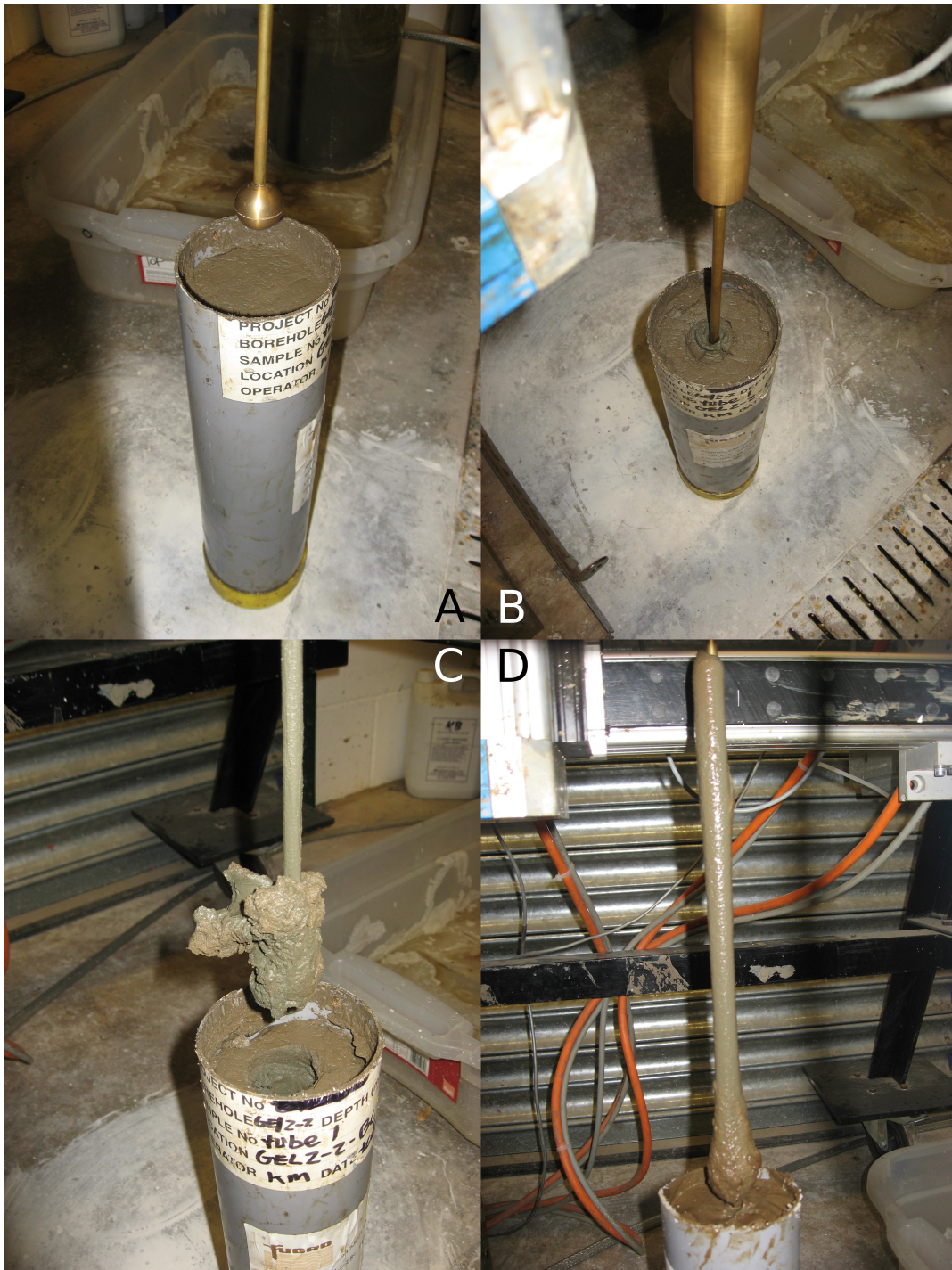
Fig. 3.35 Photographs of mini-ball penetrometer tests of natural crust cores. Note the core of material present on top of the ball after the first cycle of one core (C), and the remoulded crust material coating the shaft after 10 cycles (D).

3.6   Discussion and Conclusions

Given the extraordinary strength exhibited by intact crust material, one might have expected the degradation behaviour to be markedly different from a laboratory-prepared, reconsolidated slurry containing 'no intended' structure. This was not found to be the case. Thus, the remoulding mechanism generated by the ball penetrometer does not completely destroy the existing 'structure' of the natural soil, and/or the natural fabric comprises a bi-fold strength distribution of strong 'micro-elements' in a weak matrix. Perhaps the process of shearing with a full-flow penetrometer only disturbs the bulk structure of the matrix whilst predominantly allowing the micro-elements to retain their inherent strength. This is shown as a hypothetical schematic diagram in Figure 3.36, which proposes that the natural crust material comprises strong agglomerates or packets of clay, within a matrix. The strength of the natural sediment may result from the relatively tight packing of strong agglomerates within the matrix. Though exhibiting a higher strength than normally-consolidated sediment, the strength of the matrix is lower than that of the agglomerates themselves. Disturbance caused by testing with a full-flow penetrometer is sufficiently violent to disaggregate the agglomerates and remould the matrix, that is, disrupt the natural packing. However, this activity is unable to destroy the strong agglomerates, which may flow unhindered round the penetrating ball. This would result in a 'less-structured', partially-remoulded clay. This hypothesis is similar to that implicitly expressed by Hattab and Favre (2010), the key difference being that here it is proposed that the origin of the *crust strength* may be the *two-part* structure of agglomerates and matrix. Furthermore, it is proposed that the agglomerates have an inherent strength that is not readily destroyed.

When this is compared to the results for the Cam-shear testing presented in Section 3.4, it is observed that the process of shearing on an interface (particularly of high roughness) is significantly more destructive to the natural fabric than cyclic shearing with a full flow penetrometer. In situ testing remains invaluable; however, it is demonstrated here that it cannot be relied upon for parameters such as soil sensitivity. For example, remoulded strengths based on in situ T-bar or ball penetrometer testing may be considered suitable for understanding soil behaviour during the process of pipeline laying, but such testing may overestimate the remoulded soil strength by at least a factor of 2. This highlights the need for high-quality testing of intact cores on suitable pipeline coating interfaces with devices such as the Cam-shear, in order to investigate soil-interface behaviour applicable for design. Remoulded, reconsolidated samples are unlikely to exhibit the structure hypothesised in Figure 3.36, and, therefore, testing of these samples will underestimate the degradation that might be expected under shearing.

This chapter has presented the results of physical testing of natural crust material and remoulded samples. The presented results are an important contribution to the understanding
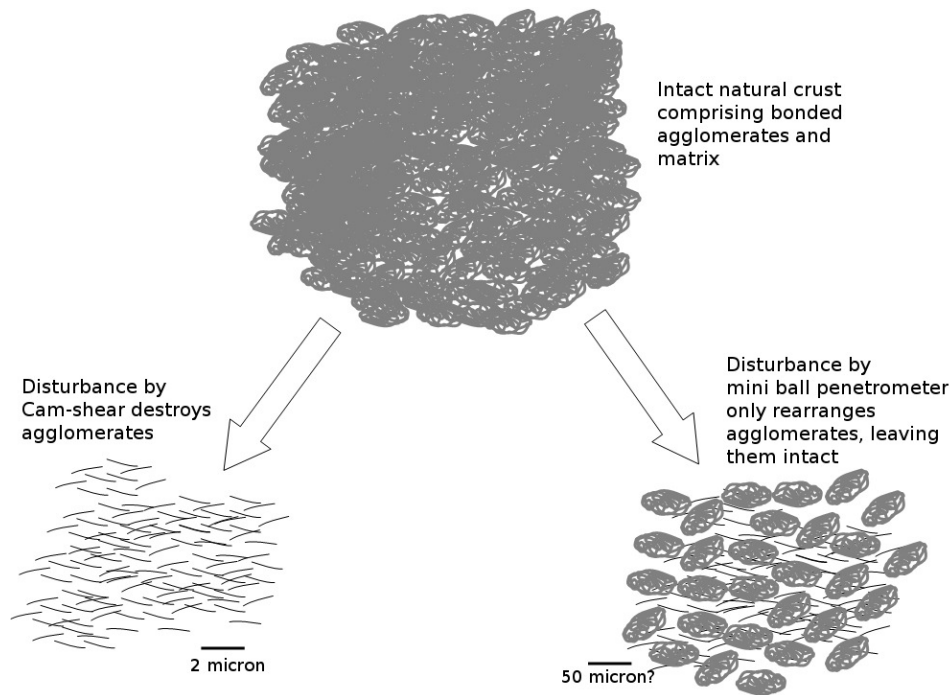
Fig. 3.36 Hypothetical structure of crust material containing both bonded, well-packed agglomerates and matrix. Destructuring by full-flow penetrometers may only remould the matrix and disrupt the packing, leaving agglomerates intact. Interface testing on a rough interface with the Cam-shear device may destroy the structure of both the matrix and the agglomerates.

of the mechanical behaviour of these sediments, as previous laboratory tests have only involved reconstituted, reconsolidated samples. The key findings from these results are:

- the natural samples exhibit very high water contents and high strength;
- significant variations in strength are observed when natural samples are sheared against a pipeline-coating interface;
- the peak strength of natural samples may be as low as zero;
- testing of natural samples on smooth interfaces result in higher friction values than rough interfaces;
- a sensitivity of 3 in natural samples is indicated by both laboratory and in situ testing;
- full-flow penetrometers in natural samples, after 10 cycles of shearing, are unable to replicate the low strengths observed from interface testing with the Cam-shear device;
- the remoulded strength of natural samples, after 10 cycles with a mini-ball penetrometer remains higher than normally consolidated strengths; and
- it is hypothesised that the high strength of crusts is attributed to two features; an aggregate strength and an inter-aggregate, packing strength, of which full-flow penetrometer testing disturbs only the latter.

3. LABORATORY TESTING OF WEST AFRICAN CLAYS

This first phase of physical testing has provided evidence for variation in natural crust-sediment properties, and for variation in mechanical behaviour depending on the type of test undertaken. These conclusions suggest that the crust's natural structure or lack thereof, strongly influences the mechanical behaviour of the sediment, and subsequently defines the parameters required for pipeline design. These findings further demonstrate the significance of the origins of the crust structure, and the need for an improved understanding of the observed crustal behaviour. An investigation of these topics will also assess the suitability of the hypothesised bi-structure proposed as a simplified model of the natural crust. To achieve this, hypotheses for crust origin need to be considered and evaluated, based on the available evidence. In Chapter 4 a range of hypotheses will be considered, some of which will be evaluated in proceeding chapters.

Chapter 4

The Crust: Hypothesis Testing

The seabed-water interface, also known as the benthic boundary layer, is a complex and dynamic environment. The overlying water column supplies the seabed with debris in the form of inorganic matter of terrestrial origin and organic matter of biological origin. Upon reaching the seafloor, these components consolidate or decompose within a few centimetres of the sediment-water interface. Within the underlying soil profile, geochemical processes and biological activity may influence the rate at which new material is reduced (broken down). These processes may have a part to play in the creation of the clay crusts observed in West African sediments, and therefore the origin of the crusts is likely to be significantly more complex than what is usually assumed for terrestrial soils.

As indicated in Chapters 1 and 2, relatively few examples within the current literature consider deep ocean crust or their origin in an explicit manner. Based on the results presented in Chapter 3, it was concluded that the origin of the crust may provide an explanation for its strength and variable behaviour under interface shearing. This investigation into possible origins for crust formation, therefore begins with the formulation of several hypotheses that may be rejected or accepted as the case for or against them is developed. The proposed hypotheses for crust formation include the influence and presence of:

- submarine slope failures;
- thin sand layers;
- cementation and chemical alteration;
- organic carbon; and
- biological influences, including bacteria and burrowing invertebrates.

This chapter presents a review of the literature considering aspects of these hypotheses, beginning on the regional scale and progressing to micro-scale influences. Each hypothesis is required to reflect and/or produce a) in situ strengths higher than expected under normally consolidated conditions; b) a very high natural water content; c) high liquid and plastic limits;

and d) moderate sensitivity as based on T-bar and mini-ball penetrometer testing. The chapter concludes with the objectives for experimental work on chosen hypotheses based on the findings presented here and in Chapter 2.

4.1 Submarine Slope Failures

The simplest explanation for an overconsolidated sediment that has remained submerged for its lifetime, is a mass erosional event that removes several metres of overlying material. This exposes underlying, consolidated material to the seabed with an apparently overconsolidated strength profile. This scenario may be able to explain the high strength sediment at shallow depth; however, it is unable to explain the dramatic loss of strength at one to two metres depth. Bennett et al. (1991) discuss the generation of 'crust' zones within the Mississippi Delta, defined on the basis of shear-strength profiles with burial depth. Sharp decreases in shear strength ('cut back') are observed between 8m and 14m below sea floor, as described by Doyle et al. (1971) and Bea and Arnold (1973). These cut backs in strength are related to submarine slumping of soft, high porosity, deltaic sediments and the movement of massive amounts of sediment seaward on gentle slopes (Bennett et al., 1991). The crust zones have been described by Bennett et al. (1991) through detailed micro-fabric studies, which show areas of preferred particle alignment, but with an overall appearance of remoulding. The sediment fabric within zones of slumping is characterised by remoulding, with particle rearrangement and reorientation into the direction of the principal shear stress (Pusch, 1970). Crusts, as defined by Bennett et al. (1991), represent overconsolidated sediment overlying a sheared zone. To create the strength profile observed in West African sediments, two stages of slumping would need to occur. The first, as discussed previously, would act to remove material from above the current seabed-water interface to form the overconsolidated crust strength; and the second, would act to cause remoulding of soil and hence a reduction in strength below the crust.

Based on BPExploration (2007), it has been established that the age of the sediment is approximately 10,000 years old at a depth of 1m. This equates to a sedimentation rate of about 1 centimetre per 100 years. If minimal erosional processes have occurred during this period of deposition, this sedimentation rate would be considered to be relatively slow for marine sediments at this given depth of water. Again, based on discussions with geologists, it has been concluded that no mass-erosional event has occurred to allow significant unloading of the sediment, and thus create an overconsolidated 'crust' at the depth observed. Puech et al. (2010) substantiates this by considering the uniformity of a high number of CPT profiles in the tested areas, and Puech et al. (2005) states that these areas are "*unaffected by the presence of geohazards*" (Puech et al., 2005, p1051).

Crustal strength generated by a series of submarine slope failures is therefore rejected as

a hypothesis and will not be considered further in this thesis.

4.2 Thin Sand Layers

After geological overconsolidation due to unloading, the next most obvious explanation for crust strength is the presence of coarse-grained layers within the clayey sediment. In situ CPT and borehole samples in some sections of the Nile Delta area have encountered crusts at shallow sediment depth, as shown in Figure 4.1.
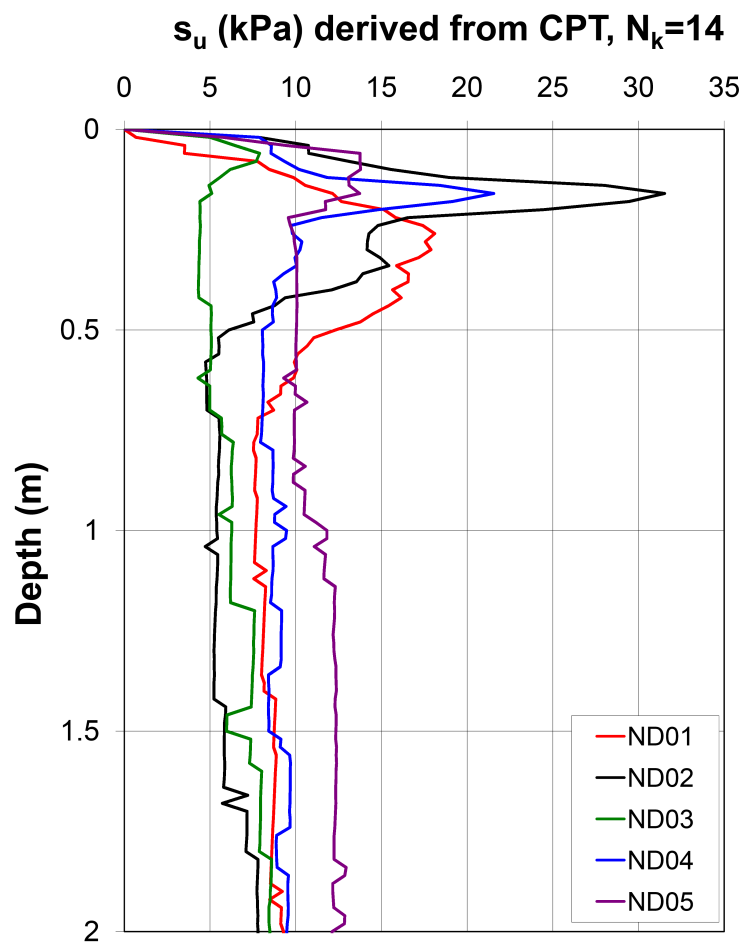
Fig. 4.1 Example CPT strength profiles from the Nile Delta showing crustal strength at shallow sediment depths (with permission from BP Exploration).

These profiles show a relatively sharp increase in undrained shear strength within the top 0.5m before an equally sharp reduction of strength by a factor of 3 to 6. Below the crust-like feature, strengths are consistent with a deposit with an overconsolidation ratio (OCR) of between 3 and 10. Based on core logging and laboratory testing undertaken by BP Exploration,

the Nile Delta sediments are predominantly very soft clays with natural water contents of between 100% and 130%, but with a thin, fine sand/shelly layer near the top of the core. Visual inspection by the author of core material adjacent to CPT locations confirms that the peaks in strength are caused by thin layers of sand resulting in a localised increase in CPT tip resistance at shallow depth.

A comparison of the Nile Delta CPT traces with those obtained from the West African clays show similar strength profiles. Both locations are influenced by terrestrial inputs from rivers that have the potential for transporting coarse-grained sediments into deeper water. Below the observed crust, West African sediments, however, tend not to exhibit OCRs as high as those found in Nile Delta sediments.

Though capable of producing comparable strengths, the shallow sand layers are unable to exhibit the high water contents or plasticities observed in West African sediments. Some West African clay samples tested in the course of this research did contain sand grains. However, the crust materials are predominantly high plasticity clays with no sand content. The hypothesis of West African crusts being formed by sand layers is therefore rejected.

4.3   Cementation and Chemical Alteration

Cementation of coarse sediments, particularly those of calcareous origin is common in marine environments. The cementation of clayey sediments is not usually evident due to the small size of the porespace, which inhibits the growth of chemical precipitation. The seabed-water interface does, however, provide an environment for the exchange of metallic ions that may promote the growth of precipitates. These precipitates may subsequently be buried with time; producing a crust-like strength increase.

Several authors (e.g. Bryant et al., 1967; Buchan et al., 1967) have observed crusts in shallow sediments on the Texan and Mexican continental slopes, and in the North Atlantic Ocean. The location of these crusts are in water depths similar to those for West African crusts. Based on the geochemical composition of these sediments, Bryant et al. (1967) suggest that the strength increase is due to: a) cementation attributed to the presence of chemically altered volcanic debris; and b) a high carbonate content. These suggestions have not been validated explicitly through experimental testing of core samples. West African clays are not exposed to volcanic activity, so it is unlikely that this explanation is the reason for the observed West African crusts. More recently, Sultan et al. (2001) considered the possible influence of physical-chemical processes that influence the ionic concentration of elements within the pore water. However, as described by Puech et al. (2010), a robust explanation for the crust's strength using this hypothesis has yet to be formulated.

In the last few decades, interest has turned toward the possible mining resource of man-

ganese nodules, which have been found in the deep Pacific, and in particular, within the Peru Basin (Grupe et al., 2001). These nodules usually occur at the sediment-water interface in water depths greater than 4,000 metres (Glasby, 2006). Diagenetic deposits may also occur, where chemical species are supplied from the underlying sediment during diagenesis. It is therefore possible that the crustal strength is caused by cementation in the form of manganese precipitates within pore spaces, or as discrete micro-nodules of less than 1mm in diameter at the sediment surface, as described by Glasby (2006) and Stoffers et al. (1984). Over time, these micro-nodules may accumulate into a layer capable of influencing the strength. Within Peru Basin shallow sediments, Stoffers et al. (1984) observed a concentration of micro-nodules, with diameters of up to 500μm within the upper 0.1m of sediment. In deeper sediments, micro-nodules were found to range between 40μm and 125μm. Using scanning electron microscopy (SEM), Stoffers et al. (1984) observed varying accretion and crystalline growth of manganese oxide on different seed materials. It was found that within the Peru Basin, extensive diagenetic remobilisation of manganese ions resulted in precipitation as micro-nodules within the upper layers of sediment.

The hypothesis of manganese precipitation may be able to provide an explanation for increased strength due to sand-like grains of high strength, however, as discussed previously, based on observations of core samples, only one particular core demonstrated the obvious presence of sand-like grains. The grains described by Stoffers et al. (1984) are likely to be too small to be readily observed in natural samples. Washing of samples and imaging with a scanning electron microscope may allow the identification of manganese precipitation in the form of micro-nodules.

4.4   Organic Carbon

Marine sediments contain variable amounts of organic carbon, depending on the availability of input sources, such as carbon dioxide and nutrients in the euphotic zone (the region of water subject to sunlight, thus allowing effective photosynthesis), and terrestrial inputs, such as rivers and glaciers. Jahnke (1990) has shown that continental slopes may be important locations for organic carbon deposition. However, according to Rullkotter (2007), the abundance is mainly restricted to the "*upwelling areas on the western continental margins*" (Rullkotter, 2007, p126). In such areas, the vertical carbon flux is water-depth dependent, as suggested by Rullkotter (2007), with major organic matter consumption occurring below the euphotic zone and within the upper sediment layer by burrowing organisms. Furthermore, as suggested by Muller and Suess (1979), the rate of sedimentation may influence the amount of organic carbon preserved within marine sediments by reducing the length of time the organic carbon is subject to benthic digestion at the sediment-water interface. Their results show that for a

tenfold increase in sedimentation rate, buried organic carbon content may increase by a factor of two.

Once organic carbon has been transported to the seabed, it is generally reported as total organic carbon (TOC) (Bennett et al., 1999). In post-glacial clays, Pusch (1973) concluded that organic matter acted as a cementing agent. Reimers (1982) suggested that the decomposition of organic matter had a significant effect on geotechnical properties of hemipelagic sediment, including a strengthening effect due to the presence of early aggregation.

The influence of TOC has been investigated by Keller (1982) in sediments found to depths of 4m off the Peru Margin. Busch and Keller (1981) suggest that organic-rich sediments have been deposited as a result of "*high biological productivity associated with the [Peru Margin] upwelling*" (Busch and Keller, 1981, p705). An upper-slope mud lens with soil properties measured by Busch and Keller (1981), is reproduced in Figure 4.2. The mud lens exhibited an unusually high undrained shear strength at approximately 1.8m depth, corresponding to about 4% to 5% TOC. Busch and Keller (1981) suggest high TOC may contribute to 'preferred orientations' of clay platelets, therefore allowing increased inter-particle bonding and aggregate formation. However, as demonstrated by Figure 4.2, at greater TOC, corresponding to shallow sediment depth, undrained shear strengths are lower. Busch and Keller (1981) conclude that "*more needs to be known about the interaction between organic matter and other sediment constituents*" (Busch and Keller, 1981, p717) before a plausible understanding of the mechanisms of apparent strengthening by non-cementing organic substances can be formed. A later study by Busch and Keller (1983) identified relatively high friction angles greater than $30°$ and up to $44°$, and suggests that these values are due to aggregation of clay particles by organic matter.
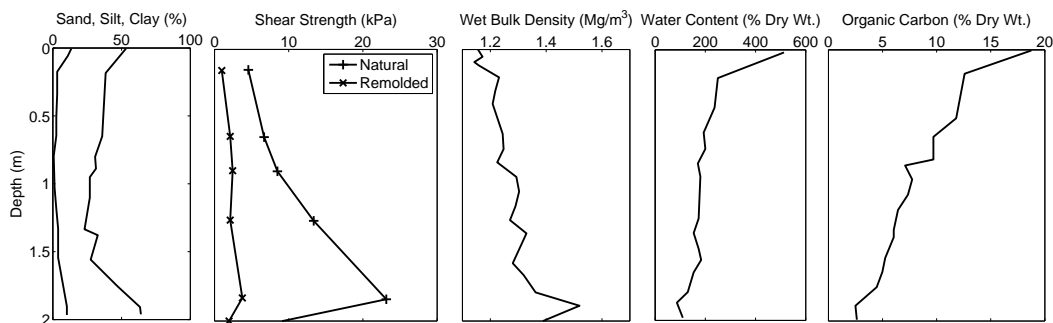
Fig. 4.2 Example of sediment properties off the Peru Margin (modified after Busch and Keller, 1981).

Lee et al. (1990) conducted further testing on samples obtained from 10m to 75m depth, to verify the results of Busch and Keller (1981). They confirmed the very high water contents of the sediments and a possible dependence on the total organic carbon. They conclude that

"high shear strengths and distinctive shear strength profiles within an organic-rich facies appear to reflect a complex interplay of diagenetic and frictional factors" (Lee et al., 1990, p650), and that this may be related to the organic content of the sediment.

More recent work by Ransom et al. (1997) considers the distribution of organic matter within the marine sediment through the use of transmission electron microscopy (TEM). By analysing continental margin sediments from northern California at water depths of between 600m and 950m, it was observed that organic matter deposits occurred in the form of: *"discrete blebs of organic goo; localized, irregular smears of undifferentiated protoplasmic or extracellular material; and bacterial cells and their related muco-polysaccharide networks"* (Ransom et al., 1997, p8).

This review of the literature indicates that there may be a link between increased undrained shear strength and the presence of organic material. However, the relationship shown in Figure 4.2 suggests a different conclusion where the trend in organic carbon is similar to that of the water content and is the inverse of the trend in bulk density and shear strength.

4.5 Biological Influences

Biological activity at the seabed and within the upper few metres of sediment is of interest to marine biologists and ecologists. Even so, the deep-sea biota remains a relatively unknown environment compared to other more accessible environments, in-part due to inhibitive costs of in situ investigations. The interaction between engineered structures, such as pipelines, which have been installed into these environments, and the existing biology is poorly understood. This section introduces some aspects of bacterial and burrowing invertebrate activity that may impact on both the creation of crusts, as well as the behaviour of installed infrastructure.

4.5.1 Bacteria in Marine Sediments

The level of bacterial activity in marine sediments rivals that of terrestrial environments. A review by Parkes et al. (2000) demonstrated the large bacterial population present in subsurface marine sediments, seen in Figure 4.3. This figure shows measurements of bacteria numbers for several marine sediments. Parkes et al. (2000) found that the top metre contained the highest populations, with between 1.4 and 4×10^9/cm^3 for the Japan Sea and Peru Margin, respectively. They suggest that temperature may limit the bacterial density at greater sediment depths. Evidently, the effect of temperature does not limit the growth of all bacteria, as several species are hyperthermophiles that thrive in temperatures in excess of 80℃. Studies at the Bent Hill Massive Sulphide site show that bacterial populations decrease by an order of magnitude from conditions suitable for mesophiles, through thermophiles and then hyperthermophiles. However, this site is influenced by hydrothermal processes, therefore allowing

large temperature gradients to dictate bacterial densities over very small depth changes.

If temperature gradients are small, other factors may dominate. Parkes et al. (2000) consider age and porosity as possible influences in areas of low hydrothermal activity, however, their discussion does not lead to conclusive results. The ability for bacteria to grow and move is related to the presence of an energy source, usually taking the form of degradable organic matter in shallow environments. As depth increases, this source becomes depleted and other means for growth are required, such as the reduction of chemical species.
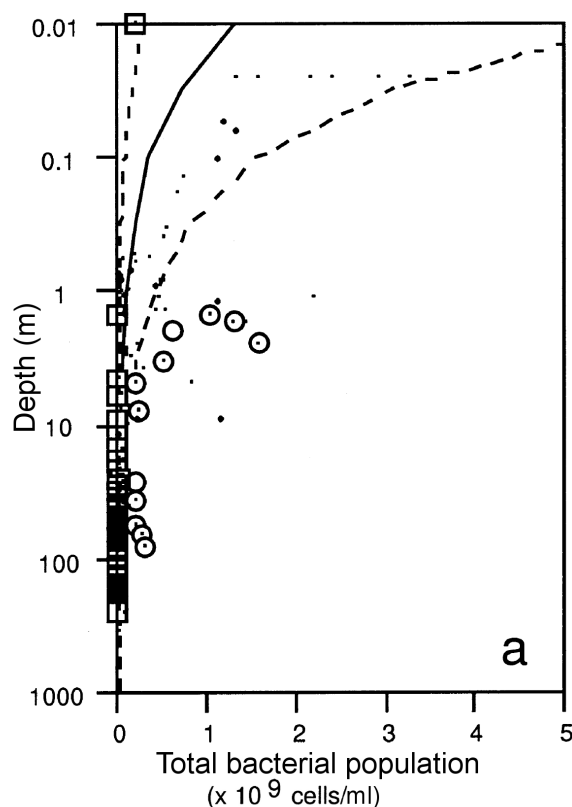
Fig. 4.3 Approximate population of bacteria in marine sediments, modified after Parkes et al. (2000).

4.5.2 Extracellular Polymeric Substances

Extracellular polymeric substances (EPS), otherwise known as extracellular polysaccharides are created by marine microorganisms such as bacteria and phytoplankton. Bhaskar and Bhosle (2005) review the importance EPS may play in the marine environment, following an increased awareness and interest in its presence from an industrial point of view. EPS may be found in many forms, ranging from biofilms and microbial mats (slime-like) to discrete particles (capsular) and free dissolved matter, which forms a component of dissolved organic matter (DOM).

74

Bacterial EPS generally contains high concentrations of uronic acid, which results in an overall negative charge. This promotes greater *"binding and adsorptive properties to the polymer"* (Bhaskar and Bhosle, 2005, p46). In shallow marine and tidal environments, EPS is suggested to assist binding of the sediment, and even when digested by invertebrate bottom feeders, the presence of EPS tends to increase the resistance of cells to destructive enzymes in the gut.

Within the water column, the presence of bacteria may influence the chance of clay platelets to produce 'bioflocculation', as suggested by Stumm and Morgan (1981) and Busch and Stumm (1968). Fast-sinking aggregates formed through the process of bioflocculation are also known as 'marine snow' after Alldredge and Silver (1988). Turley et al. (1995) propose that the formation of aggregates may either be through *"transparent exopolymer particles (TEP)"* (Turley et al., 1995, p180) or bacteria. The formation of TEPs are generally associated with sticky particulate polysaccharides generated by diatoms, which peak after a diatom bloom. Bacterial influences result in a polymer bridge produced by the bacteria exudates forming between particles, thus enhancing the aggregation of clay minerals on their way to the sea floor. In studies commenced in 1989 in the north eastern Atlantic, Turley et al. (1995) observed that the bacterial biomass was equivalent to that of the phytoplankton. Thus, large numbers of bacteria (up to 32×10^9 cells/m^2/d) are transported to the seabed. Heissenberger et al. (1996) undertook optical microscopy on marine snow, which highlighted their heterogeneity. The matrix consisted of mucilaginous material holding together bacteria, diatoms, organic debris and clay platelets. The following observations were made by Heissenberger et al. (1996):

- bacteria dominate in terms of numbers of organisms,
- eukaryotes are dominated by diatoms, and
- polymer bridges are created by the mucilaginous matrix, derived from algae and bacteria.

The use of TEM allowed the resolution of those bacteria that may substantially contribute to the polysaccharide matrix of marine snow. Heissenberger et al. (1996) suggest that that *"most marine bacteria are able to adapt their ability to produce exopolysaccharides depending on the availability of colonisable surfaces"* (Heissenberger et al., 1996, p305). Furthermore, Wrangstadh et al. (1986) observed that polysaccharide production leading to bacterial adhesion on surfaces may be induced by starvation. McCave (1984) also proposes that *"given the substantial bacterial populations of bottom sediments, binding by polymer bridging may be important in accounting for some of their cohesive properties"* (McCave, 1984, p48).

Studies on the resistance to fluid flow of sediments stabilised by eukaryotes, including benthic diatoms and other micro-algae, were undertaken by Scoffin (1970) and Neumann et al. (1970) and summarised by McCave (1984). Mats up to 10mm thick and capable of resisting flows of up to 1m/s were observed. The mats consisted of diatom-produced mucilage as

demonstrated by Holland et al. (1974). Furthermore, Robert and Gouleau (1977) suggested that this process enabled stabilisation of tidal flats and an increased rate of mud deposition. A similar process was observed by Frostick and Mccave (1979) in studying mobile epipelic algae (those that bond to sediment particles), which *"leave a trail of mucous in sediment"* (McCave, 1984, p44). Several other authors (e.g. Wigglesworth-Cooksey et al., 2001; Underwood et al., 2004; Brouwer et al., 2005) highlight the ability of diatoms to produce large amounts of EPS, predominantly in shallow marine and intertidal environments. These diatoms are able to bring about 'biogenic stabilisation' of sediment, however, the structure and volume of the EPS are found by Brouwer et al. (2005) to influence strongly the ability of diatomacious EPS to stabilise sediment. Wigglesworth-Cooksey et al. (2001) note that a complex interaction exists between EPS-producing bacteria and eukaryotes such as diatoms, and that the presence of particular species may promote or hinder the generation of EPS in laboratory experiments.

4.5.3 Bacterial Interaction with Clays at the Seafloor

Deflaun and Mayer (1983) investigated the development of bacterial polysaccharides on and within intertidal sediments, and used scanning electron microscopy (SEM) to observe samples. Sediment was collected and examined at weekly intervals, with results showing the initial generation of filaments followed by a fibrous webbing and finally the presence of continuous films. Clay particles were trapped or embedded by these films, but no bacteria were observed to be attached to the platelets themselves. This suggests that although the clay platelets provide a much increased surface area to mass ratio compared to larger grains, they are *"apparently too small or too smooth to provide micro-environments for bacterial attachment"* (Deflaun and Mayer, 1983, p877).

As stated previously, Ransom et al. (1997) considered that part of the organic matter within clay sediment could be associated with bacterial cells and their related muco-polysaccharide networks. Their research suggested that rather than the formation of films or coatings over grains, microbes tended to be localised in occurrence. This observation, combined with those stated in Section 4.4, leads to the conclusion that the complex relationship between sediment, organic matter and biology may *"increase sediment cohesion and decrease sediment matrix permeability"* (Ransom et al., 1997, p8). Mitchell and Santamarina (2005) note that bio-physical mechanisms (those that involve bacteria and non-organic clay particles) may produce agglomerate-like clusters bonded by organic mucous.

4.5.4 Motility and Mobility of Bacteria in Deep Sea Sediments

Rebata-Landa and Santamarina (2006) propose that a combination of geometric constraints and mechanical interactions may influence the level of bioactivity in marine sediments. The geometric constraints include the connectivity of the pore network and the size of pore throats.

They present collated data from their own experimental study, published work and *"analyses based on particle-level geometrical-mechanical models"* (Rebata-Landa and Santamarina, 2006, p2). Their conclusions suggest that, depending on the depth and pore size represented by the particle size d_{10}, three regions of 'bacterial fate' may be present: active and motile; trapped; and dead. These conclusions would suggest that the bacteria inhabiting the sediments of the current study (at depths between 0.001m and 1m, and in sediment of d_{10} less than $1\mu m$) will be trapped within pores. This thesis is concerned with sediments with water contents in excess of 150% (even to a depth of greater than 1.5m), which may allow bacteria to be active within the upper decimetres, permitting their presence to influence the sediment properties.

4.5.5 Conclusions for Bacterial Influences

This section has shown that bacteria and diatoms may influence the sediment properties, both during the sedimentation process and also post-sedimentation. These microorganisms produce glue-like excretions in the form of extracellular polysaccharides, which may strengthen the soil. It is not currently known whether this sediment strength increase is sufficient to generate strengths observed in clay crusts. Furthermore, it is not known what bacterial species are present in West African clays, and whether they are able to generate sufficiently large quantities of polysaccharides to influence the sediment properties.

4.5.6 Burrowing Invertebrates

The influence of burrowing invertebrates in marine sediments has been documented by numerous authors (e.g. Rhoads and Boyer, 1982; Aller, 1982; Meadows and Meadows, 1994; Murray et al., 2002). The main influence these organisms have on the sediment is through their daily feeding activities. By utilising the shallow marine sediments as their source of food, they gradually modify the sediment from 'unprocessed' to 'processed' material, thus imparting a biological structure on already naturally structured sediment.

4.5.7 Burrowing and Compaction

Analysis undertaken by several authors concerning the effects of burrowing invertebrate activities on shear strength are generally inconclusive. Trevor (1976, 1977, 1978) measured pressures of between 7kPa and 15kPa in actively burrowing polychaete worms (*Nereis diversicolor*, *Neanthes virens* and *Arenicola marina*) by attaching a pressure transducer directly to the worms. These pressures were found to be produced in a cyclic fashion, as the worm used a self-anchoring system to thrust its burrowing proboscis forwards into the sediment. Alexander (1983) noted that invertebrates jammed in their burrows could produce stresses of up to 40kPa on the surrounding sediment. Murray et al. (2002) stated that compaction of

the sediment surrounding burrowing worms would occur as some or all of the internal (worm) forces are transmitted to the sediment, usually in a direction perpendicular to the direction of propagation. This is substantiated by McCave (1988), who identified the ability of some invertebrates to exert up to 200kPa on the surrounding sediment, and suggested that their propagation directly beneath buried gravel and cobble sized rocks may represent a mechanism by which these rocks could be transported to shallower depths within the sediment.

Meadows et al. (2000) presented results on the effect of the oxygen minimum zone (OMZ) on bioturbation, sediment geochemistry and geotechnical properties of samples obtained off the Oman continental slope and abyssal plain in the Arabian Sea. Shear strengths measured with a Geonor fall-cone penetrometer remained close to zero from the sediment-water interface to approximately 0.05m depth. Strengths increased with depth, generally demonstrating larger increases in regions below the influence of burrowing invertebrates (located between 2cm and 10cm below the sediment-water interface). Shear strengths of up to 20kPa were measured at a depth of approximately 30cm, which was up to 15cm below significant numbers of invertebrate burrows.

Meadows et al. (1994) completed a detailed examination of invertebrate bioturbation in cores taken from the central Southern Pacific Ocean at ultra-deep water depths from 5,000m to 5,300m. It was demonstrated that a significant number of open burrows ranging in diameter from 0.5cm to 4.5cm were present to at least 0.4m depth. Burrows were found to be oriented both vertically and horizontally, with the most abundant being the smallest diameter burrows. Undrained shear strength was measured using a Geonor fall cone penetrometer at 0.05m intervals down-core. Results from these tests are shown in Figure 4.4, and show a rapid increase in the undrained shear strength in several test locations, with values of up to 12kPa at 0.4m depth. Variations in strength were attributed to the effects of bioturbation, whereas the increase in strength with depth was suggested by Meadows and Meadows (1994) to be the result of normal consolidation of the clay due to increasing vertical effective stress. However, it is evident from Figure 4.4 that the strength associated with a normally consolidated clay (based on γ'=2.5kN/m^3) is significantly lower than the measured strengths. Meadows and Meadows (1994) also identify 'peaks' in strength, particularly at depths of 20cm and 40cm of core CRGN 76 and 25cm depth in core CRGN 83. An investigation into the relationship between peaks in strength and the number of burrows observed was inconclusive. However, even when ignoring these peaks, the measured strength is at least three times greater than the predicted normally consolidated strength profile. The strengths measured by Meadows et al. (1994) appear to be similar to those in Figure 2.6, with an average strength profile indicating approximately 25kPa/m rise in strength. It is proposed by the author that bioturbation influences the general strength profile, not just the localised fluctuations. In the literature, the term 'bioturbation' is generally used to describe all activities associated with the move-

ment of burrowing invertebrates (and similar animals) through the sediment profile. This may therefore include the creation of burrows, mixing of different soil layers, modification of grain size through sorting and/or faecal pellet creation or the generation of pseudo-pellets during feeding without ingestion and excretion. This thesis, as will be presented in Chapter 6, uses bioturbation to specifically denote the formation of burrows and faecal pellets.
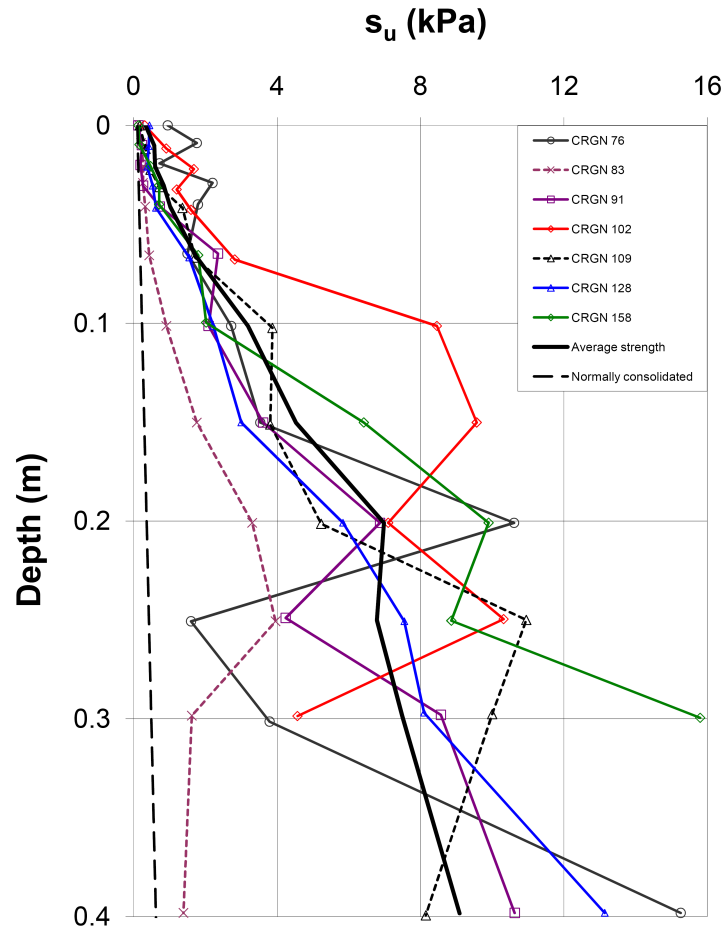
Fig. 4.4 Fall-cone tests undertaken by Meadows et al. (1994) showing crust strength in deep Pacific sediments. Also shown is an estimated normally consolidated strength profile.

Baltzer et al. (1994) present in situ cone penetration tests with pore pressure measurement (CPTU) data from the Nova Scotian Slope located on the eastern Canadian continental margin. Using a sit-on-bottom frame housing a geotechnical module with a 2m CPT, strength and induced pore pressure measurements were undertaken at seventeen locations along four transects. Sediments encountered comprised Holocene surficial clays, slumped sandy sediments of past debris flows and Pleistocene sediments of overconsolidated clays. Transect 'HMG 6'

(approximately 1200m in length) lies between 1400m and 1450m water depth and corresponds to Holocene deposits with no material removed by prior erosional events. Figure 4.5 shows undrained shear strength profiles interpreted from cone tip resistance values presented by Baltzer et al. (1994) of transect HGM 6, using a cone factor, N_k of 15. Strength values exhibit a dramatic strength increase to about 12kPa at 0.5m depth before reducing to 3.5kPa at 1.5m to 2.0m depth. These profiles are very similar to those encountered in the West African clays. Baltzer et al. (1994) suggest that the profiles broadly correspond to three sedimentary units: unconsolidated Holocene mud within the upper 0.1m to 0.25m; overconsolidated Holocene mud to about 1.5m containing many zoophycos-type burrows; and underlying sediments approximating a normally consolidated clay. Zoophycos-type burrows are usually found in the fossil record as horizontally to obliquely-oriented burrows, and are thought to be the result of multiple U-shaped burrows overlying each other (Martin, accessed 16 December 2010). It is not clear from the description provided by Baltzer et al. (1994) whether individual burrows produced the observed high strength, or whether the surrounding Holocene clay sediments were 'strengthened' by the presence of burrows.

Early investigations undertaken by Moore (1931a,b) suggest the presence of crust-like sediment strengths occurring in the Clyde Sea, Scotland. Moore (1931a) identified the presence of stiff to hard sediments at a depth of 20cm, which are comparable to the location of increased strength observed in the West African crusts. No explicit strength measurements were undertaken. In these same sediments, Moore (1931b) observed that up to 40% of the sample by dry mass, comprised faecal pellets. It was only suggested that the pellet's contribution to modification of the sediment properties was an increase in grain size and thus, porosity.

Grupe et al. (2001) identified sharp increases in sediment strength at between 0.1m and 0.15m depth within the Peru Basin whilst investigating the feasibility of manganese nodule mining. Strengths peaked at between 6kPa and 10kPa at 0.2m depth, as shown in Figure 4.6. Based on X-ray analysis of clay content, it was found that the sediments predominantly comprised smectites. Grupe et al. (2001) also observed that the different clay minerals (smectite, kaolin, illite and chlorite) were 'mixed' within the sediment profile and attributed this observation to the bioturbation of burrowing organisms.

4.5.8 Permeability and Porosity

Meadows and Tait (1989) measured increases in shear strength over a three day period for the invertebrates *Corophium volutator* and *Nereis diversicolor* using a Geonor fall-cone penetrometer. Single and mixed experiments were undertaken with the most significant results observed for *C. volutator*. Variance in sediment permeabilities due to population densities demonstrated conflicting trends. High numbers of *C. volutator* decreased sediment permeability, whereas high numbers of *N. diversicolor* increased permeability. Murray et al. (2002)
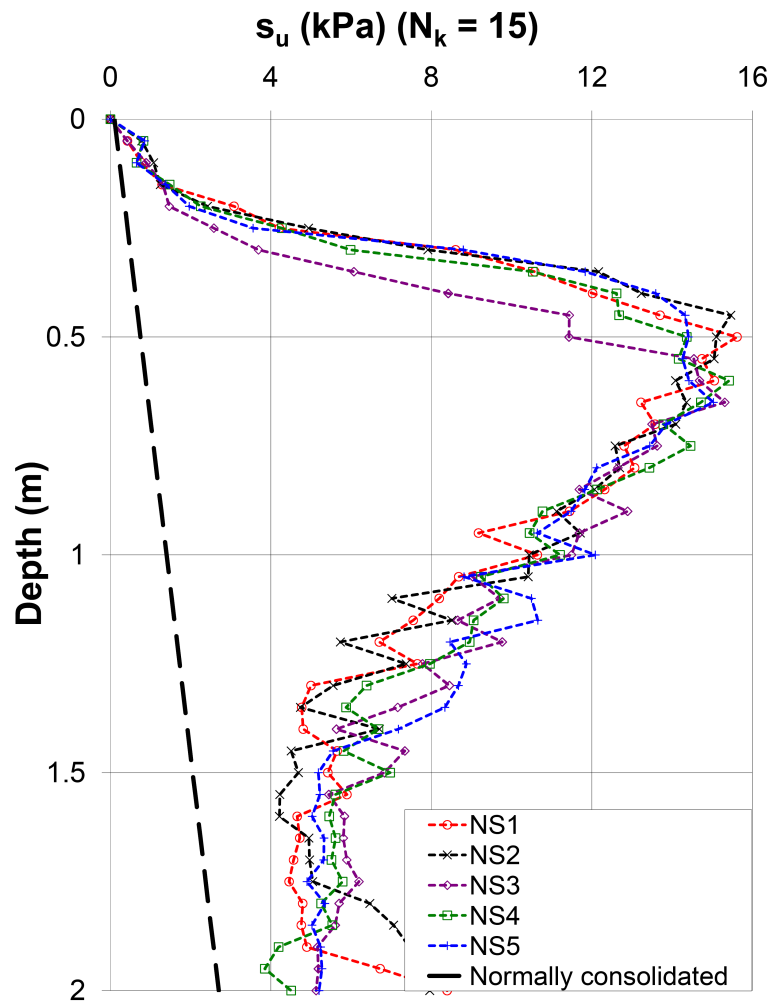
Fig. 4.5 Undrained shear strength profiles derived from cone resistance with N_k=15 by Baltzer et al. (1994), of Nova Scotian sediments showing crustal strength.

provides discussion on the results presented by Meadows and Tait (1989), suggesting that the presence of burrows increases the permeability, and hence accelerates pore water dissipation and shear strength development. They conclude that as the inverse effect is observed for *C. volutator*, 'soft-cementation' may play a role. It is not made clear, however, what soft-cementation is attributed to, nor how it is formed.

Jones and Jago (1993) assessed the modification of sediment properties by burrowing invertebrates species found in sandy sediments at intertidal locations on the coast of Wales (UK) using geophysical methods. Measurements of the acoustic shear-wave velocity and electrical resistivity were taken to assess the properties of the grain framework and pore-fluid matrix of the seabed sediment.
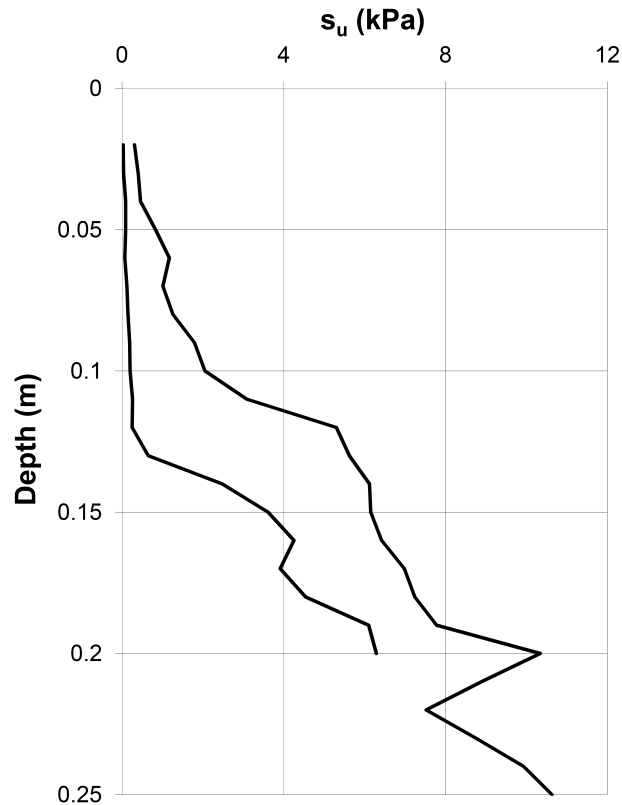
Fig. 4.6 Undrained shear strength profiles for sediments within the Peru Basin, modified after Grupe et al. (2001).

Acoustic shear-wave velocity was measured using piezo-electric ceramic 'bender' transducers acting as both the shear-wave source and the receiver after Shirley (1978). Electrical resistivity was used to determine the 'formation factor' (FF) which is a non-dimensional ratio of saturated sediment to the electrical resistivity of the pore fluid. This provides a direct measure of the structural properties of the pore fluid matrix (Jones and Jago, 1993). It was concluded that the acoustic shear-wave propagation through the bed was modified by the bio-turbation of the invertebrate species, and therefore the soil rigidity was also altered, depending on the burrow construction.

A significant reduction in the electrical formation factor due to changes in porosity and tortuosity was observed, leading to the conclusion that permeability should also be reduced. Changes in porosity and tortuosity were not only attributed to the burrow structure, but also to the remaining surrounding sediment which may be gap graded. Jones and Jago (1993) notes that no effect of burrowing on sediment porosity could be observed when using conventional porosity measurement tools, which may be due to the scale of measurement.

4.5.9 Influence on Particle Size

Rowden et al. (1998) observed an increase in mean particle size due to the "*aggregation of fine particles into faecal pellets*" (Rowden et al., 1998, p1354). This was determined by dry-sieving sediment before and after the introduction of burrowing invertebrates. These observations are similar to those made by Moore (1931b) in undertaking a measurement of the abundance of faecal pellets in Scottish sediments. Aller (1982) presents data demonstrating that the bioturbation influences of *Arenicola sp.* increase the average grain size at its preferred feeding depth of between 20 and 30 centimetres.

4.5.10 Influence on Geochemistry

The geochemical zonation of the deep seabed has been the subject of much research since the 1960s. Studies have attempted to understand the geochemical processes within marine sediments, in particular the early oxidation of organic material by sulfate (Froelich et al., 1979; Murray et al., 1978; Jahnke et al., 1982; Jahnke, 1985; Canfield, 1991; Hensen et al., 1997; Schulz and Zabel, 2006).

The role that invertebrate burrowing and 'bioirrigation' play in the modification of the geochemical profile of deep sea sediments has been considered by Fossing et al. (2000). They investigated sediments taken from two continental slope locations in the eastern South Atlantic, off the coast of Angola and Namibia, and within the influence of the Benguela Upwelling. Sulphate reduction rates (SRR) and the concentrations of dissolved sulphates and sulphides, pyrite, sulphur, total sulphur, methane and organic carbon were also presented. Clearly defined sulphate and methane zones were observed in these sediments, with the sulphate-methane transition zone (SMT) occurring between 4m and 6m depth. The SRR was modelled for both locations using a profile interpretation procedure (Berg et al., 1998). Within the SMT, the total SRRs were underestimated by up to 89%.

Fossing et al. (2000) therefore suggest that the presence of bioturbation in the form of open tubes of up to 8mm diameter to depths of 6m may allow bioirrigation of the sediment. This process would involve pore water in these tubes and burrows being exchanged with pore water in the surrounding sediment.

Aller (1982) demonstrated that burrowing invertebrates have a strong influence on the geochemical processes that occur within the upper metre of sediment. Bioirrigation, α_b, is a term used to describe the transport mechanism of burrowing invertebrates flushing their burrows. It is generally used to designate porewater movement in tubes or burrows caused by the pumping activity or movement of tube-dwelling animals (Boudreau, 1997), and can be defined as

$$\alpha_b = \frac{\text{SRR}_{\text{measured}} - \text{SRR}_{\text{diffusion only}}}{\varphi(C_0 - C)}, \tag{4.1}$$

where C is the pore water solute concentration, C_0 is the sediment water solute concentration and φ is the porosity. Boudreau (1984) suggested that α_b may be considered to exhibit units of 'fraction exchanged per unit time', and after undertaking a review of data from recent studies, Boudreau (1997) determined that it could range from 300 to 0 per year with increasing water depth. Based on measurements of SRR, C and C_0, Fossing et al. (2000) calculated α_b values of between 0.1 and 0.3, decreasing to 0 between 2m and 3m depth.

By the process of bioirrigation, Aller (1982) suggests burrows of greater than 0.6m depth may be open to the seafloor and so allow circulation of chemical species through the mucous-lined walls as the animal 'pumps' fluid while feeding at the bottom of its burrow. Furthermore, the depth to the anoxic zone may be greatly increased through such burrows, therefore permitting anaerobic bacterial influences to depths greater than otherwise expected.

4.5.11 Destabilisation of Shallow Marine Sediment

In contrast to the studies indicating increased strength, Rhoads et al. (1978) suggested that the presence of deposit feeding organisms destabilise cohesive sediments by increasing the water content and modifying the particle size composition. They suggest that higher water contents were achieved by high bioturbation rates and the feeding processes of invertebrates. Underwood and Paterson (1993) investigated the recovery time of intertidal benthic diatoms after a period of biocide and commented on the associated influence on burrowing invertebrates. Using formaldehyde to remove the influence of biological activity, Underwood and Paterson (1993) suggested that an increase in compaction of the sediment and hence sediment stability was achieved over several weeks. It was therefore inferred that the presence of burrowing invertebrates tended to destabilise the sediment by preventing consolidation. Rowden et al. (1998) suggest the process of sediment pelletisation produces a more open fabric and alters the bulk sediment properties by increasing the water content and reducing the S-wave velocity.

4.5.12 Summary on Burrowing Invertebrates

This section has considered the literature referring to the interaction of burrowing invertebrates with the marine sediment. In most of the studies, enhancement of the undrained shear strength has been noted, whether directly or indirectly, and even if only by a few kilopascals. Research undertaken by Rhoads et al. (1978) and Underwood and Paterson (1993), however, suggest results to the contrary. By the processes of bioirrigation and bio-pumping, it has also been suggested that invertebrates may influence the geochemical gradients in sediment surrounding their mucous-lined burrows. This interaction may, as suggested by Aller (1982), also impact

on the depth at which anaerobic bacteria are active.

Though these authors have considered the influence of burrowing invertebrates on shear strength, this has been undertaken from a zoological and biological perspective. More in-depth work and analysis is required in this area from a geotechnical point of view before conclusions can be made that are relevant to the offshore oil and gas industry. Table 4.1 summarises the possible influences of burrowing invertebrates on sediment properties based on the current literature.

Table 4.1 Summary of influence of burrowing invertebrates on sediment properties.

Burrows	change in permeability
	compaction of surrounding sediment
	sorting of particle sizes
	increased geochemical processes
	increased shear strength
	decreased shear strength
Faecal pellets	increase in global grain size
	reduction in stiffness
	increase in water content
	production of more-open fabric

4.6 Summary

Chapter 4 begins by presenting possible hypotheses for the crust's origin, followed by a review of background literature and evidence from the current investigation relating to these hypotheses. The following conclusions have been made. Though Bennett et al. (1991) suggest 'crusts' may be generated by slope failures, it is unlikely that such events have occurred in the geological timeframe associated with the deposition of sediments off the West coast of Africa. Further investigation into the hypothesis of geological unloading due to submarine slope failures is therefore excluded from this thesis. The West African clay samples do not exhibit thin sandy layers at the location of peak strength, and therefore, this hypothesis is also excluded from further investigation. Cementation of clayey sediments by the precipitation of manganese and ferrous elements may play a part in crustal strength in these sediments. Micro-nodules or precipitation within open porespaces may be possible, though based on observations made while testing samples in Chapter 3, it is unlikely that these exist. This hypothesis is considered further in Chapter 6 through the use of scanning electron microscopy on natural and washed samples.

Organic carbon has been shown to have an influence on the geotechnical properties of soil (Pusch, 1973; Busch and Keller, 1981; Ransom et al., 1997), however the significance of

this influence is yet to be quantified in laboratory experiments. Based on organic carbon measurements undertaken by Thomas et al. (2005) and Puech et al. (2010), it is unlikely that organic carbon will influence the sediment strength. Within the Peru Margin where it is hypothesised that organic carbon influences the strength, sediments that contain up to 20% organic carbon exhibit lower strengths than sediments that contain 5%, which is a value comparable to West African clays. It is therefore considered an unlikely source of crustal strength and will not be researched further in this thesis.

Based on the literature considering bacterial influences in marine sediments, it is concluded that bacteria may have a strengthening effect on clays. This is likely to be in the form of binding by extracellular polysaccharides. Due to their high population and relative ease of motion through the open fabric of the West African clays (aided by the presence of open invertebrate burrows), bacteria may be able to influence the matrix sediment strength. The thesis will therefore attempt to investigate the influence of bacteria on the mechanical properties of West African clays. It is suggested that the matrix in the hypothetical agglomerate-matrix model proposed in Chapter 3 may be created by a web of polysaccharide-bound clay particles.

Based on the current literature, limited scientific research has been undertaken on deep-sea sediment properties. However, several authors have considered the effects of burrowing invertebrates on shallow sediments, both in shallow and deep marine environments. In some studies, the strengthening effect of burrowing invertebrates on undrained shear strength has been affirmed, while in others it has been questioned. The mechanisms which enhance or disrupt the development of undrained shear strength remain unclear, and this therefore provides an impetus for the hypothesis of the effect of burrowing invertebrates on mechanical soil properties to be considered in this thesis. What the literature does indicate is that, like bacteria, burrowing invertebrates are extremely active in all marine environments and their modification of the sediment through burrowing and feeding has not previously been considered by geotechnical engineers.

4.6.1 Conclusions

The biological processes described in this chapter predominantly occur within a few decimetres of the seabed, and therefore represent viable avenues for further research into the formation and demise of the crust. The remainder of this thesis will take the opportunity to consider the interdisciplinary nature of the problem by incorporating aspects of microbiology, zoology, geology and geomechanics to provide a holistic explanation for the origins and subsequent behaviour of crust material under hot-oil pipeline stresses. The following chapter will consider the hypothesis of bacterial activity in deep sea sediments and their influence on sediment strength. Chapter 6 will consider evidence for burrowing invertebrates in West African clays and the possible role they play in crust formation.

Chapter 5

Bacteria

The literature review in Chapter 4 highlights the abundance of bacteria in marine sediments. The direct influence of bacteria on sediment strength in deep waters is currently poorly understood and no attempts at measuring the strength variation of inoculated samples have yet been made. No current literature considers the bacteria species present in West African crusts, nor if their presence can account for the measured crust strength. This chapter therefore describes the procedure used to discover and identify bacteria species in core samples of West African crusts. The results of an investigation into the identified bacterium's ability to alter sediment strength is then presented. This is undertaken using the Cam-shear device to measure the strength of sterile and inoculated samples. The results of these tests allow conclusions to be formed on whether the bacterium contributes to the presence of the crust. Soil-pipeline interface shear test results are also presented to provide discussion on the bacterium's influence on interface shear behaviour. Hot-oil pipelines are laid on and within the observed crust and are therefore located within sediment containing an abundance of bacteria. The conclusions made from this investigation will therefore be of importance to the design of future hot-oil pipelines installed into these sediments.

5.1   Samples and Materials

Experimental work was undertaken using samples from several stages of offshore investigation including:

- undisturbed box core and STACOR samples taken in August 2008 by Fugro on behalf of BP Exploration; and
- remoulded and reconstituted bulk samples obtained from the Norwegian Geotechnical Institute (NGI), collected between 2000 and 2003.

Bulk reconstituted samples were stored in large tanks located in an open shed, and exposed to varying external temperatures. Box core and STACOR samples were stored vertically and

87

refrigerated at between 4℃ and 12℃.

5.2 Evidence for Bacteria in Samples

Due to their size (about 1μm in length), observing bacteria in soil samples is difficult. An environmental scanning electron microscope was used to image samples taken from cores and bulk samples to identify the presence of 'intact' bacteria. No direct observation of bacteria was forthcoming in the samples imaged, which was not entirely unexpected due to the age of the samples. Furthermore, when the samples were obtained from the ocean floor a microbiological investigation into their origins had not been planned, and thus the cores had not been stored with the interests of preserving their biological content in mind. To undertake an investigation into confirming the presence of bacteria in these sediments, microbiological methods to extract bacteria DNA remaining in the sediments were therefore implemented. Though bacteria expire when removed from their required environmental growth conditions, their partially degraded DNA may remain in the sediment for decades. By targeting the DNA, it is possible to identify the species of bacteria present in the sediment.

5.3 Aims and Procedures

The aim of this section of the thesis is to discuss and apply well established microbiological techniques to isolate and identify culturable deep ocean marine bacteria in crust samples. In summary, the procedures used to achieve this aim are:

- extraction of DNA from crust samples;
- identification of potential bacteria for purchase and laboratory growth;
- trialling of preferred growth conditions including temperature and growth media;
- development of a methodology for inoculating sterile clay samples; and
- undertaking of geotechnical testing on sterile and inoculated samples.

5.4 DNA Extraction

The process of DNA extraction relies on sufficient amounts of the required DNA remaining in the sediments. Given that marine sediments have been subject to many generations of the food chain within the water column and at the bottom of the ocean, DNA from a large number of biological origins will be present. Extraction is therefore required to target DNA specific to bacteria. Crust samples were remoulded in a beaker at a water content of 220% prior to extraction of DNA using direct lysis of bacterial cells. The process of cell lysis involves the breaking down of bacterial cell walls by physical means such as bead beating. Boivin-Jahns et al. (1996) undertook DNA extraction from deep clay samples and showed that this method

significantly improved the DNA recovery compared to the method of removing bacterial cells from the soil samples prior to DNA extraction. Bead beating involves placing approximately 3ml of remoulded sample into a test tube and adding 2mm-diameter ball bearings. The test tube is then given five to ten pulses using a bench-top test-tube vibrator. This physically breaks down the cell walls.

Two extraction kits were trialled in the current investigation: a QIAamp Stool Mini Kit and a ZR Soil Microbe DNA Kit™to compare the effectiveness of DNA extraction. Procedures stated in the kit handbooks were followed, resulting in DNA suitable for the polymerase chain reaction (PCR). The QIAamp protocol optimises the non-human DNA in stool samples, which are of similar consistency to the remoulded soil samples. The ZR kit is able to "*successfully isolate DNA from cultured bacteria, fungi, and yeast*" (Zymo, 2007, p3) by using a 'bead beating' process.

5.5 PCR Set-up and Running of Gels

Once the DNA was extracted, polymerase chain reactions (PCRs) were set up to amplify the DNA. The PCR process theoretically amplifies the existing DNA by an over 10^9-fold increase (Howe, 2007) using a simple, direct enzymatic process. The process involves cyclically heating and cooling a reaction mixture containing the extracted DNA, primers and chemicals for synthesising the DNA, as shown in Figure 5.1. This process promotes the melting and annealing of DNA strands to generate a complementary strand of each existing DNA strand. The repetitive process of temperature cycling allows the PCR to be largely automated and the individual temperatures may be programmed into commercially available thermal cyclers or PCR machines (Howe, 2007). As no PCR programs were available in the literature for these particular sediments, programs that had given positive results for 16S RNA primers and bacteria samples following Howe (2007) were trialled in this thesis.

The PCR set-up was completed in a perspex set-up box to limit environmental contamination. The set-up box contains a built-in UV irradiation light to degrade unwanted DNA by 'nicking'. A 'nick' is a "*break in the sugar-phosphate backbone of a double-stranded DNA molecule*" (Howe, 2007, p14) that permits the rapid degradation of DNA.

The design of primers requires prior knowledge or at least an educated guess of the 'start' and 'end' of the DNA sequence to be amplified. These small sections of DNA, which are included in the PCR reaction mix, may be manufactured to be specific or general, depending on the target DNA sequence. Two 16S RNA primer sets; P1+P2 and P3+P4 were used in this thesis as shown in Table 5.1. These are paired as forward (f) and reverse (r) sequences and are of two different base-pair lengths (A-T, C-G etc.): 190bp for P1+P2; and 120bp for P3+P4. These were chosen to be general primers to maximise the number of bacterial DNA
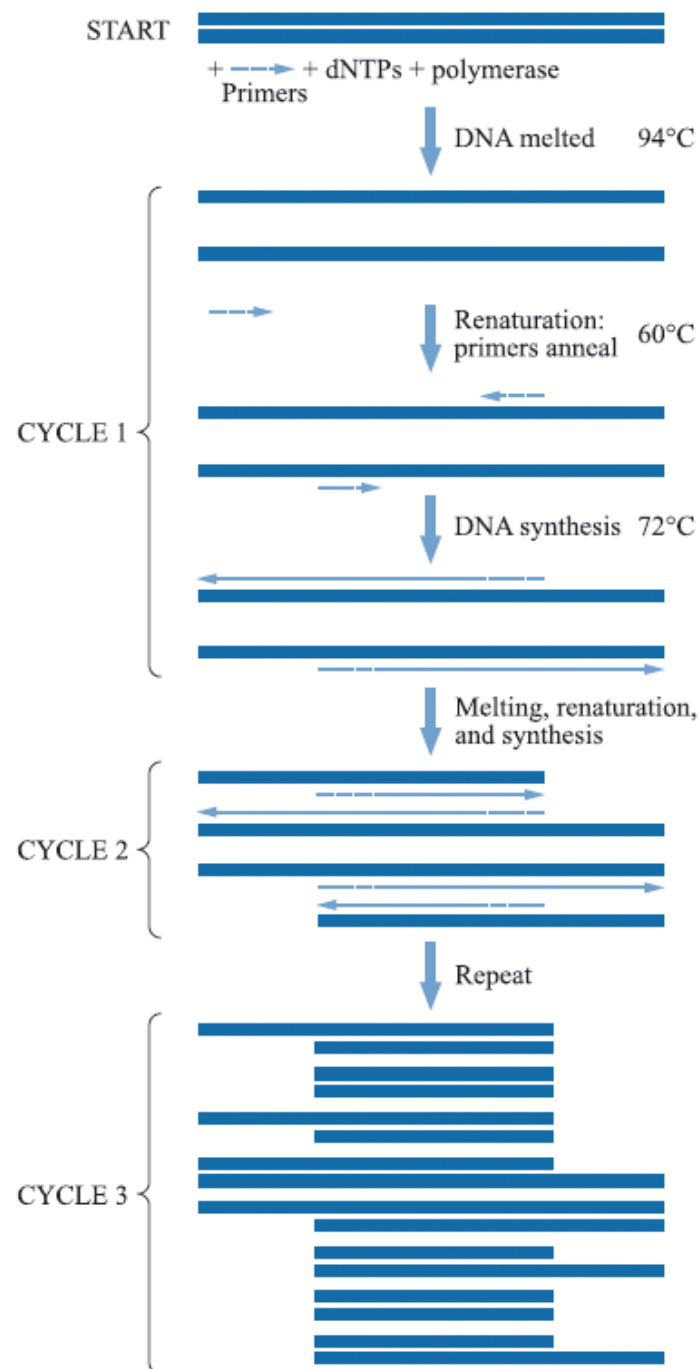
Fig. 5.1 Schematic diagram illustrating the PCR process with three cycles. Denoted temperatures may be modified for specific reaction mixes. Modified after Howe (2007).

amplified. A drawback of this is the increased likelihood of also amplifying contaminants. The PCR mix also contains proteins; buffers, including $MgCl_2$ to control the salinity; a Taq polymerase (DNA polymerase of the bacterium *Thermus aquaticus*, which is required for the extension step to add dNTPs) that is heat stable; and deoxynucleoside triphosphates (dNTPs) that provide a base ('building blocks') for the primers to bind to in the annealing step of the process, and enable synthesising of the DNA sequence.

Table 5.1 Primers used for bacteria DNA

Name	Target	Primer sequence
16S P1f	All prokaryotes	GTGCCAGCAGCCGCGGTAATAC
16S P2r	All prokaryotes	TCTACGCATTTCACCGCTACAC
16S P3f	All prokaryotes	CTTGTACACACCGCCCGTCACACCATC
16S P4r	All prokaryotes	TACCTTGTTACGACTTCACCCCA

Initial PCR conditions, based on the requirements of the chosen primers were:

1. 95℃ for 5 minutes
2. 30 cycles of 95℃ for 1 minute; 53℃ for 1 minute; 72℃ for 1 minute
3. 72℃ for 15 minutes
4. hold at 4℃

Once the PCR process is complete, the generated reaction products are analysed by gel electrophoresis to provide:

- a visible check on the presence of any contamination, and
- a check that the PCR was successful in annealing the primers to the DNA.

The distance that a given PCR product travels through the gel is proportional to its molecular weight, and can be compared with a given DNA ladder of known sizes to determine the length in base pairs that it represents. The gel is prepared by adding agarose to the buffer tris-acetate EDTA (TAE) at a concentration of between 2% and 2.5% in a conical flask. The solution is heated until all agarose has dissolved, and is then left to partially cool. Ethidium bromide at a concentration of $3\mu L$ in 120ml solution is added to the cooled solution to promote fluorescence of the DNA, which is visible as orange bands under UV light. The solution is then poured into a gel mould containing a plastic comb which that 'wells', into which the PCR product is pipetted. A loading buffer is mixed with the solution to increase its density, causing it to sink to the bottom of the well during pipetting.

5.5.1 Contamination Controls

The most likely source of contamination is the water used during the PCR set-up. This may be observed as duplicate bands, or bands in the negative controls when viewed under UV light.

To provide negative controls and check that the DNA extraction process and PCR set-up had captured the 'right' DNA, environmental; DNA-extraction; and water blanks were included in the PCR amplification process. Extraction blanks were created by leaving 1.5ml tubes open on the bench where DNA extractions were done, and environmental blanks were created where the PCR set-up was completed.

5.5.2   Results from PCR and Gels

The analysis of initial PCR reactions demonstrated the presence of contaminants within the water blanks, and no amplification of the bacterial DNA (no visible bands). This result suggested that contaminants had entered the reaction mix either during the extraction of DNA from the samples or during the PCR set up processes. A lack of bands may due to the use of expired Taq; primers that have not annealed correctly to the DNA; an incorrect choice of primers; an incorrect $MgCl_2$ concentration; and/or the addition of an excessive amount of DNA product. As both contamination and no amplification were present, and as contamination could be the cause of both results, this was investigated first.

A common source of contamination is the reaction water, and therefore the second PCR set up was run using purified water from a different source, placed in a glass vial and irradiated under UV light. Controls were also run to test the effectiveness of the primers.

Results from the second PCR still demonstrated strong amplification of contaminants and also suggested that the primers were not working as none of the primer controls showed bands. It was decided that fresh dH_2O, this time irradiated in plastic vials, and new dNTPs, BSA and Taq should be used to investigate if any of these components were the source of the primers not working or failure of the PCR reaction. To help limit the amount of environmental contamination, the PCR set up was also carried out in a perspex set-up box. All equipment was irradiated within the box for 15 minutes then turned over and re-irradiated for another 15 minutes prior to use. The results from this third set up showed clear bands for DNA samples at 120bp and 190bp, as seen in Figure 5.2. No contamination is present. This result indicated that the source of contamination was likely to be the dH_2O. Though the previous set up used water which had been irradiated, it was realised that UV light cannot penetrate through glass, thus the water in that particular reaction mix may still have been contaminated. The results of the negative controls indicated that no environmental contamination had occurred during the DNA extraction process or the PCR set up.

5.6   Cloning and Sequencing

As a PCR product free from contamination was visible under UV light, it was therefore possible to run a PCR 'clean-up' and then undertake direct-sequencing of the cleaned PCR product
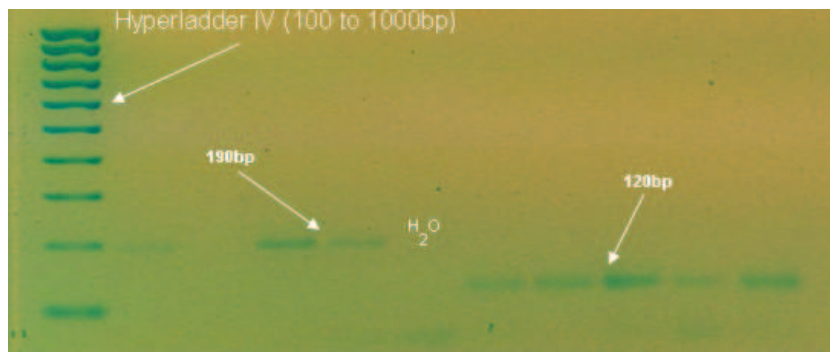
Fig. 5.2 Contamination-free gel showing clear bands of 120bp and 190bp for P3+P4 and P1+P2 primers, respectively.

using a Qiagen QIAquick PCR purification kit. This kit removes unincorporated primers and excess dNTPs from the product. Four cleaned PCR product were direct-sequenced in this thesis following this procedure. If general primers are used, direct sequencing can often return 'failed' results due to multiple amplified DNA with different sequences. As general primers were used in the PCR, the results of direct sequencing did indeed produce 'failed' results, an example of which is shown in Figure 5.3. DNA cloning was therefore used to separate the different PCR products and obtain sequences from each. An explanation follows of the cloning process that was used.
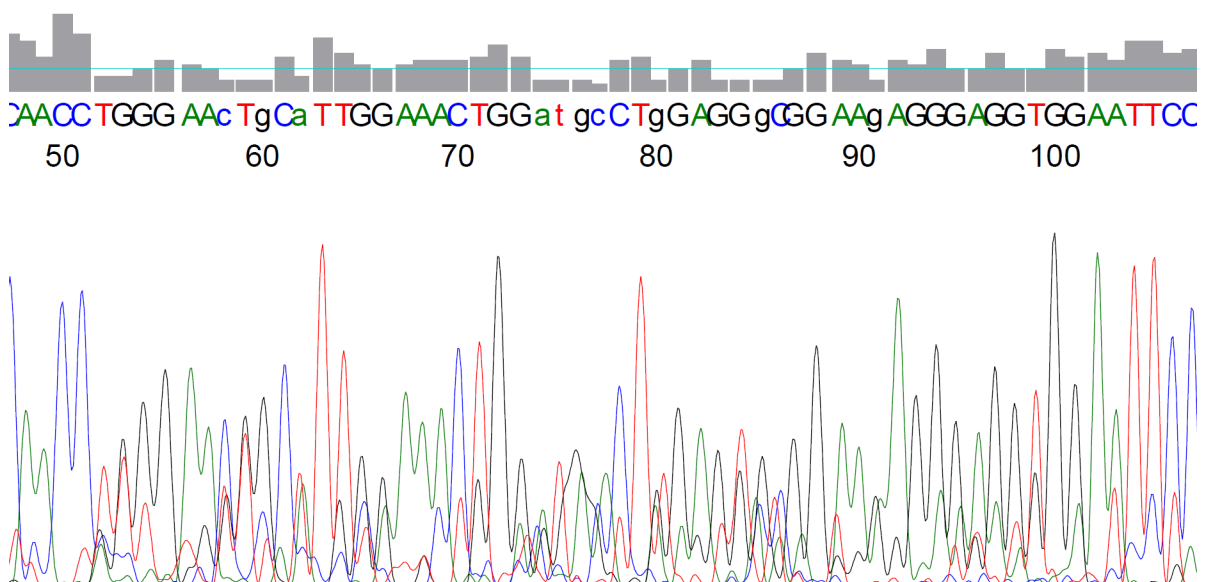
Fig. 5.3 Sequencing result for failed sample Q2P1 when viewed using FinchTV. Note significant overlapping of different sequences.

The PCR product of several reaction results were ligased into the PCR cloning vector pGEM-T Easy Vector kit (Promega) which is ampicillin resistant, and incubated overnight at 4℃. DNA ligation is the process of joining linear DNA fragments together with covalent

bonds, thus creating a phosphodiester bond between the 3′ hydroxyl of one nucleotide and the 5′ phosphate of another. This is represented in Figure 5.4. The ligation reaction was then added to *E.coli* JM109 competent cells, heat-shocked, chilled and incubated at 37℃ for 1.5 hours. The transformed culture was then plated onto Luria Broth (LB) plates containing ampicillin (0.2%), IPTG (0.05%) and Xgal (0.16%) in a sterile laminar flow cabinet (see Appendix C for LB recipe). The plates were incubated overnight at 37℃. If the ligation and transformation is successful, individual blue and white colonies will be present on the plates. White colonies represent those that contain the PCR inserts (those that were resistant to ampicillin due to the ligation with the cloning vector), and are picked off and placed onto master plates. Over time, however most colonies will turn blue (see Figure 5.5).
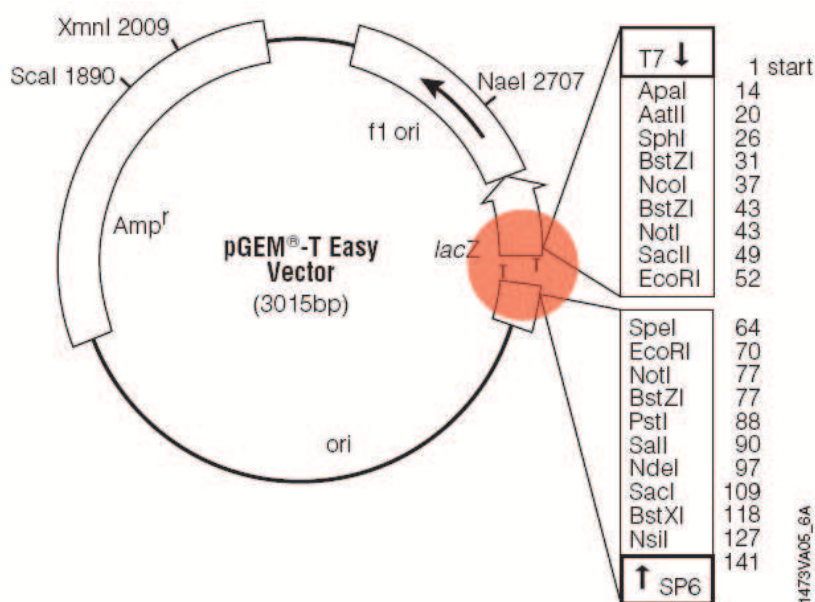
Fig. 5.4 Schematic diagram of the pGEM-T Easy Vector map and sequence reference points. Cloned inserts attach at T-T, circled in red.

To allow sequencing of the transformant colonies, sterile 50ml Falcon tubes containing 10ml LB and ampicillin (0.1%) were made-up. Colonies of interest were touched using a sterile toothpick and dropped into the Falcon tube containing liquid culture, and grown overnight in a shaking incubator at 37℃ and 150rpm. The liquid cultures were then centrifuged to obtain plasmid DNA, which was then recovered and 'cleaned' using a Qiagen Miniprep kit.

Thirty four cloned and cleaned products were sent to a commercial sequencing company, 'Geneservice', with all but four returning positive results. Results comprise a sequence read as A, T, C or G, with the inserted primers attached at the start and end of the length.

94
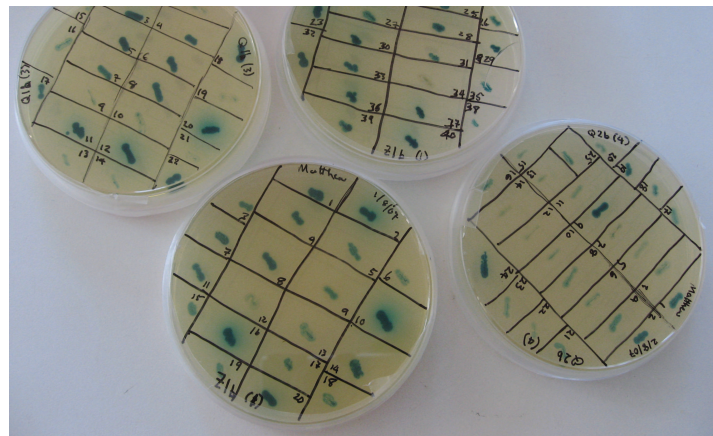
Fig. 5.5 Colonies (originally white) of bacteria on master plate.

5.6.1 Bacterial Sequencing Results

The results of cloned sequences received back from the sequencing service were viewed using a commercially available DNA sequence viewer, 'FinchTV'. FinchTV creates chromatograms of sequences and allows checking and editing of sequences, if necessary. The results were either 120 or 190 base pairs in length due to the two primer sets used, with one example of sample Q2al shown in Table 5.2 and in Figure 5.6, identifying the P3f and P4r primers and cloned insert.

Table 5.2 Sequencing result for Q2a1 showing locations of primers P3f (red) and P4r (blue), and cloned insert (black).

Basepair	Cloned Sequence
1	CTTGTACACA CTTGTACACA CACCATGGGA GTGGATTGCA
41	CCAGAAGTAG TTAGTCTAAC CTTCGGGAGG ACGATTACCA
81	CGGTGTGGTT CATGACTGGG GTGAAGTCGT AACAAGGTA
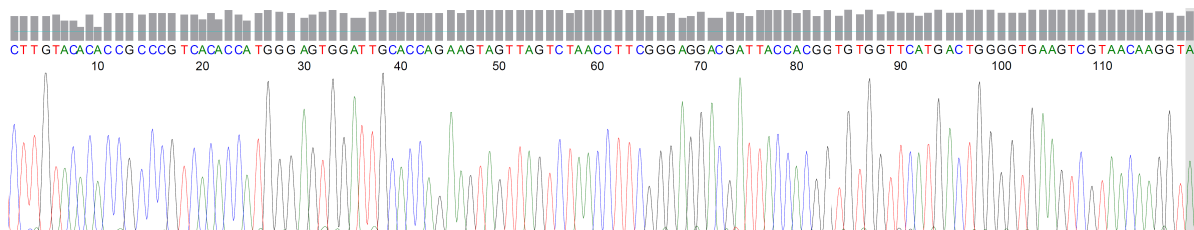
Fig. 5.6 Sequencing result for sample Q2a1 when viewed using FinchTV.

Sequences can be compared against an online database provided by the National Centre for Biotechnology Information, which is termed a 'nucleotide blast'. This contains the se-

quencing results of known and unknown bacterial genes, and provides information on whether a complete gene sequence is available. The database provides positive matches in decreasing probability, depending on the number of matching base pairs, an example of which is shown in Table 5.3. A longer matching sequence will suggest a 'more positive' match. The difficulty however, in amplifying and sequencing bacterial DNA from marine sediments is the likelihood of encountering new, uncultured species. Uncultured bacteria cannot be ordered from a culture collection and therefore cannot be grown in the laboratory. Out of the 34 results, 20 returned an uncultured bacterial sequence. The remaining 10 sequences matched bacteria of varying origins; three of which, suggested the presence of the *Marinobacter* species.

Table 5.3 Results from a nucleotide 'blast' of samples Q2a1 showing the strong match to *M. aquaeolei*.

Accession	Description	Max score	Total score	Query coverage
EF659426.1	Uncultured bacterium clone N2-A1 16S ribosomal RNA gene, partial sequence	215	215	100%
DQ768638.1	*Marinobacter hydrocarbonoclasticus* isolate MARC4F 16S ribosomal RNA gene, partial sequence	215	215	100%
CP000514.1	*Marinobacter aquaeolei* VT8, complete genome	215	647	100%
AB176073.1	Uncultured bacterium gene for 16S rRNA, partial sequence, clone: SSmCB10-15	215	215	100%
AB176042.1	Uncultured bacterium gene for 16S rRNA, partial sequence, clone: SSmNB04-69	215	215	100%
AB175989.1	Uncultured bacterium gene for 16S rRNA, partial sequence, clone: SSmNB04-14	215	215	100%
DQ282120.1	*Marinobacter bacchus* strain FB3 16S ribosomal RNA gene, partial sequence	215	215	100%

Of the bacteria identified, only *Marinobacter* sp. represented a viable option based on its growth characteristics, occurrence in marine waters and availability as a culturable bacterium in laboratory conditions. It was therefore decided that this bacteria would be incorporated in laboratory work to provide an understanding of how to best cultivate and utilise it in experiments. The successful extraction of bacteria DNA and the identification of a culturable bacterium from sediment was unlikely given the quality of samples and the low number of culturable marine bacteria available for laboratory growth.

5.6.2   Purchase and Use of *M. aquaeolei*

Marinobacter aquaeolei was purchased as a freeze-dried sample from the The National Collection of Industrial, Food and Marine Bacteria. The bacterium sample was revived following the provided procedures (see Appendix D) and placed in prepared sea water agar following the recipe given in Appendix E. Three conical flasks of approximately 25ml were incubated overnight at the optimum growth temperature of 30℃. The cultures were checked visually after approximately 20 hours, and it was observed that growth had been successful. The cultures were then sub-cultured twice by:

1. autoclaving new 25ml aliquots of sea water media in conical flasks, plugged with cotton wool;

2. pipetting 1ml of liquid culture containing grown bacteria into new autoclaved flasks under aseptic conditions;

3. incubating overnight at 30℃; and

4. repeating the process.

The newly subcultured bacteria were then plated on a petri dish containing a media of sea water agar for medium-term storage and refrigerated at 4℃. This temperature significantly retards the growth of bacteria. To confirm that the correct bacterium had been grown, a PCR set up was completed using a reaction mix to allow sufficient PCR reaction mix for running a gel and to allow sequencing, following the description given in Sections 5.5 and 5.6. Three samples of different bacterial concentrations and two positive controls were prepared using the following procedure:

1. a sterile toothpick was used to pick off bacteria from a previously prepared plate and placed into the PCR reaction mix;

2. another sterile toothpick was used to add bacteria to 100μm of sterile water and mixed thoroughly. 1.7μL was then pipetted into the second reaction mix;

3. a 1:9 dilution of the second mini-prep bacteria sample was made and added to the third reaction mix;

4. a positive control of *M. aquaeolei* (Q2a1) was determined from the cloned sequence results. 1.7μL of the recovered bacteria and plasmid DNA for this sequenced sample was added to the fourth tube; and

5. 1.7μL of a 1:10 dilution of the positive control in tube 4 was added to tube 5.

Sequencing results confirmed that *M. aquaeolei* had been cultured in the laboratory samples.

5.6.3 *Marinobacter* sp.

Marinobacter sp. currently comprises 18 different species, that have been identified in waters off Japan, Vietnam and Korea, as well as two varieties found near the Kerguelen islands (subantartic conditions) and in the Red Sea. *M. aquaeolei*, shown in Figure 5.7, is a moderately halophilic and mesophilic bacteria and was originally isolated from the "*head of an oil-producing well on the offshore oil/gas platform*" (Huu et al., 1999, p367) off the coast of Vietnam. The bacterium is rod-shaped, between 0.4μm to 0.5μm in width and 1.4μm to 1.6μm in length. Huu et al. (1999) observed growth between 13 and 50℃, and at pH levels between 5 and 10. Optimal growth occurred at 30℃ and a pH of 7.3. Like many other marine isolates, *M. aquaeolei* appears to have the "*ability to grow over a range of salinities as well as to utilise a variety of substrates*" (Huu et al., 1999, p372). The cells are "*actively motile by the presence of a single, frequently polar flagellum*", and are "*characteristically found growing singly or in pairs*" (Huu et al., 1999, p369).
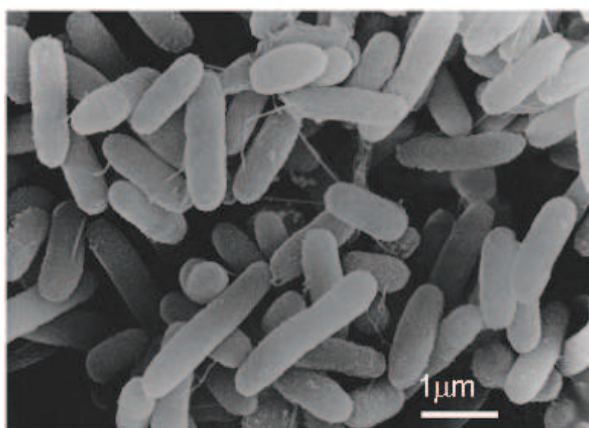
Fig. 5.7 *Marinobacter Aquaeolei* (after Huu et al., 1999).

5.6.4 Other Bacteria in Samples

It is highly likely that other culturable bacteria apart from *M. aquaeolei* are present in the sediments from the west coast of Africa. However, based on the available samples, and in their conditions, it is not unexpected that only one culturable bacteria was identified. This thesis solely considers the influence of *M. aquaeolei* on the sediment, though the techniques and procedures developed herein may be used for future investigations of other core samples.

Although controls on environmental contamination during the extraction and preparation of DNA for PCR were completed, contamination of samples themselves during collection and while on-ship may have occurred.

5.6.5   Conclusions

This section has detailed the successful identification of the culturable bacterium *M. aquaeolei* in sediments obtained from 1,400m water depth off the coast of West Africa. This result demonstrates that even after successive reconstitution and remoulding of sediment, DNA from bacteria are still present and amplifiable using the PCR process. *M. aquaeolei* has been purchased and successfully grown in the laboratory, therefore allowing the progression of geotechnical testing of samples inoculated with this bacterium.

Future core samples that are obtained from offshore site investigations may utilise the same methods and protocols used in this phase of research with confidence of producing a positive result.

5.7   Testing of Samples Inoculated with *M. aquaeolei*

5.7.1   Introduction

To provide a quantitative assessment on the influence of *M. aquaeolei* on the undrained shear strength of West African clays, a reliable and repeatable method of shear measurement was required. Two possible methods of sample preparation were considered: large, 0.3m diameter, 0.4m long samples with shear strength measurement undertaken using a mini-ball penetrometer, or small, 0.075m diameter, 0.04m high samples for use with the Cam-shear apparatus. Large diameter samples would require significant volumes of inoculated samples, and large consolidation periods prior to testing. Controlling the environmental conditions by preventing contamination of samples from external sources would also be difficult. The Cam-shear device was therefore chosen for these investigations as it allowed both soil-soil and soil-interface measurements under small vertical effective stresses and promised conclusions relevant to pipeline design. The Cam-shear device also allowed ease of cleaning between tests, thus allowing a controlled and contamination-free testing environment.

If this bacterium was the origin of the crustal strength, normally consolidated inoculated samples would produce strengths of between 10kPa and 15kPa, and exhibit significantly higher strength than sterile samples. This phase of testing therefore considered an initial set of tests on sterile and inoculated samples to determine the influence of this bacterium. If it was observed that crustal strength was achieved, additional tests would be undertaken to further investigate the mechanism of strength increase. If, however, the initial tests demonstrated that bacteria were unlikely to be the origin of the crustal strength, no further tests would be undertaken.

5. BACTERIA

5.7.2   Experimental Procedure

No existing procedures are available in the literature for the inoculation and testing of sterile offshore clay samples in relation to investigating strength variation. It was therefore required to develop and implement new protocols that are straightforward and repeatable. The procedure shown below was used to prepare inoculated samples and is founded on elements from microbiological techniques and geotechnical laboratory testing methods:

1. prepare sea-water liquid medium and autoclave in conventional laboratory autoclave at 121℃ for 20 minutes;

2. in a laminar flow cabinet, 'pick-off' bacterial colony from sea water agar plate with sterile toothpick and swirl toothpick in approximately 50ml autoclaved sea water liquid medium in a 150ml conical flask;

3. incubate bacterial sample in flask for 2 days at 30℃ (optimum growth temperature) while gently agitating in an incubator with an orbital shaker;

4. obtain West African clay samples and thoroughly remould in a beaker at the natural water content;

5. autoclave approximately 300ml remoulded sample at 120℃ for 20 minutes;

6. thoroughly mix 40ml bacterial solution with 250ml autoclaved clay slurry in sterile conditions; and

7. measure water content.

The sample sizes presented above are considered to be nominal, and represent sample volumes which are readily prepared and handled in the laboratory. A sterile sample was prepared in identical fashion to the inoculated sample, with the exception of the addition of the bacterial colony. The sterile sample serves as a control and direct comparisons in strength can be made between this and inoculated samples.

The PTFE shear box and pipe-coating surface were cleaned with 70% methylated spirits. The box was placed onto the pipe-coating surface and water-resistant sealant was used to seal the box to the surface. The inoculated slurry was then poured into the box and incubated, submerged in a seawater water bath for two days at 30℃. The sample was then normally consolidated for 48 hours using a 0.9kg mass, producing a vertical stress of 2kPa. Upwards drainage during consolidation was permitted through filter paper and a porous-plastic disk. The sample was then kept under a vertical effective stress of 2kPa during the shear tests.

If bacterial activity is the dominant biological process producing crust material, shear test results would show strength behaviour comparable with natural samples, and strength values higher than control samples.

5.7.3   Cam-Shear Inoculated Soil-Soil Results

Figure 5.8 shows the soil-soil shear strength of a remoulded sterile sample compared with soil-soil shear tests undertaken on natural samples at a vertical effective stress of 2kPa. The reconstituted sterile sample has a water content of 175% which is lower than those measured for natural clays. The average water content of natural clays is 210%, as shown in Figure 2.2. As expected, due to the disruption of the pre-existing fabric during remoulding, it is observed that the sterile sample lies close to the lower bound of the natural samples tested. Due to the variation in fabric, and the behaviour during shearing, the natural sediment is observed to exhibit strengths that might approximate that of a remoulded sediment as shown in Figure 5.8.
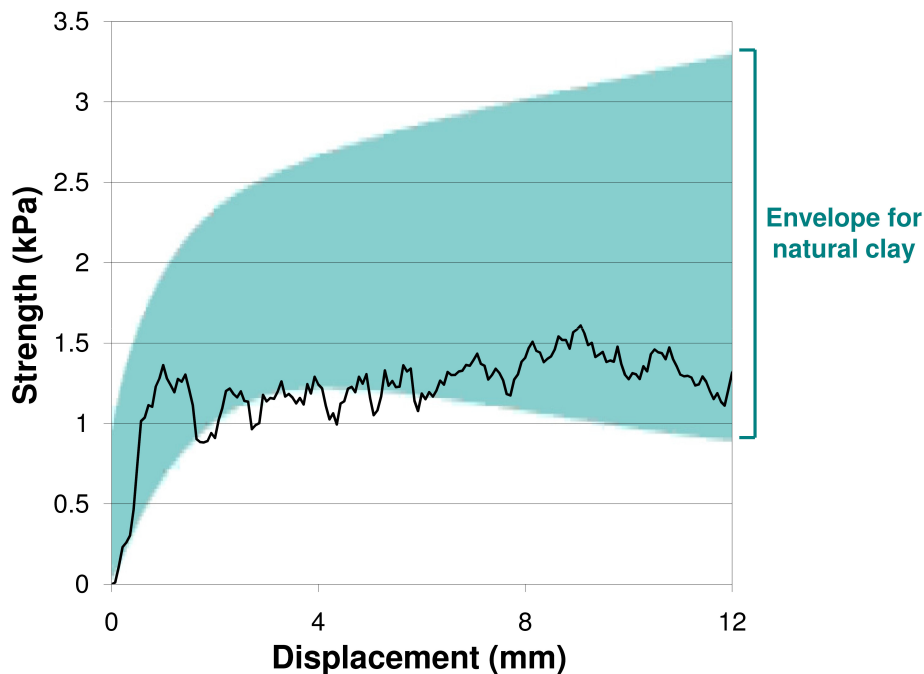
Fig. 5.8 Cam-shear soil-soil test of a remoulded, sterile sample, normally consolidated under a vertical effective stress of 2kPa, underlain with strength envelope of soil-soil strengths from natural clay tests.

Figure 5.9 presents the results of soil-soil shearing of an inoculated sample compared to the sterile control sample, both having been prepared following the procedures outlined previously and consolidated under a vertical effective stress of 2kPa. The following points are noted:

- peak undrained shear strength of the inoculated sample is about 1.6kPa compared to about 1.4kPa for the sterile sample;
- the strength of the inoculated sample decreases to about 1kPa by a shearing distance of 8mm; and

- the inoculated sample strength tends to be lower than the sterile sample strength after several millimetres of shearing.
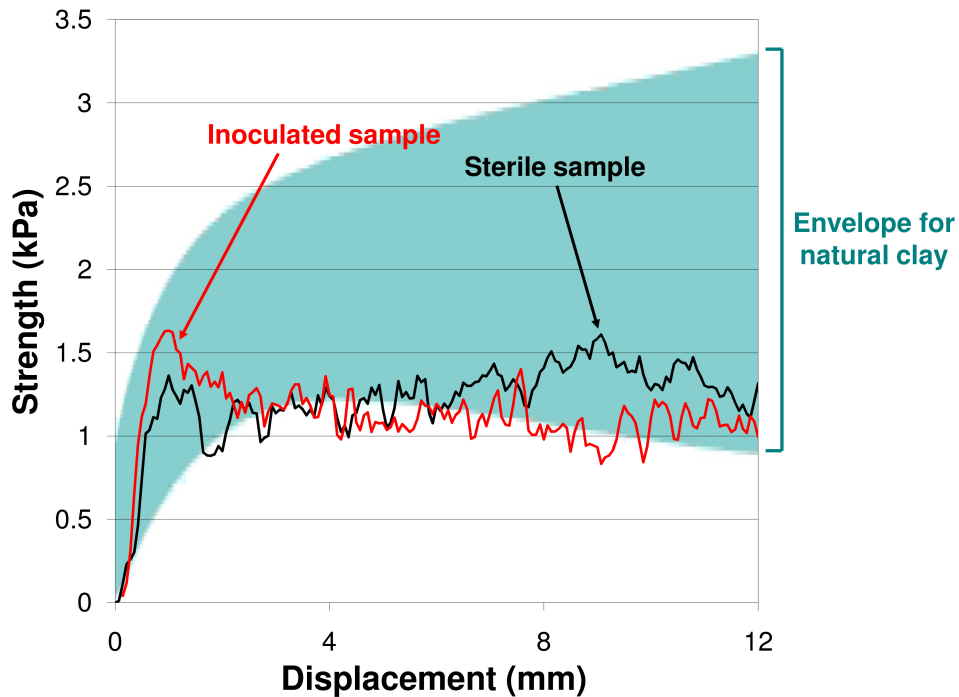
Fig. 5.9 Comparison of Cam-shear soil-soil test of a remoulded, inoculated and sterile samples, normally consolidated under a vertical effective stress of 2kPa, underlain with strength envelope of soil-soil strengths from natural clay tests.

The strength of the sterile sample remains relatively constant over the distance of the test, without a well-defined peak in strength. Strength traces from natural sediments consolidated under σ'_v=2kPa and shown in Figure 5.10, show a gradual increase in strength or demonstrate minor strain softening. Though these samples are from between 0m and and 0.05m depth (above the crust), they still exhibit natural structure which produces relatively high strengths. The inoculated sample in contrast, shows a sharp peak at small strain before softening by over 30%. This sample, if having been structured into 'crust material' by the added bacterium, would have been expected to produce strengths higher than the natural samples. The strength would therefore, also have been significantly higher than the sterile control sample. Though producing a measurable increase in peak strength over the sterile sample, these results demonstrate that the presence of *M. aquaeolei* does not create the high strengths measured in crusts samples. Therefore *M. aquaeolei* and similar bacteria are not considered to be the originators of the crust.

Validation of the growth of bacteria was unable to be undertaken using the ESEM due to
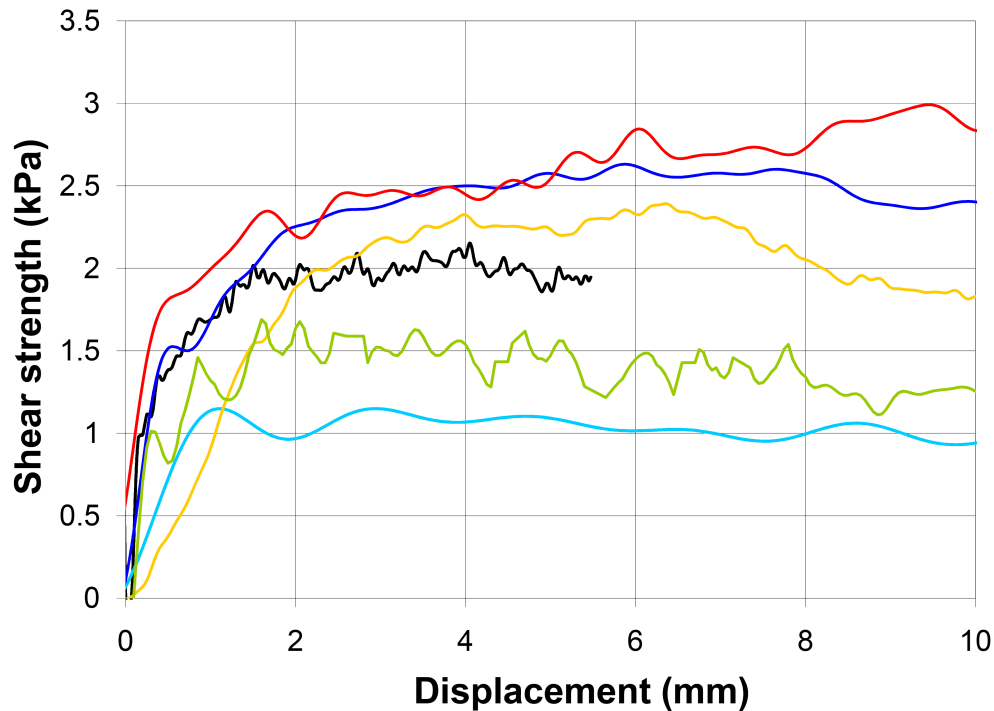
Fig. 5.10 Collated Cam-shear soil-soil strength profiles for natural samples consolidated under 2kPa. These samples represent material overlying the crust.

restrictions of its use for microbiological samples. Fresh sea-water agar plates were therefore prepared following the procedures provided in Appendix E. After the Cam-shear tests with sterile and inoculated samples, samples of each were mixed with sterile sea-water liquid media and placed on the sea-water agar plates. The plates were then allowed to grow for two days at room temperature. The results of these tests are shown in Figure 5.11. This figure demonstrates that the sterile sample remained sterile during the testing as no growth is observed within or surrounding the clay samples. The inoculated sample shows the active growth of *M. aquaeolei*, with white, cloudy bacterium colonies surrounding the sample.
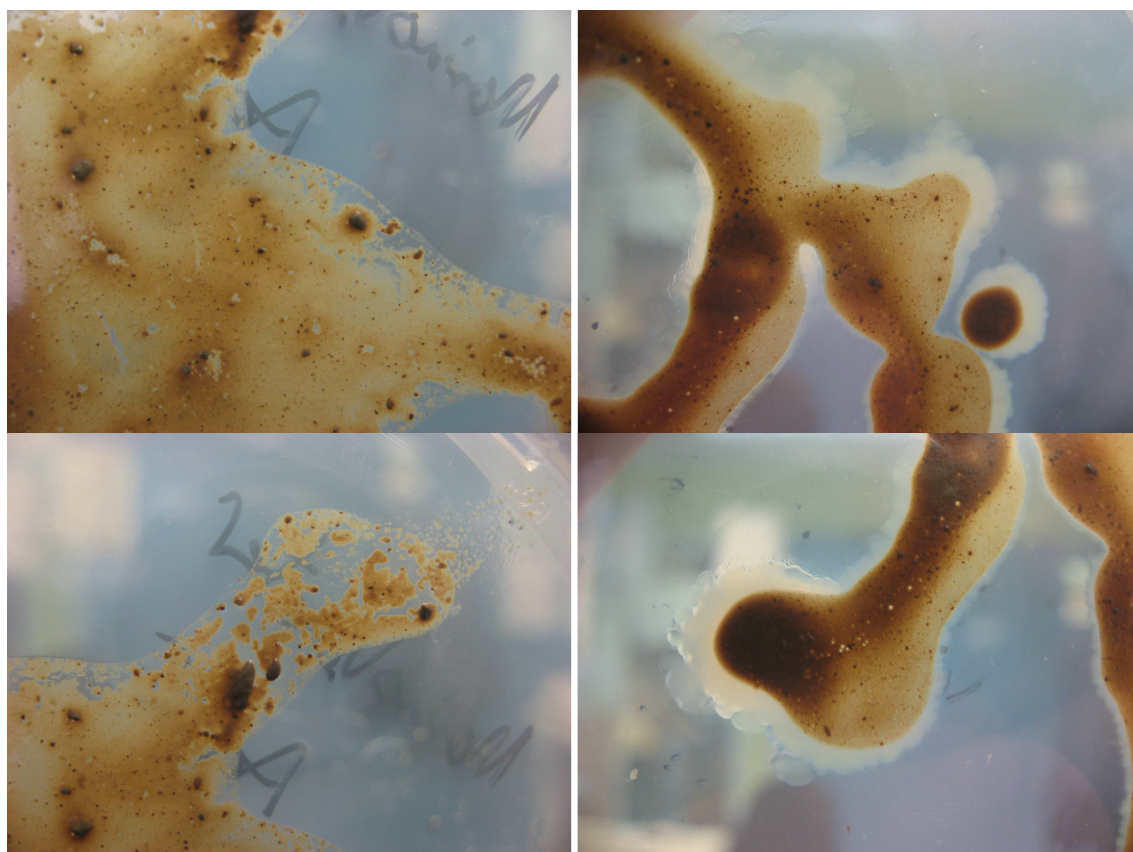
Fig. 5.11 Sterile sample (left) showing no growth of bacteria surrounding tested sample; inoculated sample (right) showing growth of *M. aquaeolei* around the clay sample.

5.7.4 Cam-shear Inoculated Interface Results

Figure 5.12 shows the results of the control sample sheared on a rough pipe coating with roughness of 100μm. The results demonstrate that the sterile sample produces consistent strengths with an interface friction coefficient of μ=0.25, which is about 60% of the value observed for the natural sediment. It is also noted that the rate of shearing (from 0.5mm/s to 0.005mm/s) does not significantly influence the value of μ. In comparison, Figure 5.13 shows the interface shearing results of the inoculated sample, again sheared on the rough coating. This figure shows that the inoculated sample produces a more erratic behaviour, and that the interface strength may fall to zero. This is reminiscent to results obtained when testing some natural crust samples. The following points are noted from Figure 5.13:

- after an initial peak of about 1kPa strength (μ_{peak}=0.5), a shearing rate of 0.5mm/s tends to about μ_{res}=0.3;
- shearing at 0.05mm/s shows a large loss of strength from about μ_{peak}=0.3 to zero before recovering towards μ_{res}=0.2; and
- shearing at 0.005mm/s tends to produce a μ_{res} of about 0.4.
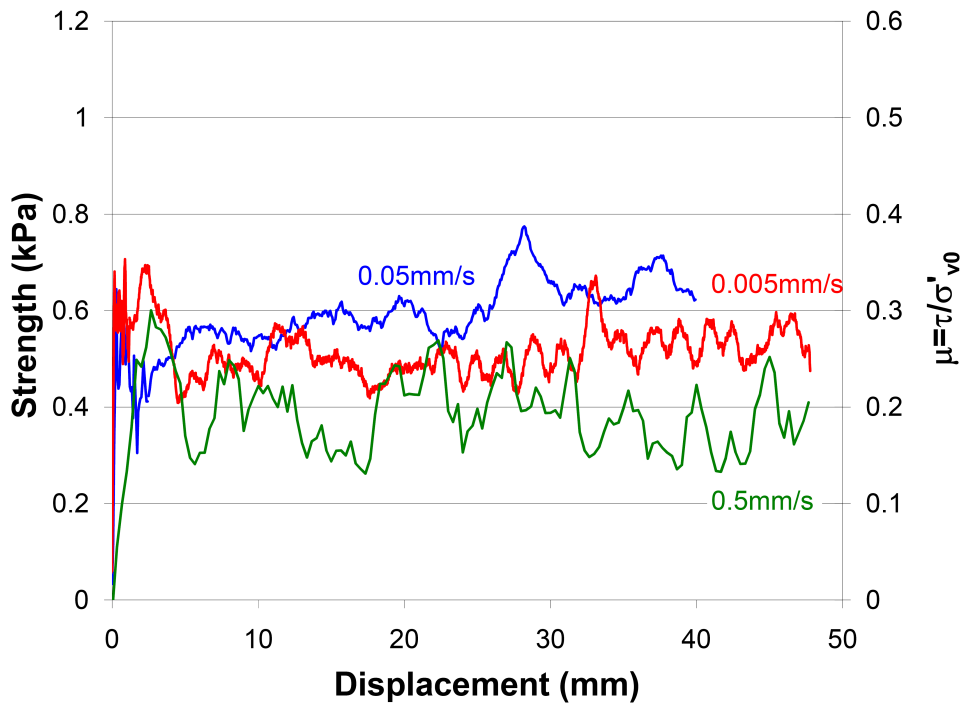
Fig. 5.12 Cam-shear test of a normally consolidated, sterile sample under a 2kPa vertical effective stress. Shearing on a rough interface.
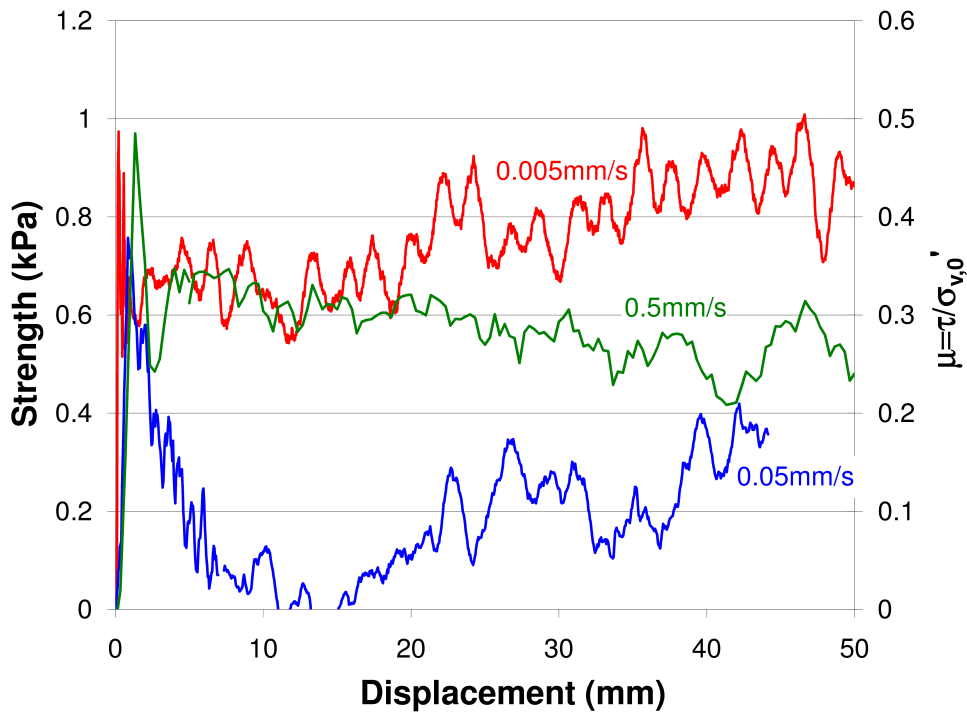
Fig. 5.13 Cam-shear test of normally consolidated, inoculated sample under a 2kPa vertical effective stress. Shearing on a rough interface.

A direct comparison of the control and inoculated samples shown in Figures 5.12 and 5.13 indicates that the remoulded, sterile sample lacks a 'strengthening' structure. Therefore, shearing on a rough interface results in a relatively constant friction value. By inoculating an initially sterile sample, a strengthening structure is introduced to the remoulded clay, which, in the process of shearing on a rough interface, may be destroyed. This is reminiscent of behaviour observed by the natural sediment. The process of structure destruction with natural samples was suggested to generate positive excess pore pressure, which may cause the friction values to drop to zero. A similar process may be induced by shearing inoculated samples, as seen by the sample sheared at 0.05mm/s. At larger strains, and presumably once the structure has been fully remoulded, no further positive excess pore pressures are generated and the strength is able to recover slightly. By comparing the results of the sterile and inoculated samples sheared at 0.5mm/s and 0.005mm/s, it is observed that the inoculated sample may be capable of producing an increase in interface friction coefficient of between 0.1 and 0.2 (between 0.2kPa and 0.4kPa strength).

5.8 Conclusions and Discussion

Based on the work presented in this chapter, *M. aquaeolei* is found to modify the structure of a remoulded clay, but insufficiently so to create crustal strength. It is likely that the generation of polysaccharides by the bacteria is the main contributor to the slight increase in soil strength, and its presence may also play a role in the behaviour observed in interface shear results. Recent studies on the DNA extraction of *M. aquaeolei* highlight the ability of this bacterium to produce significant amounts of polysaccharides (Wang and Edwards, 2009). Given that the samples prepared for the experiments in this chapter were subject to 'ideal' growth conditions, it is therefore considered likely that polysaccharides were present in abundance in inoculated samples. The aim for this phase of investigation was the evaluation of *M. aquaeolei*'s ability to produce crustal strength. It is therefore shown through the completed investigation, that the influence of this bacterium alone is insufficient to produce the observed crustal strength in natural sediments, and therefore, no further testing with this bacterium will be undertaken.

5.8.1 Comments on Experimental Conditions

Sources of energy for bacteria in deep ocean sediments are limited to the presence of organic material either as an environmental system input via 'marine snow', or through the production of faecal matter by invertebrates and other forms of marine life. As discussed previously, Thomas et al. (2005) found that the organic content of these sediments range from 2% to 6%. By providing the tested bacteria with an ideal organic carbon source (sea water agar), the preparation of inoculated samples has approximated a organic content source of about 25%

based on a water content of 175%. This far exceeds the organic content levels expected in the natural sediment.

What is not physically possible to investigate in the laboratory environment is the continual recycling of organic material which takes place close to the benthic boundary layer over decades and centuries. This recycling may result in long-term effects on sediment properties as generations of bacteria process and reprocess the material. With time being the experimental parameter limiting the ability to model 'true' biological activity in these sediments, this requires laboratory experiments to compress the processes into a more manageable time frame. The experiments undertaken in this chapter are therefore likely to be a significant simplification of the bacterial activity in the sediment found off the coast of West Africa, where thousands of competing bacteria have significant amounts of time to modify the sediment. Nevertheless, by providing the optimum growth conditions of 30℃ (compared to the severely limited rate of biological activity at 4℃), this accelerates the biological activity by many orders of magnitude. This may therefore provide experimental conditions which reflect several decades or centuries of bacterial 'work' on the sediment, albeit of one bacteria species.

The completed work demonstrates that bacteria are present in marine sediment, and they have the ability to modify the soil structure. Natural soil cannot therefore, be assumed to be sterile.

5.8.2   Application to Hot-Oil Pipelines

The laboratory conditions utilised in these experiments are evidently not representative of in situ conditions. However, hot pipelines embedded within crust material exhibit external temperatures several degrees higher than the ambient temperature of about 4℃, depending on the specific pipeline and soil characteristics (Bruton, 2010). This increase in temperature will have a significant influence on microbiological processes, both by increasing their activity and by encouraging new species to colonise the sediment adjacent to the pipeline. The significance of this on soil-pipeline interface behaviour is yet to be considered by the oil and gas industry. A temperature of 4℃ is considered to be suitable for the medium-term retardation of bacterial growth in microbiological practice. In contrast, raising the temperature by 25℃ to 30℃ accelerates bacterial growth by several orders of magnitude, potentially representing several years or decades of bacterial 'work'. This chapter, does not identify the originators of crustal strength, however, it does illustrate that elevated growth temperatures, such as those from installed hot-pipes will have a significant impact on the microbiological activity in the surrounding sediment.

5.8.3 Closing Comments

This chapter has described procedures used to identify the presence of bacteria in deep sea sediments. These procedures confirmed that culturable bacteria in the form of *M. aquaeolei* is present in West African clay samples. It is highly likely that other bacteria are also present. The influence of *M. aquaeolei* on the sediment strength has been demonstrated through the application of novel techniques linking microbiological and geotechnical procedures. It has been shown that the presence of this particular bacteria may increase the sediment strength by a factor of 1.3. Though this is a measurable amount in laboratory experiments, this increase in strength is not significant enough to be considered as the sole contributor to the crustal strength which requires an increase of over 200%. Interface shearing of inoculated samples does however, demonstrate the ability of this bacterium to alter the fabric of the sediment sufficiently for variation in mechanical behaviour on a rough interface to occur.

The findings described here therefore suggest that further investigation of the crust's main originator is required. The following chapter will consider the influences of burrowing invertebrates on sediment properties.

Chapter 6

Burrowing Invertebrates

Chapter 5 demonstrated that *M. aquaeolei* has little influence on sediment strength, so further investigation into the origins of the crust material is required. A review of the literature showed that the influence of burrowing invertebrates in marine sediments has largely been inconclusive, with some authors suggesting that burrowing invertebrates strengthen the sediment, and others suggesting the contrary. In this chapter, the natural sediment comprising the crust is analysed in order to identify any evidence that burrowing invertebrates are the source of the crustal strength. Based on the findings of this investigation, further experimental work involving oedometer tests and fall-cone tests were conducted on a variety of samples. This chapter concludes with a discussion on the results of these experiments.

6.1 Evidence for Burrowing Invertebrates

Natural core samples have been investigated using a range of methods to identify evidence for the influence of burrowing invertebrates. The results are presented in this section.

6.1.1 Burrows

Evidence for burrowing invertebrates is observed in box cores collected by Fugro and BP Exploration, shown in Figure 6.1. This figure shows the presence of several large, open burrows within crust material, underlying oxidised, red-brown, soft ooze.

Visual examination of split cores, and sample preparation for Cam-shear testing also identified numerous open burrows of various diameters distributed throughout the sediment. X-ray computer tomography (CT) equipment (X-TEK, HMX 160) was used to image undisturbed core samples prior to laboratory testing. Samples were prepared by cutting intact core samples to 60mm lengths to allow sufficient resolution to be achieved over the entire sample. Samples were placed on a pedestal within the machine and subject to X-rays in a pre-programmed array of slices. Raw image data in three dimensions was generated by the machine, which was
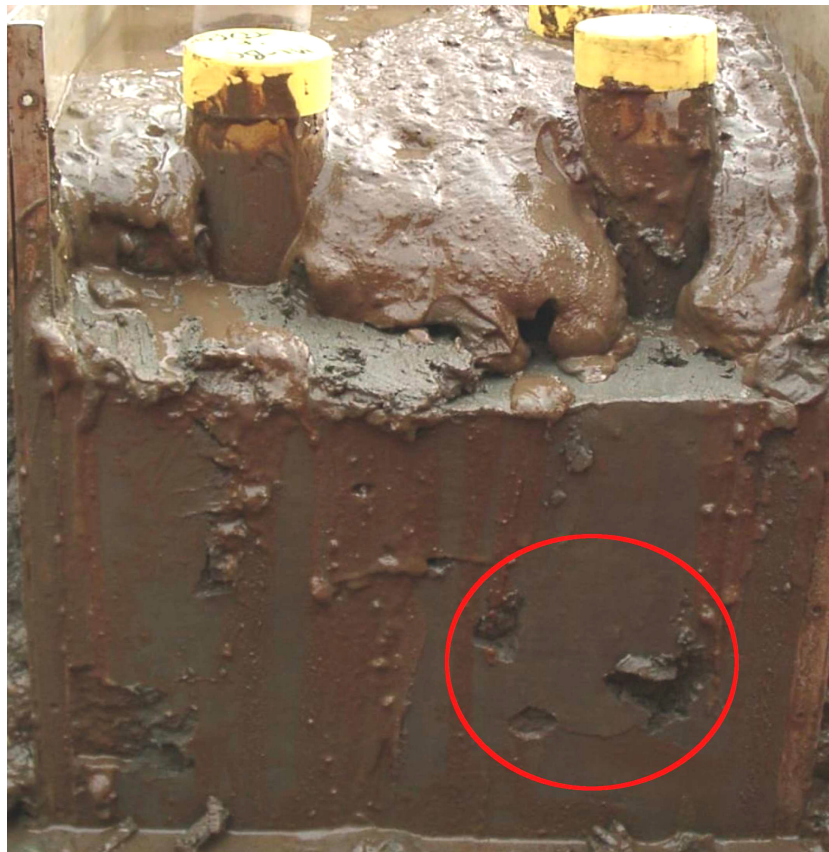
Fig. 6.1 Box core sample taken from, off the West coast of Africa, showing large open burrows. Shown with permission from BP Exploration.

then collated by imaging software to produce a 3D digital render of the sample. The image was trimmed to exclude data corresponding to the plastic core liner. The contrast was manipulated to enhance information pertaining to materials exhibiting different X-ray 'densities'. Due to the very high water content of the tested samples, it was not possible to resolve the matrix structure of intact cores. It was, however, possible to exclude the X-ray densities of wet clay and thus display the residual image of open, elongate burrows within the samples.

Images produced with X-ray CT scanning are shown in Figures 6.2 and 6.3. Burrows of between 1mm and 3mm diameter are observed in these scans, with random orientations in both sub-vertical and sub-horizontal directions. These burrows are filled with water; however, during the process of sub-sampling, they are able to partially drain. Some observed burrows may still have been connected to the seabed if they were currently in use by animals, whereas others may have been abandoned.

As demonstrated from the review of the literature in Chapter 4, several authors have considered the influence of open burrows on sediment properties. An example of this is the ability to increase permeability and hence accelerate consolidation. They may also act as

conduits for advancing the rate of chemical alteration of surrounding sediment.

With reference to the design of hot-oil pipelines, the presence of abundant open burrows in crust material will influence the time required for laid pipelines to consolidate, and if the burrows remain open, they may allow excess pore pressures to dissipate more rapidly during shearing. If, however, the pipe laying process significantly disturbs the seabed sediment, burrows may be closed by smearing and thus the permeability will be reduced by several orders of magnitude. In terms of laboratory testing of natural samples, the presence of randomly-oriented burrows will influence results, which may therefore be reflected in a wide range of values.
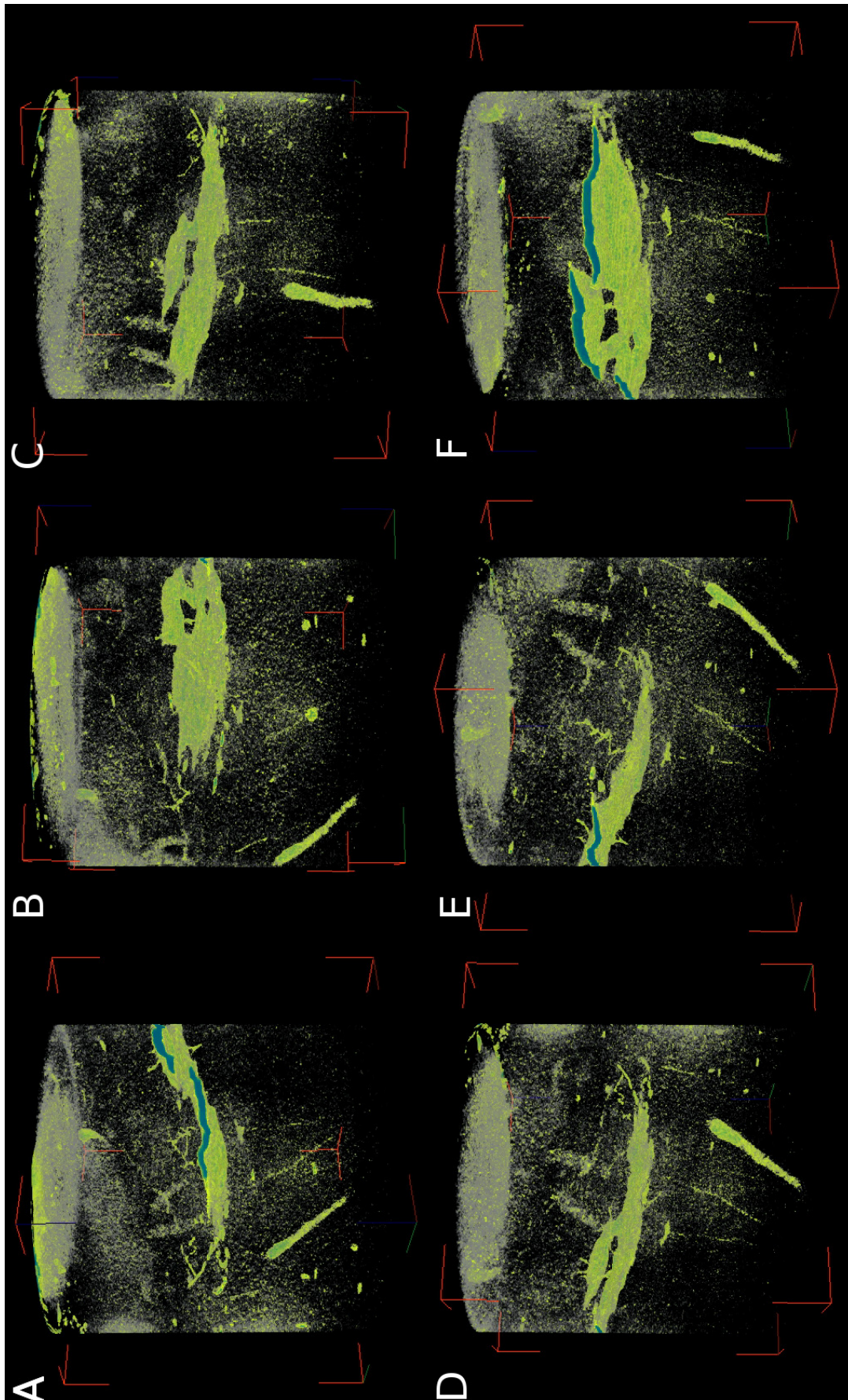
Fig. 6.2 A series of still images obtained using X-ray CT of crust material at a depth of 0.2m showing one large, open burrow rising from the bottom of the core. A large sub-planar crack can also be seen through the centre of the sample. Sample diameter is 8.5cm.
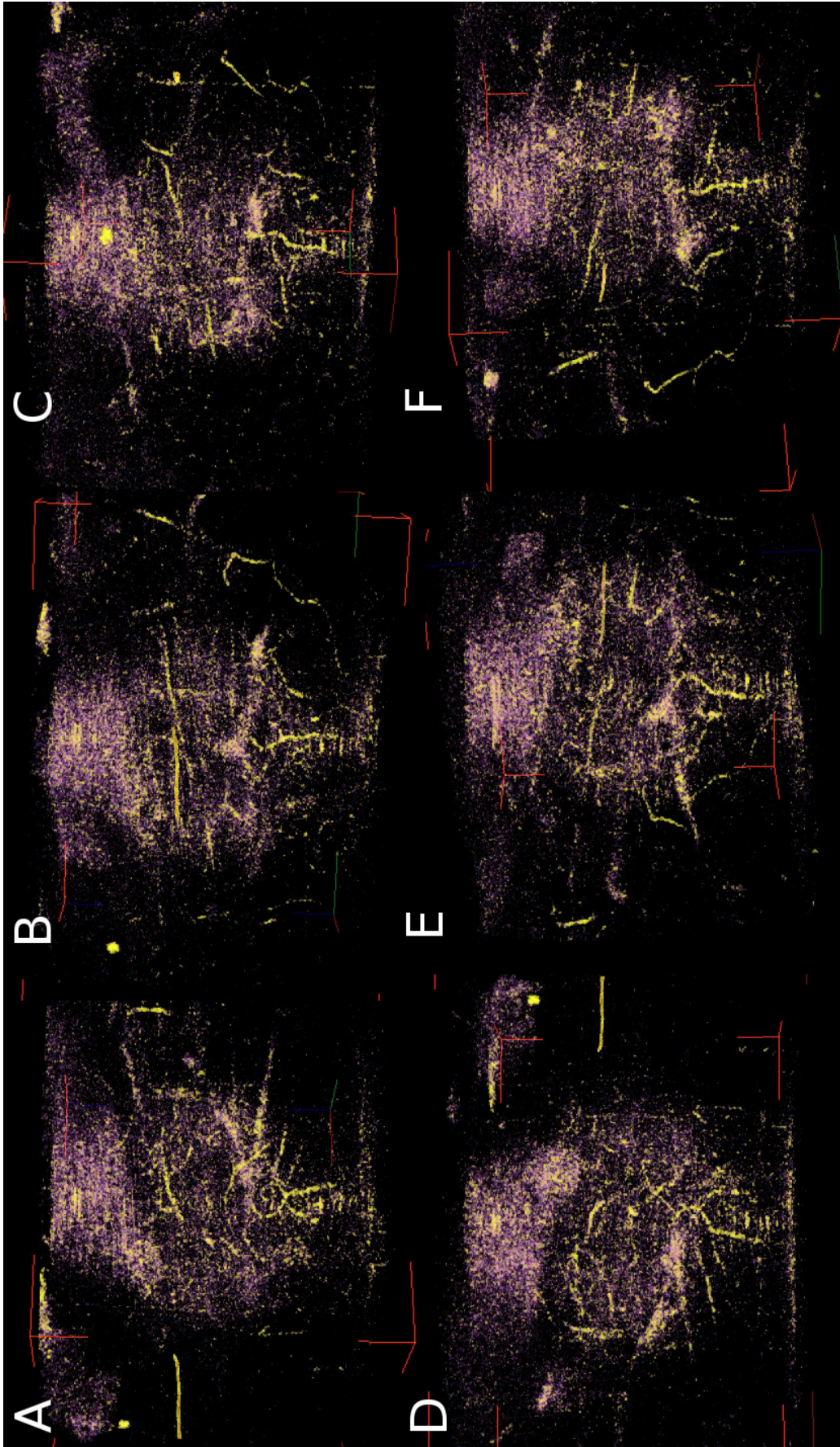
Fig. 6.3 A series of still images obtained using X-ray CT of crust material at a depth of 0.3m, showing numerous open burrows of 1mm to 3mm diameter. These burrows (shown in yellow) are observed to be oriented in all directions; both sub-horizontally and sub-vertically. Sample diameter is 8.5cm.

6.1.2   Faecal Pellets

Faecal pellets with a size comparable with rice grains were observed in box cores, as seen in Figure 6.4. Their influence on the bulk sediment properties was not generally deemed to be significant as they appeared to only occur in discrete, random pockets within core samples.

Fig. 6.4 Rice-grain-sized faecal pellets found within a box core taken from deep water West African sediments, with permission from BP Exploration.

West African sediments have been classified by Evans (2002) and Thomas et al. (2005). Tests undertaken by Evans (2002) followed the 'falling drop method', which is "*primarily a sedimentation method based on Stoke's Law*" (Evans, 2002, p10). Sample preparation for this method requires the samples to be treated with water and hydrogen peroxide to dis-aggregate clay particles prior to washing through a 60μm sieve and centrifuging. Thomas et al. (2005) undertook a study on the ability of cation exchange resins, disodic phosphates and ultrasound to disperse the sediment. It was concluded that samples should be treated with a combination of cation exchange resins and ultrasound to obtain the particle size distribution. Figure 6.5 presents the relative particle size distributions obtained by Evans (2002) and Thomas et al. (2005). Almost all material passes the 63μm sieve indicating that the sediments predominantly comprise clays or silty clays. These results masked the need to undertake further particle size distribution (PSD) analysis on natural cores.

Only after observing the unexpectedly rough and undulating surface of samples prepared for Cam-shear tests did the question of particle size arise. As shown in Figure 6.6, the surface of core material cut with cheese wire is not smooth and smeared as might be expected for a clay sample. Wavy ridges are observed throughout the cut surface, which expose a 'grainy'
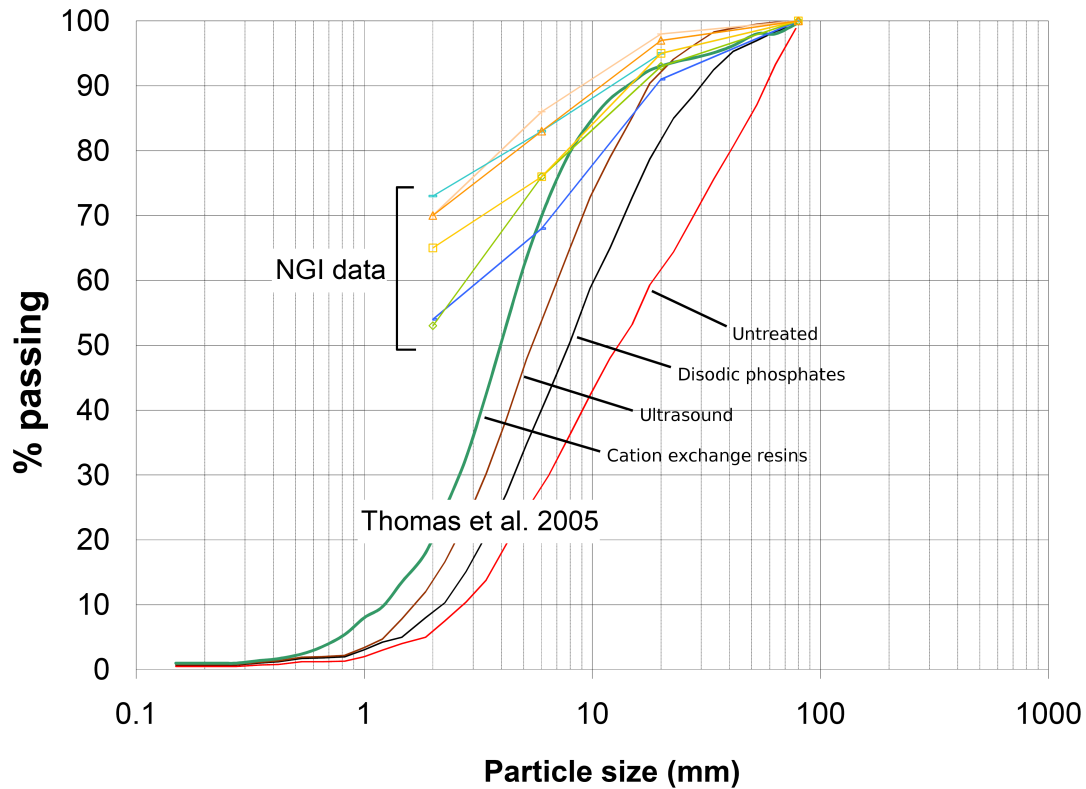
Fig. 6.5 Particle size distribution of West African clay as determined by the Norwegian Geotechnical Institute and Puech et al. (2005), indicating predominantly clay or silty clay material.

fabric. This suggests that discrete, fine-sand-sized soil particles may be present in samples.

A 'quick' wet sieve of natural clay exhibiting the rough cut surface was undertaken through a 225μm sieve. This exposed thousands of smooth, capsule-shaped 'agglomerates' of clay. This finding gave preliminary support to the observation that the clay appeared to contain material coarser than originally assumed. Based on the available literature (e.g. Bayliss and Syvitski, 1982; Martens, 1978; Moore, 1931a) and discussion with experts at the National Oceanography Centre, Southampton (Gooday, 2009), it was concluded that the observed agglomerates were faecal pellets produced by a range of different burrowing invertebrate species, including those from the *polychaete sp.* Abundant faecal pellets within these sediments may have a significant influence on the mechanical behaviour of the soil. Depending on their individual (and collective) strength and distribution, a sufficient number of pellets may increase the bulk grain size from a clay to a silt or even fine sand. This could increase the effective permeability and strength by several orders of magnitude over that of a normally consolidated clay. The abundance of faecal pellets in the crust material clearly required investigation. The procedure and results of this investigation are presented in the proceeding section.

115

Fig. 6.6 Photograph showing the grainy, undulating texture of a
core sample cut with a cheese wire, suggesting the presence of
coarser grains.

6.2 Faecal Pellet Percentages

Conventional particle size distribution (PSD) analysis of clayey soils based on ASTM D442-
63 was found to be an inappropriate method for investigating the individual pellets found
within these sediments, due to the mechanical breakage of pellets during preparation. Pellet
preservation was achieved by utilising the author's previous experience of techniques used
in sedimentological washing of foraminifera. Using this method, bulk natural samples were
carefully washed with running water through a series of sieves without prior drying, crushing
or remoulding of the sediment. This process ensured the survival of pre-existing biologically-
bonded aggregates for post-washing analysis. As water is used as the deflocculating agent
in this method, results cannot be presented as a percentage of the natural sediment's mass.
Instead, results are presented as pellet percentages by original total dry mass. The sieve sizes
used included 465μm, 300μm, 212μm, 125μm, 75μm, 63μm, 53μm, 38μm, and 20μm, with
material passing the smallest sieve being discarded.

Samples were prepared by measuring the water content of cuttings adjacent to the test
sample following the procedure given in ASTM D2216. The test sample was then weighed
to determine the total mass prior to wet sieving. Once thoroughly washed through the stack
of sieves, the material remaining on each sieve was then removed and dried in an oven at

105℃ for at least 24 hours. The dried samples were weighed and the dry masses converted to a percentage of the original test sample whose dry mass was determined from the original measured water content. This is referred to herein, as the 'faecal pellet percentage'. Optical imaging was undertaken on dried samples, however, the resulting images were not a true representation of the original pellets due to shrinkage during drying.

6.2.1 Faecal Pellet Wet Sieving Results

Cores from several depths were wet-sieved to determine the percentages of faecal pellets larger than 63μm, shown in Figure 6.7, and as summarised in Table 6.1. Figure 6.8 presents the percentage passing each sieve size for Core B shown in Figure 6.7. The sieve fraction percentages shown in this figure are typical for most cores tested. The majority of pellets in the cores are found in the 63μm to 125μm fraction, and the smallest percentage are found in the $>300\mu$m fraction. Faecal pellet sieve fraction plots of the other core samples are shown in Appendix F. Core G represents material containing a significantly high fraction of sand, discussed in more detail in Section 6.3. The results of this particular sample are not considered representative of the crust material, and will not be considered in the following discussion concerning the crust.

Based on in situ and laboratory testing, the crustal strength observed in these samples generally develops from a depth of about 0.15m below the seabed. The peak strength of crust material, however, may vary from 8kPa to 12kPa in specific core samples, based on mini T-bar, mini ball and cone penetration testing. Figure 6.9 shows the relationship between the percentage of faecal pellets in the various cores, as shown in Figure 6.7, and the undrained shear strength obtained from adjacent penetrometer probes at the depth appropriate to the wet-sieved sample. These figures indicate that crusts contain 20% to over 50% faecal pellets by dry mass, and that there is a strong correlation between the measured strength and the faecal pellet content in crust material. The 2m long STACOR sample exhibiting peak strength at a depth of about 1m was provided as two 1m long core sections. These core sections were found to be in poor condition, with desiccation evident at the core tops and softening at the core bottoms. The wet sieving of this particular core indicates a small increase in the percentage of pellets down to 1m depth followed by a reduction in pellet percentage. The maximum percentage of pellets, however, is only 22%. Core disturbance during sampling and subsequent transportation and storage is considered to be the likely cause of these lower results.

Table 6.1 Summary of samples wet sieved for faecal pellets.

Core	Depth	w_c	Dry mass	% pellets >63mm by dry mass
	m	%	g	
A	0.2	164	8.48	55
	0.25	176	9.47	53
	0.3	174	6.29	55
	0.42	188	10.2	46
B	0.27	211	8.66	33
	0.4	190	8.73	35
C	0.04	163	15.47	46
	0.2	149	12.99	32
	0.4	156	15.7	33
D	0.07	287	7.59	28
	0.17	260	7.86	27
	0.28	220	8.72	30
E	0.03	247	14.46	22
	0.1	198	8.6	20
	0.2	189	10.16	21
	0.3	189	7.28	19
F	0.35	225	9.87	17
	0.6	198	13.68	21
	0.8	216	11.74	18
	1	186	6.75	22
	1.2	181	10.87	20
	1.3	209	10.44	19
	1.6	212	13.38	17
	1.9	211	17.59	15
G	0.25	61	46.15	71
	0.3	62	22.31	62
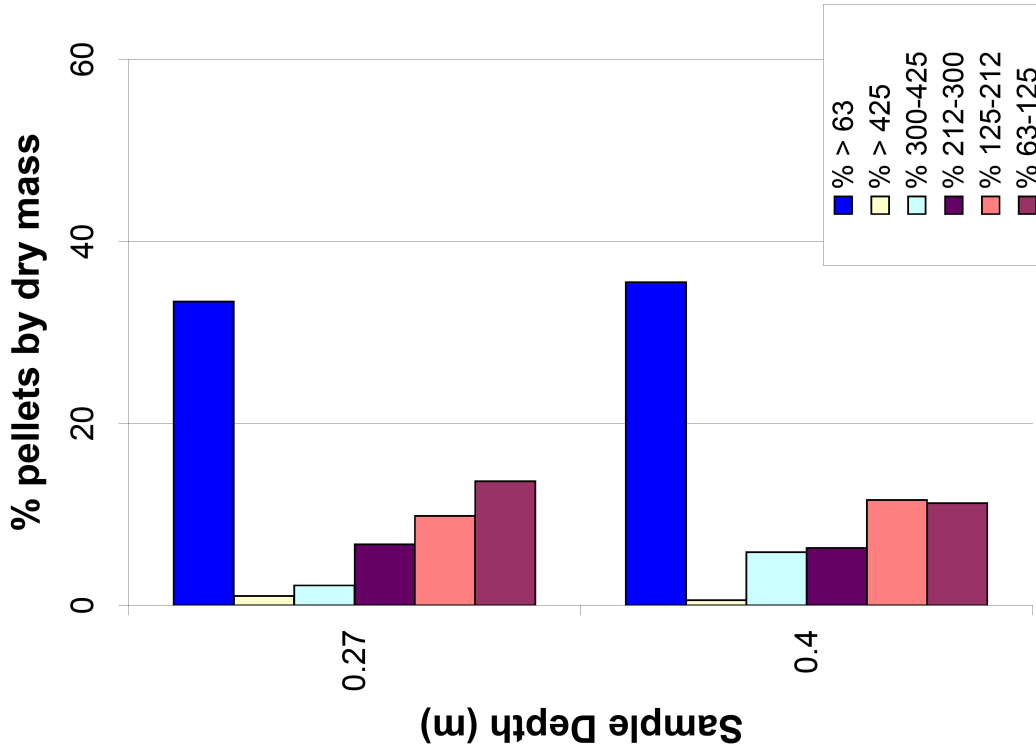
Fig. 6.8 Percentage of faecal pellets remaining on each sieve fraction for Core B. Fractions are typical for most cores tested.
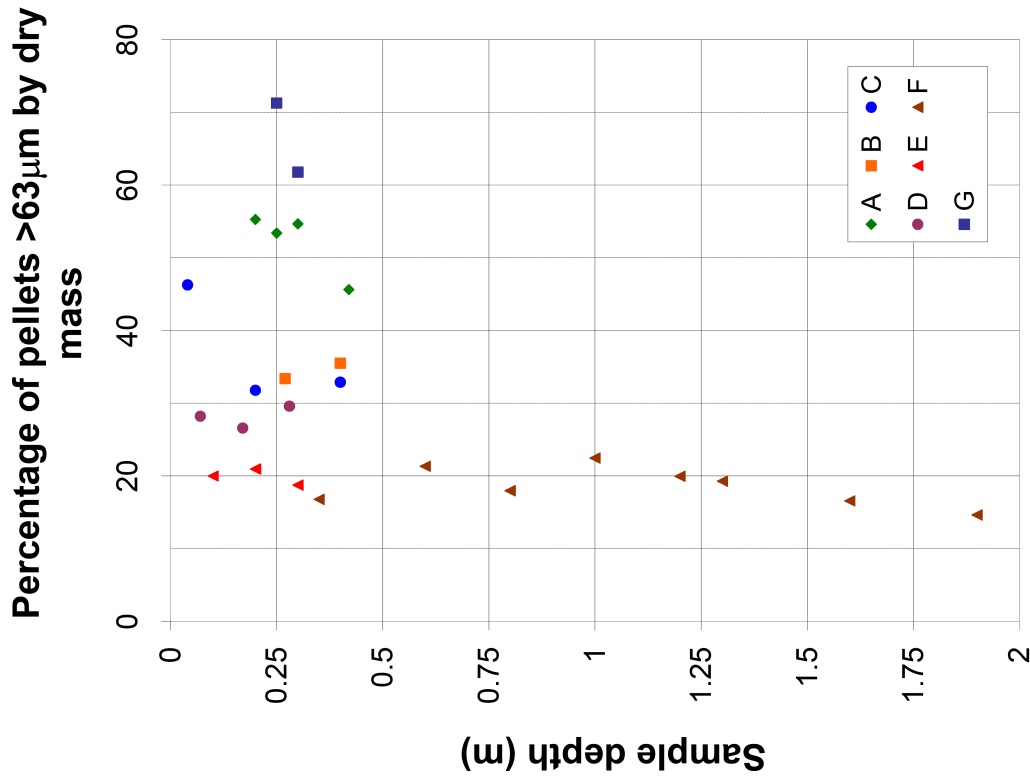
Fig. 6.7 Faecal pellet percentages by dry mass for core samples of crust material.
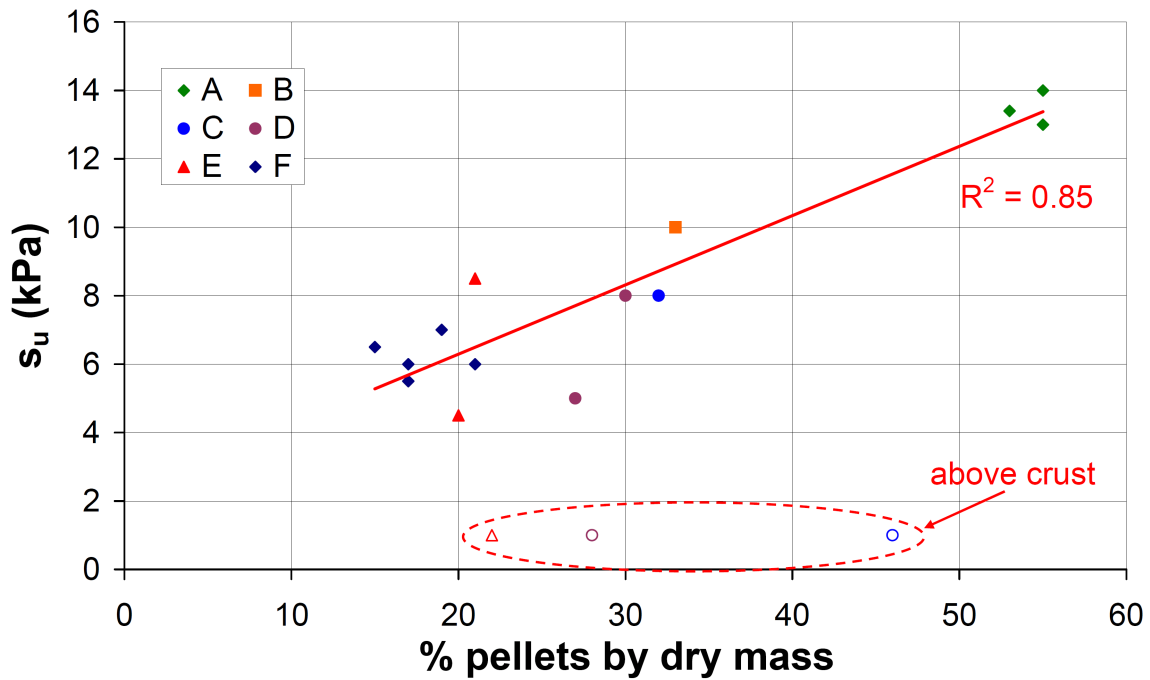
Fig. 6.9 Relationship between the percentage of faecal pellets in natural crust samples and the undrained shear strength measured using mini T-bar, mini ball and cone penetrometers.

PSD profiles are presented in Figure 6.10 with comparisons to previous testing undertaken by Evans (2002) and Thomas et al. (2005) who used different techniques, as discussed previously. This figure illustrates the difference in particle size distribution that is obtained when samples are subject to different methods of preparation. Wet-sieving natural samples under running water is shown to shift the particle size curve by at least one order of magnitude of grain size. This demonstrates that pellets are robust enough to withstand careful washing. If allowed to desiccate, be remoulded or subject to shear stresses, as required by sample preparation following ASTM D442-63, pellets will disintegrate into their constituent parts of clays, diatoms and detrital fragments, such as sections of foraminifera, shell fragments and sponge spicules.
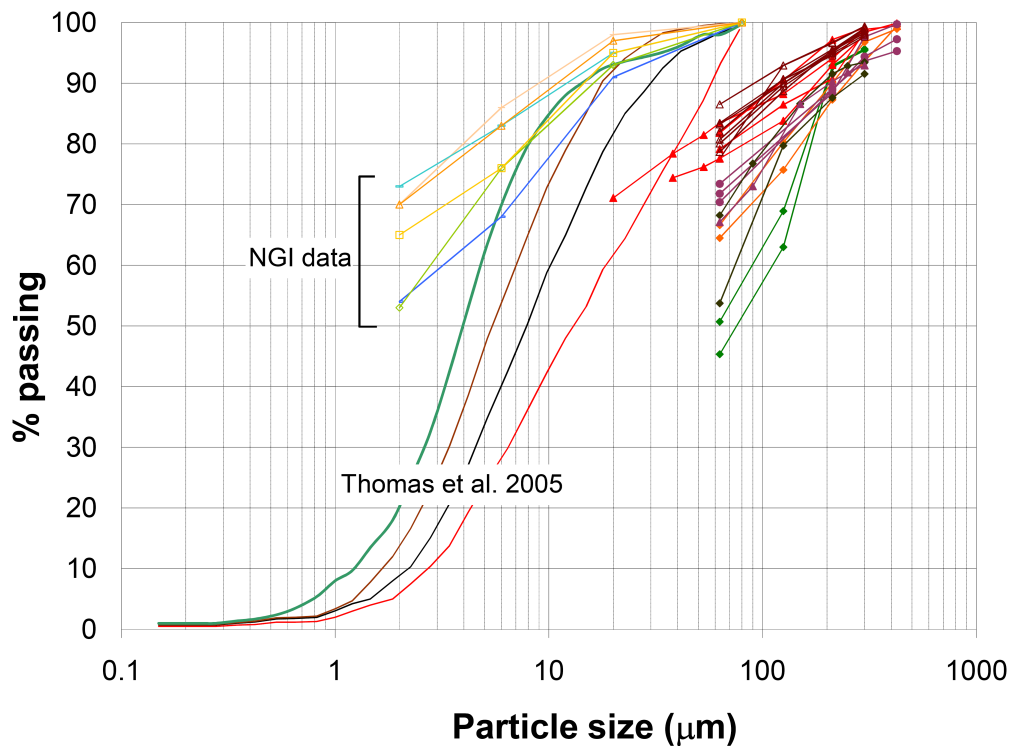
Fig. 6.10 Comparison of particle size distributions for wet-washed samples and previous results from Evans (2002) and Puech et al. (2005), showing a change in mean grain size by approximately an order of magnitude.

Images of wet faecal pellets are shown in Figure 6.11. An environmental scanning electron microscope (ESEM, Zeiss EVO LS15 type) image of a typical intact pellet is shown in Figure 6.12, demonstrating the well-defined ellipsoidal, capsular shape, and the presence of diatoms within a matrix of clay.

6.2.2   Discussion

According to a study of sand-clay mixtures, Kumar and Muir Wood (1999), the percentage of granular material required to significantly influence the mechanical properties of the mixture is approximately 50%. A similar study on the shear strength of clay-sand mixtures by Vallejo and Zhou (1994) suggests that a sand content of greater that 50% would result in the shear strength being influenced by the presence of the sand. Below this amount, the strength would remain largely that of the clay. Based on the wet-sieving method, the percentage of faecal pellets in some samples suggests that it might be plausible for these pellets to influence the mechanical behaviour of the sediment if they behave like fine sand grains, and especially if they cause jamming and potential dilation during shearing. Figure 6.11 demonstrates that sieved material greater than 63μm in size predominantly consists of faecal pellets. To determine whether the material smaller than 63μm also comprises faecal material, samples from 0.03m,

(a) Pellets of greater than 300μm diameter.

(b) Pellets of 212μm to 300μm diameter.

Fig. 6.11 Typical photographs of wet-sieved faecal pellets.
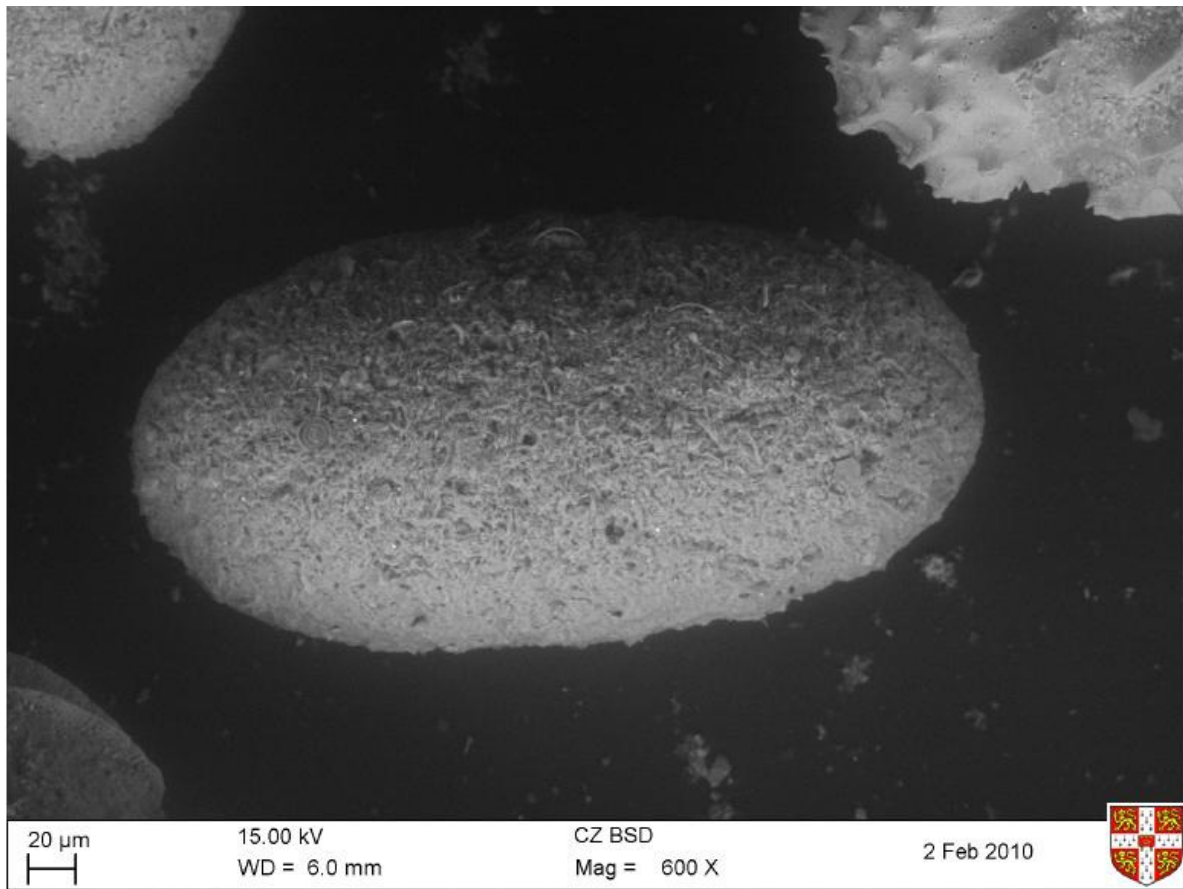
Fig. 6.12 A faecal pellet of greater than 300μm diameter, imaged using an ESEM. Note the ellipsoidal shape and the embedded diatoms, seen as arcs projecting from top of pellet.

0.2m and 0.3m depths were sieved to 20μm.

Figure 6.13 shows an ESEM image taken of material between 20μm and 53μm. This image shows that the material within this fraction comprises agglomerates of clay which have not dispersed during sieving. These agglomerates do not exhibit the well-defined shape of the faecal pellet shown in Figure 6.12; however, given their apparent compactness, they may represent pellets in various stages of decomposition. The material sieved to 20μm was found to contribute between 8% and 12% by dry mass to the percentage of non-clay-sized material. This indicates that the results presented in Figure 6.7 under predict the percentage of agglomerated material within natural crust samples.

The faecal pellet percentage above the crust is not significantly less than that within the crust. Based on previous studies, invertebrate activity is most prevalent within the upper 0.2 m of sediment. This would suggest that most faecal material will be produced and deposited above this depth. As discussed in Section 3.1.1, the sediment to a depth of about 0.15m exhibits extremely high water contents (often above 300%) and is essentially 'unconsolidated ooze'. It is suggested that the crustal strength develops when the material is subject to a
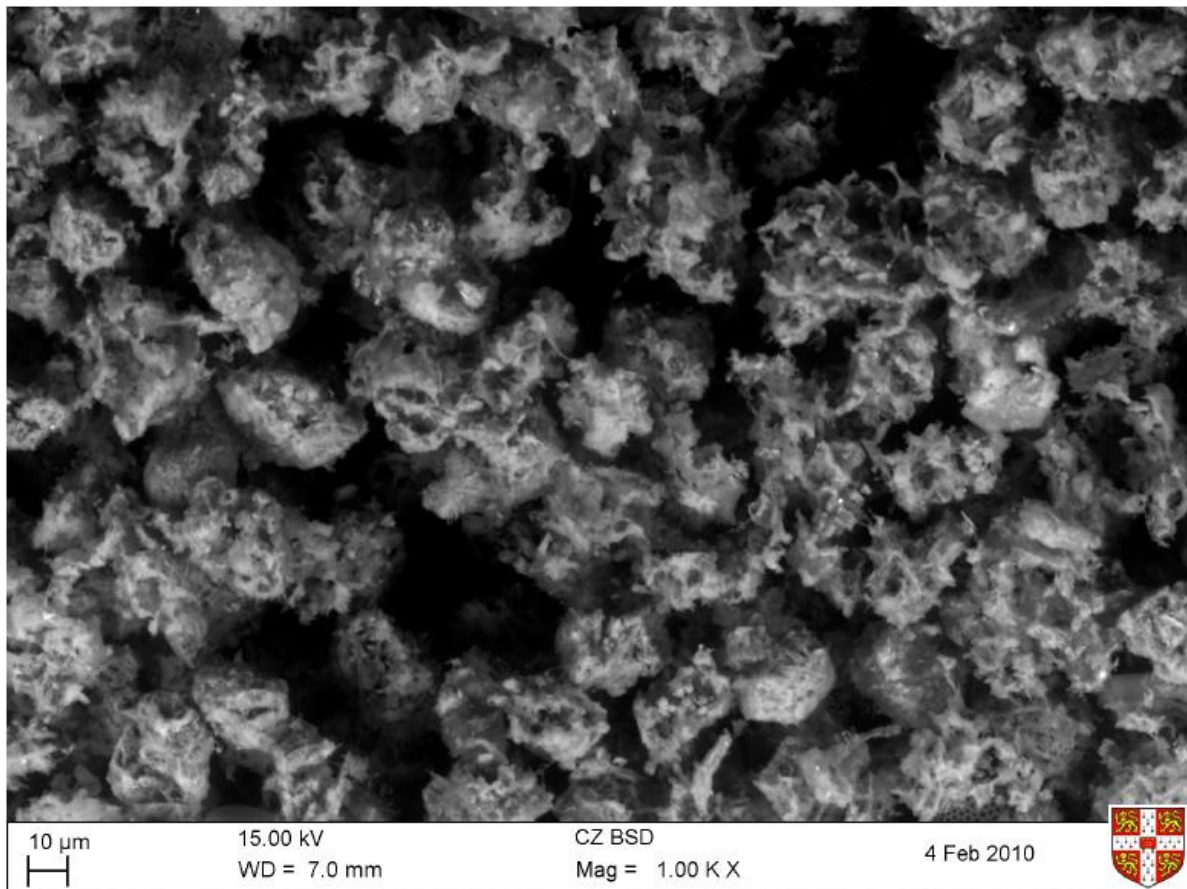
Fig. 6.13 Agglomerates of 20μm to 53μm imaged using an ESEM. These may be the remains of decomposed faecal pellets.

confining stress due to overburden that resists the dilation of pellets during shearing.

Below the crust, at depths greater than 1.2m, the percentage of pellets decreases to below levels that would influence the mechanical behaviour, and hence the strength of the sediment should revert to that of a conventional clay sediment, based on the behaviour of clay-sand mixtures considered by Kumar and Muir Wood (1999); Vallejo and Zhou (1994). Visual inspection of cores indicate that no discrete pellets remain by about 1.9m depth. A 'remnant' pelletal texture, however, is evident in some sections of core at this depth. This indicates that burial of more than about 1.2m may generate sufficient vertical effective stress to cause pellets to crush and resediment their contents, coinciding with a loss in crustal strength. To test this hypothesis, oedometer tests on crust material were undertaken, and the results are presented in Section 6.4.

6.3 Microscope Observations

This section presents typical images of natural sediment containing pellets and wet sieved pellets, taken with a conventional optical microscope. Images were taken during Cam-shear sample preparation to illustrate the natural fabric of samples, and highlight the variability encountered in core samples. Figure 6.14 shows examples of high plasticity clay and sandy crusts. Within both types of samples, an apparently clear distinction between pelletised and matrix material is observed. Large pellets are seen to exist either randomly within the matrix or to populate a particular zone of the sample. Wet sieving the clay matrix, however, demonstrates the existence of pellets within the matrix, which cannot be seen from visually examining fresh core samples. Sieving of the sandy material (Figure 6.14(b)) shows that the sand grains are likely to be faecal pellets that have been chemically altered. These grains retain their ovoid form, but behave as incompressible sand grains.

Pellets within the crust material (Figure 6.14(a)) range in colour from dark grey and pale grey to brown and pale brown. Some pellets show a darker brown discolouration that may be the result of minor mineral alteration. Broken or crushed grains exhibit consistent colouration to the external surface. For comparison, samples from 1.9m depth, representing material from below the crust are shown in Figures 6.15 and 6.16. Examples of both wet and oven-dried samples are presented, showing distinct green-brown colouration consistent with glauconite replacement of the pellet's original minerals through dissolution, with "*iron and potassium rich glauconitic smectites*" (Odin and Matter, 1981, p631). Other references to glauconite may only consider the appearance of the material as being pellet-shaped and greenish in colour, as indicated by Birch (1979). As considered by Takahashi and Yagi (1929); Moore (1939); Bayliss and Syvitski (1982); Chafetz and Reid (2000), faecal pellets are ideal environments for glauconisation to occur due to alteration of clay mineralogy during sediment digestion by burrowing invertebrates. It has been shown that "*faecal pellets have an abundance of the necessary ions for the growth of glauconite in the clay minerals originally comprising the pellets*" (Chafetz and Reid, 2000, p30).

In other samples from this depth, there is evidence for minor pyritisation (Figure 6.16), predominantly of foraminifera and within the structure of siliceous sponge spicules. At 1.9m depth, pellets make up about 15% of the total dry mass. Based on observations from optical microscopy presented here, it is likely that these pellets remain following chemical alteration, due to a combination of their resistance to mechanical crushing and their chemical inertness.
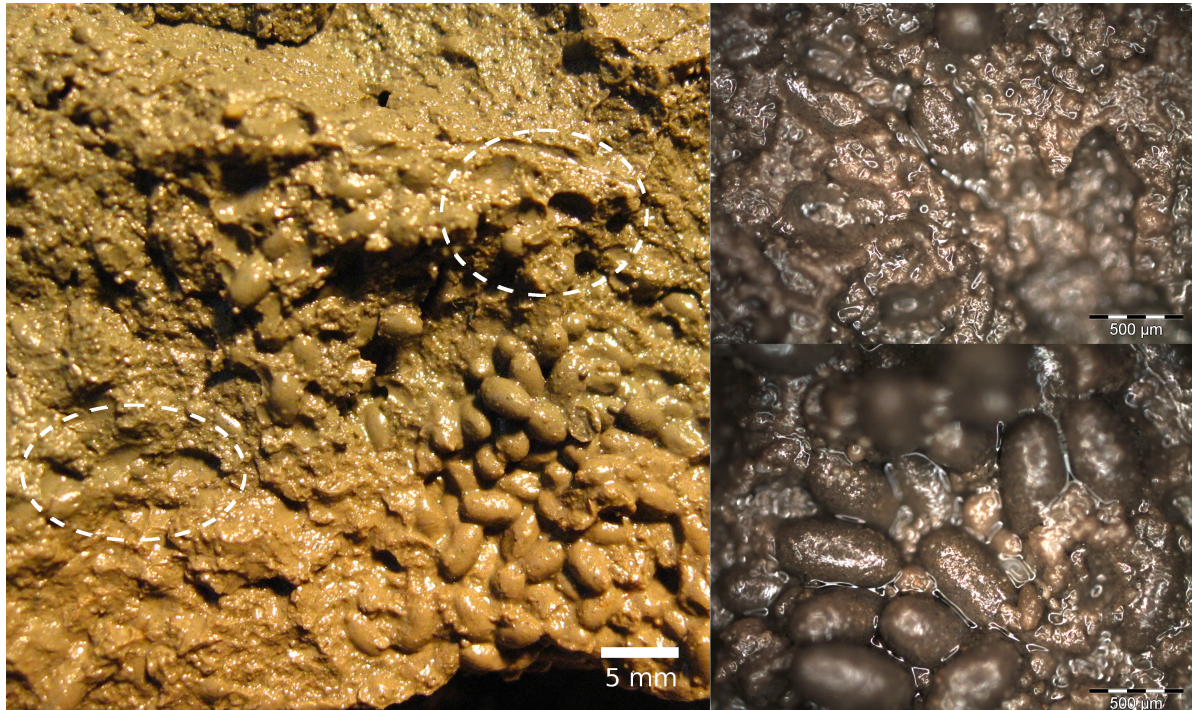
(a) Clay crust material containing pellets. Note the imprint left in the clay matrix (circled) when pellets are removed from the sample.

(b) Sandy crust samples. Black sand grains are likely to be chemically altered faecal pellets.

Fig. 6.14 Photographs taken with a digital camera (left) and an optical microscope (right) of clay and sandy crust samples.
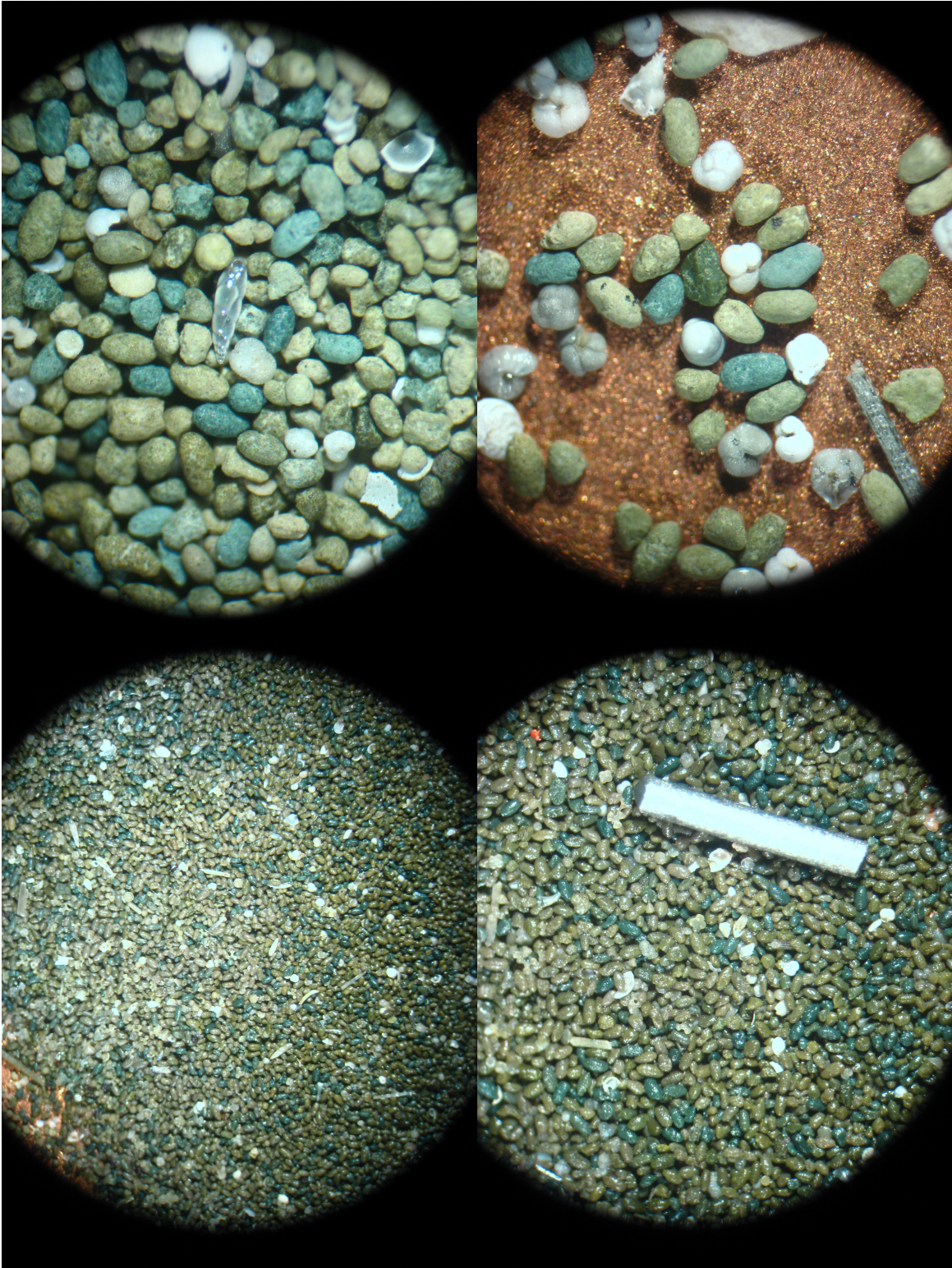
Fig. 6.15 Digital photographs taken through the eye piece of an optical microscope of samples from 1.9m depth. Wet samples are shown on the left and oven-dried samples are shown on the right. A 0.5mm diameter pencil lead is shown for scale in the bottom left hand photograph. Note the green and brown discolouration of pellets due to glauconisation.
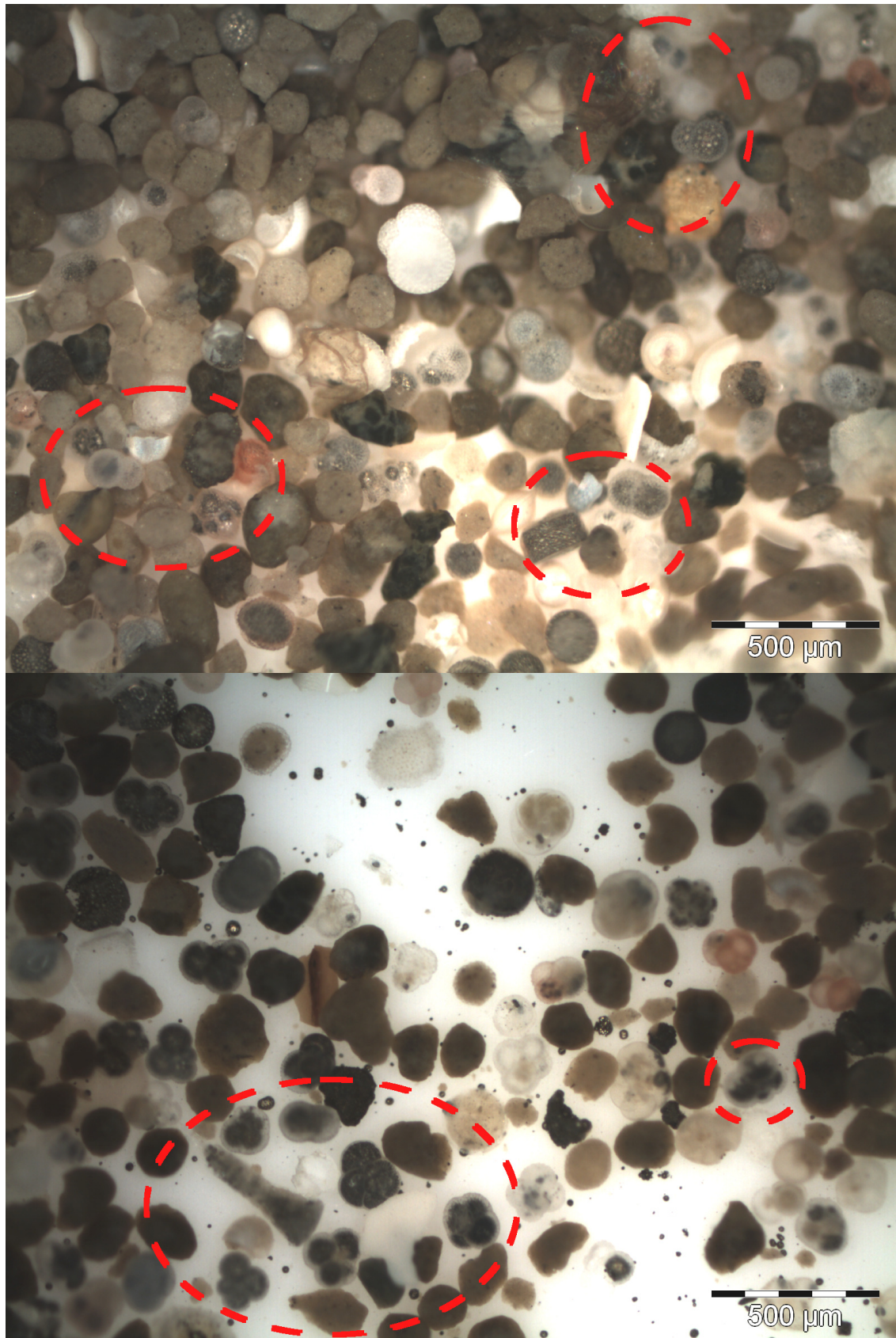
Fig. 6.16 Photographs taken using an optical microscope of samples from 1.9m depth. Samples were lit from below, allowing the imaging of internal pyritisation of foraminifera, examples of which are circled.

6.3.1 X-ray CT Imaging and ESEM of Faecal Pellets

Initial imaging of pellets was undertaken using a conventional scanning electron microscope (SEM). The sample preparation to produce high resolution images requires the drying of samples and coating with an element of high valency, such as gold. This allows the machine to operate under a vacuum, thus minimising the interference experienced by the electron beam due to air molecules within the chamber. Drying clay samples with high water content such as those from marine sediments results in structural collapse under suction. Samples are therefore no longer representative of the natural sample. The SEM was therefore unsuitable for imaging wet pellets. An environmental scanning electron microscopy (ESEM) was instead used to investigate the structure of intact pellets, as well as fragments of faecal pellets. The ESEM allows imaging of moist samples by retaining a relatively high water vapour pressure within the chamber. Retention of a high vapour pressure, however, usually results in images that are less sharp than SEM images. To provide evidence for the natural sediment structure surrounding pockets of pellets, X-ray CT imaging was undertaken on pellet subsamples following the sample preparation described in Section 6.1.1.

A photograph of a natural sample containing large faecal pellets of approximately 1.5mm diameter is shown in Figure 6.17. X-ray computer tomography (CT) images of the same sample are presented in Figure 6.18. These show the presence of macro-voids of a few millimetres in diameter adjacent to pellets. Figure 6.19 presents ESEM images of washed pellets, which indicate the presence of micro-voids within the structure of the pellets. These micro-voids are observed to be less than 1μm to 3μm in diameter. ESEM imaging with the variable pressure secondary electron (VPSE) detector also allows the identification of 'wet textures'. Evidence for mucin or peritrophic membranes (as discussed by Bayliss and Syvitski, 1982) surrounding pellets is acquired using this method. The pellet membrane is produced within the gut of burrowing invertebrates to ease passage through the digestive system. Peritrophic membranes surrounding the pellet and mucous within the pellet produce robustness by providing a protective sheath for the pellet contents and by sticking the digested fragments together. By imaging with a back scatter detector (BSD) in the same wet chamber as for VPSE imaging, information about the internal structure of pellets can be resolved. This demonstrates the arrangement of clay platelets at the surface of pellets and allows the imaging of micro-voids within pellets.

Fig. 6.17 Photograph of sample prior to X-ray CT imaging. Note the large faecal pellets, and the open voids adjacent to pellets.
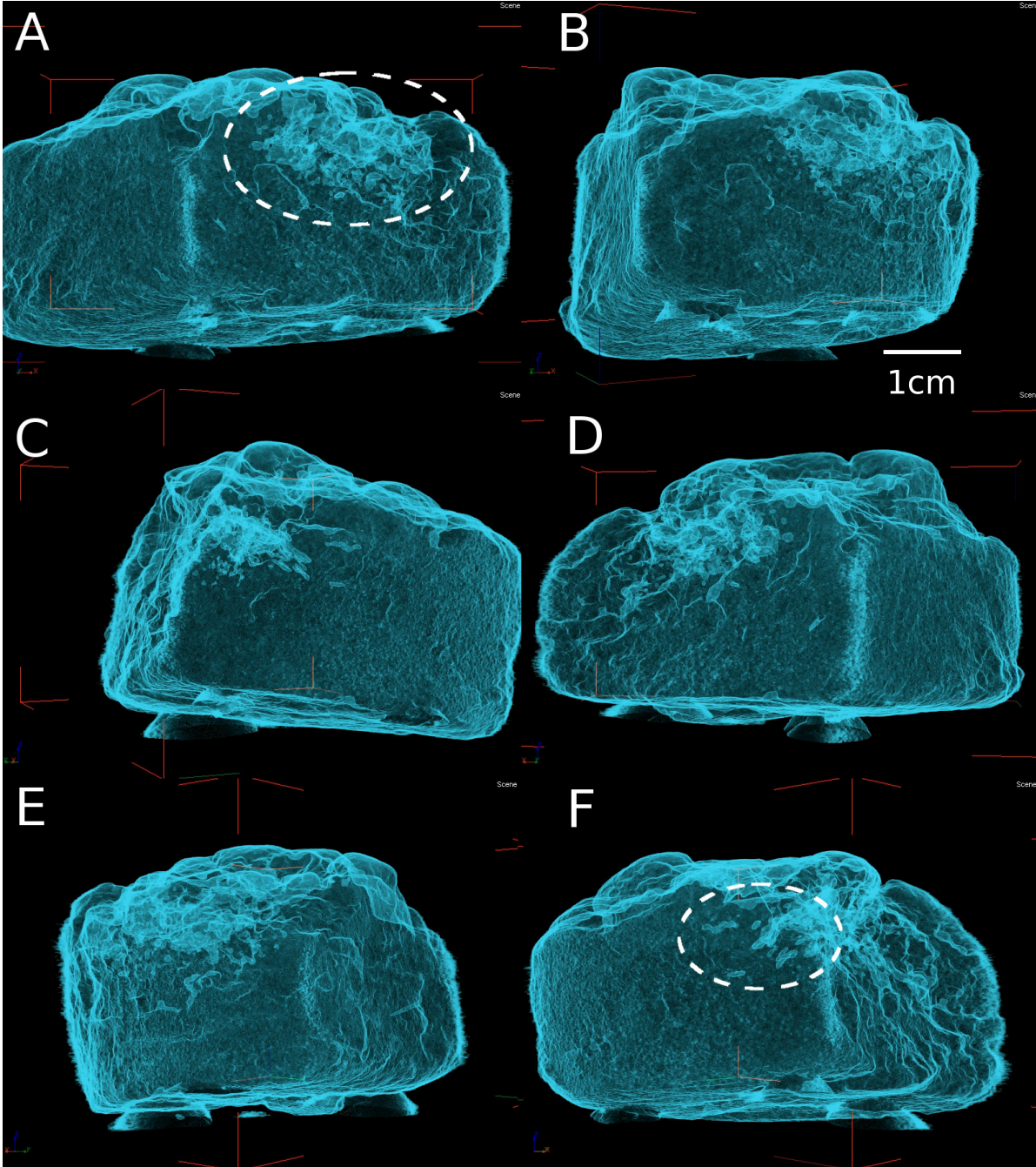
Fig. 6.18 X-ray CT images of a natural sample containing pellets. These images show the presence of internal macro-voids located adjacent to faecal pellets, examples of which are highlighted in images A and F.
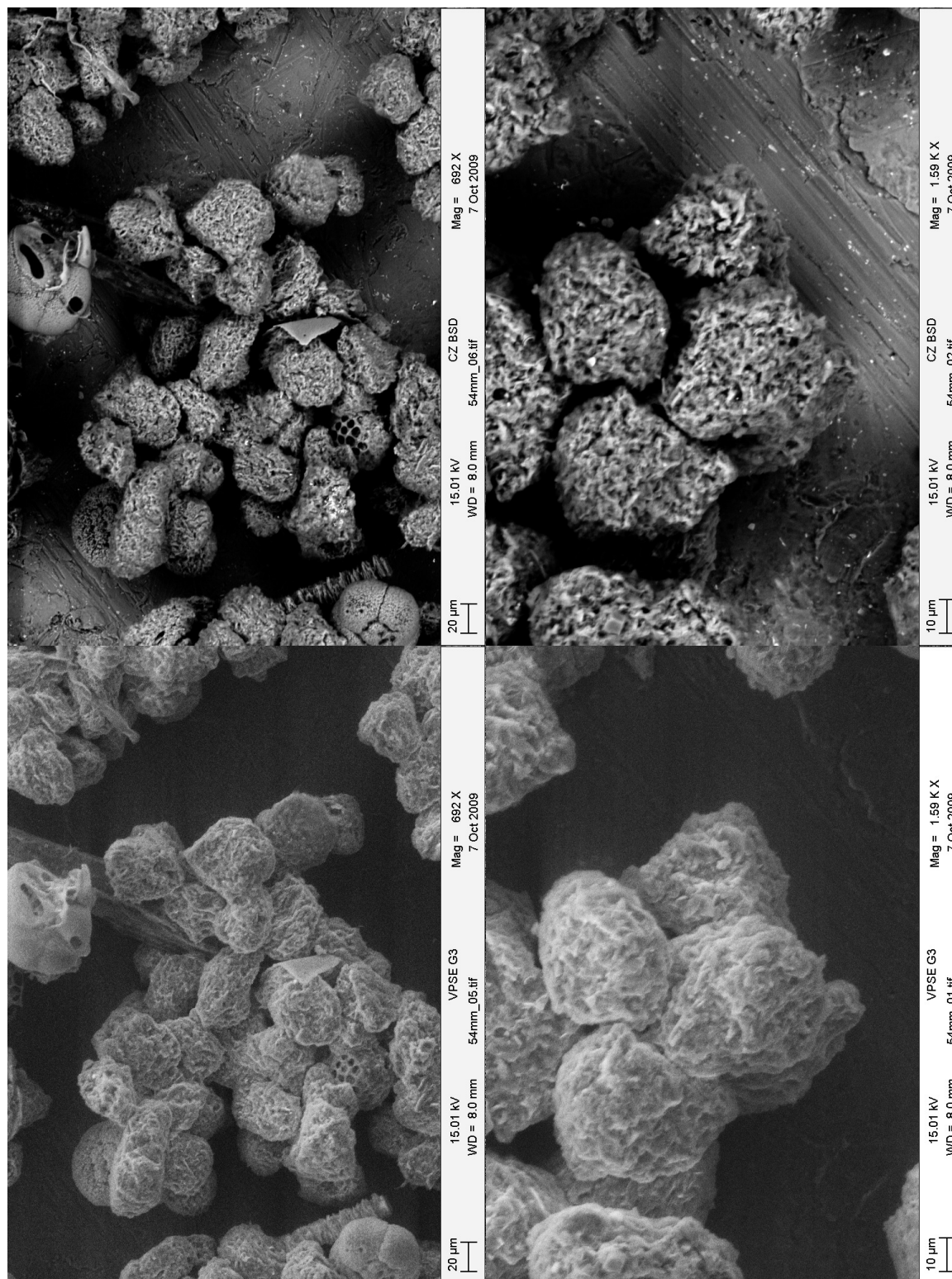
Fig. 6.19 Comparison of information obtained from ESEM variable pressure secondary electron (left) and back scatter (BSD) (right) detectors of wet-sieved pellets ranging from 54μm to 63μm diameter. Note the BSD's ability to highlight the structural elements of pellets, including micro-voids, which are on the order of microns in size.

As the vapour pressure drops within the ESEM (typically after 40 to 60 minutes), samples tend to dry, causing disruption of the pellet's outer membrane and, eventually, cracking of the clay pellets. This, allows images of pellet disintegration and provides information on their internal composition. Figure 6.20 shows the presence of sponge spicules, diatom fragments and remoulded clay exposed by drying.
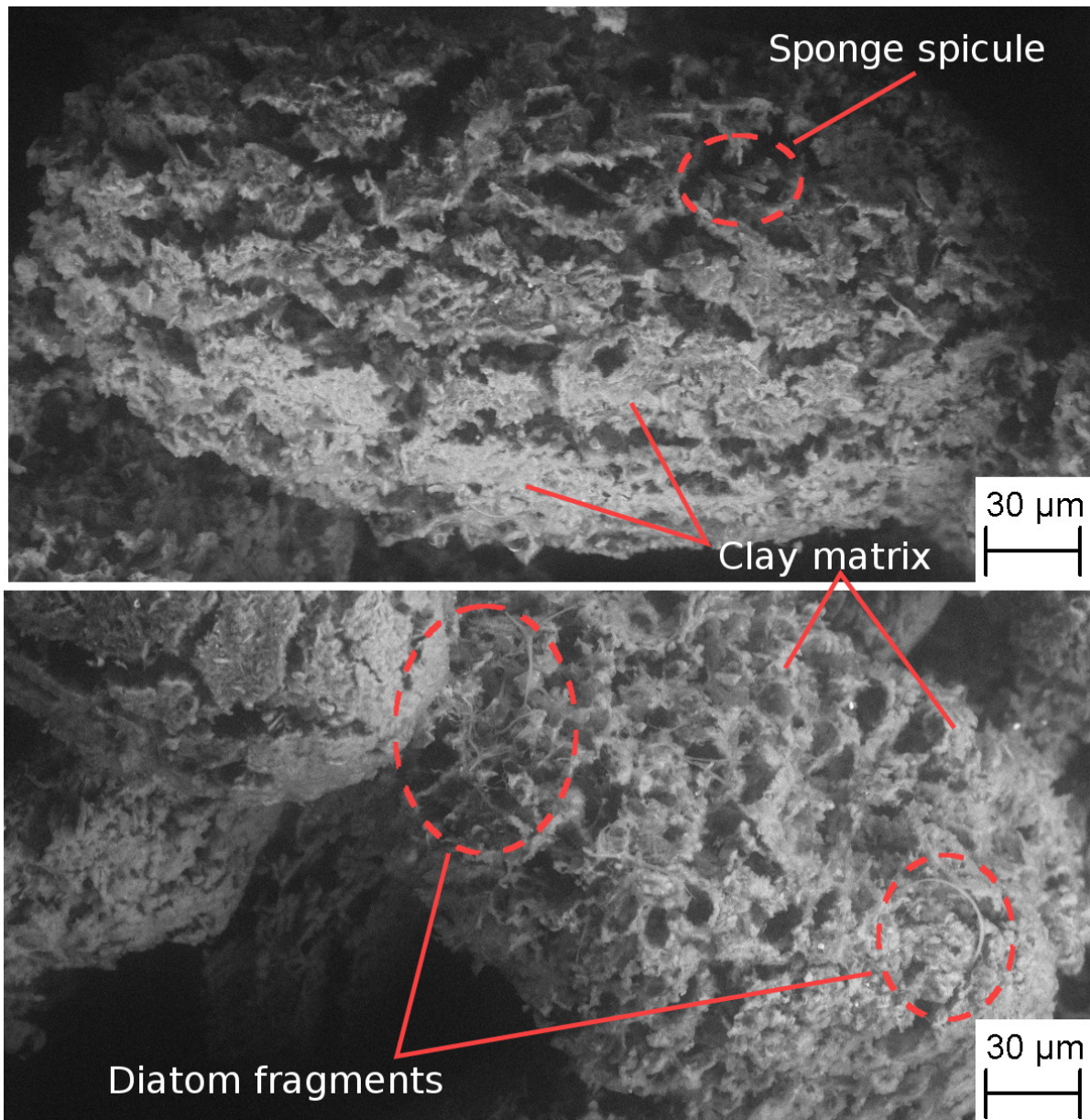
Fig. 6.20 Pellets gradually dried within the ESEM reveal internal contents comprising diatoms, sponge spicules and a clay matrix.

6.3.2 Energy Dispersive X-ray Spectroscopy

To identify the chemical composition of natural crust, energy dispersive X-ray spectroscopy (EDX) was undertaken on two crust samples from 0.25m depth during imaging with a scanning electron microscope (Leica Stereoscan 430). This method of chemical analysis produces a series of traces that show the relative abundance of specific elements in relation to others. The two results are shown in Figure 6.21. This figure indicates that the dominant elements in the crust material are Al, Si, Na, Cl, Fe and smaller amounts of K. Samples were coated with gold prior to imaging and EDX analysis, resulting in a large peak for Au. Na and Cl correspond to the presence of salt (halite). The major constituents are consistent with glauconite, and the proportion of Fe is significantly smaller than what might be expected compared to Hassan and Baioumy (2006). These elements are, however, also typical of clay minerals including muscovite, kaolinite and illite (of which glauconite is a alteration mineral). The EDX analysis cannot therefore conclusively prove that glauconisation has occurred. It does, however, indicate that precipitation of FeO or MgO is unlikely to be the origin of the crustal strength due to the relatively low abundance of these elements.

6.3.3 Concluding Comments

The results and observations presented in Sections 6.2 and 6.3 demonstrate the abundance of faecal pellets in natural samples, including information on their shape and size, and their collective and internal structure. It is concluded that the crust material contains 30% to over 50% faecal pellets by dry mass, which are predominantly smaller than 300μm in diameter. Based on these conclusions, the hypothetical bi-fold structure proposed in Chapter 3 is found to be a reasonable model of the natural crust. However, it was not explicitly known how the abundance of pellets influenced the sediment properties. To address this question, the next section considers the one-dimensional compression of samples of natural crust, no-crust and pellet-only samples. These tests investigate compressibility, coefficient of consolidation, stiffness and permeability of samples, and whether pellet abundance has an influence on these soil properties.
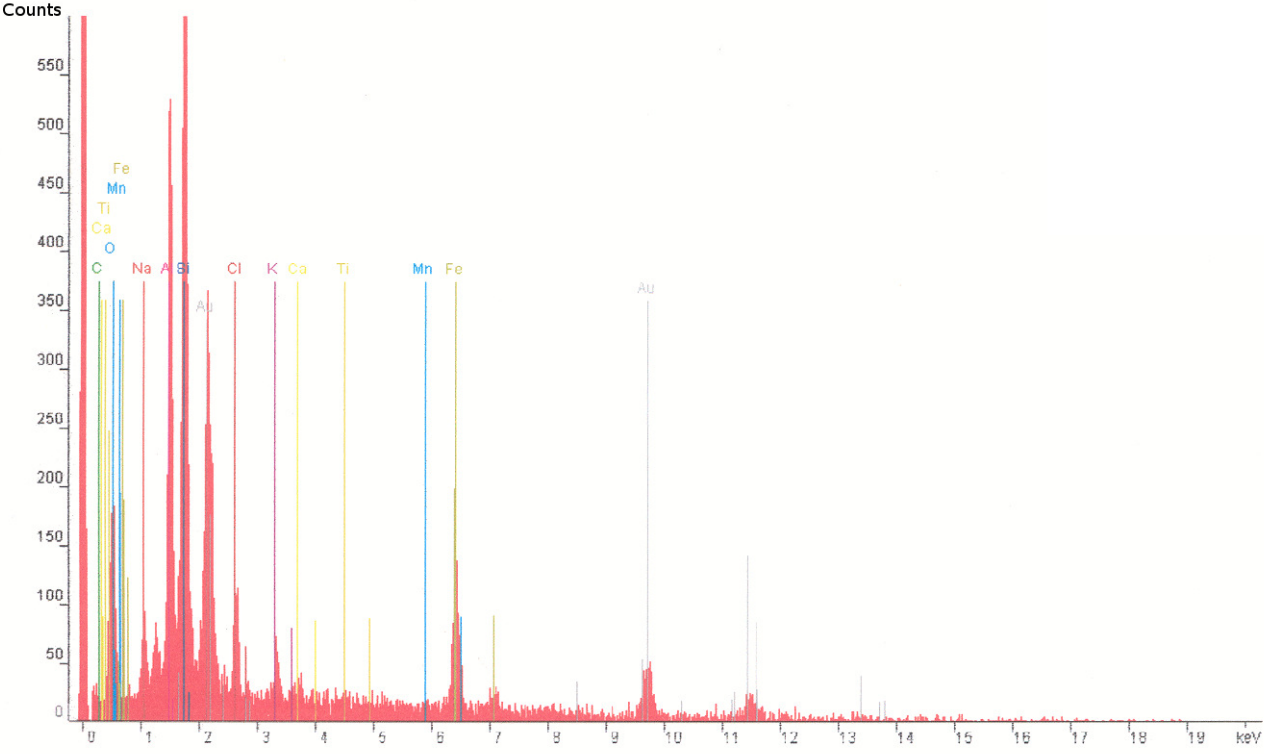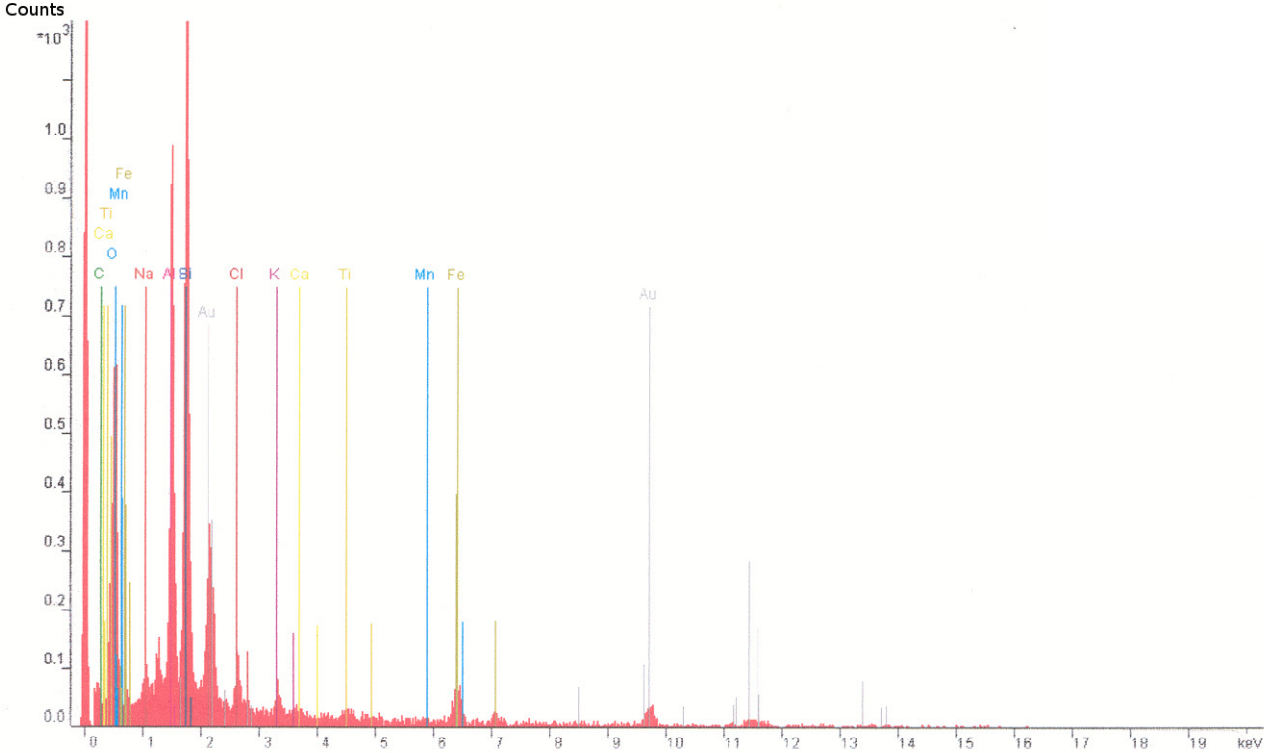
Fig. 6.21 Results of two EDX analyses on crust samples from 0.25m depth showing abundance of Al, Si, Na, Cl, Fe and smaller amounts of K.

6.4   Oedometer Testing

The observation that natural samples from below the crust contain only 15% faecal pellets by dry mass suggests that the process of burial plays a major role in reducing pellet numbers. This correlates with the observation that the crustal strength is limited to shallow depths. The demise of pellets due to crushing under overburden stress was one hypothesis for the loss of crustal strength. Oedometer tests were therefore undertaken to investigate the behaviour of crust sediments under stresses exceeding their in situ stress state.

6.4.1   Testing of Natural Samples

The following objectives were considered during oedometer tests:

- estimation of the preconsolidation stress of natural samples;
- investigation of the compression and unloading behaviour at both very low stresses and beyond the in situ vertical effective stress;
- investigation of the variation in physical properties during compression; and
- comparison with existing oedometer data from similar geographic locations, which considered samples taken from below the crust.

6.4.1.1   Sample Preparation

A conventional rear-loading oedometer apparatus was used to test crust samples from 0.25m and 0.3m depth. A stress range of 1kPa to 282kPa, doubling the load at each stage, was applied to the samples in order to investigate stresses from below to well past the in situ vertical effective stress. Oedometer test samples were prepared using the following procedure:

1. take a sub-sample approximately 0.03m thick from box core tube by cutting through the tube liner;
2. extrude the sample from the core tube liner;
3. trim the sample to a 0.075m diameter sample with a sharpened stainless steel cutter;
4. extrude the trimmed sample into a 0.02m high PTFE ring and trim flush with ring;
5. place the PTFE ring containing the sample on filter paper and a porous plastic disc and wrap in cling film;
6. X-ray CT scan the sample;
7. place the PTFE ring and the sample into an aluminium sample holder with a brass drainage disc at the base and clamp in-place;
8. place the entire set-up into a waterbath, reducing swelling by application of a seating stress comprising a porous plastic disc and a PTFE perforated drainage disc;
9. measure any volume change with a LVDT placed on upper surface of the PTFE disc and allow to stand for 5 hours or until changes in volume have ceased;

10. measure the water content of cut-offs;

11. wet-sieve the remaining cut-offs to determine the particle size distribution between 300μm and 38μm; and

12. apply consolidation masses to the loading frame.

The samples were permitted to consolidate for at least 24 hours at each stage or until primary consolidation was completed. Settlements were measured using an LVDT connected to a USB junction box and laptop running commercial data-logging software. To investigate the small-stress consolidation behaviour of the West African clays at 0.03m (above the crust), a low-friction, one-dimensional set-up was used comprising a light weight, self-hanging loading frame. Sample preparation and the testing procedure was the same as for the conventional oedometer apparatus although no doubling of the applied load was used for this test.

If the hypothesis that faecal pellet destruction is due to increasing vertical effective stress, the specific volume-vertical effective stress (v-σ'_v) relationship might have been expected to show the behaviour of a sensitive soil with large volume reduction at a preconsolidation stress, σ'_c of approximately 2.5kPa, corresponding to the in situ effective stress near the bottom of the crust. Furthermore, the percentage of pellets at each sieve fraction before testing should be significantly higher than the percentage following the test.

6.4.2 Faecal Pellet-Only Oedometer Tests

To provide comparisons with natural samples containing different percentages of faecal pellets, a pellet-only oedometer sample was prepared. This sample was created by sieving natural pellets of 125μm to 212μm diameter from bulk samples, and prepared by the following procedure:

1. seal a 40mm high PTFE split-plane oedometer shear-box using silicone sealant, to a steel baseplate containing a pre-embedded mini pore pressure transducer;

2. submerge the shear-box in a waterbath containing de-aired water;

3. decant the saturated pellets into the oedometer box;

4. allow settlement and rearrangement to occur under gentle vibration of the sample; and

5. level the pellet sample, if required, and measure the water content of the wet pellets.

An LVDT was used to monitor settlement at each loading stage and a pore pressure transducer was located at the centre of the base of the sample to indicate when the pore pressures had dissipated. The sample was consolidated in stages to a maximum vertical effective stress of 55.4kPa.

6.5 Oedometer Testing Results

Analysis and interpretation of the oedometer test results focused on the influence of faecal pellets. The sample containing pellets only was considered to be the upper bound of a series

of pellet-sediment mixtures ranging from 100% pellets, through crust containing over 50% pellets to the non-crust sample containing less than 20% pellets. Initial water contents for these samples were 253% for the non-crust sample from 0.03m depth, and 174% and 194% for crust samples from 0.25m and 0.3m, respectively.

6.5.1 One-Dimensional Stiffness

The tangential one-dimensional stiffness, determined by averaging adjacent pairs of stiffness values calculated for each stress increment, is plotted against the cumulative applied vertical effective stress on log-log axes in Figure 6.22. The corresponding specific volume, v-σ'_v relationship on semi-log axes is shown in Figure 6.23.

Figure 6.22 indicates that the relationship between the natural clay samples' one-dimensional stiffness and cumulative applied vertical effective stress falls within a relatively well-defined band of values, where the relationship may be approximated by a power law. In contrast, the relationship for the pellets-only sample is more complex. It is initially observed that the tangential one-dimensional stiffness increases with cumulative applied stress to a maximum of about 22MPa at approximately 1.6kPa vertical stress (path 'A' shown in Figure 6.22), before reducing to a relatively consistent stiffness of 6.6MPa to 7.8MPa (paths 'B' and 'C'). A 'collapse' in the structure and thus sudden drop in voids ratio corresponding to this rapid reduction in stiffness may have been expected. The reduction in stiffness to one third of the original value corresponds to a relatively large change in specific volume per stress increment in Figure 6.23. Lateral support for individual pellets will only be in the form of point contacts with adjacent pellets. Large, water-filled macro-voids will therefore be present initially. The reduction in stiffness may be due to the crushing of some pellets.

With a further increase in the vertical effective stress, it is observed that the tangential stiffness remains relatively constant (path 'C'). This may be due to continual breakage of pellets and particle rearrangement with increasing stress, which does not permit the stiffness to increase. The stiffness behaviour of the pellets then approaches a trend similar to the natural samples containing 50% pellets (path 'D'). Wet sieving of the pellet sample at the end of the pellet oedometer showed that 71% of pellets remained intact. 9% of the sieved material represented crushed pellet fragments sized between 63μm and 125μm. The remaining 20% of material represented crushed fragments less than 63μm. During consolidation, the crushed pellet material will progressively fill the macro-voids between intact pellets. The resulting mixture of pellet and pellet-fragment material will therefore approach the behaviour of a pellet-clay matrix typical of natural crust sediments.

Figure 6.23 also presents results obtained by De Gennaro et al. (2005) for samples taken from 4m depth (below the crust). The following points on the relative compression behaviours are noted:
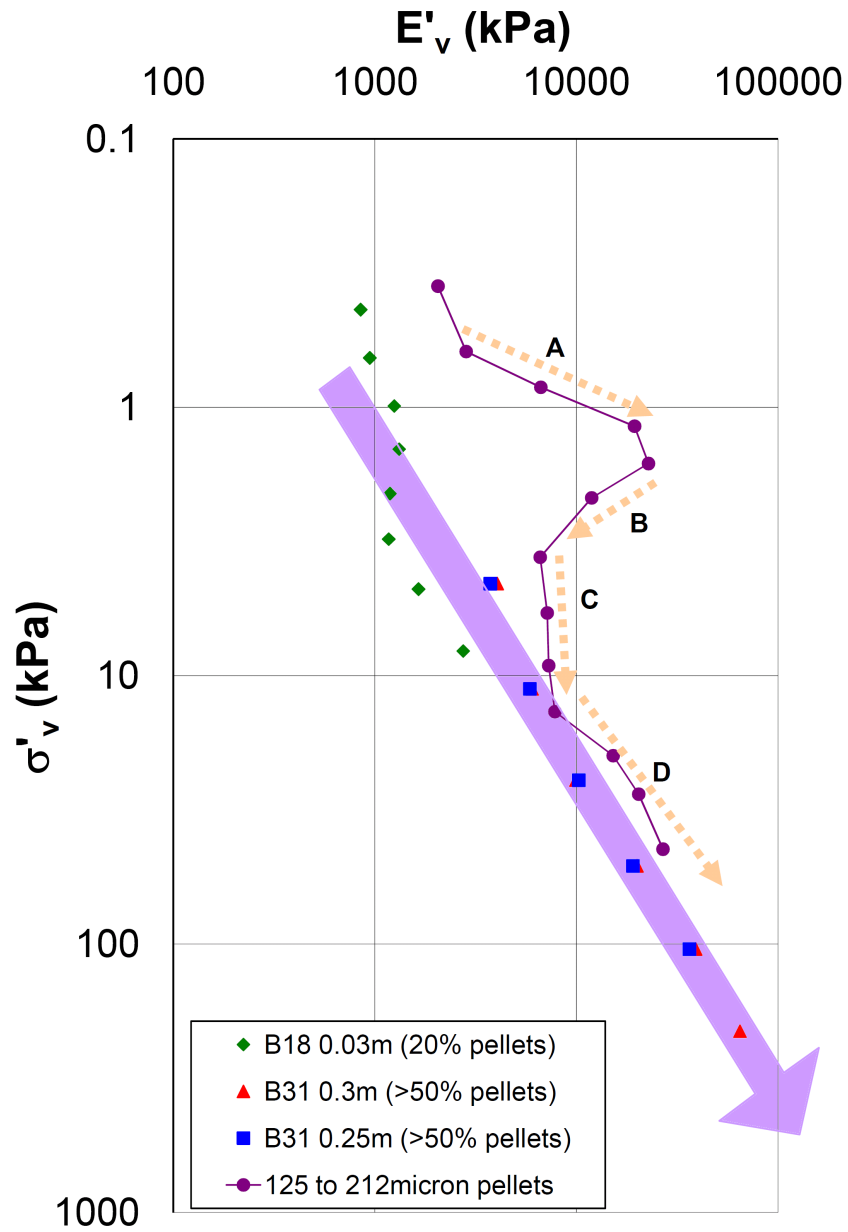
Fig. 6.22 Tangential one-dimensional stiffness E'_v plotted against cumulative applied vertical effective stress σ'_v for samples of only-pellets (125μm to 212μm diameter) and natural samples containing 20% to over 50% pellets (sample depths of 0.03m, 0.25m and 0.3m).

Fig. 6.23 Specific volume plotted against the applied vertical effective stress for samples of only-pellets and natural samples containing 20% to 50% pellets, compared to samples tested by De Gennaro et al. (2005).

- an apparent preconsolidation stress, σ_c' of 10kPa is suggested by crust material based on the method proposed by Casagrande (1936), and following ASTM 2435. Material above the crust exhibits σ_c' of 1kPa, and material below the crust apparently has σ_c'=25kPa.

- once past σ_c', the slope of the curve defines the compression index, c_c, which is found to be 1.88 above the crust and between 1.01 and 1.22 within the crust. Below the crust at 4m depth, De Gennaro et al. (2005)'s data indicates that c_c approaches the intrinsic compression line (ICL) defined by Burland (1990), with a value that is comparable to the crust;

- the swelling index, c_s is defined as the slope of the unloading-reloading section of the curves, and is found to be between 0.08 and 0.14 with an arithmetic mean of 0.11 for material above and within the crust;

- for the pellets-only sample, σ_c' is 9kPa; c_c approximates 1.34; and c_s is found to be between 0.02 and 0.07 with an arithmetic mean of 0.04.

Above the crust, the sediment exhibits a higher water content, with a more open structure. Pellets in this material are less well supported and therefore during one-dimensional

compression, some will crush and resediment as clay, resulting in a reduction in the number of pellets. Based on the compression index values, crust material is less compressible than overlying material. Le (2008) undertook oedometer tests on natural and remoulded samples of similar material, ranging from 0.5m to 18m depth, and measured a c_c of between 1.45 and 1.80 for natural non-crust samples and 1.20 for remoulded samples. The values obtained in this thesis suggest that the crust material is less compressible than the material below the crust based on a comparison with Le (2008)'s findings. The swelling index (c_s) values measured for the sample taken from 0.03m depth suggest that compression was irreversible up to 3kPa, which is consistent with crushing of pellets and the gradual collapse of the natural fabric.

The ratio of c_s to c_c is approximately 0.1 for crust material and 0.06 for material above the crust. These values are consistent with clay material. Burland (1990) suggests that this ratio may be a *"sensitivity indicator of fabric and inter-particle bonding in natural soil"* (Burland, 1990, p356). The c_s/c_c values are likely to be influenced by the bulk natural fabric of the crust, as well as variation in water content and specific fabric elements such as the percentage of pellets in a sample.

Figure 6.24 presents the information shown in Figure 6.23 on a normalised vertical axis of the void index (I_v), defined in Equation 2.1 following Burland (1990). De Gennaro et al. (2005) found the intrinsic void ratio at 100kPa, e_{100}^* and coefficient of consolidation, c_c^* for West African clays to be 2.13 and 1.03, respectively. Burland (1990), having investigated a wide range of natural and remoulded, reconstituted clays, identified that most natural clays lay on a line approximately parallel to and above the intrinsic compression line (ICL) defined by the remoulded, reconstituted clays. Cotecchia and Chandler (2000) extended Burland (1990)'s work and observed that a sensitivity framework could encompass the 'post-sedimentation'-compression behaviour of natural clays. The clays examined by Burland (1990) are found to lie between sensitivities of 3 and 5 when interpreted using the framework proposed by Cotecchia and Chandler (2000). The curves corresponding to various soil sensitivities for samples tested in this thesis are shown in Figure 6.24.

This figure indicates that the materials above, within and below the crust exhibit different sensitivity behaviour. De Gennaro et al. (2005)'s sample from 4m approaches S_t=5 before dropping towards the ICL (S_t=1). The sample from 0.03m crosses S_t=10 before dropping below 10 and suggests a continuation towards the ICL with increasing stress level. The rate of reduction in I_v is, however, much less than the sample from 4m depth. This shows that the natural structure of material above and below the crust is able to support a significantly higher vertical effective stress than a remoulded material before the structure begins to collapse under increasing stress. In contrast to both of these, the samples from crust material (0.25m and 0.3m depth) tend to approach and then follow sensitivity curves defined by S_t=5 and S_t=10. The pellet-only sample exhibits extraordinary behaviour, remaining on S_t of approximately 50.
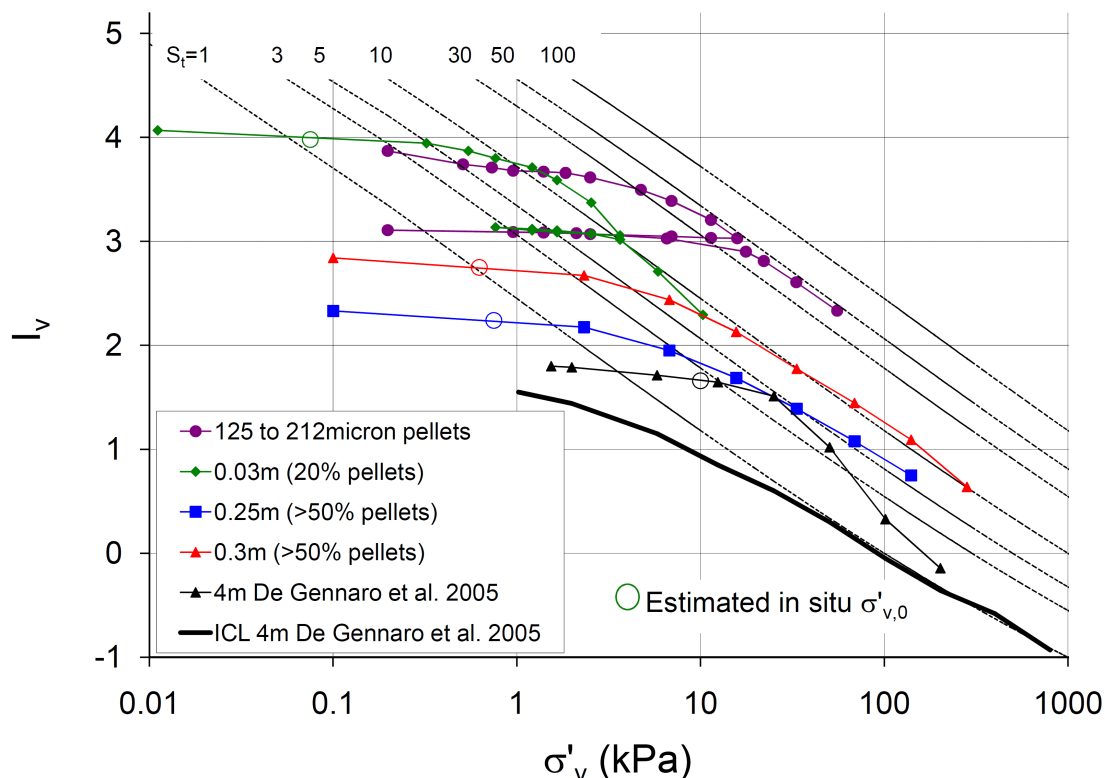
Fig. 6.24 Void index I_v plotted against the logarithm of applied vertical effective stress for samples of only-pellets and natural samples containing 20% to 50% pellets and compared to a sample from De Gennaro et al. (2005).

Its location, far above natural clays, is due to the large initial voids ratio produced by open, water-filled pores between individual pellets. The crust and pellet-only samples do not exhibit significant collapse of structure during one-dimensional loading. It is therefore proposed that a unique normal consolidation line does not exist for clays starting with these structures; rather, a family of normal consolidation curves for such pellet-rich samples may be developed. These observations also show that the crushing of pellets is *not* associated with loss of crustal strength.

6.5.1.1 Faecal Pellet Percentages in Natural Samples

Wet sieving of oedometer trimmings prior to testing, and of the consolidated sample after testing, was undertaken to provide quantitative information on the amount of pellet crushing caused by the tests. Figure 6.25 presents the results of the wet sieving. The following points are noted:

- total pellet percentages of non-crust material from 0.03m depth fell from 21% to 16% over a total stress change of 10kPa;

- the most significant reductions for non-crust material occurs for the 212μm to 300μm and 63μm to 125μm fractions;

- pellet percentages pre- and post- testing for crust material from 0.25m and 0.3m depth are comparable, with less than 4% variation in pellet percentage over a total stress change of 280kPa; and

- large reductions in pellet percentages are observed in fractions greater than 212μm for crust material, with a corresponding increase in material within the 63μm to 212μm fraction.

Within the crust, pellets are supported by adjacent pellets and an in-filling matrix of clay, which prevents pellets from excessive deformation and crushing. Nevertheless, larger pellets are more susceptible to crushing than smaller pellets, resulting in the reductions for pellets greater than 212μm in Figure 6.25. The increase in material from 63μm to 212μm must be due to crushed pellet fragments. De Gennaro et al. (2005) do not observe faecal pellets in the 4m-deep sample, which is consistent with the observation that pellets only comprise about 15% of the total dry mass by about 2m depth and the tendency for the $I_v - \sigma_v'$ curve to approach the ICL. It is noted, however, that the absence of a reference to pellets may only mean that they were not identified during the testing of samples.

6.5.2 Coefficient of Consolidation

The coefficient of consolidation (c_v) was determined following the procedure outlined in ASTM 2435. The general solution for determining the coefficient of consolidation is in terms of

$$c_v = \frac{T_v d^2}{t}, \tag{6.1}$$

where T_v is the dimensionless time factor; d is the drainage distance assuming pore pressure dissipation through a unit cell; and t is the time to reach the calculated proportion of primary compression completed. The dimensionless time factor, T_v, was determined using the square-root of time method (Taylor's Method), and interpolating the value for T_{90}, that is, the dimensionless time factor for 90% primary consolidation, and the corresponding time, t to achieve this condition. The variation of c_v with the cumulative vertical effective stress (σ_v') applied by the oedometer for the natural and pellet-only samples is shown in Figure 6.26. Figure 6.27 presents c_v plotted against the specific volume, v.
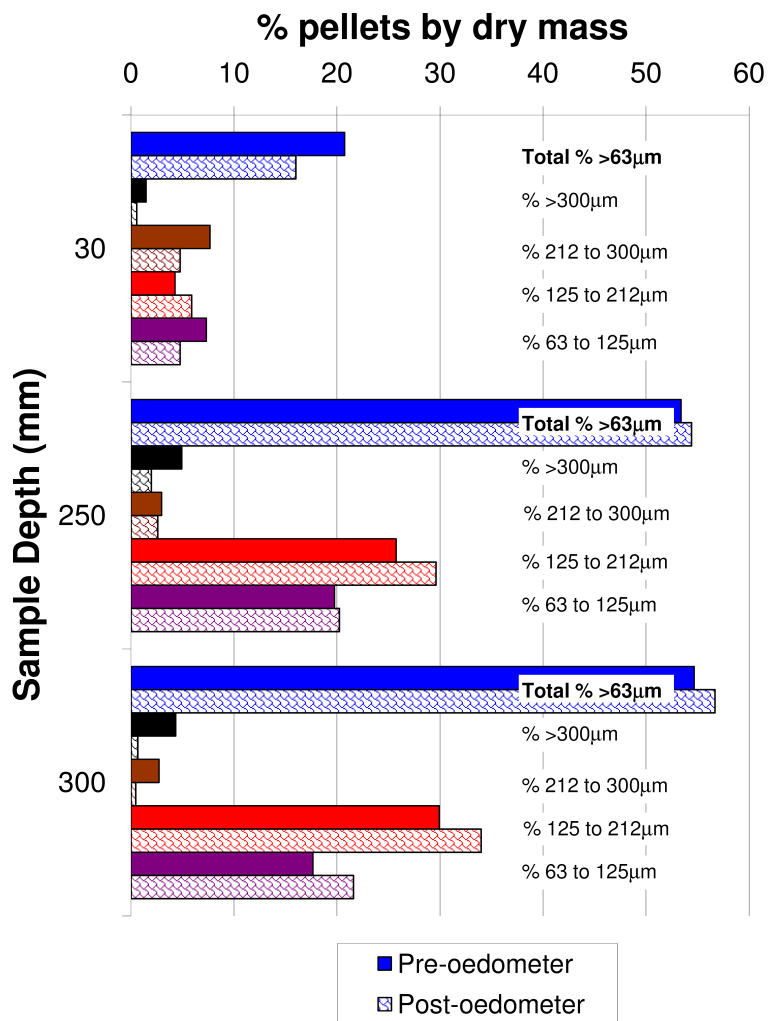
Fig. 6.25 Comparison of faecal pellet percentages before and after oedometer tests for natural samples of depths 0.03m, 0.25m and 0.3m.
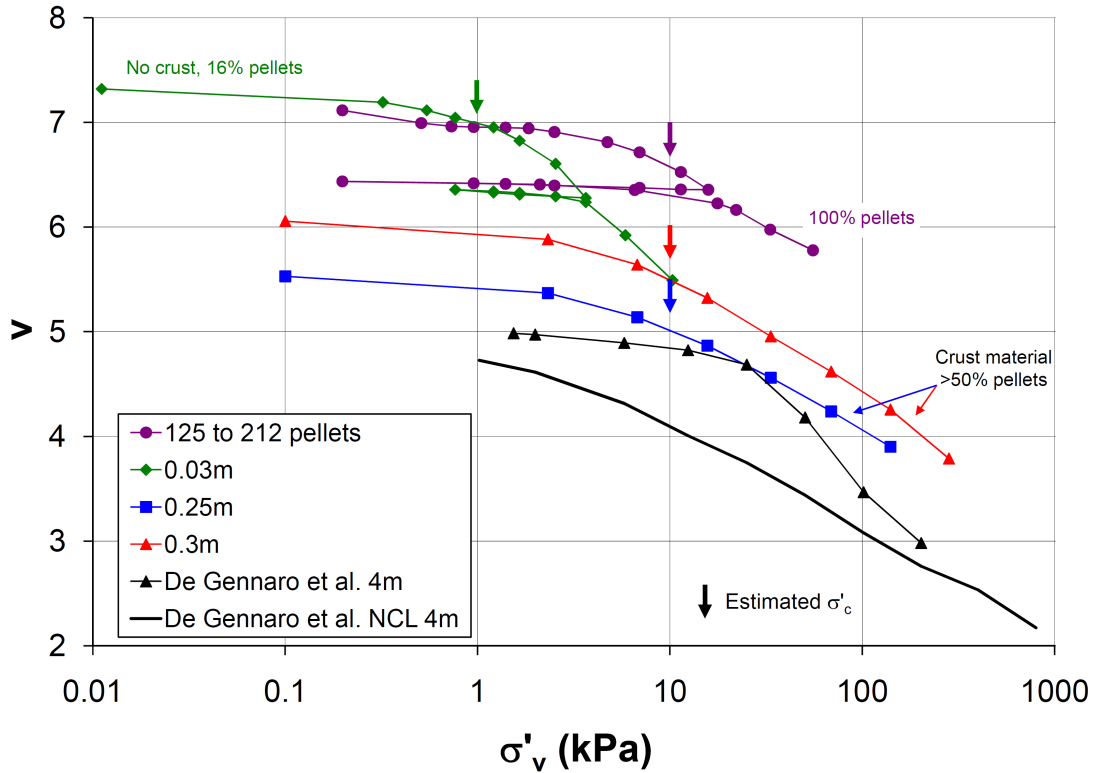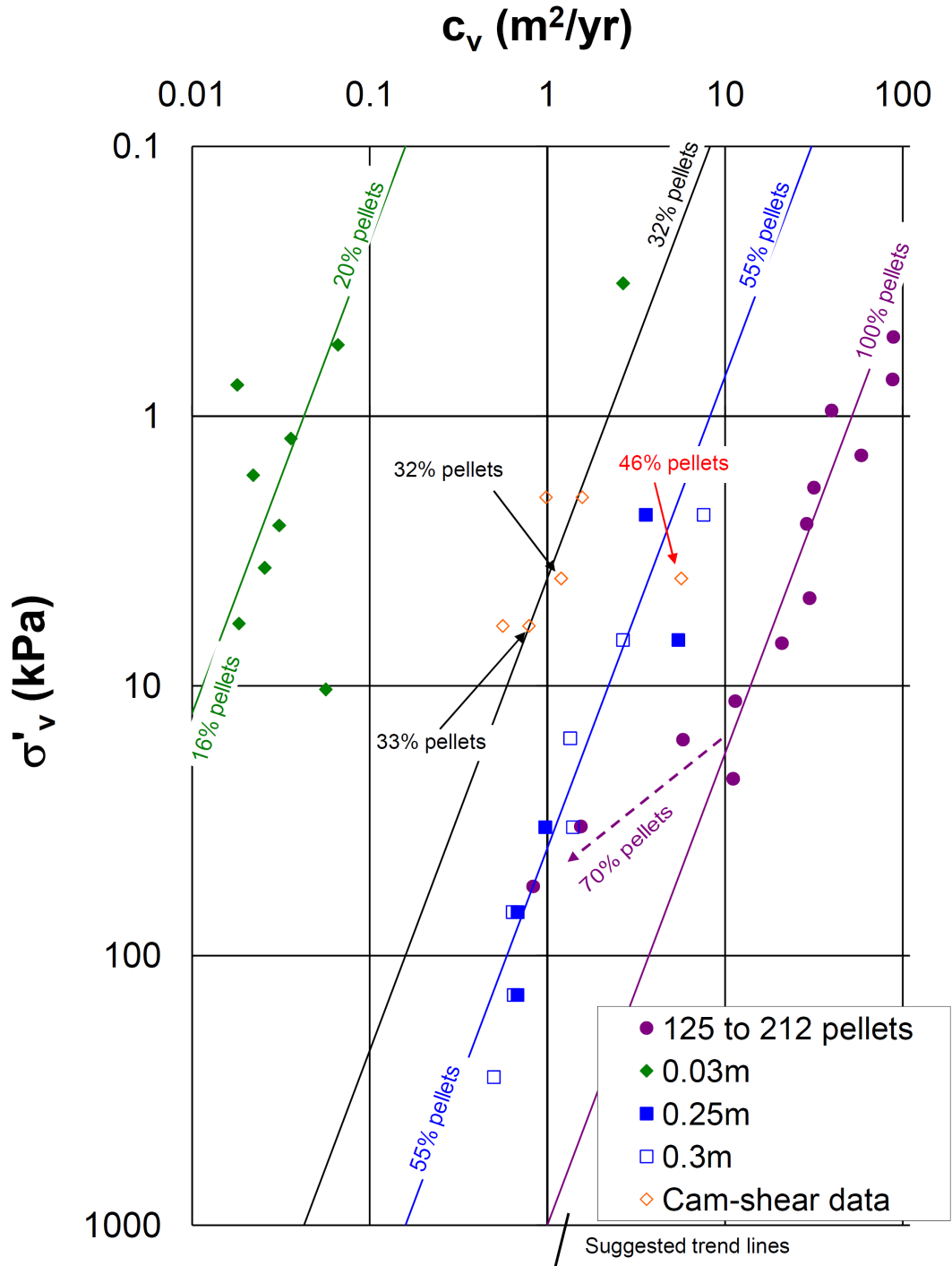
Fig. 6.26 The coefficient of consolidation plotted against the applied vertical effective stress for samples of only-pellets and natural samples containing 20% to 50% pellets.
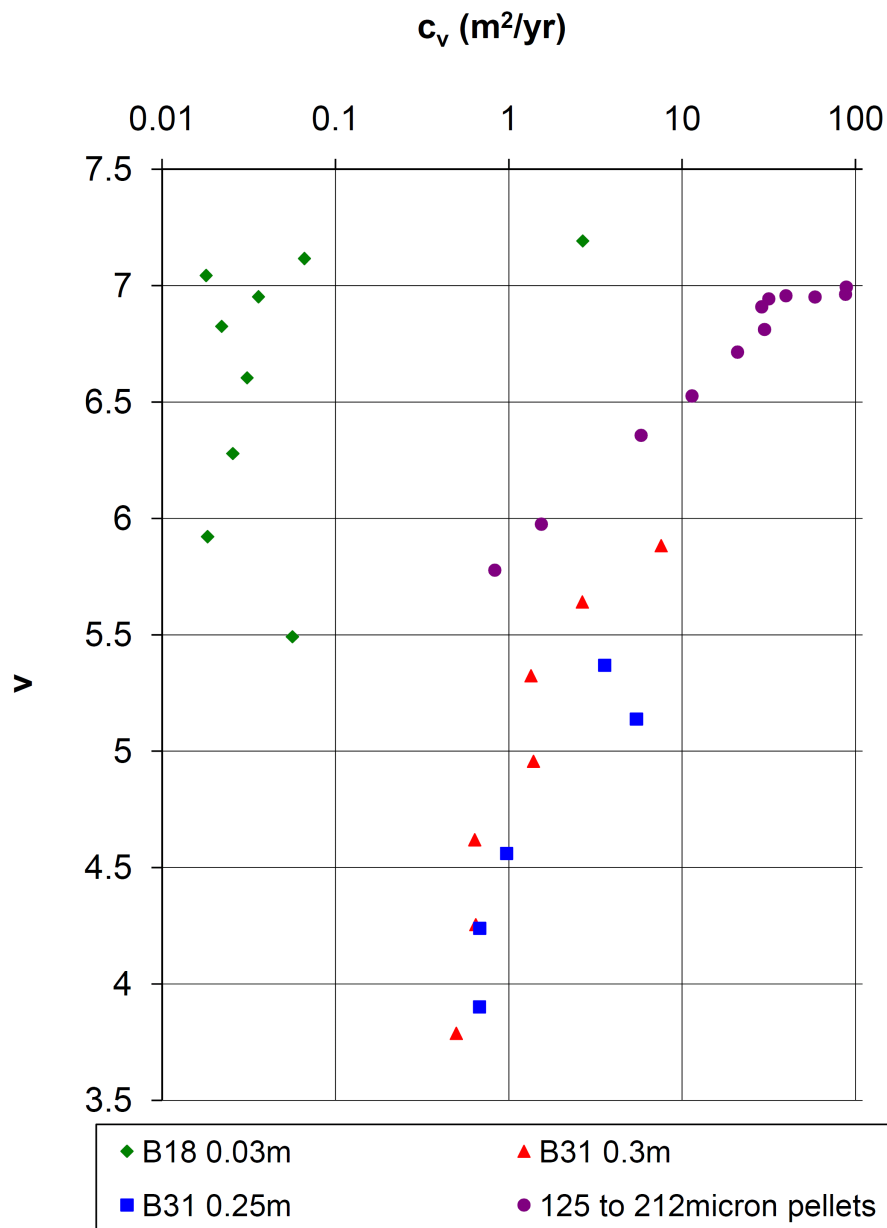
Fig. 6.27 The coefficient of consolidation plotted against the specific volume for samples of only-pellets and natural samples containing 20% to 50% pellets.

The following points are drawn from Figure 6.26:

- natural samples at different in situ vertical effective stresses exhibit significant variations in c_v with increasing vertical effective stress;

- samples at higher in situ vertical effective stresses (corresponding to crust material) exhibit c_v values at least one order of magnitude higher than the sample at a lower in situ vertical effective stress; and

- when compared to the literature, samples of crust material from 0.25m and 0.3m depth have significantly higher c_v values than would be expected for marine clays. For example,

146

Singapore Marine Clay has c_v of 0.5m^2/yr to 1.7m^2/yr (Chu et al., 2002) and 0.47m^2/yr to 0.6m^2/yr (Arulrajah and Bo, 2008).

A series of curves are drawn in this figure, which relate the percentage of faecal pellets to the variation of the coefficient of consolidation at a particular vertical effective stress. It is shown that a sample containing 100% pellets (diameters 125μm to 212μm) initially exhibits a c_v of up to 100m^2/yr. In contrast, a natural sample initially containing 20% pellets exhibits a c_v four magnitudes smaller. Natural samples with faecal pellet percentages of 30% and 50% map intermediate parallel lines on the logσ'_v - logc_v plot in Figure 6.26. The coefficient of consolidation for the pellet-only sample is found to reduce by an order of magnitude as the vertical effective stress rises from 20kPa to 40kPa. This results in c_v of the pellet-only material falling to values comparable with a natural sample containing over 50% pellets due to the fragmentation of pellets and the associated filling of void space. These observations are consistent with those made by Rowe (1972) who considered the importance of soil fabric on soil properties. Rowe (1972) noted the closure of open plant-root tubes due to increasing vertical effective stress, which caused a reduction in the coefficient of consolidation.

For a particular natural clay sample of known faecal pellet content subject to a proposed pipe stress, the coefficient of consolidation can be predicted. Figure 6.28 presents a summary of the empirical relationship between percentage of faecal pellets and the coefficient of consolidation for typical pipeline stresses in the form of a design-chart. The c_v values shown in this figure implicitly account for any crushing of pellets under the applied pipeline stress and therefore it is only necessary to measure the natural material's initial pellet percentage. It is observed from this figure that a dramatic decrease in the coefficient of consolidation occurs when the pellet percentage drops below 30%. This may coincide with a transition zone, where the behaviour of the natural soils move from being dominated by pellets to being dominated by the clay matrix.

By plotting the coefficient of consolidation against the specific volume v in Figure 6.27, it is shown that the pellet-only sample initially has c_v values three orders of magnitude greater than the very shallow (0.03m depth) natural sample at a comparable voids ratio. The arrangement of open voids within these two samples is thus demonstrated to be significantly different. The pellet-only sample comprises compact pellets of clay surrounded with large macro-voids, thus allowing the dissipation of excess pore pressures to occur. The natural sample, by comparison, is an open clay matrix containing only a few compact pellets, and permeability is controlled by the matrix alone. A transitional zone may be present for the pellet-only sample and the natural samples containing over 50% pellets between specific volumes of 5.5 and 6. In this region, the percentage of pellets of the natural and pellet-only samples are within 15%, and they may therefore exhibit similar mechanical properties.
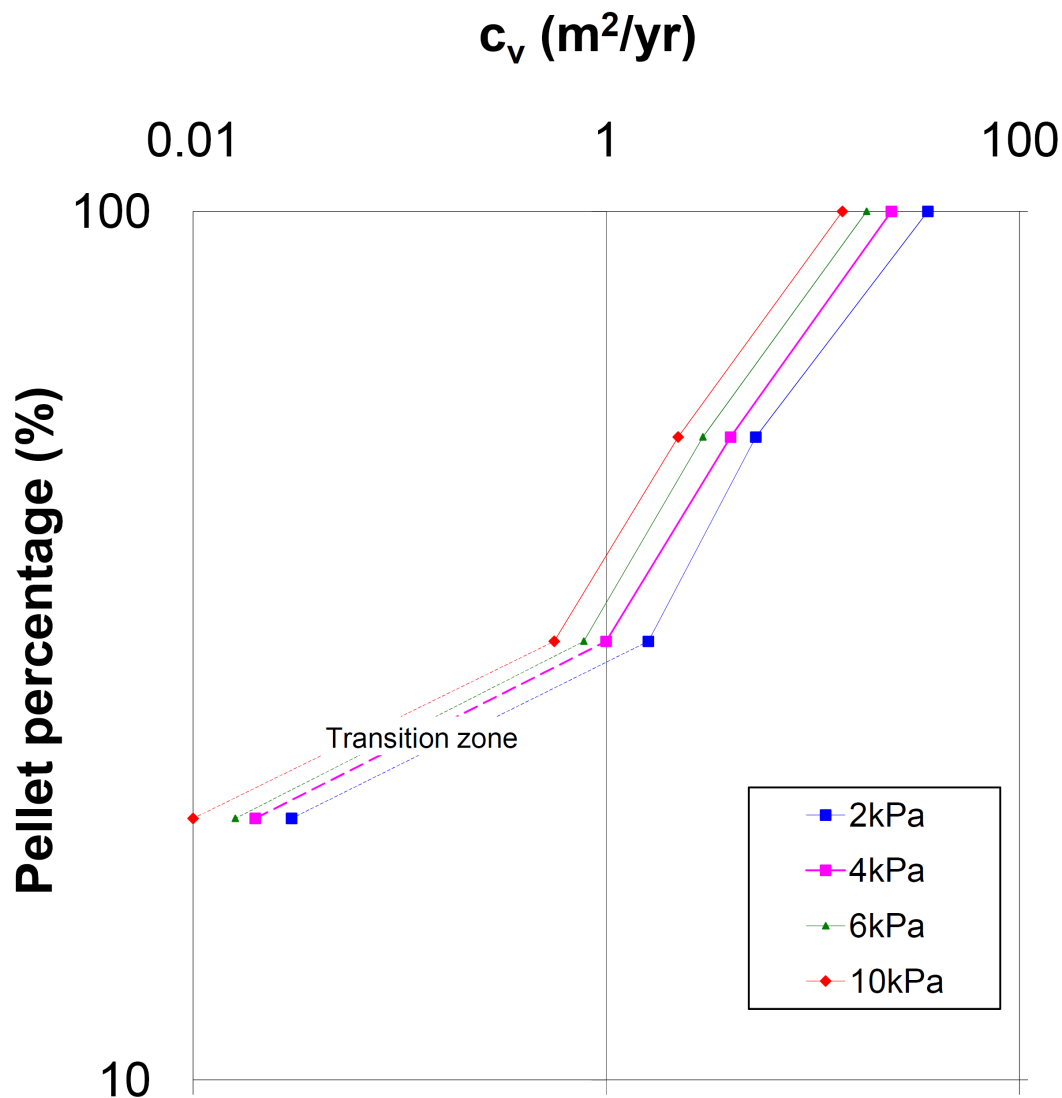
Fig. 6.28 Empirical design chart showing the relationship between the percentage of pellets, measured by wet sieving a natural sample and to the coefficient of consolidation.

6.5.3 Variation in Permeability

The variation in permeability, k, with respect to the one-dimensional stiffness is shown in Figure 6.29. It is observed that the pellet-only sample tends towards the behaviour of the natural samples as the stiffness increases. The permeabilities of deeper samples are found to be higher than shallower, more compressible samples that exhibit a more open fabric. Furthermore, it is observed that the relationship between the permeability and the one-dimensional stiffness of material containing over 50% pellets may be approximated by a power law. As noted from

measuring the percentage of faecal pellets before and after compression, comparable numbers of pellets were present at both stages in these samples. The permeability, however, decreased by over two orders of magnitude. This suggests that the matrix of unpelletised clay surrounding pellets has compressed, and elastic deformation of the pellets and minor crushing has occurred. The initial permeability at low confining stress may represent drainage predominantly around pellets, facilitated by the open fabric of the matrix clay and open burrows. During one-dimensional compression, the matrix fabric collapses, resulting in forced drainage through a mixture of both pellet material and compressed matrix clay, thus decreasing the permeability.

As expected, material containing fewer pellets exhibits lower permeabilities and lower one-dimensional stiffness. The pellet-only sample initially exhibits high, and relatively constant permeability before dropping by two orders of magnitude towards the crust samples containing over 50% pellets at comparable stiffness. This corresponds to the transitional zone between these samples, observed in Figure 6.26 and 6.27.
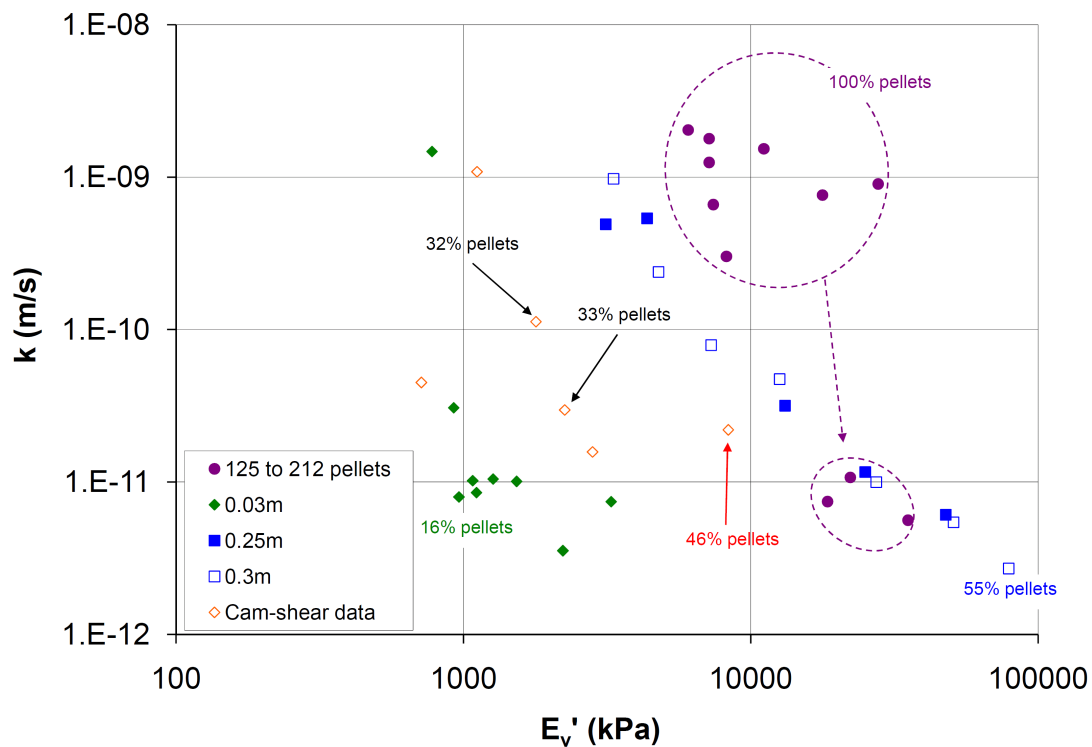
Fig. 6.29 The permeability, k plotted against the tangential one-dimensional stiffness, E_v' for samples of only-pellets and natural samples containing 20% to 50% pellets.

6.5.4 Discussion on Physical Processes During Consolidation

Based on the sieving of samples before and after oedometer tests, it is not explicitly known when the majority of the pellet crushing occurs. During an oedometer test on 'conventional' soils, some crushing and rearrangement of particles occurs during initial loading. It is likely that a similar process occurs for the samples tested in this thesis. With increasing load, crushing occurs, initially of asperities and then of an increasingly larger proportion of particles (e.g. McDowell and Bolton, 1998; Bolton et al., 2008). The v - σ'_v relationship will thus define the compression index, c_c. This interpretation of the mechanical behaviour during one-dimensional compression of the tested natural samples is likely to be a simplification of the actual process. The tested material consists of robust grains (pellets) within a highly compressible matrix, so during loading, two phases of consolidation may occur concurrently, one of the matrix and the other of the pellets. Furthermore, the percentage of pellets will have an influence on whether the consolidation behaviour is dominated by pellets or the matrix. Initially, at low stress levels, the behaviour is likely to be dominated by the more compressible matrix. Robust pellets may be free to move within the matrix or, conversely, the matrix is free to flow round the pellets. As the stress level increases, deformation of poorly-supported pellets may contribute to the bulk consolidation characteristics, and some pellets may begin to crush. Finally, as the stress level reaches the crushing stress of individual grains, the proportion of clay matrix to grains increases due to resedimentation of the contents of crushed pellets. This stress level was not achieved in testing undertaken in this thesis as most pellets are still present after oedometer tests.

Stresses of over 280kPa during oedometer testing are reached in situ by sediments at over 100m depth. As noted previously, at a depth of 1.9m, corresponding to material below the crust, the sediment contained only 15% faecal pellets by dry mass (see Figure 6.7). It is impossible to believe that the species of invertebrates responsible for faecal pellets in recent, shallow sediments were not also acting in sediments tens of thousands of years ago, which are now more deeply buried and found to be relatively free of pellets. The observation that only a minimal change occurs in the number of pellets present in crustal samples loaded to high stresses, demonstrates that increasing overburden stress is not, on its own, the cause of pellet destruction, nor of loss of crustal strength. Another explanation for the loss of strength and reduction of pellets in the sediment must be sought.

6.6 Strength of Faecal Pellets

The faecal pellets observed in tested samples are likely to have been produced by a large number of different invertebrate species. Their presence illustrates the significant biological influence of burrowing invertebrates on the crust material. The processes involved in pellet

formation by invertebrates vary depending on species, but include activity within three sections of the digestion system: fore-gut, mid-gut and hind-gut following Barnes et al. (1988). Factors that may influence the robustness of pellets, and their mechanical behaviour once excreted, include:

- the presence of salivary glands which coat ingested food with mucous in the fore-gut;
- mechanical break-down and sorting by contraction of muscle cells in the mid-gut wall (Barnes, 1974);
- desiccation by osmosis; and
- formation of distinct pellets with mucus, described as 'moulding' by Barnes (1974) and 'consolidating' by Moore (1931a) in the hind-gut.

Moore (1931a,b) discusses the faecal pellets in muddy sediments within the Clyde Sea Area, West Scotland, which can represent the entire composition of the sediment. Pellet formation generally occurs close to the sediment-water interface, where animals have access to sufficient oxygen. By contrast, at greater sediment depths, conditions remain favourable for smaller and more robust creatures such as nematodes. Information relating to relative soil stiffness was reported by Moore (1931b), who observed comparatively stiff, clayey conditions at a depth of 0.2m in the Clyde Sea sediments. No explicit description of the stiffer layer is given; however, its location corresponded to sediment containing over 50% pellets ranging from 0.1mm to 1mm in length. This suggests a strong relationship between faecal pellets and sediment strength.

The resilience of moulded pellets has also been noted by Moore (1931a), as the pellets were resistant to fairly rough handling, and able to withstand boiling in sulphuric acid and strong caustic soda. These observations led Moore (1931b) to suggest that pellets may remain in their pelletised form for hundreds of years in an accumulating sediment.

A reference to faecal material along the African coast is described by Moore (1939) in quoting Buchanan (1890). The 'mouse-dropping-like' pellets were in such abundance around the mouth of the Congo River that Buchanan (1890) designated it as a 'coprolitic mud', defined as castings of mud-eating organisms by Amstutz (1958). Thorp (1931) describes the occurrence of ovoid pellets off the coast of Panama in water depths ranging from 2,000m to over 3,500m; and their relative abundance in sediments ranging from 26.1% to 44.1%. Their discussion suggests that the shape and size of these pellets indicate an organic excrement, however, due to their apparent robustness, Thorp (1931) considered them to more likely be the creation of chemical and physical aggregation. Thorp (1931) suggests that the presence of bacteria in sediments surrounding pellets would tend to disseminate the internal contents, as the pellets become the food source for the next smaller order of organism. As demonstrated by Moore (1931b), however, pellets are robust enough to withstand hundreds of years within the soil profile.

Schafer (1972) considers the preservation of faecal pellets in sediment. Based on the modification processes within the invertebrate gut, and the method of expulsion, faeces may or may not become a constituent of the sediment profile. Schafer (1972) suggests that faecal material suited to the formation of deposits are those produced by sediment dwellers, such as burrowing invertebrates, which require expelled material to be transported away from their immediate surroundings, or which deposit pellets in abandoned sections of burrows. Such creatures create either segmented or egg-shaped pellets. These pellets are "*dehydrated, very compact and suited for transportation*" (Schafer, 1972, p426). Finally, it has already been demonstrated by Figure 6.9 that in West African crust samples, a linear relationship exists between the percentage of faecal pellets and the undrained shear strength of the same core.

6.6.1 Faecal-Pellet Crusher

The strength of individual faecal pellets, has not been explicitly investigated by previous researchers. Indeed, pellets have not been considered as an engineering material. To provide a quantifiable measure of pellet strength, a novel pellet-crushing device was designed, and is shown in Figure 6.30. Individual pellets were placed on a saturated porous-plastic platform and covered with a thin, impermeable, plastic membrane. A suction pressure, s, was applied to the pellets through the porous plastic in 0.1kPa increments by lowering a reservoir of water (open to the atmosphere) relative to the porous plastic platform. The plastic membrane was forced onto the pellets by the atmospheric pressure acting on the outside of the membrane. As most pellets encountered in the natural samples were between 63μm and 300μm, a microscope was used to observe the point at which individual pellets crushed.

The results of several pellet-crushing experiments are presented in Figure 6.31. Results are plotted as the number of individual pellets crushed at a particular suction pressure. A typical example of a pellet before and after crushing is shown in Figure 6.32. Figure 6.31 demonstrates that pellets crush at pressures ranging from about 0.1kPa to 1kPa. This represents a significant variation in pellet strength, which may be due to the age, stage of degradation, internal composition and in situ alteration experienced by the pellet post-excretion. The strength of groups of pellets is found to be strongly influenced by the presence of adjacent pellets, as seen by the 'grouped pellets' region in Figure 6.31. Groups allow arching of the applied stress around centrally located pellets. The mechanism involved in the crushing of pellets using this pellet crusher is considered to approximate the crushing of grains between platens, with the pellet failing in tension at its mid-plane.

Converting the suction stress, s to an unconfined compressive strength, σ_c is undertaken with caution due to the complexity involved in applying the crushing force via a flexible membrane. It is evident from the loading process that the pellet will experience not only force applied over the physical contact area, but also a tensile force due to the area of plastic mem-

Fig. 6.30 Novel pellet-crushing device used to apply a crushing stress onto pellets by the application of suction to a thin plastic membrane.
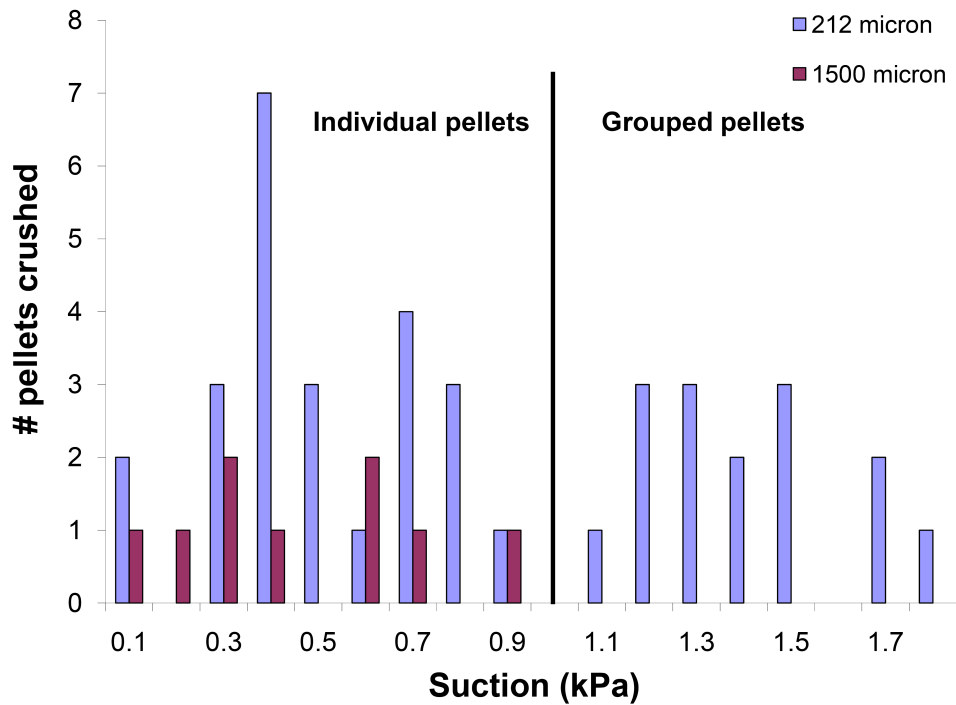
Fig. 6.31 Results of pellet-crushing tests, showing the number of pellets crushed at each stress increment for pellets between 212μm to 300μm, and greater than 300μm.
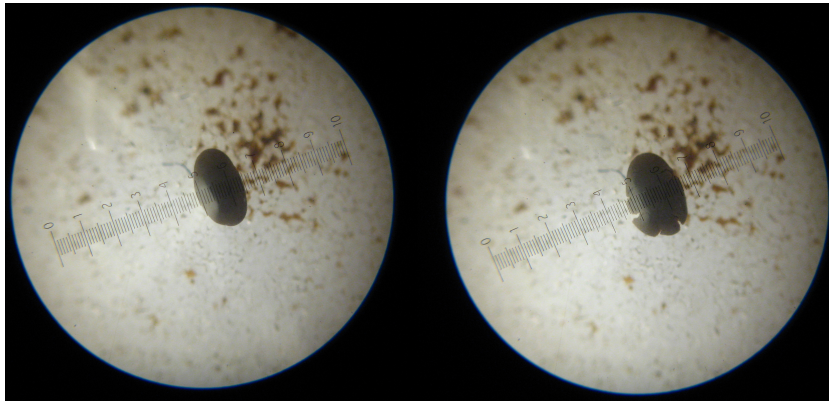
Fig. 6.32 Photographs of pellets before and after crushing.

brane which drapes over the extremities of the pellet, as shown in Figure 6.33. To accurately determine the stress at which the pellet crushes, the elasticity and variance in shape of the plastic membrane needs to be accounted for. As an initial estimation, it is appropriate to assume that the pellet experiences a stress that acts over the membrane's draped area, approximated as an ellipse with draped distances of d_{pellet} (the pellet's diameter) from the pellet as shown in Figure 6.34.

Fig. 6.33 During crushing, the thin plastic membrane may be seen to drape over pellets, resulting in a water-filled void between the sides of the pellet and the membrane.

Based on Shipway and Hutchings (1993), the tensile stress, σ_t at failure of lead glass spheres may be approximated by:
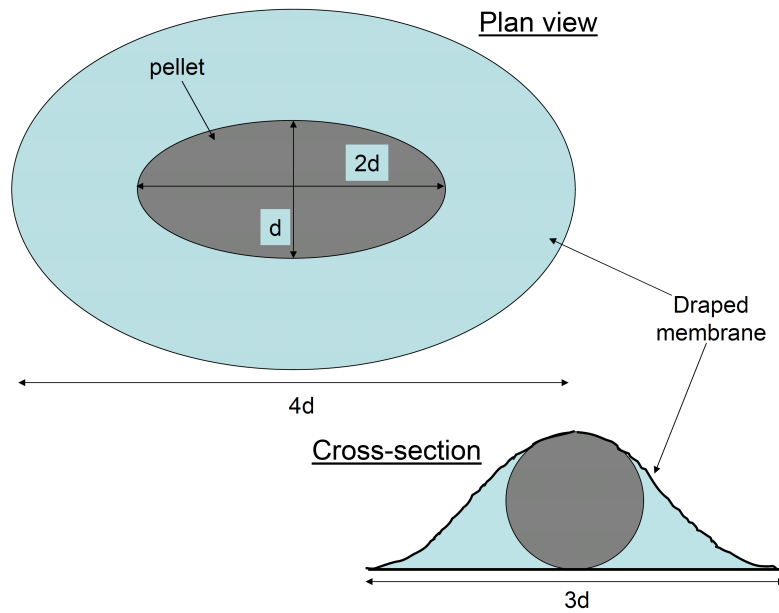
Fig. 6.34 Schematic diagram of an idealised pellet in plan view and cross-section showing the approximated drape of the plastic membrane.

$$\sigma_t = \frac{0.4F_0}{\pi R^2}, \tag{6.2}$$

where F_0 is the platten force at failure, found to be $3\pi s d_{pellet}^2$ based on the assumption of an elliptical drape, and R is the radius of the sphere ($\frac{d_{pellet}}{2}$). The faecal pellets fail in tension, producing vertical failure planes as shown in Figure 6.32, which is similar to that of the spheres investigated by Shipway and Hutchings (1993). The tensile force at failure for the tested pellets is therefore approximately five times the applied suction pressure. An unconfined compressive strength (UCS) can then be determined by assuming a conservative strength factor of 10 (e.g. Hudsen and Harrison, 1997). The individual pellets therefore exhibit UCS values ranging from 5kPa to 50kPa.

6.6.2 Shearing of Faecal Pellets

To provide a comparison with Cam-shear tests on natural samples, interface and internal shearing of pellet-only samples were undertaken. Pellets with sieved diameters of 125μm to 212μm were normally consolidated in the Cam-shear split-plane box under vertical effective stresses ranging from 0.3kPa to 3.5kPa. Samples were prepared by the method described in Section 6.4.2 for the pellet-only oedometer sample. Shearing at the split-plane to obtain the pellet-pellet strength was then completed. Interface tests on rough (100μm) and smooth (5μm) interfaces were also undertaken at confining stresses ranging from 1kPa to 4kPa. All

tests were completed at a shearing rate of 0.05mm/s. Though this shearing rate represented undrained shearing for natural soils, pellet-only samples have shown to exhibit coefficients of consolidation of up to $100\text{m}^2/\text{yr}$, and therefore, this shearing rate is considered slow enough to induce drained behaviour.

The results of peak strength for all tests are shown in Figure 6.35. This figure presents a linear relationship between the peak shear strength and the applied effective stress. This relationship is contrary to the Cam clay yield surface proposed by Schofield and Wroth (1968), and the test results of natural samples presented in Chapter 3. It is, however, reminiscent of the shear behaviour proposed by Hoek (2006) for rough and smooth rock joints, which assumes that the behaviour may be modelled by the Mohr-Coulomb equation,

$$\tau, \tau^* = c' + \sigma'_v tan\phi', \tag{6.3}$$

where τ, τ^* are the interface and soil shear strengths, respectively, c' is the cohesion intercept produced by cementation at the sheared interface, σ'_v is the applied vertical effective stress during shearing, and ϕ' is the measured angle of friction.
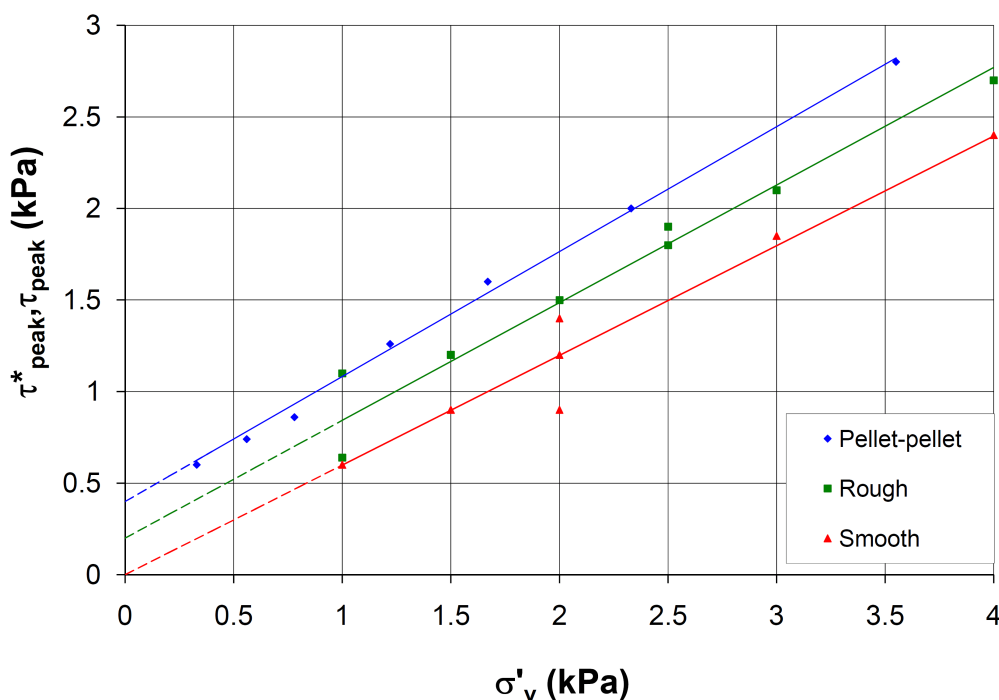
Fig. 6.35 Peak strength results from Cam-shear testing of 125μm to 212μm pellets. Soil-soil, smooth and rough interface results are shown, demonstrating a linear relationship for all tests.

Figure 6.35 shows that the smooth interface tests exhibit a relationship that passes through the origin, whereas the rough interface exhibits a cohesion, c' of 0.3kPa. Soil-soil tests approx-

imate the shearing behaviour between very rough platens, giving a c' of 0.4kPa. Figures 6.36 and 6.37 present strength-displacement data for these tests. These figures demonstrate that samples sheared on rough interfaces reach a peak in strength within a shear displacement of about 5mm, before strain softening by between 15% and 35%. Conversely, samples sheared on the smooth interface either remain at a constant strength for the duration of the test, or demonstrate a slight increase in strength before reaching a constant value after a shearing distance of about 90mm.
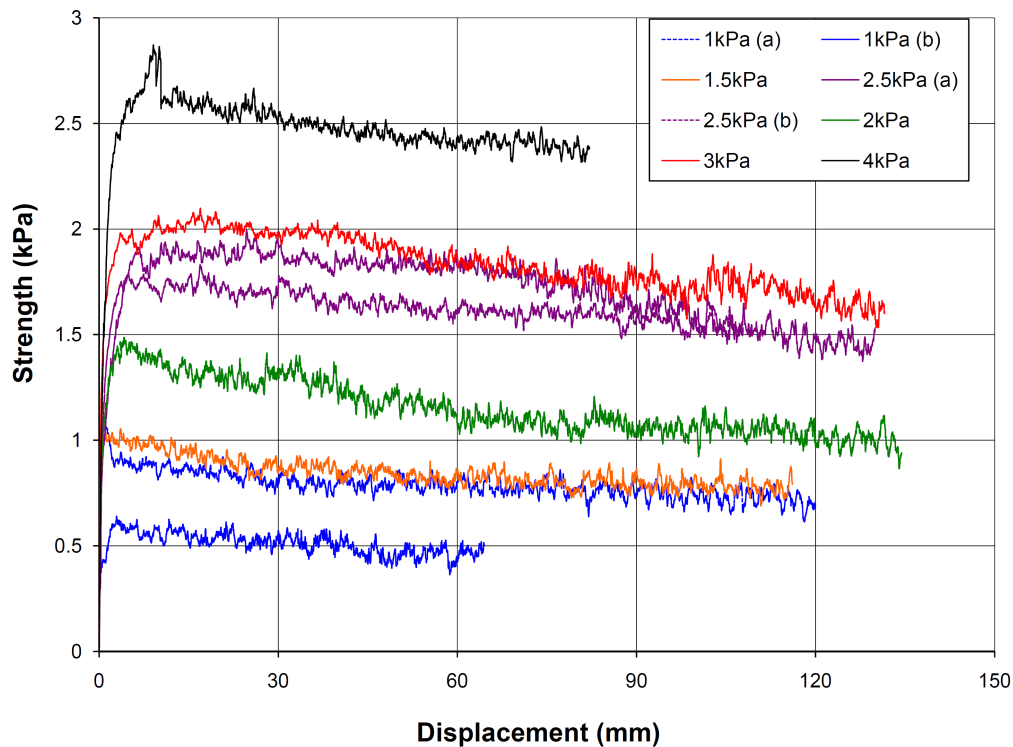
Fig. 6.36 Rough interface, strength-displacement plots for pellet-only samples, showing peak strength before softening behaviour at large displacements.

The strengths exhibited at the end of interface shear tests are plotted in Figure 6.38. This figure shows that when sheared on either smooth or rough interfaces for sufficient distance, the pellets will continue shearing at constant volume, that is, the pellets reach a critical state. The interface friction coefficient indicated from this figure is $\mu=0.6$. This is the same value as μ^*; the soil-soil friction coefficient assumed for Cam-shear testing of natural samples in Chapter 3.

Figure 6.39 shows rough and smooth pipeline coating interfaces after shearing. This figure clearly demonstrates that when sheared on an interface with roughness of 100μm, pellets are continuously ground, crushed and destroyed. In contrast, little to no grinding or crushing is observed for the smooth interface. This indicates that different shearing mechanisms are

157
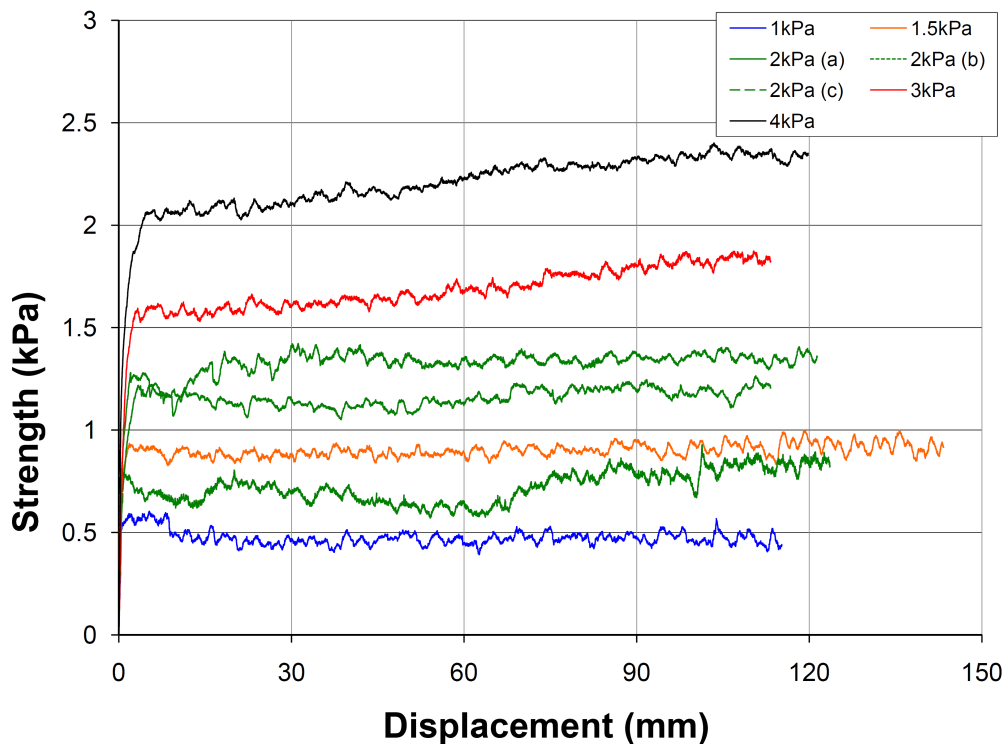
Fig. 6.37 Smooth interface, strength-displacement plots for pellet-only samples, showing relatively constant strength after about 90mm shearing distance.
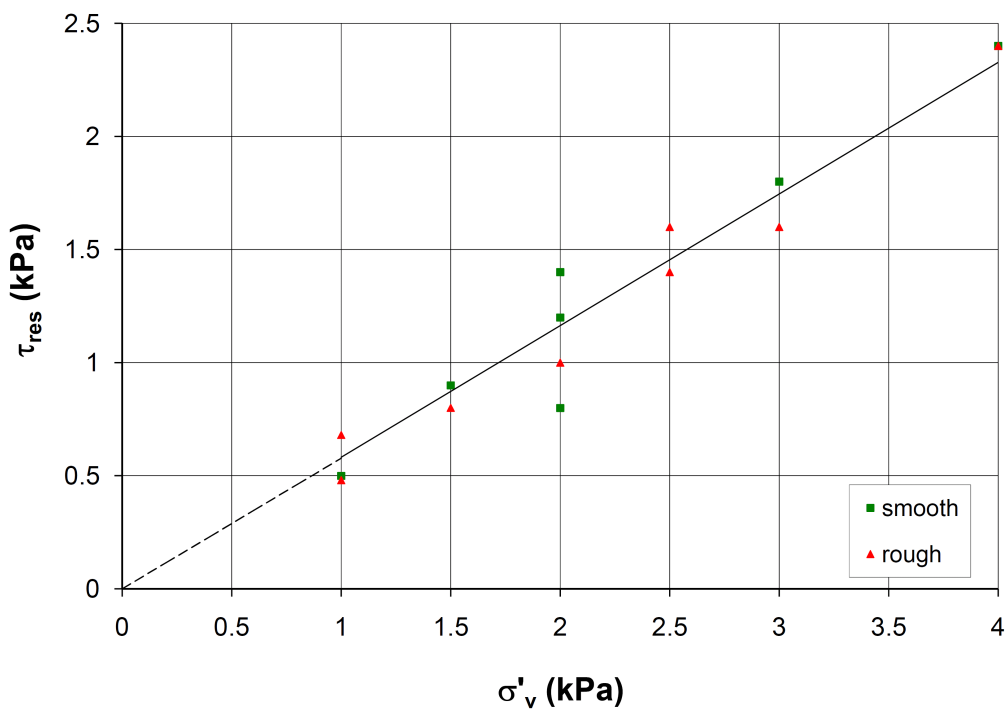
Fig. 6.38 Residual strengths for all rough and smooth interface, pellet-only Cam-shear tests. All tests approach a critical state interface friction coefficient of μ=0.6.

induced to produce the measured strength on rough and smooth interfaces. For a rough interface, the shear strength is governed by the breakage and shearing of individual pellets. For smooth interfaces, the measured strength is purely due to sliding and/or rolling of pellets along the interface. Figure 6.40 shows the pellets located at the smooth interface after shearing, demonstrating that they remained intact during the shearing process. The implications of this observation on pipeline interface design is discussed in Chapter 7.

6.6.3 Autoclaving of Faecal Pellets

In microbiological experiments, the process of autoclaving degrades biological content present in samples. The autoclaving process involves subjecting the biological sample to high pressure steam at 121℃. Autoclaving of intact faecal pellets was undertaken in a conventional laboratory bench-top autoclave to investigate the influence of biological degradation on pellet structure. A review of the literature suggests that pellets are coated both internally and externally with mucous generated in the gut of burrowing invertebrates, and that a peritrophic membrane may exist surrounding the pellet. This feature was observed in ESEM imaging of pellets in Section 6.3.1. The process of autoclaving may therefore degrade the biological bonding and cause a break-down of the pellet structure. Pellets were placed in glass beakers containing sea water and autoclaved twice for 20 minutes each time at 121℃ prior to ESEM imaging. Visual examination of pellets before and after autoclaving suggested minimal degradation during the sterilising process, with pellets retaining their ellipsoidal shape. Figure 6.41 and 6.42 compares ESEM images of pellets before and after autoclaving. These images show that the process of autoclaving does have an impact on the surface structure of pellets. Prior to autoclaving, a relatively smooth, membrane-like structure is observed to cover the surface of pellets. After autoclaving, the surface clay platelets and the smooth peritrophic membrane are found to have been degraded.

Pellets were also subject to boiling with the addition of sodium hexametaphosphate, which is commonly used to aid the dispersion of clays in sedimentological studies. After 15 minutes of boiling and mixing, pellets remained intact. This observation demonstrates that though the process of autoclaving does alter the structure of pellet surfaces at the micron-scale, it is unlikely that the overall strength is influenced by the sterilisation process. Furthermore, the process of ingestion and excretion is capable of compacting the clay structure into a significantly more robust packet than unpelletised material. These conclusions suggest that though the peritrophic membrane will gradually decompose through the activities of organisms such as bacteria and nematoda, the pellets themselves will remain largely intact. Only after hundreds or thousands of years of bacterial action and the activities of similar microorganisms, may pellets finally resediment once more as normally consolidated material.

(a) Photograph of smearing due to crushing of pellets observed while shearing on the rough interface.
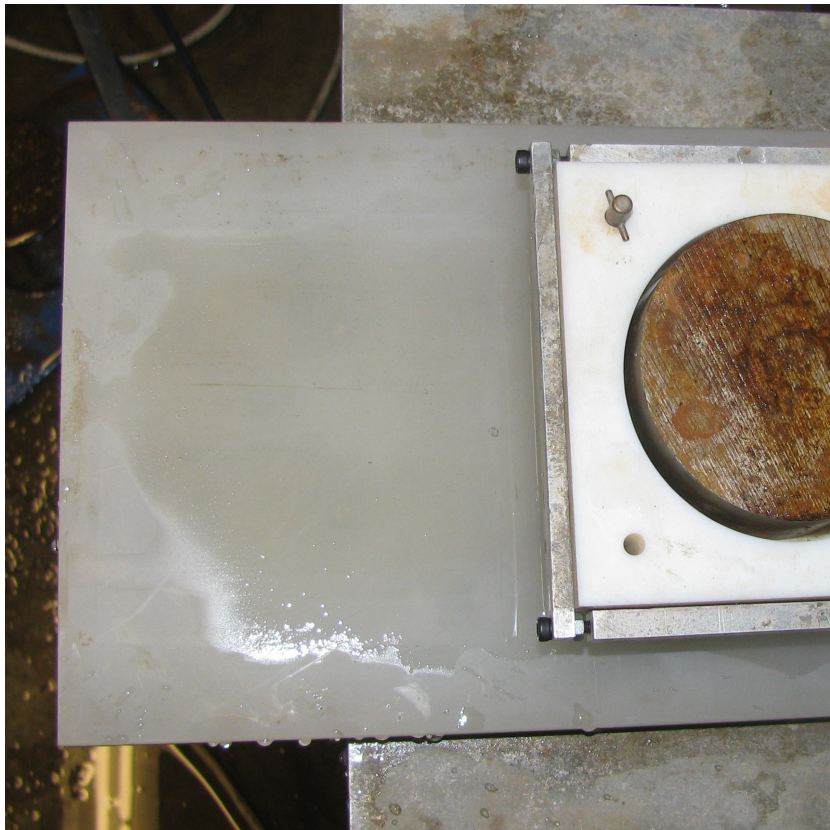
(b) Photograph showing no crushing of pellets occurs when shearing on the smooth interface.

Fig. 6.39 Photographs showing the difference between shearing on rough and smooth interfaces.

Fig. 6.40 Photograph of intact pellets that were located at the smooth interface after shearing, demonstrating that no crushing had occurred.
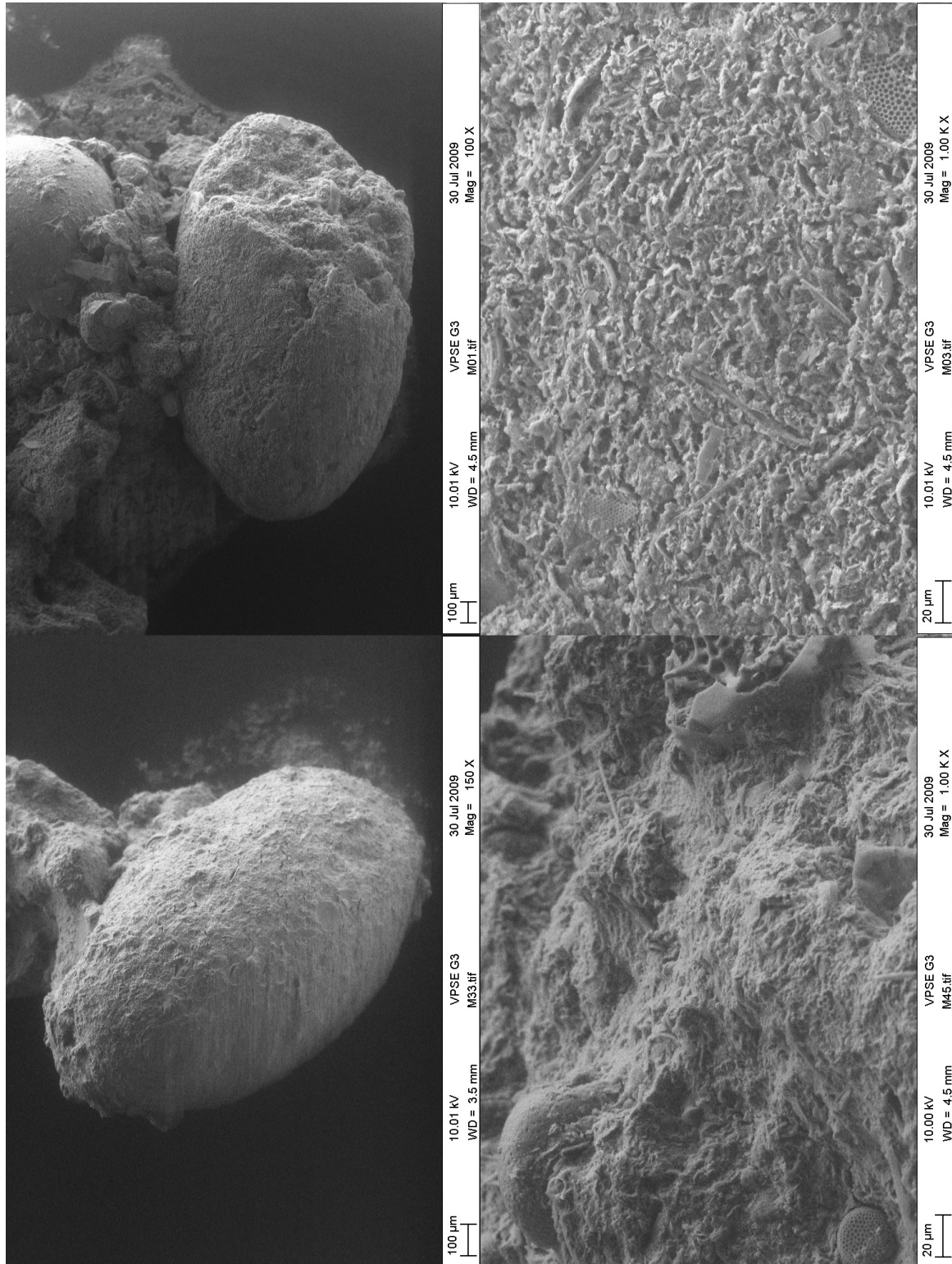
Fig. 6.41 Comparison of fresh (left) and autoclaved (right) pellets with ESEM at lower magnification.
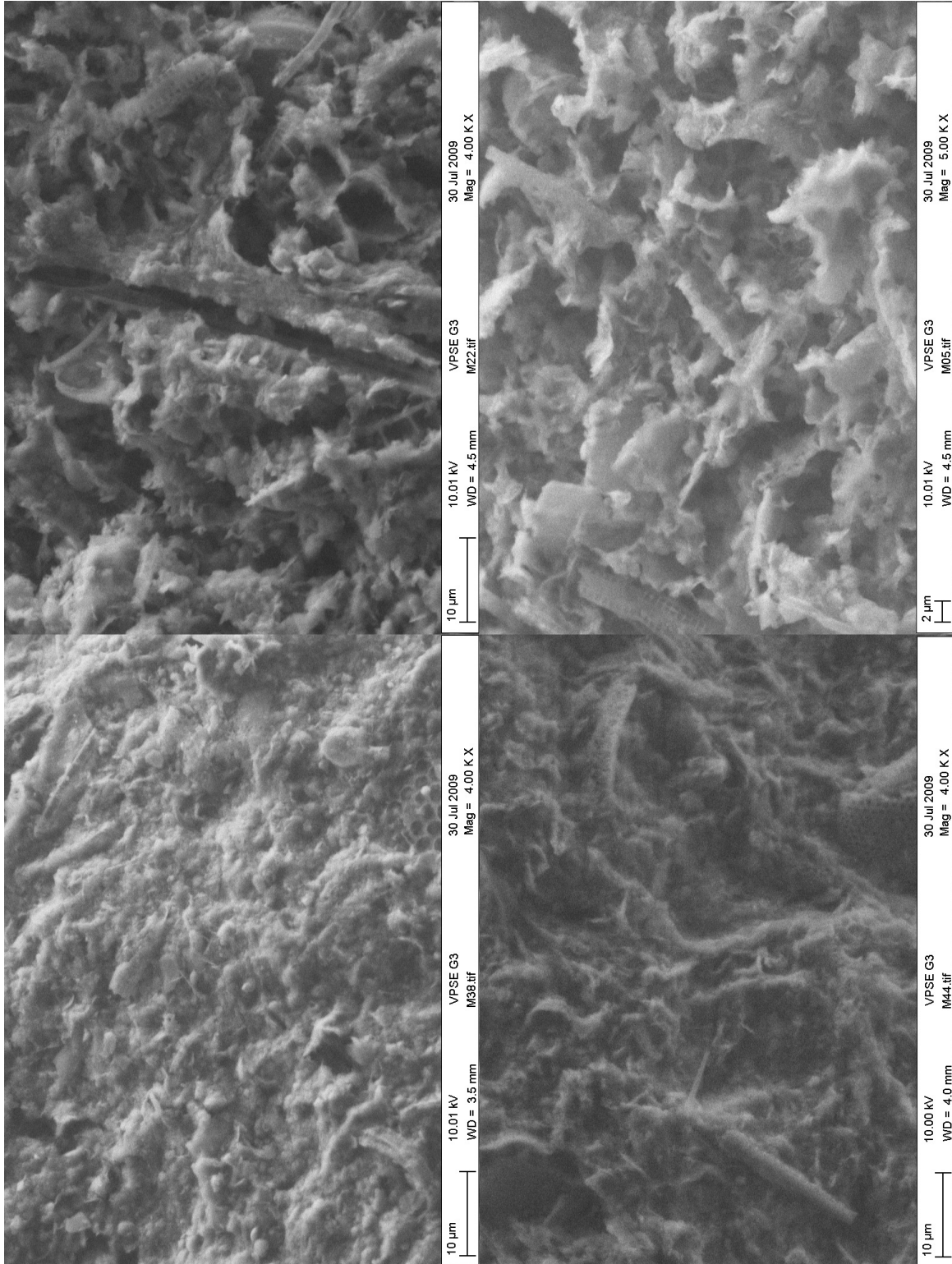
Fig. 6.42 Comparison of fresh (left) and autoclaved (right) pellets at higher magnification.

6.7 Fall-Cone Testing of Natural Samples

Fall-cone testing was undertaken on four natural core samples from two box cores to investigate the variation in strength within the crust. Core samples were cut and trimmed at 0.1m intervals and tested using a Geonor fall cone with a 80g cone. Each test location was noted for the presence of large (visible) pellets, burrows and other sedimentological features that might influence the measured strength. Between five and seven tests were completed at each depth to provide information on strength variation within the 0.092m diameter cores. Tested samples were then remoulded at constant moisture content and re-tested in a standard 50mm diameter brass cup to determine the remoulded strength, and hence, the sensitivity of the soil. Boundary effects caused by the core liner and adjacent tests were minimised by locating tests at a spacing of 30mm. Given the structure of the natural cores, plastic deformation of the samples during the fall-cone tests are unlikely to follow the theoretical models (e.g. Houlsby, 1982). Indeed, the usefulness of the fall cone for natural sediments exhibiting significant variability is limited and the results should be interpreted accordingly.

6.7.1 Fall-Cone Shear Strength Results

Figure 6.43 show the results of fall-cone tests on core samples with faecal pellet percentages shown for five sub-samples and these are compared with a strength profile from the mini ball penetrometer using a ball factor, N_{ball} of 10.5. Determination of pellet percentage was undertaken by wet-sieving a representative portion of the tested sample. Detailed inspection of fall-cone test locations after strength measurements indicated that the percentage is an average value. Locations that exhibited a higher strength had higher numbers of visible pellets. Conversely, locations adjacent to open, water-filled burrows produced lower strengths due to softening of the clay fabric. The main points drawn from these results are:

- a large amount of scatter is observed in samples below 0.1m depth, a location corresponding to the transition between 'unconsolidated' ooze and the crust material;

- the presence of pellets observed without magnification and the open, water-filled burrows significantly influence the measured strength; and

- an unexpected decrease in natural strength is observed for the 0.39m sample, corresponding to a remoulded strength lower than the expected trend based on shallower measurements.

It is likely that the sample from 0.39m depth was disturbed during sampling, given it was located close to the end of the length of core. A slightly higher measured water content is also noted for this particular depth, which may account for the lower strengths. The measured

strengths may reflect an increased number of water-filled burrows. The relatively good comparison between the fall-cone measurements and the mini ball penetrometer suggests that a value of $N_{ball} = 10.5$ is suitable. However, it is accepted that given the highly variable nature of the natural sediments, this value may be location-, or even core-specific.
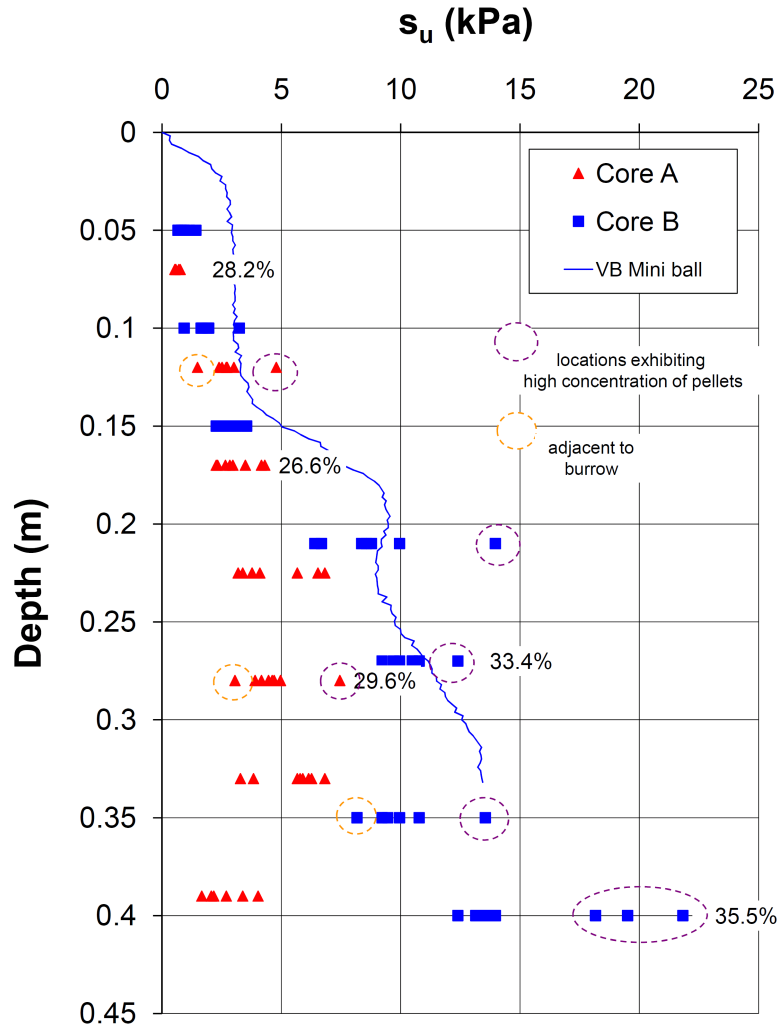
Fig. 6.43 Fall cone test results for cores of crust material. A large range of strengths may be obtained from cores containing material from the same parent box core. Tests undertaken adjacent to faecal pellets and open burrows are noted.

Figure 6.44 shows a comparison of fall-cone measurements for core X, the corresponding mini-T bar tests undertaken in the box core while on ship (by BP Exploration), and an in situ CPT (by Fugro). This figure shows a relatively good correlation between the peak strength measured using the fall-cone and mini T-bar penetrometers with a bar factor, N_b of 10.5, and an average measurement of strength by the CPT. Figure 6.44 also presents the remoulded strengths, determined by thoroughly remoulding the sample at constant water content and

repeating the fall-cone test. It is observed that the remoulded strengths are comparable to a normally consolidated sediment and, as expected, do not exhibit the variation in strength observed in natural, undisturbed samples. The variation in sensitivity has been determined from the ratio of peak strength to remoulded strength for each test depth, and is shown in Figure 6.45. This figure shows that the sensitivity may vary with depth, with a minimum value ranging from 1 for the shallowest sample to 5 for samples at about 0.3m depth. An upper-bound on the sensitivity shows that values of over 10 may be achieved if large (visible) pellets are present. Comparison with the strength shown in Figure 3.32 of a different core of crust after 10 cycles of a mini-ball penetrometer, demonstrates the large difference in sensitivity measurements for the different tests. Peak strengths measured by both devices are similar, though it is acknowledged that the ball penetrometer will tend to average strengths over the area of the ball. The strengths of apparently remoulded material, however, are significantly different. Remoulded fall-cone tests produce strengths from 0.3kPa to 0.8kPa, generally increasing with depth. Non-crust material above 0.1m depth produces a remoulded strength comparable with crust material at 0.3m depth. Conversely, the ball penetrometer measures remoulded strengths of 1kPa for non-crust material and 5kPa for remoulded crust material. This result indicates that the ball penetrometer is unable to fully remould the strongly structured crust containing faecal pellets. As demonstrated by Figure 6.45, a remoulded strength of about 1kPa throughout the natural material implies that the crust sensitivity values are approximately equal in magnitude to the measured peak (undisturbed) strength of the crust.
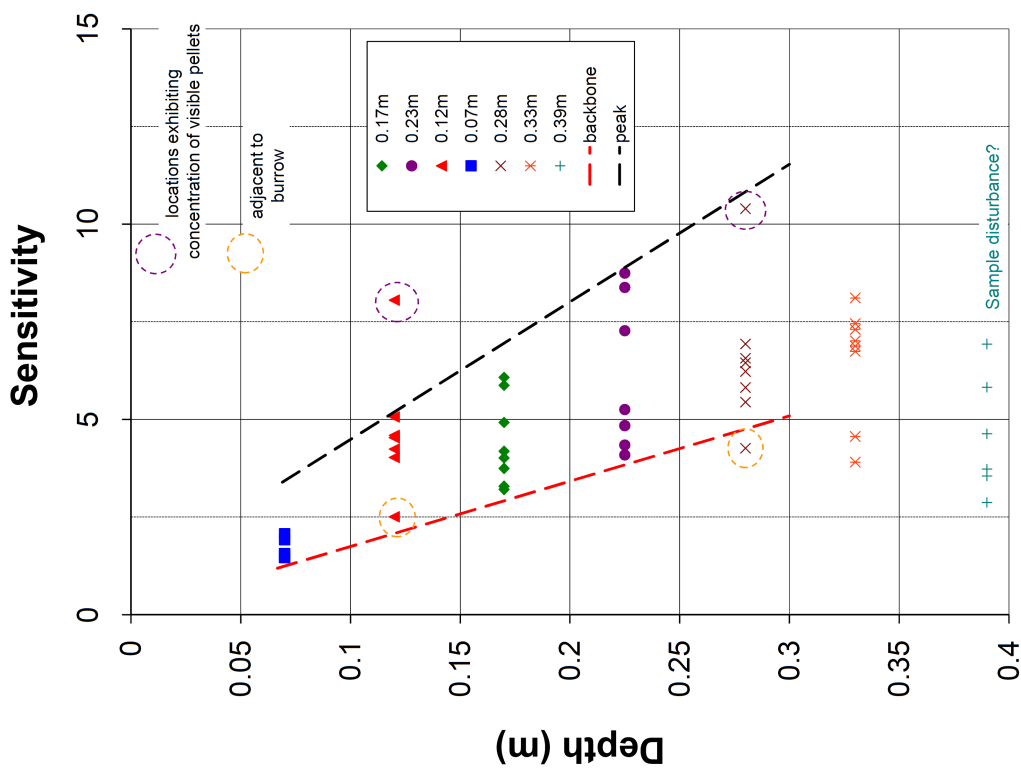
Fig. 6.45 Sensitivity plotted against depth, where residual strengths are determined by fully remoulding natural samples at constant water content and re-testing with the fall cone.
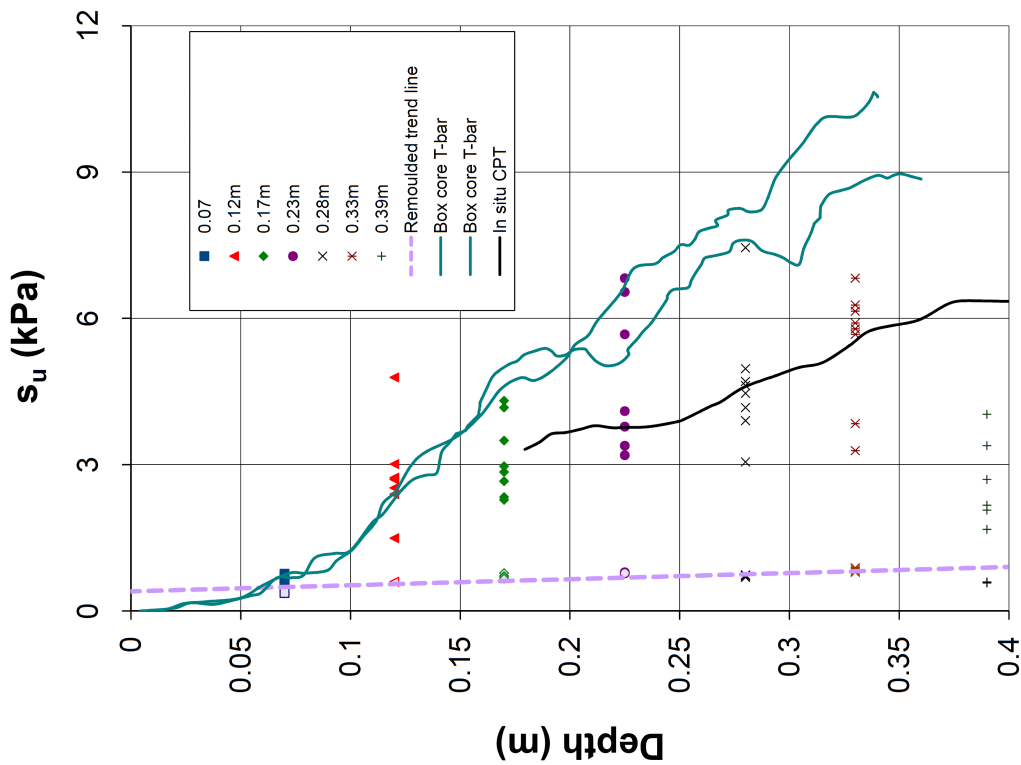
Fig. 6.44 Comparison of fall-cone test results, in situ CPT and on-ship mini-T bar tests. The CPT profile is found to measure an average sediment strength whereas T bars measure peak strength comparable to the fall cone.

6.8 Concluding Comments

This chapter has presented evidence for the presence of burrowing invertebrates within crust material. A significant number of burrows and faecal pellets have been observed in natural core samples of crust material. X-ray computer tomography has allowed non-intrusive, three-dimensional imaging of burrows within cores, which demonstrates varied burrow orientations and complexity within individual samples. By utilising wet-sieving techniques, it has been shown that thousands of faecal pellets exist within the crust, representing, in some samples, over 55% of the total dry mass. Oedometer testing of natural and pellet-only samples highlights the robustness of pellets and their significant influence on consolidation behaviour. It has been shown that a series of normal consolidation lines exist, depending on the percentage of pellets within tested samples. The presence of pellets has also been shown to strongly influence permeability and the coefficient of consolidation. The strength of individual pellets has been estimated through the design and use of a novel pellet-crusher. The results suggest that pellets may exhibit unconfined compressive strengths between 5kPa and 50kPa. By completing Cam-shear testing on pellet-only samples, it has been shown that the peak strength of normally consolidated pellets exhibit linear shear-strength-confining-stress behaviour. 'Apparent cohesion' intercepts are found to be governed by the interface roughness. Residual interface strengths are found to approximate a constant interface friction coefficient of 0.6. The robustness of faecal pellets is further demonstrated by sterilisation in an autoclave and by boiling with sodium hexametaphosphate. Only surficial disruption of the peritrophic membrane and outer clay platelets are observed, with the pellet structure remaining largely intact. The testing of natural samples with a fall cone demonstrates the large variation in measured strength, which is dependent on the proximity of the test location to large pellets or burrows. Furthermore, the sensitivity of the crust material, as determined by fall-cone testing, is found to be largely dependent on the measured shear strength. This is in contrast to the sensitivity determined by mini-ball penetration tests undertaken in crust material, which suggested a constant sensitivity value of 3.

Based on the results of this chapter, it is concluded that faecal pellets created by burrowing invertebrates play a significant role in the generation of extraordinary strength, manifested as a crust, in the marine sediments tested. A discussion of the applicability and implications of this conclusion to marine geotechnics and the design of hot-oil pipelines is presented in Chapter 7. In this chapter, a discussion of the testing methods used in this thesis and a summary of the hypothetical life-cycle of deep ocean clay crusts is also presented.

Chapter 7

Discussion Points

This chapter presents a discussion of the key findings of this thesis, including consideration of the results of the completed mechanical tests and the observations made of crust material. The limitations of equipment and analysis methods are considered, as are the potential applications to pipeline design.

7.1 Cam-Shear Testing

The procedure used to complete interface tests with the Cam-shear device involved shearing at three different rates after consolidation against the pipeline interface. A shearing distance of approximately 50mm was completed at each speed. Chapter 6 presented evidence that the natural fabric comprises crushable faecal pellets, and that the shearing behaviour is strongly dependent on the destruction of the fabric, particularly on rough interfaces. It is therefore concluded that by undertaking interface tests on the same soil sample at three different speeds in sequence, the fabric will be intact only for the first speed trial, which in these tests was always undertaken at 0.05mm/s. This explains why tests undertaken at 0.05mm/s are generally able to attain a higher interface strength than the subsequent tests at 0.5mm/s and 0.005mm/s, as shown in Figure 3.19. The alteration of fabric caused by each successive speed trial can also provide an explanation for some of the variability in "residual strength" seen in Figure 3.21. The first test on each sample was conducted at 0.05mm/s and gave variable residual strength, sometime apparently "drained" and sometimes apparently "undrained". Being previously undisturbed, the sample will have high initial permeability, but on the other hand it will have degraded during shearing. The second test at 0.5mm/s takes place on soil that is already sheared and whose permeability will have fallen due to disruption to the natural fabric. Being also 10 times faster, it is not unexpected that much smaller residual strengths are measured (see Figure 3.21). The third test at 0.005mm/s also takes place on soil that is already sheared, however, the slower shearing rate allows the partial dissipation of excess pore pressures and a

larger strength to be measured.

7.1.1 Limitations of the Cam-Shear Device

The Cam-shear device generates information of particular interest to pipeline designers. Due to low internal friction values and the simplicity of the design, the Cam-shear device is capable of determining the interface friction between very soft clays and pipeline coatings, at a range of shearing speeds. The shear box's small diameter permits the testing of natural cores that have been sub-sampled from box cores, as well as remoulded, reconsolidated samples.

The Cam-shear device, however, does have some limitations, which are:

- variable volume shearing; 'new' soil is sheared for the duration of the test; and

- a small shearing sample size.

These limitations are discussed in turn, below.

As shown in Figure 6.39, shearing on rough coating interfaces causes the tested sample to smear and fill undulations in the coating material. This smeared material is left behind as the shear box progresses forward. This indicates that the volume of material within the box reduces as 'new' clay is continuously dragged down at the front of the shear box to fill the surface undulations in the clean interface that it is traversing. Based on shear test observations, smooth interfaces are less prone to this phenomenon. The measured interface strengths will be influenced partially by this process. The strengths measured at the end of tests, particularly on rough interfaces may be 'residual' values only in the sense that the Cam-shear process has become steady and repeatable after 50mm of sliding, and not necessarily that the breakdown of soil fabric has reached its maximum possible extent.

During the shearing of samples, it is possible for water to be entrained beneath the PTFE shear box and cause an increase in excess pore pressures. This may influence the test results due to the relatively small surface area of clay sample tested. To avoid this, Arasu (2010) undertook tests with a 8m long pipe, which achieves a significantly larger soil-coating interface area. Any water entrained under the front of the pipe would be negligible compared to the surface area tested. This experimental set up can only be used for reconstituted samples and not for natural soil samples. Arasu (2010)'s results indicate that though the influence of entrained water is minimised, interface strengths still exhibit low residual strengths.

7.2 Biology: the Key to Understanding Natural Sediment Behaviour

7.2.1 Variation in Strength

The Cam-shear test results presented in Figures 3.19 to 3.22 highlight the significant variability in strength that is encountered when testing natural clays on interfaces. An investigation into the structure of the tested samples provides an explanation for these observations. Natural clay samples were found to be inhomogeneous; containing faecal pellets with random orientations and numerous open, water-filled burrows. The measured interface strengths will be strongly dependent on the arrangement of pellets, burrows and clay matrix on the shearing plane. Furthermore, as observed in pellet-crushing tests, a large variation in pellet strengths will be present at the interface. If particularly weak pellets are located at the interface, they will tend to break down more easily, releasing water as the broken fragments re-pack more efficiently. At higher shear speeds, this may generate excess pore water pressures that reduce local shear strengths. This conclusion does not provide much comfort for pipeline designers seeking a robust design value, however, it does highlight a need for the testing of natural samples rather than remoulded, reconsolidated samples.

7.2.2 Comparison of Cam-Shear, Mini Ball Penetrometer and in situ T-bar Tests

A comparison of the strength values that are obtained from different types of tests is provided here, though difficulty exists when attempting to describe the mechanisms involved with each type of test. Soils subject to cyclic testing with full-flow penetrometers experience large shear strains, resulting in the strength falling from $s_{u,max}$ to $s_{u,res}$. The mechanisms involved are generally considered to involve the generation of positive excess pore pressures (thus reducing effective stresses), or destruction of the soil's natural fabric during the passage of the T-bar or the ball through the soil.

The processes involved with reducing soil strength from peak to residual values on a pipeline interface are considered by Bolton et al. (2007). They provide a non-dimensional framework in which the shearing against asperities on a rough pipeline coating may be considered analogous to the displacement of a penetrometer device moving past a particular piece of soil. However, as discussed by Bolton et al. (2007), this hypothetical mechanism can not be verified due to the minuscule size of coating asperities.

Based on the Cam-shear and mini-ball penetrometer test results presented in this thesis, it is concluded that the process of shearing on a rough interface is at least an order of magnitude more destructive to the natural fabric than moving a ball penetrometer through the soil over 10 cycles. Cam-shear tests samples are consolidated under applied pipeline stresses prior

to shearing. The observation that a very low peak strength is obtained in Cam-shear tests on rough interfaces before equally low residual strengths indicates that shearing at a rate of 0.05mm/s induces an immediate destruction of the fabric with accompanying generation of positive excess pore pressures. The penetration of a relatively smooth brass ball through the same material does not achieve the same destructive behaviour as material flows over its surface. It has been shown that the crust material contains robust pellets that break down during shearing on a rough interface. It has also been shown that when subject to one-dimensional compression, the surrounding clay matrix undergoes sufficient deformation such that pellets are able to re-arrange themselves without the need for breakage. It is therefore suggested that during the first cycle of a mini-ball penetration test, the crust material deforms around the ball, resulting in only minor breakage of pellets and allowing the majority of pellets to remain intact for subsequent cycles. After ten cycles, a sensitivity of 3 is measured. This value is found to be small compared to fall-cone results, which indicated sensitivities of over 7 may be measured.

Recent full-flow penetration tests in crust material undertaken by Puech et al. (2010) show that the sensitivity only reaches the values indicated by the fall-cone after 20 to 30 cycles.

7.2.3 Influence of Shearing Rate

Figure 3.21 shows that residual friction values range from 0.1 to 1 with an average of 0.3. The large range in values indicates that drained conditions were not achieved even during shearing at 0.005mm/s. Although natural samples exhibit very high coefficients of permeability, and open burrows are observed in the samples tested, disruption of the natural fabric must be preventing dissipation of excess pore pressures generated by the shearing of pellets on the coating interface. By shearing at an even slower rate, truly drained shearing conditions could be induced, producing a constant drained friction value, presumably of the order of 0.5 (see Figure 3.21).

7.2.4 Faecal Pellets and Interface Friction

Cam-shear testing of natural, inoculated samples and pellet-only samples on smooth and rough pipeline coatings facilitate discussion on the behaviour and mechanisms invoked during shearing. A summary of the key observations from the results of shearing these three materials on rough pipeline coatings is:

1. natural samples are capable of generating very small interface friction values, presumably due to hydroplaning brought about by generation of positive excess pore pressure. These excess pore pressures are considered to be caused by the crushing of faecal pellets; creating fragments that fill adjacent water-filled voids during collapse. This forces water

out along the interface.

2. shearing of sterile, remoulded West African clays samples that have been inoculated with *M. aquaeolei* can produce strength values even lower than typical of normally consolidated clays. This may be caused by the collapse of a polysaccharide-enhanced structure, resulting in the clogging of water-filled voids.

3. pellet-only samples crush during shearing, however, they do not generate the very small interface friction values observed in natural samples.

It is suggested that collapse of natural structure - however it has occurred - is responsible for producing variable and very low friction values. As hypothesised previously, in Section 3.6, the natural sediment contains two parts: a biologically enhanced component of grains, found to be predominantly in the form of faecal pellets; and a matrix comprising of clay interlaced with bacterial polysaccharides. A sample containing only faecal pellets can exhibit permeabilities higher than that associated with clays, as indicated in Section 6.5.3, particularly when subject to the low confining stresses imparted by a pipeline. This implies that during shearing on a rough interface, water forced from voids that are being filled by crushed fragments of pellets is permitted to drain through the permeable pellet-only fabric.

On the contrary, a natural sample containing 50% faecal pellets is an order of magnitude less permeable due to the clay matrix surrounding the pellets. During shearing and crushing of pellets, the matrix prevents drainage, inducing the generation of positive excess pore pressures.

A comparison of soil-soil Cam-shear tests undertaken on pellet-only (see Figure 6.35) and natural-crust samples highlights the significant influence the clay matrix has on measured strengths. Soil-soil tests show that natural samples can exhibit strengths that are 60% to 100% greater than those of normally consolidated, pellet-only samples. This is due to the matrix, which provides support to shearing pellets in natural clay. The initial structure of pellet-only samples, which is formed during normal consolidation, will be comparatively unstable, and will collapse when sheared, filling void spaces adjacent to pellets. Due to the high permeability of pellet-only samples, the measured strength may be considered to be a drained value. Indeed, tests undertaken on natural samples at a slow shearing rate of 0.005mm/s lie close and slightly below the trend presented by the pellet-only samples.

During consolidation of pellet-only samples on a rough interface, pellets that are located at the interface will squeeze between the asperities, forming an interlocked structure. When sheared, positive excess pore pressures generated by filling of water-filled voids by pellet fragments quickly dissipate through the permeable fabric of the sample. Comparison of Figures 6.35 and 3.19, show that values from pellet-only samples are almost universally higher than peak strength values from natural samples. Smearing of the interface by the clay matrix and the relatively low permeability of natural samples, prevents dissipation of positive excess pore pressures. Through the process of void-filling due to fragment generation during

pellet crushing, significantly lower interface friction values are measured by the inducement of hydroplaning due presumably to excess pore pressures.

It can therefore be concluded that the percentage of faecal pellets will dictate the interface shear behaviour of pipelines on rough coating interfaces. Samples containing greater than 70% pellets will (initially) allow drainage of excess pore pressures and will therefore exhibit a larger interface strength. Samples with sufficient clay matrix to fill the spaces between pellets will retain excess pore pressures more easily and so will be more susceptible to hydroplaning.

7.2.5 Comments on Previous Cam-Shear Testing of West African Clays

Wet-sieving of bulk samples used in investigations by Bolton et al. (2007, 2009) identified the presence of abundant, robust faecal pellets in samples that had undergone mechanical mixing to create a remoulded slurry for Cam-shear testing. Based on wet-sieving, pellet percentages of at least 15% are likely to have been present in the tested samples. These percentages are smaller than those in the natural crust samples tested in this thesis. However, the shearing behaviour at the interface, which involves pellets being crushed when sheared, will have the potential to exhibit the behaviour observed when testing natural samples. These pellets provide an explanation as to why large variations in, and low values of interface shear strength were measured in apparently homogeneous, remoulded samples. It is therefore recommended that in future, shallow marine core samples not only those from West African locations, are analysed for the presence of invertebrate faecal pellets and other biological activity prior to testing.

7.2.6 Applicability of the Cam Clay Model

The analysis of Cam-shear data undertaken in this thesis has used the Cam clay model proposed by Schofield and Wroth (1968) as a framework. This is justified by previous research undertaken by Bolton et al. (2007, 2009), which suggested that the data from the shearing of remoulded, reconsolidated West African clays could be adequately represented by the Cam clay yield surface. The results presented in Chapter 3 exhibit similar Cam clay yield surfaces when appropriate α-factors are applied to account for the interface testing of natural samples. Upper and lower yield surfaces obtained by calculating values for the apparent pre-consolidation stress, $\sigma'_{c,0}$ for each test have been drawn. However, it is noted that due to the heterogeneous nature of natural samples, the model is unable to provide an adequate prediction of the influence and effects of biological activity. Part of this limitation is due to a difficulty in the interpretation of stress-strain data for natural core samples, presented in Appendix A, and the variability present in any sample. The plots in Appendix A illustrate that the stress-strain behaviour rarely follows conventional profiles, such as an initially elastic phase followed by elastic-plastic softening or hardening.

Furthermore, only the vertical effective stress applied to the sample during consolidation and shearing, and the measured shear strength are known. The effective stress path taken by a particular soil sample during the shear tests is unknown.

For soil-soil tests, strain-softening to the critical state is expected to occur after yielding, given that most samples exhibit overconsolidated to heavily overconsolidated behaviour when subject to shearing under pipe stresses. This would imply that an interface friction coefficient, μ of 0.6 would be experienced under large strains. This would correspond to low values of strength, particularly for smaller pipelines that subject the sample to a 2kPa vertical effective stress. For interface tests, it is observed that most samples, particularly those at 2kPa and 4kPa vertical effective stress, exhibit *peak* shear strengths that are a fraction of what would be predicted by the Cam clay model. Furthermore, after shearing a distance of 50mm, the strength does not recover. As discussed previously, this is due to immediate disruption of the natural structure at the onset of shearing and the generation of positive excess pore pressures and subsequent hydroplaning. Based on the Cam clay model, these samples would then be expected to approach the critical state line (CSL) by strain-hardening, but instead, residual values are grouped below the CSL, having either reduced in strength or never exhibited strength at all. This is particularly evident for samples sheared at 0.5mm/s and 0.05mm/s. Samples sheared at the slower rate of 0.005mm/s largely remain at the same shear strength for the duration of the shear test.

The Cam clay model can account for crushing of grains during shearing (e.g. Cheng et al., 2004), which is shown in this thesis to occur in both natural and pellet-only samples. This model is however, largely unable to model soil sensitivity, and is therefore unable to predict the behaviour experienced by these particular natural samples during shearing on interfaces. It is therefore appropriate that the Cam clay model be used for the analysis of homogeneous, remoulded and reconsolidated samples that do not contain robust faecal pellets. This model will be less suitable for the analysis of heterogeneous samples where large variability in natural structure, and thus sensitivity, is expected within the soil.

7.2.7 Applicability of One-Dimensional Consolidation Theory and Analysis Using a Faecal-Pellet Framework

This thesis has used one-dimensional consolidation theory based on a unit cell model to analyse oedometer test results. As for the Cam clay model, it is expected that the results of this analysis will be strongly influenced by the heterogeneity of natural samples, particularly faecal pellets and open, water-filled burrows. These structural elements will alter both the horizontal and vertical permeability, and the sample stiffness. Smearing of sample surfaces during preparation will also influence the permeability. Furthermore, the consolidation of robust pellets within a compressible clay matrix causes difficulties in identifying the transition from primary

consolidation to creep. For example, under a given vertical effective stress, the clay matrix may undergo normal consolidation by travelling down a normally consolidated line, whereas pellets that have experienced a significantly higher preconsolidation stress may move down a unload-reload line. It is clearly observed that the natural crust material is influenced by these inclusions, and the results of this thesis highlight the significant differences in stiffness and one-dimensional consolidation values that may be attained by testing natural core samples.

The methods used to attain these values produce results that are comparable with those for in situ measurements of permeability and one-dimensional stiffness. Though these methods do not provide an exact value for these parameters, they are applicable to pipeline design because they determine the order of variance and the correlation between the percentage of faecal pellets. It is therefore proposed that future analysis of consolidation characteristics of deep ocean sediments be undertaken using a faecal-pellet framework. The results from previous studies on remoulded samples, such as De Gennaro et al. (2005); Bolton et al. (2009); Puech et al. (2010) can therefore, also be included in this framework.

7.3 Influence of Soil Structure on Soil Strength and Shearing Behaviour

This thesis identifies that biological activity plays a significant part in post-depositional structuring of marine soils through the creation of burrows and faecal pellets and possible subsequent destructuring of material. Future efforts in classification of marine sediments, particularly for engineering purposes would therefore benefit from the inclusion of post-depositional factors, especially biological activity.

It is generally accepted that due to their sedimentation history, natural clays may have a degree of "improved strength" above unstructured, normally consolidated clays. This is described and considered by many authors, including Skempton (1970); Burland (1990); Cotecchia and Chandler (2000). The importance of this natural strength to geotechnical engineering usually manifests itself in the consideration of soil sensitivity. As has been described in this thesis, the sensitivity of West African clays is difficult to measure, even with modern, conventional methods such as remoulding with full-flow penetrometers. In many sensitive soils, consolidation of natural samples induces collapse of the structure, resulting in a familiar v-logσ'_v or if normalised, I_v-logσ'_v profile. The crust materials considered in this thesis, however, have a natural structure with an unusually high resistance to collapse. Figure 6.24 indicates that the normal consolidation line is dependent on the percentage of pellets in a given sample. The structure produced by pellets is therefore significantly different from the structure observed by De Gennaro et al. (2005), though both are natural samples from the same geographical region. Samples containing pellets are difficult to classify as they can either exhibit a sensitivity close

to unity (if it is considered that a family of normally consolidated lines exist), or increasing sensitivity, depending on the percentage of pellets. These natural soils are thus similar to those investigated by Nocilla et al. (2006), where 'transitional' behaviour was observed for various gradings of an Italian silt.

7.3.1   Strength of Clay-Sand Mixes

This thesis demonstrates that the crust material consists of a mixture of robust faecal pellets and a clay matrix. This may behave in a manner similar to mixtures containing sand or gravel and clay. As discussed in Section 6.2.2, Kumar and Muir Wood (1999) and Vallejo and Zhou (1994) investigate the influence of varying clay contents on the strength of gravels and rocks. They conclude that approximately 50% granular material by dry weight is required to significantly influence the strength characteristics. This is dependent on the dry densities of the materials considered. When applying the conclusions of Kumar and Muir Wood (1999) to a pellet-clay mixture, it is more appropriate to convert the faecal pellet percentage to sand or gravel using the ratio of dry weight to wet volume, in order to account for the influence of water content. Faecal pellets contain water, with water contents between 130% and 170% being measured in pellets found in the tested crust samples. Gravel and rock fragments, however, obviously do not contain water. Thus, by assuming a mean water content of 150% for pellets and by using a clay-matrix water content of 200% for both pellet and gravel mixes, the relative wet and dry volumes and masses can be determined for different coarse-fines mixtures. Figure 7.1 shows the percentage sand by dry mass and percentage pellets by dry mass curves against percentage granular by wet volume. This figure allows the conversion of pellet percentage in a given crust sample to the equivalent percentage of granular material in a clay-gravel or sand mixture.

The conclusion from this figure is that the strength characteristics of samples with faecal pellet percentages above 40% by dry mass are dominated by the behaviour of pellets. This faecal pellet percentage corresponds to 60% sand or gravel by dry mass. Samples containing between 20% and 40% pellets by dry mass lie within a transitional zone where both pellet and matrix influence the strength behaviour. The behaviour of samples with less than 20% pellets will be dominated by the clay matrix alone. Kumar and Muir Wood (1999) identify key fractions that define changes in the sample-mix behaviour, which are shown on Figure 7.1. This conversion exercise shows that the proportion of faecal pellets observed in crust samples is sufficient to dominate the strength behaviour. This supports the hypothesis that faecal pellets are the origin of the crustal strength.
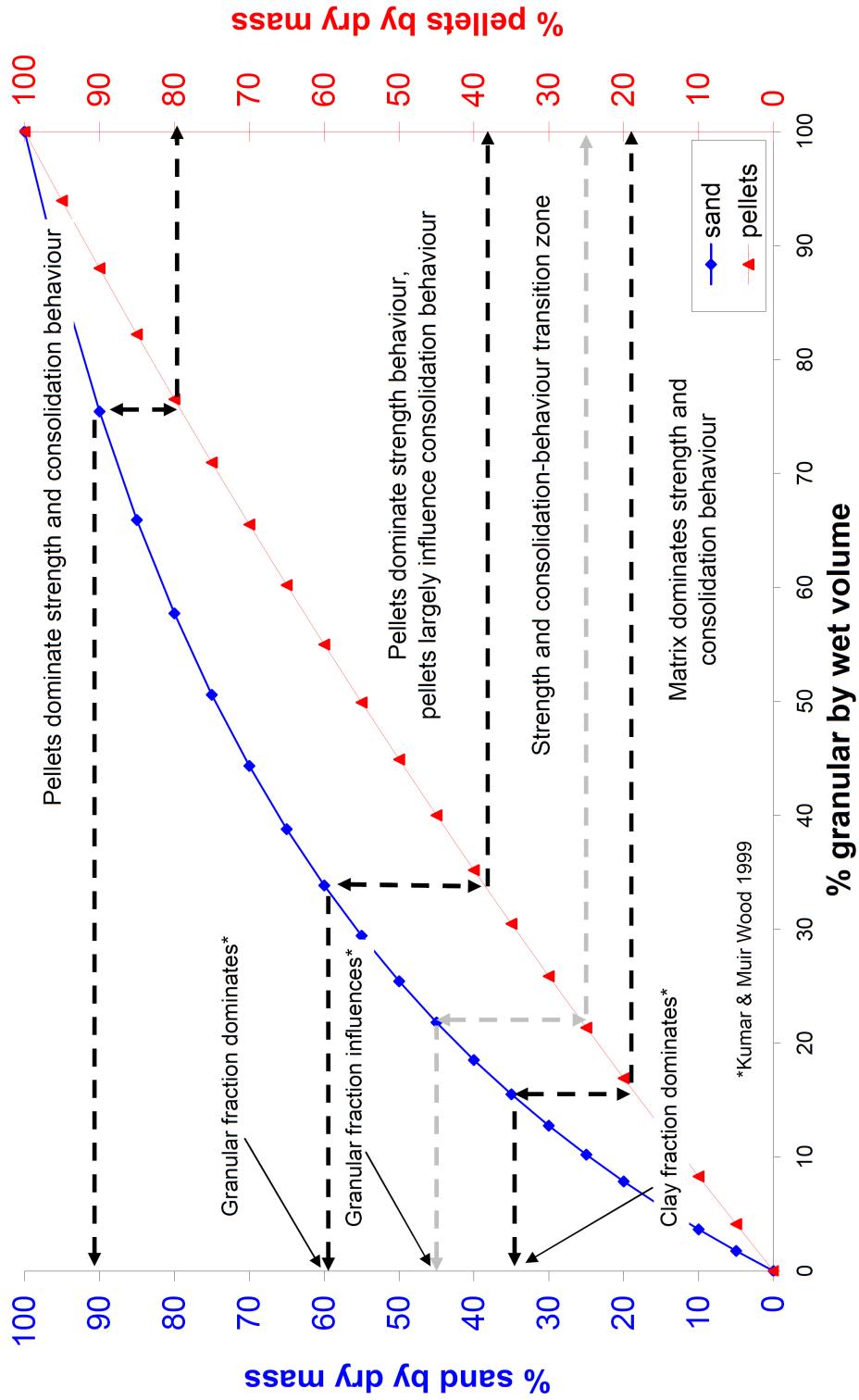
Fig. 7.1 Plot showing equivalent % faecal pellets and % sand by dry mass values and the different areas of soil behaviour.

7.3.2 Shearing of Clay-Sand Mixes

Lupini et al. (1981) considered the drained residual strength of clay and clay-sand mixtures during testing of samples with a ring-shear device and identified the presence of three main shearing behaviours: turbulent, transitional and sliding. These behaviours were found to be dependent on particle shape and angularity, which controls the inter-particle friction. Turbulent shearing is described by Lupini et al. (1981) as being dominated by rotund particles, whereas sliding behaviour is usually induced by the presence of platy, low-friction particles. A transitional zone exists between the two defined modes of shearing, where neither particle shape (rotund or platy) dominates. It was observed that sliding behaviour exhibited low residual strengths whereas turbulent shearing produced higher residual strengths. The application of this conclusion is that clayey soils will tend to produce lower strengths, whereas samples with a high granular component will tend to exhibit higher strengths.

Skempton (1985) considered the residual strength of natural clay-sand mixtures present in landslides, and compared the behaviour of mixtures observed in the field to those observed by Lupini et al. (1981). Skempton (1985) concluded that the proportion of clay within a particular sample will only influence the shearing behaviour when the clay content exceeds 50%. In samples with a lower clay content, the residual strength is largely controlled by the granular material. Lemos and Vaughan (2000) undertook interface shear tests with ring shear and conventional direct-shear boxes. Interfaces of varying roughness were used to investigate the influence of interface roughness on interface shear strength. It was concluded that samples with a high clay content produced residual interface strengths that were independent of the interface roughness, and of comparable value to soil-soil residual strengths. The mode of shearing was determined to be sliding, as observed by Lupini et al. (1981). Conversely, samples with clay contents less than 40% were observed by Lemos and Vaughan (2000) to be strongly influenced by the interface during during shearing. In this situation, the interface allowed the generation of a thin veneer of clay between the granular material and the interface, thus inducing sliding behaviour.

The results presented in this thesis are used to extend the observations and conclusions made in these studies. Figures 7.2 and 7.3 present schematic diagrams of the results from this thesis underlain by the interface shearing behaviour suggested by Lupini et al. (1981), and other interface shearing results by Lemos and Vaughan (2000) and Bolton et al. (2009). S_1 is defined by Lupini et al. (1981) as being a region of *"possible sliding shear when soil is failed against a smooth interface"* (Lupini et al., 1981, p209). It is observed from Figure 7.2 that sliding or rolling of faecal pellets on smooth interfaces (5μm roughness) can occur (though, not within the defined S_1 region). This behaviour may be due to the relative smoothness of faecal pellets, which do not exhibit the same angularity as sand grains. This results in the

generation of a lower shear resistance than might be expected when compared with the London Clay-Happisburgh Till mixture investigated by Lemos and Vaughan (2000). Conversely, the behaviour of natural crust and remoulded crust material produce higher strengths than what might have been expected based on previous studies.

Figure 7.3 shows the transition of pellet-only samples into a purely turbulent mode of shearing, but again, at lower residual friction coefficients than that suggested by Lemos and Vaughan (2000). It is observed that the natural crust samples containing pellets may produce larger variation in the interface friction coefficients, representing both sliding and turbulent shearing modes. Based on the work completed in this thesis on crust samples, an additional 'hydroplaning' mode is indicated in this figure. When the natural structure and most of the faecal pellets are destroyed by remoulding, a higher interface friction coefficient is obtained, as shown by the results from Bolton et al. (2009).

It is observed that a residual μ value of 0.6 was measured whilst shearing the pellet-only sample on the smooth interface. No pellet crushing was induced during these tests. This is the same value as that measured in pellet-only tests on the rough interface, where pellets were clearly seen to crush. This suggests that the modes of shearing induced by these tests are strongly governed by the permeability of the soil's fabric.

The influence of the roughness of the pipeline coating on the measured residual strength can be assessed by comparing Figures 7.2 and 7.3. The various modes of shearing behaviour are:

- extremely high percentage of pellets (70% to 100%): residual strength is independent of roughness;

- high percentage of pellets (20% to 70%): residual strength is dependent on roughness, but only because of the destruction of pellets, and the production of positive excess pore pressures that cannot dissipate; and

- low percentage of pellets (less than 20%): variable residual strengths, though this material is less likely to generate hydroplaning behaviour due to fewer crushing pellets.
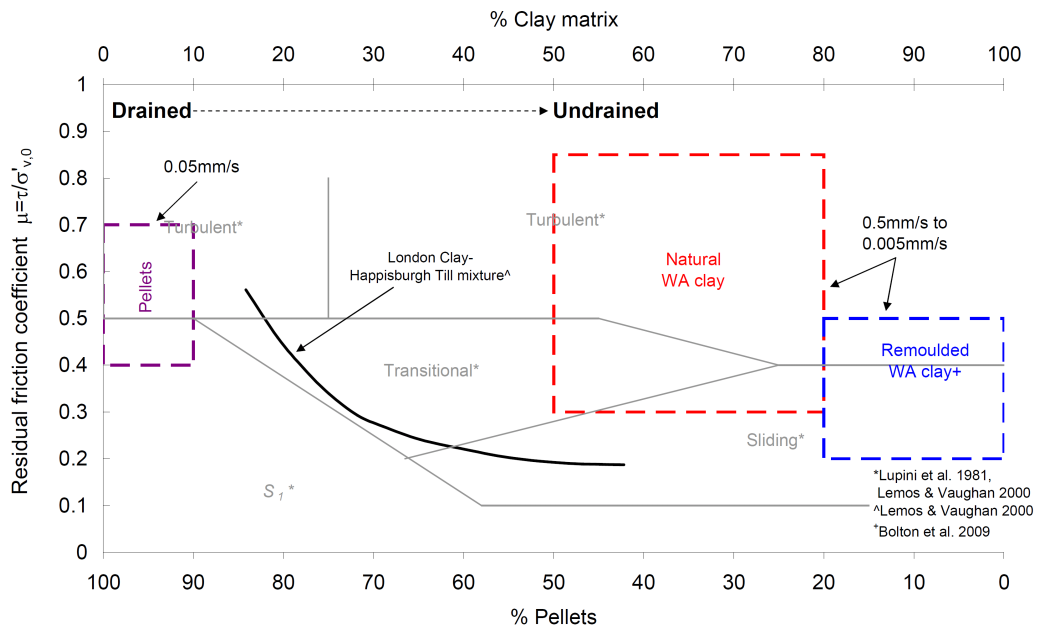
Fig. 7.2 Interface shearing regions for smooth interfaces based on the percentage of pellets and Lupini et al. (1981).
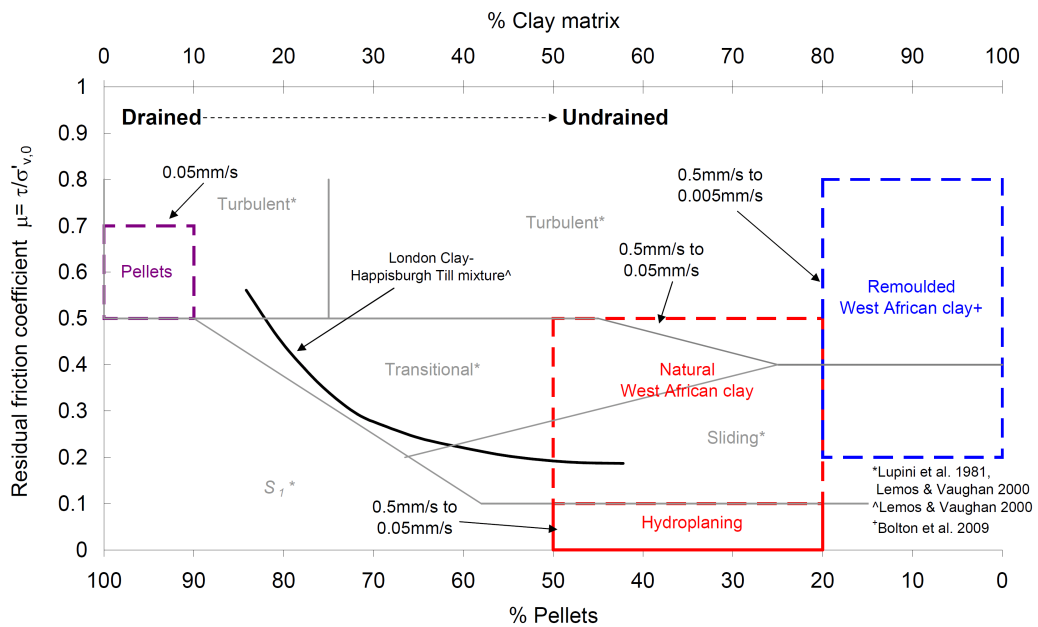
Fig. 7.3 Interface shearing regions for rough interfaces based on the percentage of pellets and Lupini et al. (1981).

7.4 Relevance to Pipeline Design and Offshore Site Investigations

Geotechnical offshore site investigations for pipeline routes currently focus on sediment mechanical behaviour specific to pipeline design. Geologists and geophysicists may be consulted to provide historical (geological) and seismic information. However, very rarely are marine ecologists, including zoologists or biologists consulted, apart from providing a broad ecological review of the proposed developments. The low interest in the possible influence of biological aspects on marine sediments is seldom highlighted in academia industry literature. This thesis may provide the impetus for further research into the formal linking of marine geotechnics and marine ecology with specific application for the design of hot-oil pipelines and associated structures, such as pipeline end terminations and manifolds.

7.4.1 Influence of Pipeline Roughness

Both natural and pellet-only testing demonstrate that smooth pipelines do not crush faecal pellets. This observation implies that the design of pipeline coating roughnesses needs to consider the biologically enhanced structure of natural clays. Current and previous pipeline designs predominantly assume embedment into soft clay. This thesis demonstrates that the natural sediment contains a significant proportion of coarse grains in the form of robust faecal pellets. The question pipeline designers must address is how the pipelines will destroy the structure in the generation of soil-pipeline interface strength. As a simplified example, Figure 7.4 provides a schematic diagram of faecal pellet-containing sediment located against a range of pipeline coating roughnesses.

A pipeline designer is required to consider the wavelength and the roughness amplitude of individual asperities that collectively produce the coating interface surface. This decision will depend on the abundance and size of faecal pellets in the sediment. Pipeline coating roughnesses are relative to the dimension of the natural material that shears upon it. High roughness amplitudes will increase the risk of water-filled macro-voids at the soil-pipeline interface. Pipeline coating interfaces are usually highly variable. It is therefore suggested that the design of roughness wavelength, λ should consider defining the roughness with respect to the faecal pellet diameter, ϕ_{pellet}. Smooth and rough pipelines would then be defined as:

$$\text{smooth: } \lambda_{min} > \phi_{pellet}; \text{ and}$$
$$\text{rough: } \lambda_{min} < \phi_{pellet}.$$

For conservative designs that minimise the risk of very low interface friction coefficients due to crushing of pellets, it is suggested that pipelines are designed to be smooth. The widely believed notion that rough pipes (e.g. roughnesses greater than 100μm) will generate

a) Smooth interface

b) Rough interface 1

c) Rough interface 2
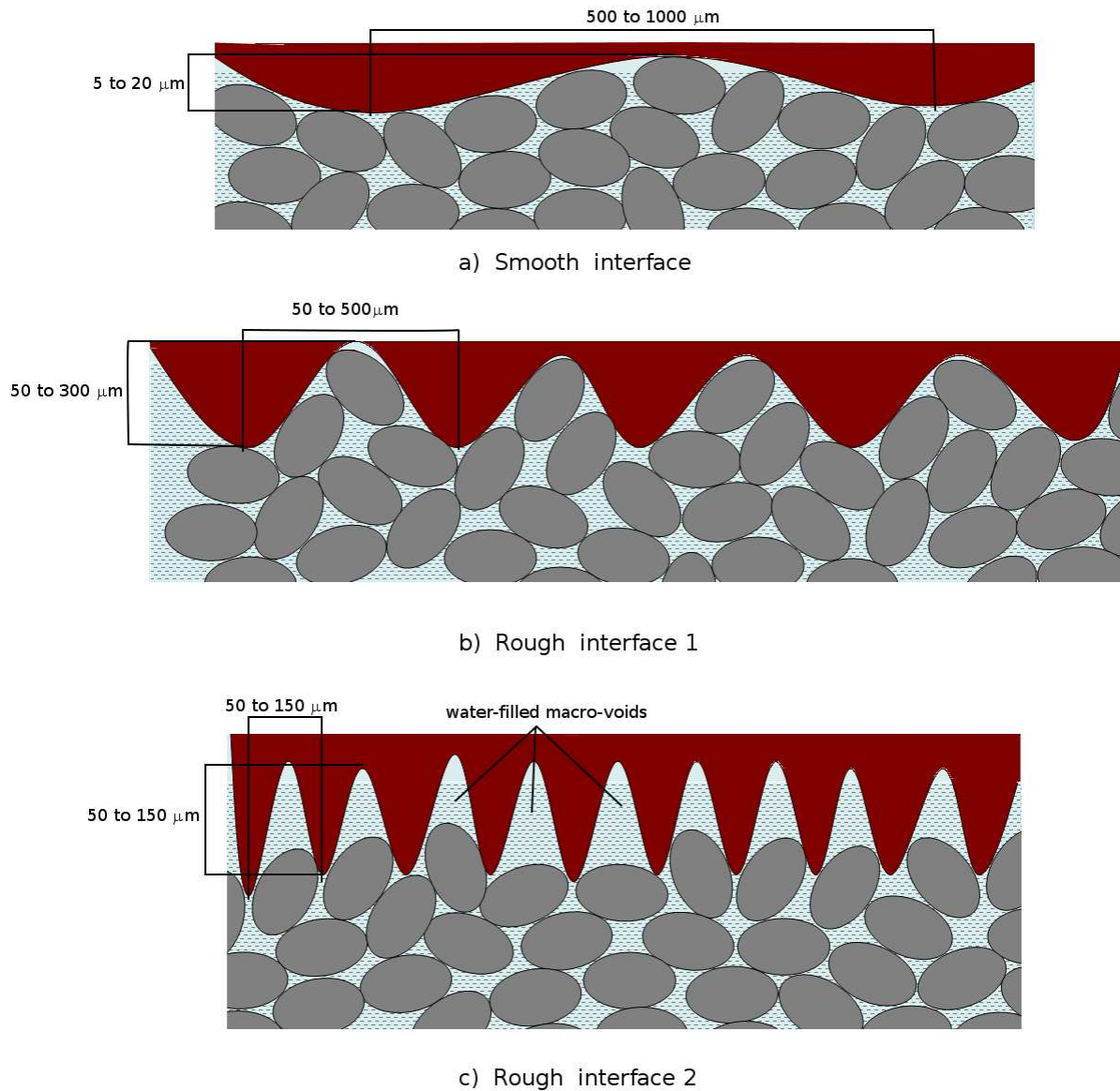
Fig. 7.4 Schematic diagram of faecal pellet-containing sediment against pipelines of different roughnesses.

more frictional resistance when shearing on these sediments is only true under specific soil conditions.

7.4.2 Particle Size Distribution

This research has highlighted the importance of the natural structure of sediment. In particular, the presence of faecal pellets that are either deposited in situ by burrowing invertebrates, or are transported some distance prior to sedimentation, will effect sediment behaviour. The current practice of undertaking a particle size distribution on core samples following standards

such as ASTM D442-63 will result in a significantly skewed interpretation of the grain size. This is due to the remoulding and destroying of all natural fabric prior to the analysis, resulting in a PSD-interpreted clay. If faecal pellets were structurally weak and only represented temporary structures within the crust, they might be expected to crush under pipe stresses. However, faecal pellets exhibit significant robustness, and will modify the grain size distribution and the soil properties with the degree of modification depending on their size and abundance.

It is therefore concluded that the wet sieving of marine sediments, preferably to 20μm, should be routinely undertaken to provide an accurate indication of the natural sediment's grain size distribution. The results of this analysis will aid in the interpretation of interface shear tests and the consolidation behaviour of natural samples. These results are key to understanding the behaviour of hot pipelines installed into these sediments.

7.5   Biology: the Origin of the Crust

The findings from the microbiological work on crust material presented in this thesis, and the testing of inoculated samples highlight the minor but measurable influence bacteria have on the strength of clay sediments. Given the abundance of bacteria in deep ocean sediments, natural material containing either one dominating species, or several co-existing species, may generate a more significant influence on the strength than that measured in simple laboratory experiments. This implies that natural sediments, particularly from marine environments, can not continue to be assumed 'sterile' during geotechnical testing, nor can micro-organisms be assumed to be absent.

No burrowing invertebrates were observed in core samples obtained from West African deep sea sediments. Their presence, however, is irrefutable based on the abundant physical evidence for bioturbation in the form of open burrows and faecal pellets. The experimental work has demonstrated the exceptional robustness of individual pellets through wet sieving, crushing, shearing and one-dimensional compression. The review of the literature indicates that biological processes predominantly occur within the benthic boundary layer; in close proximity of the seabed-water interface. The correlation of crustal strength with abundant bioturbation in the form of faecal pellets and burrows and bacteria indicate that biology is the cause for the crust. The largest influence on strength is the presence of thousands of robust faecal pellets that are continuously being created and replenished by burrowing invertebrates by digestion of nutrients from the above ocean. The proposed biological and mechanical genesis of crust sediments is demonstrated by Figure 7.5. This presents the formation of faecal pellets in one-dimensional compression space, and provides an explanation for the behaviour under 1-D compression during oedometer tests of crust material; and sediment from below the crust.
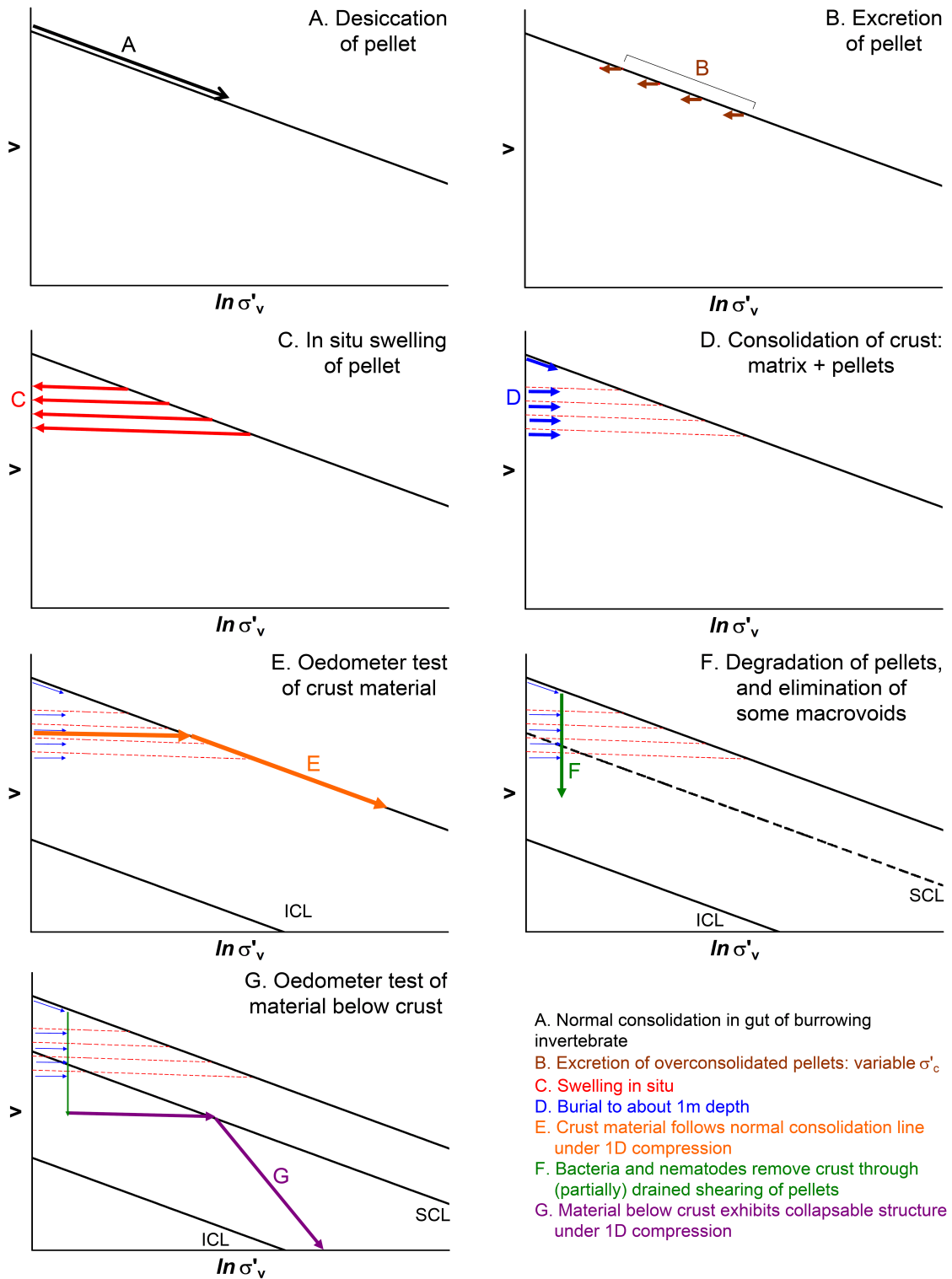
Fig. 7.5 Schematic diagram showing the biological and mechanical formation and degradation of crust material in v-σ'_v space.

7. DISCUSSION POINTS

Based on completed oedometer tests on crust material, it has been demonstrated that crushing of pellets under increasing vertical effective stress cannot be the cause of low percentages of pellets below the crust region. Therefore, the crushing of pellets cannot be the cause of the loss of crustal strength. The loss of strength at sediment depths greater than 1m coincides with a reduction in invertebrate activity as indicated by the literature, and evidenced by few in situ faecal pellets. By this depth, the sediment is approximately 10,000 years old, which is a significant length of time for biological processes to work at breaking down the crust material.

The sedimentation process in the considered water depths may be at least three orders of magnitude slower than the bioturbation processes that initially produce the crust. It is therefore feasible to suggest that over the same time frame, but at a greater depth, bacteria or animals such as nematodes may be degrading the crust. Removal of the crust might be manifested through reworking of larger pellets into smaller agglomerates or by complete destructuring of pellets by removal of the mucins and peritrophic membrane that bind the pellets together. This may then allow resedimentation of material within pellets that were initially overconsolidated, forming a normally consolidated zone (in terms of strength) below the crust. Under 1-D compression, however, this material still exhibits 'structure' as evidenced by Figure 6.23.

The estimated rate of sedimentation in the West African sediments is 0.1mm per year. Suppose that one worm of 3mm diameter is capable of bioturbating one burrow through 300mm depth of sediment each 'worm week'; then each worm can be responsible for an order of 10^5mm^3/year of bioturbation. Worms spaced at 1m centres are more than sufficient to completely bioturbate the sediment. This may be a very conservative approximation of the ability of burrowing invertebrates to modify the soil. A study by Gingras et al. (2008) presents estimated rates of bioturbation for a range of invertebrate species. It is suggested that ten worms may require less than 15 years to completely bioturbate a 1x1x0.1m volume of sediment that takes 1,000 years to accumulate. It is therefore feasible for worms, through their daily activities, to engineer into pellets all the material that falls to the seabed.

Figure 7.6 summarises the suggested input parameters and subsequent modification processes leading to crust formation and subsequent demise. The input from the overlying water shown in this figure includes both organic (degrading biological matter) and inorganic (terrestrial material including clay). Upon reaching the sediment floor, the inputs are consumed by invertebrates, transforming them into faecal matter. Invertebrates that burrow and produce compact faecal pellets significantly modify the geotechnical properties of the sediment. Pellets are more abundant within the top 0.5m of sediment, corresponding to the high crustal strength. With depth, the proportion of pellets decreases, corresponding to a reduction in sediment strength. Sediment strength profiles from in situ T-bar and CPTs are shown with a description of the biological and geomechanical activities occurring at key sediment depths.

The early observations of faecal pellets in Scottish lochs by Moore (1931a,b) have gone unnoticed by modern-day geotechnical engineers; and the geotechnical implications of the observation made by Schafer (1972) that faecal pellets are compacted and overconsolidated packets of clay, have not been considered until now. The process of faecal pellet production in clay sediments has remained unchanged for hundreds of millions of years, but their influence on geotechnical engineering is only now being discovered.
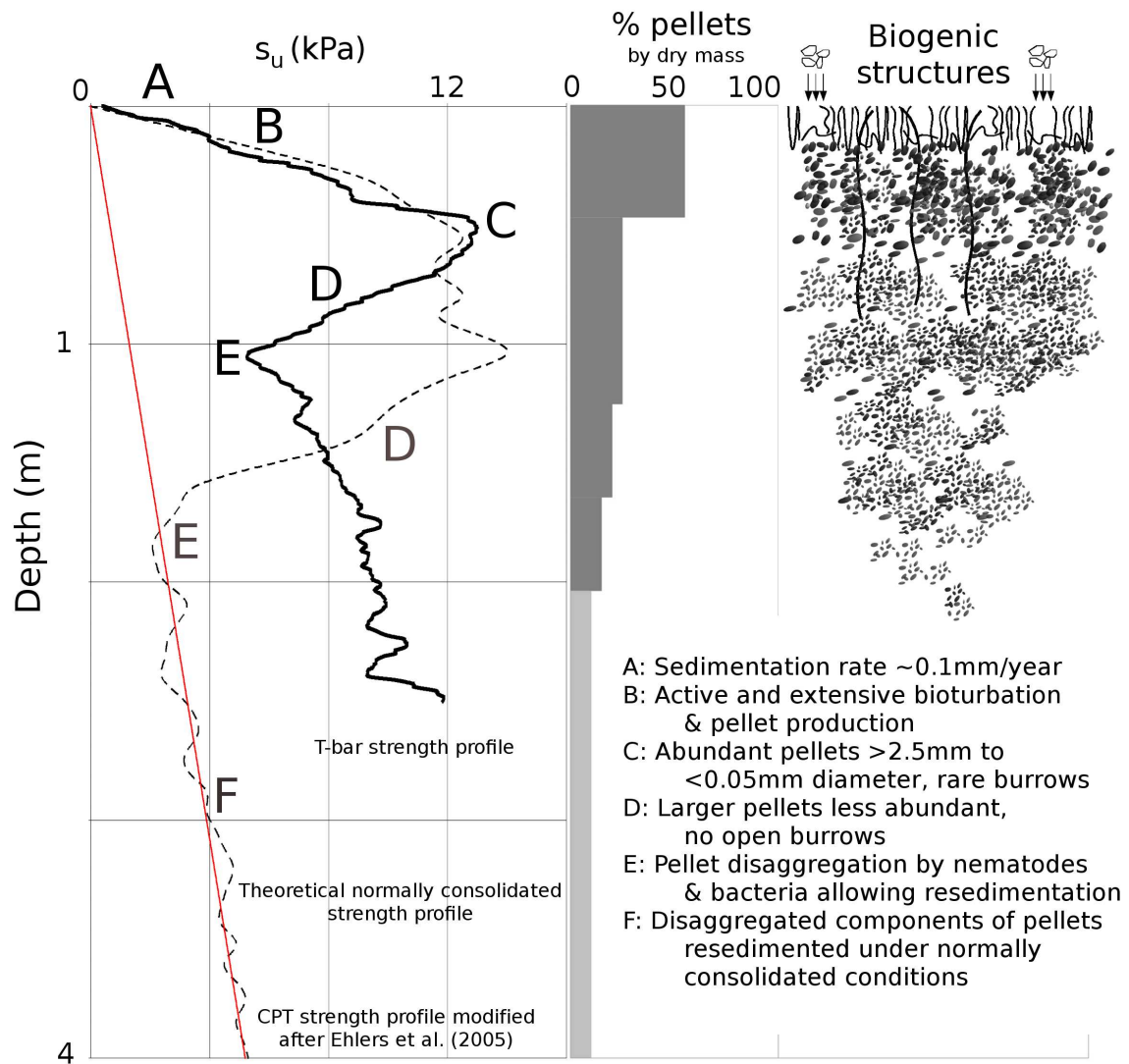
Fig. 7.6 Schematic of the hypothetical lifecycle of marine crust sediments from deposition of sediment from the water, biological structuring into faecal pellets and subsequent destructuring by bacterial activity.

Chapter 8

Conclusions and Recommendations for Future Work

8.1   Key Conclusions of this Thesis

Chapter 1 provides an introduction to this thesis by explaining the present context of the offshore oil and gas industry, and the previous neglect of biological processes in geotechnical engineering. This highlights the unique contribution of the current work: an attempt at interfacing marine ecology and marine geotechnics with specific application for the design and behaviour of hot-oil pipelines. Chapter 2 presents a review of the literature directly relating to the in situ and laboratory testing of West African clays. This demonstrates the presence of an anomalously high undrained shear strength in the upper metre of sediment; a phenomenon which, prior to this thesis, was not understood. This chapter also presents an overview of the literature describing similar crustal strengths at a global scale. This suggests that the phenomenon is more common that initially thought, with a direct implication for the offshore oil and gas industry, in that pipelines are likely to encounter crust material in future projects. This highlights the need for a better understanding of the mechanical behaviour of pipelines embedded in crust material, particularly through laboratory testing of natural cores.

8.1.1   Laboratory Testing

Chapter 3 presents the bulk sediment properties of samples obtained from the west coast of Africa determined using a multi scan core logger. This highlighted the unusual correlation of high strength and high water content, presumably due to some previously undescribed natural structure. A description of the Cam-shear apparatus and testing method was given, followed by results and discussion of soil-soil and pipeline coating interface testing with natural clay samples. The key results from Cam-shear testing are:

- the observation of a significant variation in interface strength on both smooth and rough

pipeline coatings;

- the occasional total loss of interface strength, especially after 50mm of sliding over rough coatings; and

- the discovery that smooth interfaces generally show more frictional behaviour than rough interfaces.

A mini-ball penetrometer was developed and used to test natural crust material, and provide degradation curves over ten cycles. It was found that peak strengths were comparable to in situ and T-bar strength profiles and that a sensitivity of about 3 was measured after ten cycles. The behaviour of the crust material during disturbance with the mini-ball penetrometer did not suggest that exceptionally low interface strength values would be recorded in Cam-shear tests. This led to the conclusion that the crust's natural fabric is complex, perhaps comprising of two or more structural components. The mini-ball penetrometer may disturb the clay in the fashion of pipe laying and embedment. The Cam-shear test, however, may be representative of axial sliding due to in-service temperature changes. The two processes apparently degrade the natural clay structure at different rates, with the fretting of a rough interface being particularly severe.

A better understanding of the natural fabric and its origins will assist the interpretation of in situ and laboratory test results.

8.1.2 Hypotheses for Crust Origin

No previous research has explicitly considered the origins of the crustal strength. This thesis presents a review of possible hypotheses in Chapter 4, considering chemical, organic, geological and biological origins, respectively. Through a review of the literature on each of these topics and knowledge already gained from laboratory testing of natural samples, it was concluded that chemical precipitation and high organic content were unlikely to contribute significantly to the crustal strength. These conclusions were based on an absence of evidence of chemical precipitation within the natural clay matrix when using SEM and ESEM imaging, and previous organic content measurements (Thomas et al., 2005) identifying less than 6% organic material in these sediments. The two strengthening agents that could not immediately be discounted on current knowledge were both biological in nature: bacteria and burrowing invertebrates. The existing literature on these two possibilities highlighted two aspects that might contribute to the sediment strength by the following broad attributes:

- generation of extracellular polysaccharides by bacteria; and

- bioturbation, specifically the creation of burrows and faecal pellets by burrowing invertebrates.

These two aspects needed to be investigated further to verify their role and relative contributions towards producing crust material.

8.1.3 The Role of Bacteria

Chapter 5 presents the experimental work undertaken in a microbiological laboratory that provided controlled environmental conditions for microbiological experiments reducing the likelihood of contamination. This chapter details the process of bacterial DNA extraction from bulk core samples using two commercially available extraction kits. It was concluded that an extraction method using a bead beating process was the most suitable based on existing literature of DNA extraction from deep sea bacteria. Typical microbiological procedures were undertaken to amplify extracted DNA using the polymerase chain reaction (PCR), followed by the running of gels to confirm the amplification of suitable, uncontaminated material. Following PCR clean-up and sequencing, the bacterium *Marinobacter aquaeolei* was identified as being present in the tested sediment.

Chapter 5 then details the purchase and successful growth of this bacterium under laboratory conditions on sea water agar plates, and the inoculation of sterile, remoulded samples. A procedure for inoculation of clay slurry is described and used to create samples for testing with the Cam-shear device. Tests were undertaken on sterile and inoculated samples at three different shearing rates. It is observed that a sterile sample produces a shear strength comparable to the lower bound of natural samples. An inoculated sample produced a similar strength, albeit with a slightly higher initial peak strength. It is therefore concluded that bacteria are unlikely to be the main contributor of crustal strength. However, given their abundance in deep-sea shallow marine sediments, their collective contribution to the sediment properties may be significant enough to influence geotechnical sediment properties, particularly permeability through the clogging of pores.

8.1.4 The Role of Burrowing Invertebrates

Chapter 6 is the final of the investigative chapters and presents the laboratory and exploratory work on the role of burrowing invertebrates in crust formation. A number of imaging methods were used to collect evidence for the presence of burrowing invertebrates in crust samples, including environmental scanning electron microscopy (ESEM), X-ray computer tomography (CT scanning) and optical microscopy. Using these methods, numerous open, water-filled burrows ranging from 0.5mm to 3mm diameter were identified. Wet-sieving techniques were used to wash cores of natural crust samples, uncovering the presence of thousands of apparently robust faecal pellets ranging from less than 60μm to larger than 300μm. The abundance of pellets in crust material, determined as a percentage of total dry mass, was found to range from 20% to greater than 55%. A further $\sim$10% by dry mass of agglomerates was found

8. CONCLUSIONS AND RECOMMENDATIONS

between 20μm and 60μm in size; these appeared to be irregular fragments, and may have been the result of some process of faecal pellet breakdown. Particle size distribution curves based on the wet-sieving method resulted in a shift by one order of magnitude of grain size compared with previous studies of the same material. Furthermore, a linear relationship exists between the percentage of faecal pellets and the measured undrained shear strength of crust samples. The proportion of pellets in crust samples is converted to the equivalent proportion of sand in a sand-clay mixture by determining the percentage of pellets by wet volume to account for the water content of faecal pellets. This conversion provides evidence supporting the hypothesis that faecal pellets are the originators of the crustal strength, by demonstrating that the proportion of pellets in crusts is sufficient to dominate the strength behaviour.

The strength of pellets was approximated by the use of a novel pellet-crushing device, resulting in estimated unconfined compressive strengths of between 5kPa and 50kPa. By undertaking fall-cone tests on natural core samples, it was demonstrated that the presence of pellets at or adjacent to the test location positively influenced the measured strength. Conversely, tests undertaken adjacent to open burrows produced a lower strength. One-dimensional consolidation tests of natural samples containing less than 20% pellets, greater than 50% pellets and 100% pellets (a pellet-only sample) were undertaken. The pellet-only sample contained sieved pellets ranging from 125μm to 212μm. The observations drawn from these tests are:

- the pellet percentage within samples has a measurable influence on one dimensional tangential stiffness, coefficient of consolidation and permeability;
- a pellet-only sample has a significantly higher permeability than natural samples;
- increased vertical effective stress causes the behaviour of a pellet-only sample to tend towards natural samples with 50% pellets; and
- pellet crushing due to increasing vertical effective stress with burial is not the cause for loss of crustal strength, based on comparable pellet percentages before and after oedometer tests.

It is concluded that the crustal strength is the result of the presence of abundant faecal pellets in natural core samples.

The thesis closes with a discussion on key points, and which considers the limitations of laboratory testing equipment and the methods used to analyse test results. This discussion suggests that the Cam-shear device is currently the most appropriate pipeline interface shear apparatus, due to its ability to complete tests at very low vertical effective stresses. The test results should be applicable to the design of axial anchor lengths of pipelines.

Pellet crushing has been shown to occur during shearing on rough interfaces. It is suggested, therefore, that the pipeline interface coefficient of friction will depend on the proportion and size of pellets in natural samples. Pipeline roughness values are suggested to be dependent on

the roughness wavelength and amplitude, which in turn, will be relative to the size of pellets. For conservative design, it is therefore proposed that smooth pipeline coatings be utilised to minimise the risk of low friction values.

A new key soil classification parameter should therefore be included in investigations for pipeline design: the determination of faecal pellet proportion. This value will dictate both consolidation and strength behaviour of natural soils, and will also strongly influence the behaviour of hot-oil pipelines shearing on natural sediments.

The discussion is concluded by providing a summary of the life cycle experienced by deep ocean crusts, from creation by burrowing invertebrates to possible destruction by bacteria or nematodes. It is demonstrated that in their collective lifespan, burrowing invertebrates will have the capacity to generate the shallow crusts observed in deep marine sediments. Offshore engineers and offshore engineering projects should therefore acknowledge and respect the biological aspects of the sediments into which structural and lifeline elements are founded. By considering the influence of biology on geotechnical properties of sediments, this will potentially allow for safer and more economical designs to be implemented.

8.2 Recommendations for Future Work

This section outlines avenues for future research into this topic. Suggested research includes the extension of work undertaken in this thesis; development of new laboratory testing equipment; the influence of temperature on the properties of marine sediments containing biological activity; and numerical analyses to better-understand the behaviour of complex, heterogeneous, natural sediments.

8.2.1 Extension of Cam-Shear Testing

The Cam-shear testing undertaken for this thesis has considered very low effective stresses of 2kPa to 6kPa, correlating to expected pipeline stresses, and has indicated highly variable interface strengths. Other researchers (Puech et al., 2010) have used the ring-shear apparatus to investigate shear behaviour. Due to limitations with equipment sensitivity at very low effective stresses, these tests have been undertaken at stress conditions larger than those achieved during the Cam-shear tests presented in this thesis. To provide a direct comparison with the large volume of existing ring-shear data, it is suggested that further Cam-shear testing be undertaken to confirm the nature of interface properties up to vertical effective stresses of 30kPa.

Tests on remoulded samples by Bolton et al. (2009) demonstrated that strength was influenced by shearing rate, which is in contrast to the ring-shear results presented in Figure 3.24. Neither Puech et al. (2010) nor Bolton et al. (2009) considered the influence of pellets that

may remain in apparently remoulded samples. As shown in Chapter 7, robust pellets may be present and will influence the interface strengths measured. There is, therefore, need for further testing of both natural and remoulded samples at higher effective stresses with the Cam-shear device to understand these behaviours. Pore pressure measurement should be attempted (taking into account the difficulties outlined in this thesis), to provide evidence for the generation of positive excess pore pressures during shearing on interfaces.

8.2.2 Cam-Tor Device

The limitations of the Cam-shear device as a means for characterising the soil-pipeline interface properties have been discussed in Chapter 7. To address some of the highlighted limitations, a torsional soil-pipeline interface shearing device can be proposed. The key features of such a device would be:

- unrestricted shearing distance on soil-coating interfaces;
- measurement of true residual strengths at very large strains;
- prevention of new sample material being dragged down to the interface due to smearing;
- prevention of water entrainment during shearing; and
- continuous pore pressure measurement via a pore pressure transducer located within the coating material.

8.2.3 Influence of Temperature

Pipeline designers currently assume that the crust is a permanent feature of these sediments, and consider the phenomenon of crustal demise only in relation to geological timescales, if at all. It is commonly assumed that pipelines will self-embed into the crust and remain there for the duration of their lifetime. This assumption, may not be as robust as first believed. As discussed in Chapter 7, this thesis proposes that the observed loss of crustal strength with depth is due in part to the action of bacteria that degrade and resediment faecal material into sediment with normally consolidated strengths. This process is likely to take hundreds of years to complete at an in situ ambient temperature of 4℃, as the metabolic rates of bacteria are influenced by temperature. For cold-water pipelines, the results of shear testing without consideration of temperature effects may be appropriate for design.

Flowlines transporting oil at 160℃ will increase the ambient sediment temperature by 10℃ or even 20℃. This increase in temperature will significantly increase the metabolic activity of biological processes in the sediment and encourage new species of fauna to colonise the area disturbed by the pipeline. It is hypothesised that pellet disintegration will occur directly beneath the pipeline at a much increased rate, thereby reducing soil strength and the safety of hot flowlines.

An assembly of intact pellets could be inoculated with a solution of *M. aquaeolei* under long term monitoring, and at temperatures expected to exist at hot-pipe-soil interfaces, based on data obtained from industry. Visual comparisons could be made with control samples considering:

- pellets kept at an in situ ambient temperature of 4℃ without *M. aquaeolei*;
- pellets kept at an in situ ambient temperature of about 4℃ inoculated with *M. aquaeolei*; and
- pellets kept at pipeline-soil interface temperatures without *M. aquaeolei*.

The results of this investigation would provide information on the role of bacteria in pellet degradation under increased interface temperatures. This will assist in determining the vulnerability of medium and long-term crustal strength in hot-pipe installations.

8.2.4 Extension of Investigation with Burrowing Invertebrates

To provide supporting evidence for the strengthening of sediment surrounding burrows and by faecal pellets, burrowing invertebrates could be collected from muddy estuarine sediments. Using a mini-ball penetrometer, it would be possible to obtain continuous strength profiling within and around sediment which has been bioturbated both in situ and in core samples brought back to the laboratory. As with core samples investigated in this thesis, samples should be subject to X-ray computer tomography to identify the presence of burrows, and a physical determination of pellet percentages should be undertaken to provide evidence for changes in strength with sediment depth.

Field studies involving marine ecologists and geotechnical engineers should be considered to allow the interfacing of biological, microbiological and engineering research interests, particularly through the collection of water and core samples for laboratory testing. An offshore location that could provide direct comparisons with existing literature detailing the presence of faecal pellets is along the west coast of southern Scotland, within the Clyde Sea area.

Numerical analyses of the influence of open, water-filled burrows on one-dimensional consolidation characteristics would also be an important aspect of future work, particularly as the consolidation of hot-oil pipelines is initially dependent on the natural, in situ condition of sediments which contain numerous burrows of varying diameters.

8.2.5 Application to Pipeline Design Practice

A validation of the results presented in this thesis through the recommended future work will ultimately allow the implementation of the conclusions into pipeline design guidelines. This will represent the direct transfer of academic knowledge to industry practice. Finite element

8. CONCLUSIONS AND RECOMMENDATIONS

models that include consideration of the influence of bacteria and burrowing invertebrates on pipeline design parameters will result in safer and more economical designs.

References

R. McN Alexander. *Animal Mechanics.* Blackwell, Oxford, 2nd edition, 1983.

A. L. Alldredge and M. W. Silver. Characteristics, dynamics and significance of marine snow. *Progress in Oceanography*, 20(1):41–82, 1988.

R.C. Aller. *The effects of macrobenthos on chemical properties of marine sediment and overlying water.* Animal Sediment Relations. Plenum Press, New York, 1982.

G.C. Amstutz. Coprolites: A review of the literature and a study of specimens from southern washington. *Journal of Sedimentary Petrology*, 28:498–508, 1958.

S.G. Arasu. *Unknown.* PhD thesis, University of Cambridge, 2010.

A. Arulrajah and M. W. Bo. Characteristics of Singapore Marine Clay at Changi. *Journal of Geotechnical and Geological Engineering*, 26:431–441, 2008.

A. Baltzer, P. Cochonat, and D. J. W. Piper. In situ geotechnical characterisation of sediments on the Nova Scotian Slope, eastern Canadian continental margin. *Marine Geology*, 120(7): 291–308, 1994.

R. D. Barnes. *Invertebrate Zoology.* W. B. Saunders Company, Philadelphia, 3rd edition, 1974.

R. S. K. Barnes, P. Calow, and P. J. W. Olive. *The Invertebrates: a new synthesis.* Blackwell Scientific Publications, Oxford, 1st edition, 1988.

P. Bayliss and J.P.M. Syvitski. Clay diagenesis in recent marine fecal pellets. *Geo-Marine Letters*, 2:83–88, 1982.

R. G. Bea and P. Arnold. Movements and forces developed by wave induced slides in soft clay. *Fifth Annual Offshore Technology Conference*, 2(1899):11, 1973.

R. H. Bennett, N. R. O'Brian, and M. H. Hulbert. Determinants of clay and shale microfabric signature: processes and mechanisms. In A.H. Bouma, editor, *Microstructure of Fine-Grained Sediments: From Mud to Shale*, volume IV. Springer-Verlag, New York, 1991.

R. H. Bennett, B. Ransom, M. Kastner, R. J. Baerwald, M. H. Hulbert, W. B. Sawyer, H. Olsen, and M. W. Lambert. Early diagenesis: impact of organic matter on mass physical properties and processes, California continental margin. *Marine Geology*, 159(1-4):7–34, 1999.

P. Berg, N. Risgaard-Petersen, and S. Rysgaard. Interpretation of measured concentration profiles in sediment pore water. *Limnology and Oceanography*, 43(7):1500–1510, 1998.

P. V. Bhaskar and N. B. Bhosle. Microbial extracellular polymeric substances in marine biogeochemical processes. *Current Science*, 88(1):45–53, 2005.

G. F. Birch. The nature and origin of mixed apatite/glauconite pellets from the continental shelf off South Africa. *Marine Geology*, 29:313–334, 1979.

REFERENCES

V. Boivin-Jahns, R. Ruimy, A. Bianchi, S. Daumas, and R. Christen. Bacterial diversity in a deep-subsurface clay environment. *Applied and Environmental Microbiology*, 62(9): 3405–3412, 1996.

M. D. Bolton, S. A. Ganesan, and D. J. White. SAFEBUCK Phase II: Axial pipe-soil interaction testing using the Cam-shear device. CUTS Report no. SC-CUTS-0609-R2. Technical report, University of Cambridge, 2007.

M. D. Bolton, Y. Nakata, and Y. P. Cheng. Micro- and macro-mechanical behaviour of DEM crushable materials. *Geotechnique*, 58(6):471–480, 2008.

M. D. Bolton, S. A. Ganesan, and D. J. White. SAFEBUCK Phase II: Axial pipe-soil resistance - summary report. CUTS Report no. SC-CUTS-0705-R1. Technical report, University of Cambridge, 2009.

D. Borel, A. Puech, H. Dendani, and M. de Ruijter. High quality sampling for deep water geotechnical engineering: the STACOR Experience. *Ultra Deep Engineering and Technology, Brest*, June 2002.

B. P. Boudreau. On the equivalence of nonlocal and radial-diffusion models for porewater irrigation. *Journal of Marine Research*, 42(3):731–735, 1984.

B.P. Boudreau. *Diagenetic models and their implementation.* Springer, Berlin, 1997.

BPExploration. Age of crust sediments. Personal communication discussing the age of West African crust sediments, 2007.

BPExploration. Block 31 offshore Angola. *webpage*, accessed 19 December 2009. URL `http://www.bp.com/genericarticle.do?categoryId=2012968&contentId=7056656`.

J. F. C. Brouwer, K. Wolfstein, G. K. Ruddy, T. E. R. Jones, and L. J. Stal. Biogenic stabilisation of intertidal sediments: the importance of extracellular polymeric substances produced by benthic diatoms. *Microbial Ecology*, 49:501–512, 2005.

D. A. S. Bruton. External temperature of hot pipelines. Email discussion on external temperatures of hot-oil pipelines, 2010.

D. A. S. Bruton, M. Carr, and D. White. The influence of pipe-soil interaction on lateral buckling and walking of pipelines. *The SAFEBUCK JIP. Sixth International Offshore Site Investigation and Geotechnics Conference*, 2007.

D. A. S. Bruton, D. J. White, M. Carr, and J. C. Y. Cheuk. Pipe-soil interaction during lateral buckling and pipeline walking - The SAFEBUCK JIP. *Proceedings of the Offshore Technology Conference*, 2008.

W. R. Bryant, P. Cernock, and J. Morelock. Shear strength and consolidation characteristics of marine sediments from the western Gulf of Mexico. In A. F. Richards, editor, *Marine Geotechnique.* Univ. Illinois Press, 1967.

S. Buchan, F. C. D. Dewes, D. M. McCann, and D. Taylor Smith. Measurements of the acoustic and geotechnical properties of marine sediment cores. In A. F. Richards, editor, *Marine Geotechnique.* Univ. Illinois Press, 1967.

J. Y. Buchanan. On the occurance of sulphur in marine muds and nodules, and its bearing on on their mode of formation. *Proceedings of the Royal Society of Edinburg*, 18:17–39, 1890.

J. Burland. On the compressibility and shear strength of natural clays. *Geotechnique*, 40(3): 329–378, 1990.

P. L. Busch and W. Stumm. Chemical interactions in the aggregation of bacteria: bioflocculation in waste treatment. *Environmental Science Technology*, 2:49–53, 1968.

W. H. Busch and G. H. Keller. The physical-properties of Peru-Chile continental-margin sediments - the influence of coastal upwelling on sediment properties. *Journal of Sedimentary Petrology*, 51(3):705–719, 1981.

W. H. Busch and G. H. Keller. Analysis of sediment stability on the Peru-Chile continental slope. *Marine Georesources & Geotechnology*, 5(2):181–211, 1983.

D. E. Canfield. Sulfate reduction in deep-sea sediments. *American Journal of Science*, 291(2): 177–188, 1991.

A. Casagrande. The determination of the pre-consolida- tion load and its practical signicance. *Proc. 1st. Int. Conf. on Soil Mech. and Found. Eng*, 3:60–64, 1936.

H. S. Chafetz and A. Reid. Syndepositional shallow-water precipitation of glauconitic minerals. *Sedimentary Geology*, 136:29–42, 2000.

Y. P. Cheng, M. D. Bolton, and Y. Nakata. Crushing and plastic deformation of soils simulated using dem. *Geotechnique*, 54(2):131–141, 2004.

J. Chu, M. W. Bo, M. F. Chang, and V. Choa. Consolidation and permeability properties of Singapore Marine Clay. *Journal of Geotechnical and Geoenvironmental Engineering, ASCE*, 128(9):724–732, 2002.

F. Cotecchia and R. J. Chandler. A general framework for the mechanical behaviour of clays. *Geotechnique*, 50(4):431–447, 2000.

V. De Gennaro, P. Delage, and A. Puech. On the compressibility of deepwater sediments of the Gulf of Guinea. In S. Gourvenec and M. Cassidy, editors, *Frontiers of Offshore Geotechnics: ISFOG 2005*, pages 1063–1069, Perth, Australia, 2005. Taylor and Francis Group, London.

M. F. Deflaun and L. M. Mayer. Relationships between bacteria and grain surfaces in intertidal sediments. *Limnology and Oceanography*, 28(5):873–881, 1983.

E. H. Doyle, B. McClelland, and G. H. Ferguson. Wire-line vane probe for deep penetration measurements of ocean sediment strength. *Offshore Technology Conference Preprints*, 2 (1327):11, 1971.

C. J. Ehlers, J. Chen, H. H. Roberts, and Y. C. Lee. The origin of near-seafloor crust zones in deepwater. In S. Gourvenec and M. Cassidy, editors, *Frontiers of Offshore Geotechnics: ISFOG 2005*. Taylor & Francis Group, London., 2005.

T. Evans. Block 18 offshore Angola. Technical Report 20021117-1, Norwegian Geotechnical Institute, 2002.

H. Fossing, T. G. Ferdelman, and P. Berg. Sulfate reduction and methane oxidation in continental margin sediments influenced by irrigation (South-East Atlantic off Namibia). *Geochimica Et Cosmochimica Acta*, 64(5):897–910, 2000.

P. N. Froelich, G. P. Klinkhammer, M. L. Bender, N. A. Luedtke, G. R. Heath, D. Cullen, P. Dauphin, D. Hammond, B. Hartman, and V. Maynard. Early oxidation of organic-matter in pelagic sediments of the eastern equatorial atlantic - suboxic diagenesis. *Geochimica Et Cosmochimica Acta*, 43(7):1075–1090, 1979.

L. E. Frostick and I. N. Mccave. Seasonal shifts of sediment within an estuary mediated by algal growth. *Estuarine and Coastal Marine Science*, 9(5):569–576, 1979.

REFERENCES

M. K. Gingras, S. G. Pemberton, S. Dashtgard, and L. Dafoe. How fast do marine invertebrates burrow? *Palaeogeography, Palaeoclimatology, Palaeoecology*, 270:280–286, 2008.

G.P. Glasby. Manganese: predominant role of nodules and crusts. In H. D. Schulz and M. Zabel, editors, *Marine Geochemistry*, pages 371–427. Springer, 2006.

A. Gooday. On the faecal pellets of polychaete sp. Personal communication discussing photographic evidence of faecal pellets found in West African crusts, 2009.

B. Grupe, H.J. Becker, and H.U. Oebius. Geotechnical and sedimentological investigations of deep-sea sediments from a manganese nodule field of the Peru Basin. *Deep-Sea Research Part II*, 48:3593–3608, 2001.

M. S. Hassan and H. M. Baioumy. Structural and chemical alteration of glauconite under progressive acid treatment. *Clays and Clay Minerals*, 54(4):491–499, 2006.

M. Hattab and J.-L. Favre. Analysis of the experimental compressibility of deep water marine sediments from the gulf of guinea. *Marine and Petroleum Geology*, 27:486–499, 2010.

A. Heissenberger, G. G. Leppard, and G. J. Herndl. Ultrastructure of marine snow .2. microbiological considerations. *Marine Ecology-Progress Series*, 135(1-3):299–308, 1996.

C. Hensen, H. Landenberger, M. Zabel, J. K. Gundersen, R. N. Glud, and H. D. Schulz. Simulation of early diagenetic processes in continental slope sediments off southwest Africa: the computer model CoTAM tested. *Marine Geology*, 144(1-3):191–210, 1997.

E. Hoek. *Practical Rock Engineering*, 2006.

A. F. Holland, R. G. Zingmark, and J. M. Dean. Quantitative evidence concerning stabilization of sediments by marine benthic diatoms. *Marine Biology*, 27(3):191–196, 1974.

G. T. Houlsby. Theoretical analysis of the fall cone test. *Geotechnique*, 32:111–118, 1982.

C. J. Howe. *Gene Cloning and Manipulation*. Cambridge University Press, 2007.

J. A. Hudsen and J. P. Harrison. *Engineering rock mechanics: An introduction to the principles.* Pergamon, 1997.

N. B. Huu, E. B. M. Denner, D. T. C. Ha, G. Wanner, and H. Stan-Lotter. *Marinobacter aquaeolei sp. nov.*, a halophilic bacterium isolated from a Vietnamese oil-producing well. *International Journal of Systematic Bacteriology*, 49:367–375, 1999.

R. Jahnke. A model of microenvironments in deep-sea sediments - formation and effects on porewater profiles. *Limnology and Oceanography*, 30(5):956–965, 1985.

R. A. Jahnke. Early diagenesis and recycling of biogenic debris at the sea-floor, Santa-Monica Basin, California. *Journal of Marine Research*, 48(2):413–436, 1990.

R. A. Jahnke, S. R. Emerson, and J. W. Murray. A model of oxygen reduction, denitrification, and organic-matter mineralization in marine-sediments. *Limnology and Oceanography*, 27 (4):610–623, 1982.

S. E. Jones and F. C. Jago. In situ assessment of modification of sediment properties by burrowing invertebrates. *Marine Biology*, 115:10, 1993.

G. H. Keller. Organic matter and the geotechnical properties of submarine sediments. *Geo-Marine Letters*, 2:191–198, 1982.

G. V. Kumar and D. Muir Wood. Fall cone and compression tests on clay-gravel mixtures. *Geotechnique*, 49(6):727–739, 1999.

M. H. Le. *Caracterisation physique et mecanique des soils marins d'offshore profond*. PhD thesis, l'Institut Français du Pétrole et le CERMES (Institut Navier), 2008.

H. Lee, R. E. Kayen, and W. G. McArthur. Consolidation, triaxial shear-strength, and index-property characteristics of organic-rich sediment from the Peru continental margin: Results from Leg 112. *Proceedings of the Ocean Drilling Program, Scientific Reports*, 112:639–651, 1990.

L.J.L. Lemos and P.R. Vaughan. Clay-interface shear resistance. *Geotechnique*, 50(1):55–64, 2000.

J. F. Lupini, A. E. Skinner, and P.R. Vaughan. The drained residual strength of cohesive soils. *Geotechnique*, 31(2):181–213, 1981.

P. Martens. Faecal pellets. *Fich. Ident. Zooplancton*, 162, 1978.

A. J. Martin. Zoophycos burrows. *webpage*, accessed 16 December 2010. URL `http://www.envs.emory.edu/faculty/MARTIN/ichnology/Zoophycos.htm`.

I. N. McCave. *Erosion, transport and deposition of fine-grained marine sediments*. Fine-Grained Sediments: Deep-Water Processes and Facies. Blackwell Scientific Publications, Oxford, 1984.

I. N. McCave. Biological pumping upwards of the coarse fraction of deep-sea sediments. *Journal of Sedimentary Petrology*, 58(1):148–158, 1988.

G McDowell and M. D. Bolton. On the micromechanics of crushable aggregates. *Geotechnique*, 48(5):667–679, 1998.

A. Meadows and P. S. Meadows. Bioturbation in deep-sea pacific sediments. *Journal of the Geological Society*, 151:361–375, 1994.

A. Meadows, P. S. Meadows, F. J. C. West, and J. M. H. Murray. Bioturbation, geochemistry and geotechnics of sediments a!ected by the oxygen minimum zone on the oman continental slope and abyssal plain, arabian sea. *Deep-Sea Research II*, 47:21, 2000.

P. S. Meadows and J. Tait. Modification of sediment permeability and shear-strength by 2 burrowing invertebrates. *Marine Biology*, 101(1):75–82, 1989.

P. S. Meadows, A. C. Reichelt, A. Meadows, and J. S. Waterworth. Microbial and meifaunal abundance, redox potential, ph and shear strength profiles in deep sea pacific sediments. *Journal of the Geological Society*, 151:377–390, 1994.

J. K. Mitchell and J. C. Santamarina. Biological considerations in geotechnical engineering. *Journal of Geotechnical and Geoenvironmental Engineering, ASCE*, 131(10), 2005.

H.B. Moore. The specific identification of faecal pellets. *Journal of the Marine Biology Association , New Series*, XVII(2), 1931a.

H.B. Moore. The muds of the clyde sea area. iii. chemical and physical conditions; rate and nature of sedimentation; and fauna. *Journal of the Marine Biological Association, New Series*, XVIII(2), 1931b.

H.B. Moore. Faecal pellets in relation to marine deposits. In *Recent marine sediments*, pages 516–524. Association of Petroleum Geologists, 1939.

P. J. Muller and E. Suess. Productivity, sedimentation-rate, and sedimentary organic-matter in the oceans .1. organic-carbon preservation. *Deep-Sea Research Part a-Oceanographic Research Papers*, 26(12):1347–1362, 1979.

REFERENCES

J. M. H. Murray, A. Meadows, and P. S. Meadows. Biogeomorphological implications of microscale interactions between sediment geotechnics and marine benthos: a review. *Geomorphology*, 47:15–30, 2002.

J. W. Murray, V. Grundmanis, and W. M. Smethie. Interstitial water chemistry in sediments of saanich inlet. *Geochimica Et Cosmochimica Acta*, 42(7):1011–1026, 1978.

S. S. Najjar, R. B. Gilbert, E. Liedtke, B. McCarron, and A. G. Young. Residual shear strength for interfaces between pipelines and clays at low effective normal streses. *JOURNAL OF GEOTECHNICAL AND GEOENVIRONMENTAL ENGINEERING, ASCE*, 133(6), 2007.

NCIMB. Growth media recipies, 2007a. http://www.ncimb.com/files/NCIMB%20Culture %20Media%20v2.0.pdf.

NCIMB. Revival of cultures, 2007b. http://www.ncimb.com/files/Qf077%20- %20revival%20of%20cultures%20notice.pdf.

A. C. Neumann, C. D. Gebelein, and T. P. Scoffin. Composition, structure and erodability of subtidal mats, abaco, bahamas. *Journal of Sedimentary Petrology*, 40(1):274–, 1970.

T. A. Newson, M. F. Bransby, P. Brunning, and D. R. Morrow. Determination of undrained shear strength parameters for buried pipeline stability in deltaic soft clays. Technical report, The University of Dundee, 2004.

Newswires. Location of Blocks 18 and 31. *webpage*, accessed 12 October 2010. URL `http: //www.energy-pedia.com/article.aspx?articleid=139632`.

A. Nocilla, M. Coop, and F. Colleselli. The mechanics of an italian silt: an example of 'transitional' behaviour. *Geotechnique*, 56(4):261–271, 2006.

G. S. Odin and A. Matter. De glauconiarum origine. *Sediment*, 28:611–641, 1981.

Offshore-technology. Block 18, Angola. *webpage*, accessed 26 August 2010. URL `www. offshore-technology.com/projects/greater_plutonio/specs.html`.

O. Oung, J. W. G. Van der Vegt, L Tiggelman, and H. E. Brassinga. Adapted T-bar penetrometer versus CPT to determine undrained shear strengths of Dutch soft soils. Technical report, GeoDelf, ?

R. J. Parkes, B. A. Cragg, and P. Wellsbury. Recent studies on bacterial populations and processes in subseafloor sediments: A review. *Hydrogeology Journal*, 8:11–28, 2000.

R. C. Pedersen, R. E. Olsen, and Rauch A. F. Shear and interface strength of clay at very low effective stress. *ASTM Geotechnical Testing Journal*, 26(1):1–8, 2003.

A. Puech, H. Dendani, J. F. Nauroy, and J. Meunier. Characterisation of Gulf of Guinea deepwater soils for geotechnical engineering: successes and challenges, 21-22 October 2004.

A. Puech, J. L. Colliat, J. F. Nauroy, and J. Meunier. Some geotechncial specificities of Gulf of Guinea deepwater sediments, 2005.

A. Puech, J.-L. Colliat, H. Dendani, and J.-F. Nauroy. Gulf of Guinea deepwater sediments : geotechnical properties, design issues and installation experiences. In *Frontiers of Offshore Geotechnics: ISFOG2 2010*, 2010.

P. K. Pufahl, M. A. Maslin, L. Anderson, V. Bruchert, F. Jansen, H. Lin, M. Perez, and L. Vidal. Pithostratigraphic summary for leg 175: Angola-benguela upwelling system. In G. Wefer, W. H. Berger, and C. Richter, editors, *Proceedings of the Ocean Drilling Program, Initial Reports*, volume 175, 1998.

R. Pusch. Microstructural changes in soft quick clay at failure. *Canadian Geotechnical Journal*, 7:7, 1970.

R. Pusch. Influence of organic matter on the geotechnical properties of clays. *National Swedish Building. Resource Document*, 11:1–64, 1973.

G. W. Quiros and R. L. Little. Deepwater soil properties and their impact on the geotechnical program. *Proceedings of the Offshore Technology Conference*, 2003.

M. F. Randolph. Characterization of soft sediments for offshore applications. *2nd International Site Characterization Conference, Porto, Portugal*, 1:209–232, 2004.

M. F. Randolph and G. T. Houlsby. The limiting pressure on a circular pile loaded laterally in cohesive soil. *Geotechnique*, 34(4):613–623, 1984.

M. F. Randolph, M. Cassidy, S. Gourvenec, and C. Erbrich. Challenges of offshore geotechnical engineering. *Osaka*, 2005.

B. Ransom, R. H. Bennett, R. Baerwald, and K. Shea. TEM study of in situ organic matter on continental margins: Occurrence and the "monolayer" hypothesis. *Marine Geology*, 138 (1-2):1–9, 1997.

V. Rebata-Landa and J. C. Santamarina. Mechanical limits to microbial activity in deep sediments. *Geochemistry Geophysics Geosystems*, 7:–, 2006.

C. E. Reimers. Organic-matter in anoxic sediments off Central Peru - relations of porosity, microbial decomposition and deformation properties. *Marine Geology*, 46(3-4):175–197, 1982.

D.C. Rhoads and L.F. Boyer. *The effects of marine benthos on physical properties of sediments: a successional perspective*. Plenum Geobiology Series. Plenum Press, New York, 1982.

D.C. Rhoads, J. Y. Yingst, and W.J. Ullman. *Seafloor stability in Central Long Island Sound: Part I. Temporal changes in erodibility of fine-grained sediment*. Estuarine Interactions. Academic Press, 1978.

J. M. Robert and D. Gouleau. Experimental confirmation of role of a benthic diatom, *Navicula-Ramosissima (Agardh) Cleve*, in secretion of mucoidal materials which stabilize muddy marine littoral flats. *Comptes Rendus Hebdomadaires Des Seances De L Academie Des Sciences Serie D*, 284(19):1915–, 1977.

A. A. Rowden, F. C. Jago, and S. E. Jones. Influenc of benthic macrofauna on the geotechnical and geophysical properties of surficial sediment, North Sea. *Continental Shelf Research*, 18: 1347–1363, 1998.

P. W. Rowe. The relevance of soil fabric to site investigation practice. *Geotechnique*, 22(2): 195–300, 1972.

Rullkotter, editor. *Organic Matter: The Driving Force for Early Diagenesis*. Marine Geochemistry. Springer, Berlin, 2007.

J. Sambrook and D. Russell. *Molecular Cloning: A Laboratory Manual*, volume 3. CSHL Press, 2001.

W. Schafer. *Ecology and palaeoecology of marine environments*. Oliver and Boyd, 1972.

A. Schofield and C. P. Wroth. *Critical state soil mechanics*. McGraw-Hill, 1968.

H. D. Schulz and M. Zabel. *Marine Geochemistry*. Springer, Berlin Heidelberg, 2006.

REFERENCES

T. P. Scoffin. Trapping and binding of subtidal carbonate sediments by marine vegetation in Bimini Lagoon, Bahamas. *Journal of Sedimentary Petrology*, 40(1):249–, 1970.

P.H. Shipway and I. M. Hutchings. Attrition of brittle spheres by fracture impact loading under compression and impact loading. *Powder Technology*, 76:23–30, 1993.

D. J. Shirley. An improved shear wave transducer. *Journal of the Acoustical Society of America*, 63(5), 1978.

A. Skempton. Discussion of the structure of inorganic soil. *Proceedings of ASCE, Soil Mechanics and Foundations Division*, 80:19–22, 1954.

A. Skempton. The consolidation of clays by gravitational compaction. *Q. J. Geological Society*, 125, 1970.

A. W. Skempton. Residual strength of clays in landslides, folded strata and the laboratory. *Geotechnique*, 35(1):3–18, 1985.

K. Soga. Soga research expertise. In J. T. DeJong, B. Mortensen, and B. Martinez, editors, *Bio-Soils Interdisciplinary Science&Engineering Initiative: "Meeting societal needs through international transformative research"*, 2007.

D. P. Stewart and M. F. Randolph. A new site investigation tool for the centrifuge. In A. A. Balkema, editor, *Centrifuge 91 : International Conference on Centrifuge Testing*, pages 531–538, Rotterdam, 1991.

D. P. Stewart and M. F. Randolph. T-bar penetration testing in soft clay. *Journal of Geotechnical Engineering, ASCE*, 120(12):2230–2235, 1994.

P. Stoffers, G.P. Glasby, and G. Frenzel. Comparison of the characteristics of manganese micronodules from the equatorial and south-west pacific. *Tschermaks Mineralogische und Petrographische Mitteilungen*, 33:1–23, 1984.

W. Stumm and J. J. Morgan. *Aquatic Chemistry*. Wiley, New York, 2nd edition edition, 1981.

N. Sultan, P. Cochonat, E. Cauquil, and J. L. Colliat. Apparent overconsolidation and failure mechanism in marine sediments. *Proc. OTRC Int. Conference Honoring Prof. W. Dunlap*, 2001.

J. Takahashi and T. Yagi. Peculiar mud grains and their relation to the origin of glauconite. *Economic Geology*, 24(8):838–52, 1929.

F. Thomas, B. Rebours, J.-F. Nauroy, and J. Meunier. Mineralogical characteristics of the gulf of guinea deep water sediments, 2005 2005.

F. Thomas, A. Puech, J.F. Nauroy, E. Palix, and J. Meunier. Specific identification test procedures for deepwater sediments of Gulf of Guinea. *Proceedings of the International Conference on Offshore Site Investigation and Geotechnics, SUT, London*, 2007.

E. M. Thorp. Description of the deep-sea bottom samples from the western North Atlantic and the Caribbean Sea. *Bulletin of the Scripps Institute of Oceanography, Technical Series*, III(1):1–31, 1931.

J. H. Trevor. The burrowing activity of *Nephthys cirrosa, Ehlers (Annelida: Polychaeta)*. *Journal of Experimental Marine Biology and Ecology*, 24:307–319, 1976.

J. H. Trevor. The burrowing of nereis diversicolor o.f. muller, together with some observations on *Arenicola marina (L.) (Annelida: Polychaeta)*. *Journal of Experimental Marine Biology and Ecology*, 30:129–145, 1977.

J. H. Trevor. The dynamics and mechanical energy expendi- ture of the polychaetes *Nephthys cirrosa*, *Nereis diversicolor* and *Arenicola marina* during burrowing. *Estuarine and Coastal Marine Science*, 6:605–619, 1978.

C. M. Turley, K. Lochte, and R. S. Lampitt. Transformations of biogenic particles during sedimentation in the northeastern atlantic. *Philosophical Transactions of the Royal Society of London Series B-Biological Sciences*, 348(1324):179–189, 1995.

G. J. C. Underwood and D. M. Paterson. Recovery of intertidal benthic diatoms after biocide treatment and associated sediment dynamics. *Journal of Marine Biology*, 73:20, 1993.

G. J. C. Underwood, M. Boulcott, and C. A. Raines. Environmental effects on exopolymer production by marine benthic diatoms: dynamics, changes in composition, and pathways of production. *Journal of Phycology*, 40:293–304, 2004.

L. E. Vallejo and Y. Zhou. The mechanical properties of simulated soil-rock mixtures. *Proceedings of the 13th International Conference on Soil Mechanics and Foundation Engineering*, 1:365–368, 1994.

H. Wang and K. Edwards. Bacterial and archaeal DNA extracted from inoculated experiments: Implication for the optimization of DNA extraction from deep-sea basalts. *Geomicrobiology Journal*, 26(7):463–469, 2009.

Z. J. Westgate, M. F. Randolph, D. J. White, and S. Li. The influence of sea state on as-laid pipeline embedment: A case study. *Applied Ocean Research*, 32(3), 2010.

D. J. White and J. C. Y. Cheuk. Modelling the soil resistance on seabed pipelines during large cycles of lateral movement. *Marine Structures*, 21:59–79, 2008.

D. J. White, C. Gaudin, N. Boylan, and H. Zhou. Interpretation of T-bar penetrometer tests at shallow embedment and in very soft soils. *Canadian Geotechnical Journal*, 47:218–229, 2010.

B. Wigglesworth-Cooksey, D. Berglund, and K. E. Cooksey. Cell–cell and cell–surface interactions in an illuminated biofilm: Implications for marine sediment stabilisation. *Geochemical Transactions*, 10:75–82, 2001.

D. M. Wood. *Soil behaviour and critical soil mechanics*. Cambridge University Press, 1990.

M. Wrangstadh, P. L. Conway, and S. Kjelleberg. The production and release of an extracellular polysaccharide during starvation of a marine *Pseudomonas Sp* and the effect thereof on adhesion. *Archives of Microbiology*, 145(3):220–227, 1986.

N. J. Yafrate and J. T. DeJong. Considerations in evaluating the remoulded undrained shear strength from full flow penetrometer cycling. In S. Gourvenec and M. Cassidy, editors, *Frontiers of Offshore Geotechnics: ISFOG 2005*, 2005.

N. J. Yafrate and J. T. DeJong. Influence of penetration rate on measured resistance with full flow penetrometers in soft clay. *Geo-Denver*, 2007.

N. J. Yafrate, J. T. DeJong, and D. DeGroot. The role of full-flow penetrometer area ratio on penetration resistance and shear strength estimates. *Proceedings of the International Conference on Offshore Site Investigation and Geotechnics, SUT, London*, 2007.

T. S. Yun, G. A. Narsilio, and J. C. Santamarina. Physical characterisation of core samples recovered from Gulf of Mexico. *Marine and Petroleum Geology*, 23:893–900, 2006.

Research Zymo. Zr soil microbe DNA kit; instruction manual. Technical report, 2007.

Appendix A

Cam-shear Test Summary and Shear Stress - Displacement Plots

A. CAM-SHEAR TEST SUMMARY AND SHEAR STRESS - DISPLACEMENT PLOTS

Sample	Tested depth m	Normal stress kPa	Shear strength τ kPa		Apparent friction coefficient $\mu = \tau/\sigma'$		Apparent friction angle $\phi°$		Speed mm/s	Plane	Coating	Comments
			Peak	Residual	Peak	Residual	Peak	Residual				
A	0.02	2.1	2.1		1		45		0.05	internal	-	-
A	0.04	2.1	2.8	2.2	1.33	1.05	53	46	0.5	interface	smooth	smeared
A	0.04	2.1	2	1.6	0.95	0.76	44	37	0.5	interface	smooth	clean
A	0.04	2.1	2	1.7	0.93	0.81	43	39	0.05	interface	smooth	clean
A	0.04	2.1	1.3	1.3	0.62	0.62	32	32	0.005	interface	smooth	clean
A	0.18	4.1	4.1		0.83		40		0.05	internal	-	-
A	0.2	4.1	2	0.6	0.49	0.15	26	8	0.5	interface	smooth	clean
A	0.2	4.1	2.3	2.3	0.56	0.56	29	29	0.05	interface	smooth	clean
A	0.2	4.1	4.2	4.2	1.02	1.02	46	46	0.005	interface	smooth	clean
A	0.32	6.1	2.8		0.52		28		0.005	internal	-	-
A	0.34	6.1	1.5	0.4	0.25	0.07	14	4	0.5	interface	rough	clean
A	0.34	6.1	2.6	1.1	0.43	0.25	23	14	0.05	interface	rough	clean
A	0.34	6.1	1.1	1	0.18	0.16	10	9	0.005	interface	rough	clean
B	0.02	2.1	2.1		1		45		0.05	internal	-	-
B	0.04	2.1	1	0.3	0.48	0.14	25	8	0.5	interface	rough	clean
B	0.04	2.1	0.6	0.1	0.29	0.05	16	3	0.05	interface	rough	clean
B	0.04	2.1	0.8	0.8	0.36	0.36	20	20	0.005	interface	rough	clean
B	0.18	4.1	3.4		0.83		40		0.05	internal	-	-
B	0.2	4.1	0.6	0.2	0.15	0.05	8	3	0.5	interface	rough	clean
B	0.2	4.1	0.4	0.1	0.1	0.02	6	1	0.05	interface	rough	clean
B	0.2	4.1	0.9	0.8	0.32	0.29	18	16	0.005	interface	rough	clean

Sample	Tested depth m	Normal stress kPa	Shear strength τ kPa Peak	Residual	Apparent friction coefficient $\mu = \tau/\sigma'$ Peak	Residual	Apparent friction angle $\phi°$ Peak	Residual	Speed mm/s	Plane	Coating	Comments
C	0.02	2.1	1.2		0.62		32		0.05	internal	-	wet
C	0.04	2.1	0.2	0.1	0.14	0.05	8	3	0.5	interface	rough	wet, clean
C	0.04	2.1	0.8	0.1	0.62	0.05	32	3	0.05	interface	rough	wet, clean
C	0.04	2.1	0.7	0.6	0.29	0.29	16	16	0.005	interface	rough	wet, clean
C	0.18	4.1	3.6		0.88		41		0.05	internal	-	wet
C	0.2	4.1	1.7	0.6	0.41	0.15	23	8	0.5	interface	rough	wet, clean
C	0.2	4.1	2.4	2	0.59	0.49	30	26	0.05	interface	rough	wet, clean
C	0.2	4.1	1.3	1.1	0.32	0.32	18	18	0.005	interface	rough	wet, clean
C	0.3	6.1	3.5		0.61		32		0.005	internal	-	wet
C	0.32	6.1	2.2	0.7	0.48	0.11	25	7	0.5	interface	rough	wet, clean
C	0.32	6.1	1.5	0.9	0.25	0.15	14	8	0.05	interface	rough	wet, clean
C	0.32	6.1	1.7	1.6	0.28	0.26	16	15	0.005	interface	rough	wet, clean
D	0.02	2.1	2.6		1.24		51		0.05	internal	-	wet
D	0.04	2.1	1.8	0.4	0.86	0.19	41	11	0.5	interface	rough	wet, clean
D	0.04	2.1	1.1	0.8	0.52	0.38	28	21	0.05	interface	rough	wet, clean
D	0.04	2.1	1	1	0.48	0.48	25	25	0.005	interface	rough	wet, clean
D	0.28	5.1	3.5		0.69		34		0.005	internal	-	wet
D	0.3	5.1	1.3	0.5	0.25	0.1	14	6	0.5	interface	rough	wet, clean
D	0.3	5.1	1.6	0.9	0.31	0.18	17	10	0.05	interface	rough	wet, clean
D	0.3	5.1	1.5	1.5	0.29	0.29	16	16	0.005	interface	rough	wet, clean

A. CAM-SHEAR TEST SUMMARY AND SHEAR STRESS - DISPLACEMENT PLOTS

Sample	Tested depth m	Normal stress kPa	Shear strength τ kPa		Apparent friction coefficient $\mu = \tau/\sigma'$		Apparent friction angle $\phi°$		Speed mm/s	Plane	Coating	Comments
			Peak	Residual	Peak	Residual	Peak	Residual				
E	0.02	2.1	3		1.43		55		0.05	internal	-	wet
E	0.04	2.1	0.6	0.5	0.43	0.43	23	23	0.5	interface	smooth	wet, clean
E	0.04	2.1	1	1	0.86	0.81	41	39	0.05	interface	smooth	wet, clean
E	0.04	2.1	1.7	1.7	0.29	0.29	16	16	0.005	interface	smooth	wet, clean
E	0.18	4.1	6.7		1.63		59		0.05	internal	-	wet
E	0.2	4.1	0.5	0.3	0.49	0.49	26	26	0.5	interface	smooth	wet, clean
E	0.2	4.1	1.1	0.8	0.27	0.2	15	11	0.05	interface	smooth	wet, clean
E	0.2	4.1	0.5	0.5	0.12	0.12	7	7	0.005	interface	smooth	wet, clean
E	0.28	5.1	6.7		1.31		53		0.05	internal	-	wet
E	0.3	5.1	2	0.9	0.55	0.14	29	8	0.5	interface	rough	wet, clean
E	0.3	5.1	2	1.6	0.39	0.31	21	17	0.05	interface	rough	wet, clean
E	0.3	5.1	1.2	0.8	0.24	0.16	13	9	0.005	interface	rough	wet, clean

Sample	Tested depth m	Normal stress kPa	Shear strength τ kPa		Apparent friction coefficient $\mu = \tau/\sigma'$		Apparent friction angle $\phi°$		Speed mm/s	Plane	Coating	Comments
			Peak	Residual	Peak	Residual	Peak	Residual				
F	0.07	2.1	1.7		0.81		39		0.05	internal	internal	wet
F	0.09	2.1	0.1	0.1	0.05	0.05	3	3	0.5	interface	rough	wet, clean
F	0.09	2.1	0.1	0.1	0.05	0.05	3	3	0.05	interface	rough	wet, clean
F	0.09	2.1	2.1	2.1	1	1	45	45	0.005	interface	rough	wet, clean
F	0.18	4.1	5		1.22		51		0.05	internal	internal	wet
F	0.2	4.1	0.7	0.6	0.17	0.15	10	8	0.5	interface	rough	wet, clean
F	0.2	4.1	1.4	0.6	0.34	0.15	19	8	0.05	interface	rough	wet, clean
F	0.2	4.1	0.8	0.5	0.2	0.12	11	7	0.005	interface	rough	wet, clean
F	0.3	6.1	2.6		0.43		23		0.05	internal	internal	wet
F	0.32	6.1	1.2	0.1	0.2	0.02	11	1	0.5	interface	rough	wet, clean
F	0.32	6.1	3.4	1.5	0.56	0.25	29	14	0.05	interface	rough	wet, clean
F	0.32	6.1	1.9	1.9	0.31	0.31	17	17	0.005	interface	rough	wet, clean

A. CAM-SHEAR TEST SUMMARY AND SHEAR STRESS - DISPLACEMENT PLOTS

Sample	Tested depth (m)	Normal stress (kPa)	Shear strength τ (kPa)		Apparent friction coefficient $\mu = \tau/\sigma'$		Apparent friction angle $\phi°$		Speed (mm/s)	Plane	Coating	Comments
			Peak	Residual	Peak	Residual	Peak	Residual				
G	0.08	2.1	2.3		1.1		48		0.05	internal	-	wet
G	0.1	2.1	0.5	0.1	0.24	0.05	13	3	0.5	interface	rough	wet, clean
G	0.1	2.1	0.4	0.4	0.19	0.19	11	11	0.05	interface	rough	wet, clean
G	0.1	2.1	0.5	0.5	0.24	0.24	13	13	0.005	interface	rough	wet, clean
G	0.18	4.1	4.4		1.07		47		0.05	internal	-	wet
G	0.2	4.1	0.4	0.1	0.1	0.02	6	1	0.5	interface	rough	wet, clean
G	0.2	4.1	2.1	2.1	0.51	0.51	27	27	0.05	interface	rough	wet, clean
G	0.2	4.1	1	0.8	0.24	0.2	14	11	0.005	interface	rough	wet, clean
H	0.18	4.1	3.2		0.78		38		0.05	internal	-	wet
H	0.2	4.1	1	0.5	0.24	0.12	14	7	0.5	interface	smooth	wet, clean
H	0.2	4.1	1.5	1.5	0.37	0.37	20	20	0.05	interface	smooth	wet, clean
H	0.2	4.1	1.3	1.3	0.32	0.32	18	18	0.005	interface	smooth	wet, clean

The following figures are Cam-shear test results completed on natural samples showing both interface and soil-soil shearing at 0.5mm/s, 0.05mm/s and 0.005mm/s.
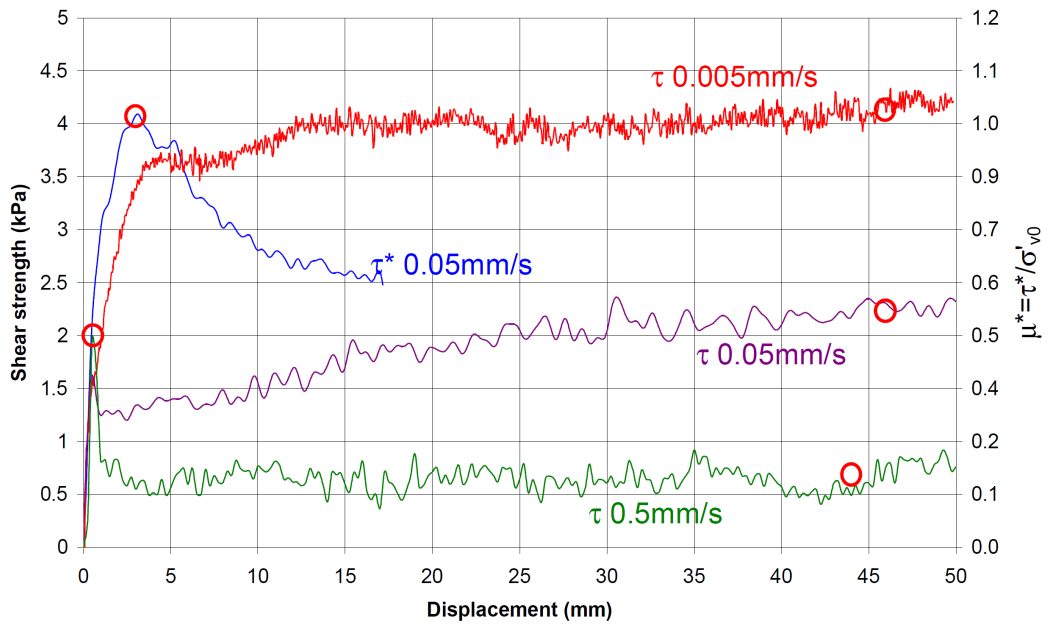
Fig. A.1 A 0.2m smooth
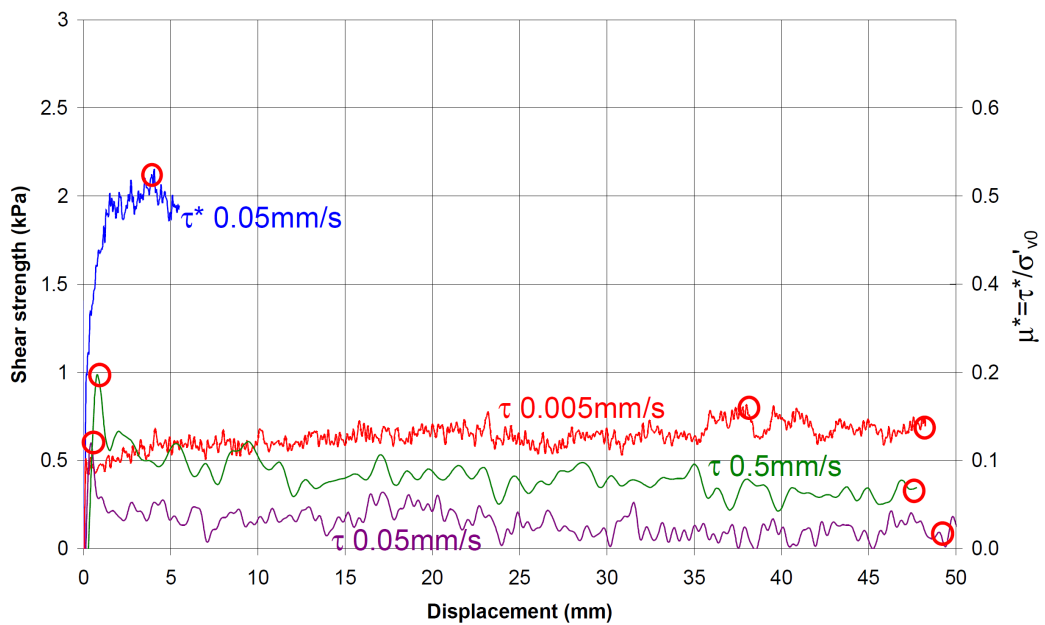
Fig. A.2 B 0.04m rough

A. CAM-SHEAR TEST SUMMARY AND SHEAR STRESS - DISPLACEMENT PLOTS
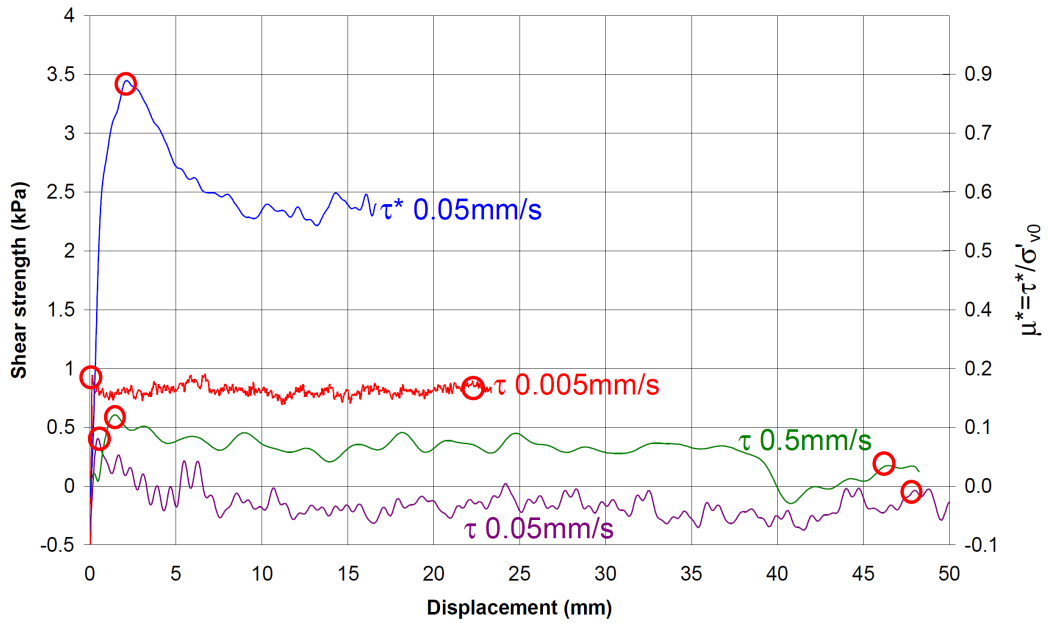
Fig. A.3 B 0.2m rough
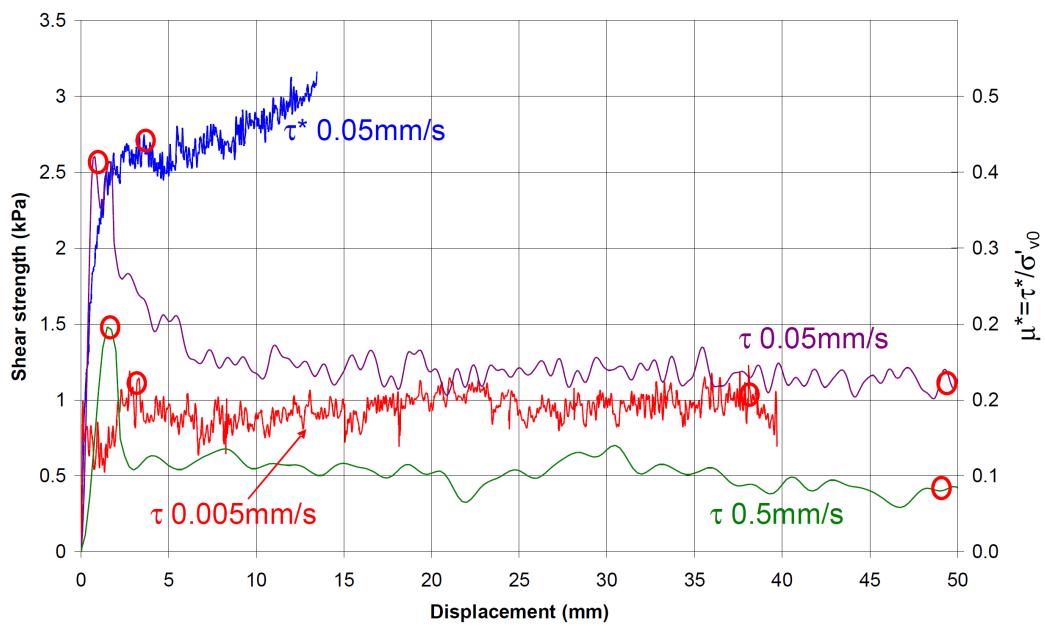
Fig. A.4 B 0.34m rough
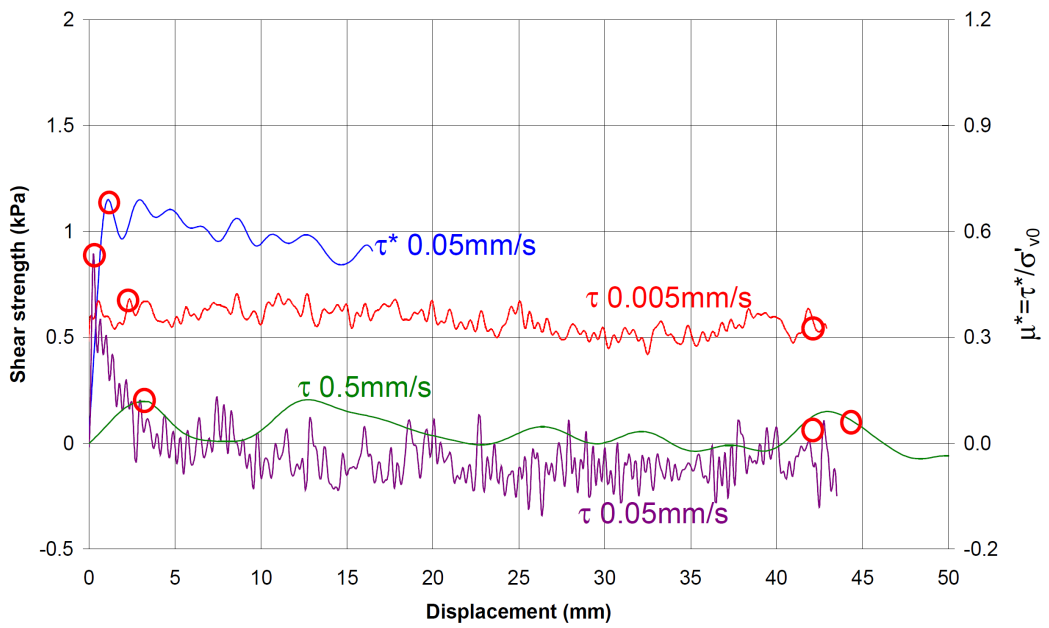
Fig. A.5 C 0.04m rough
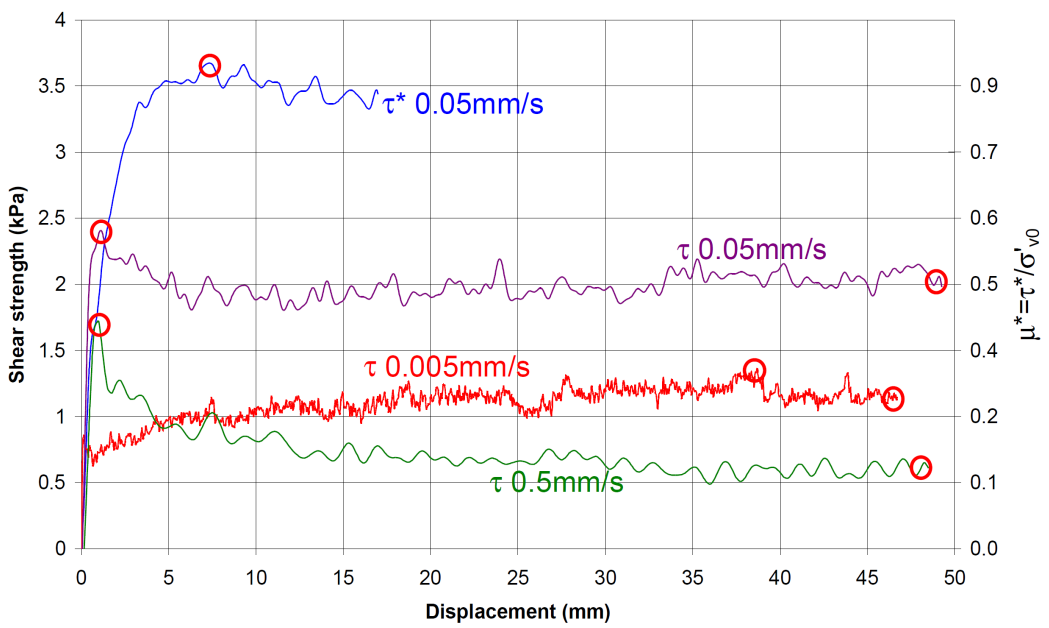
Fig. A.6 C 0.2m rough

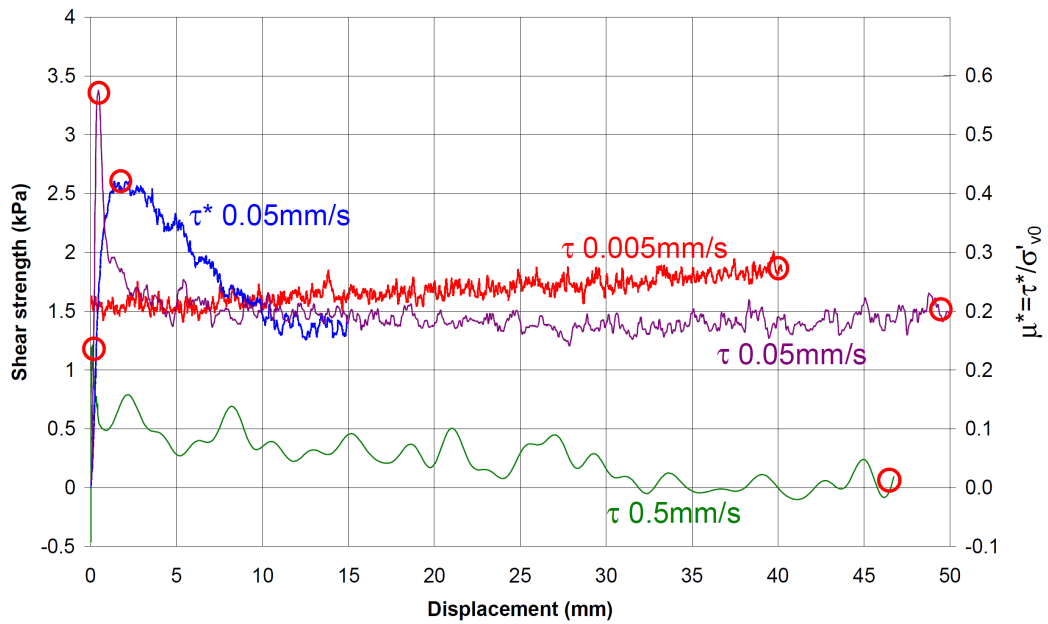# A. CAM-SHEAR TEST SUMMARY AND SHEAR STRESS - DISPLACEMENT PLOTS
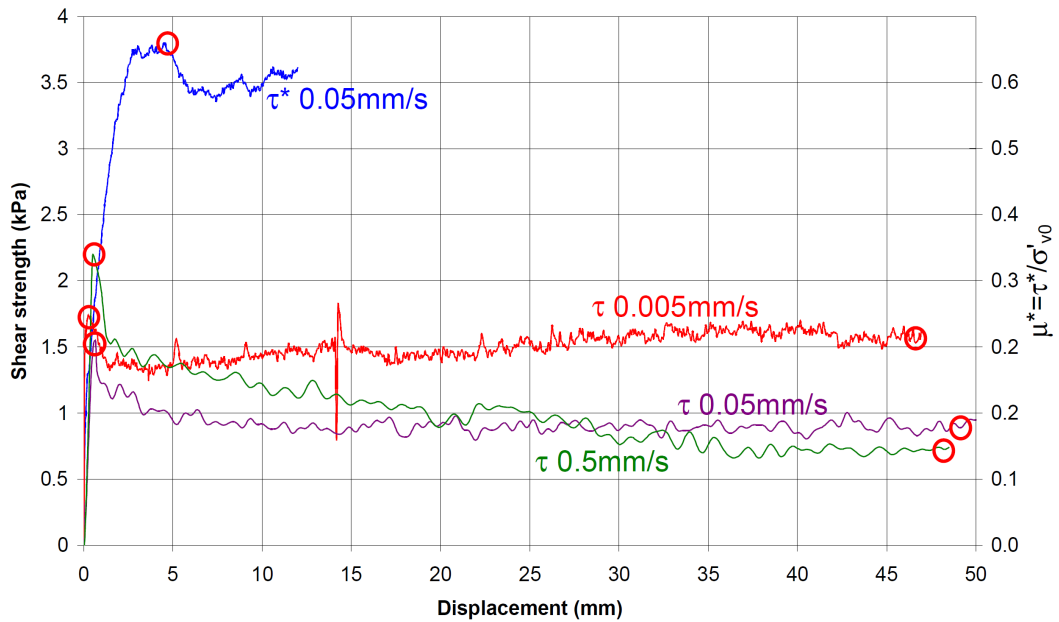
Fig. A.7 C 0.32m rough
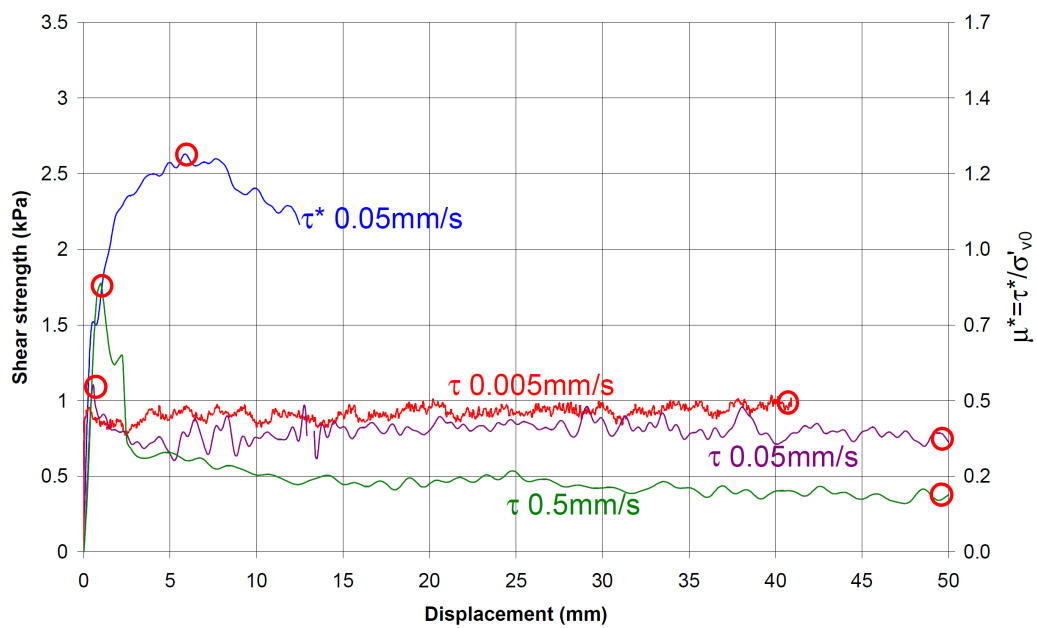
Fig. A.8 D 0.04m rough
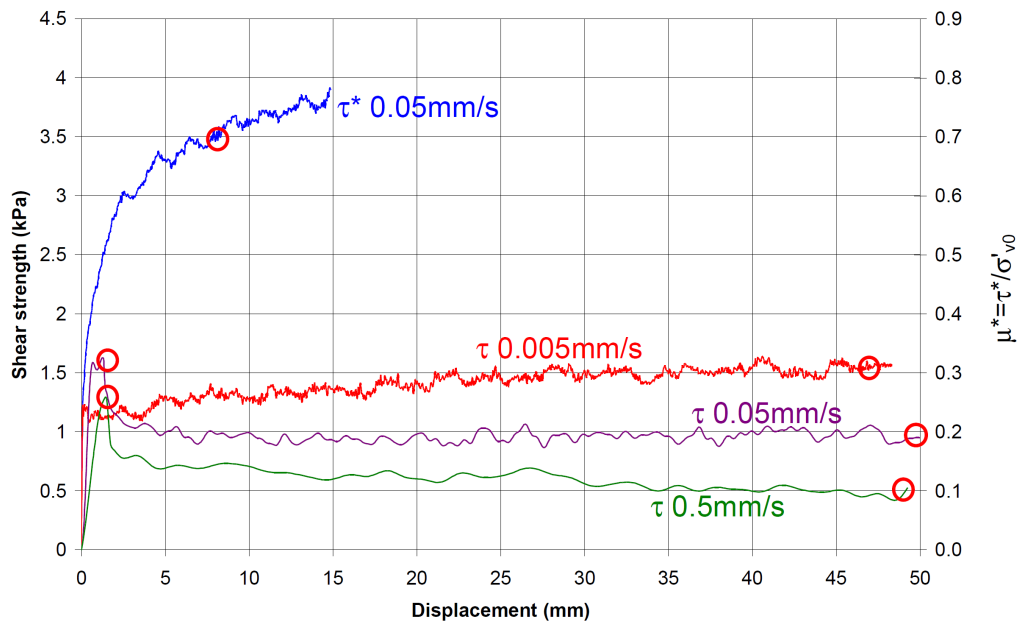
Fig. A.9 D 0.3m rough
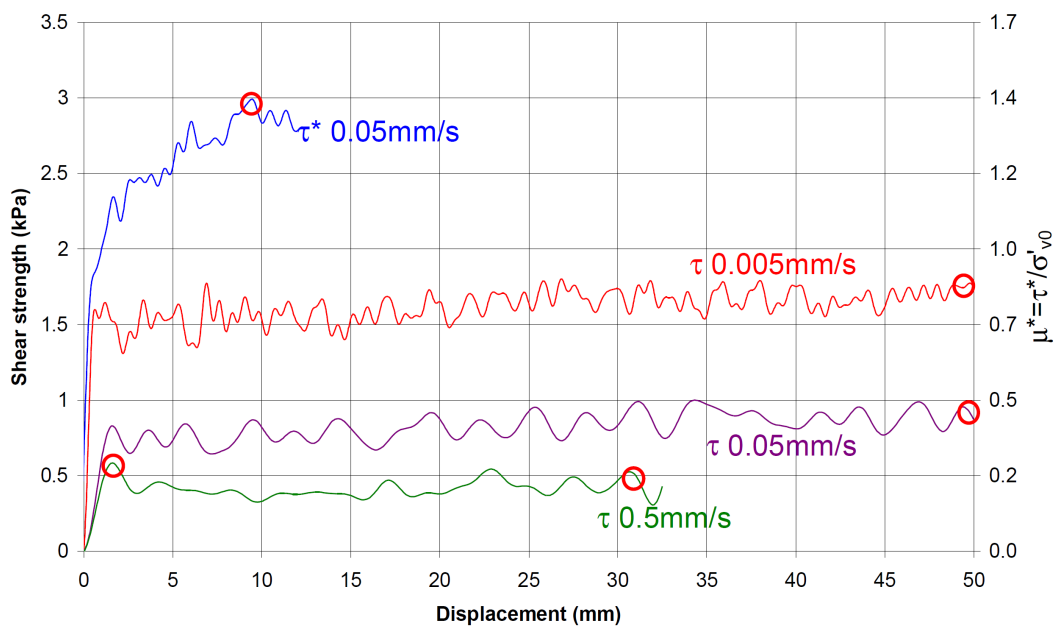
Fig. A.10 E 0.04m smooth

A. CAM-SHEAR TEST SUMMARY AND SHEAR STRESS - DISPLACEMENT PLOTS
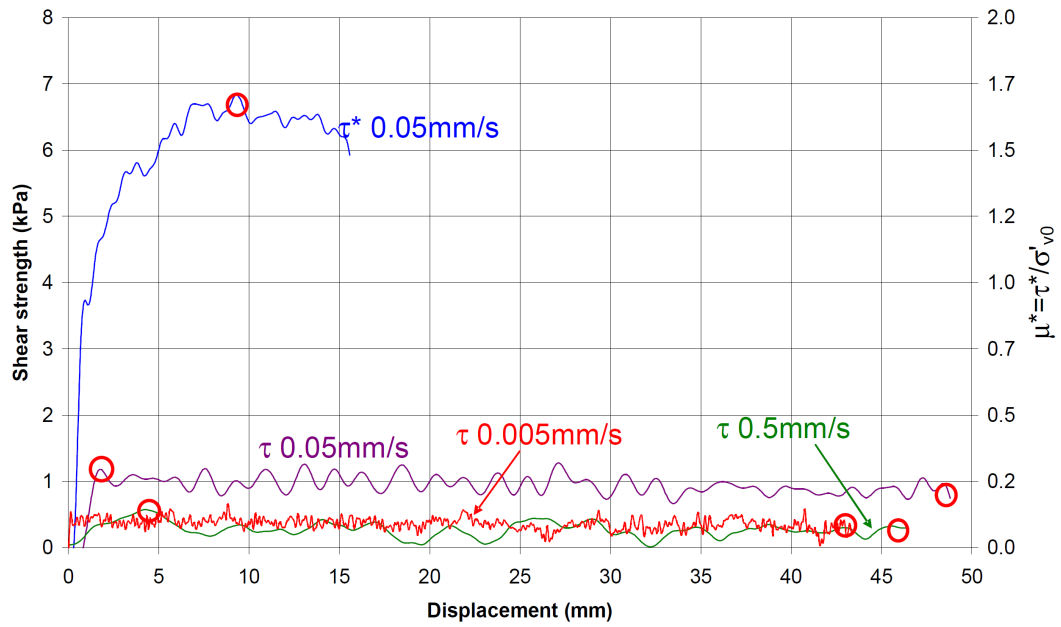
Fig. A.11 E 0.2m smooth
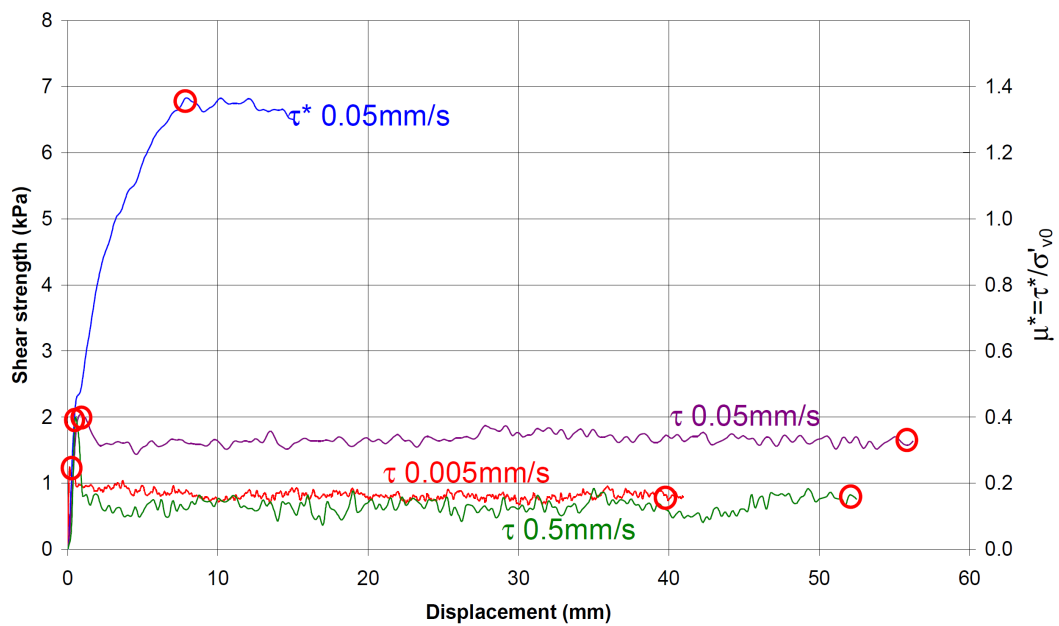
Fig. A.12 E 0.3m rough
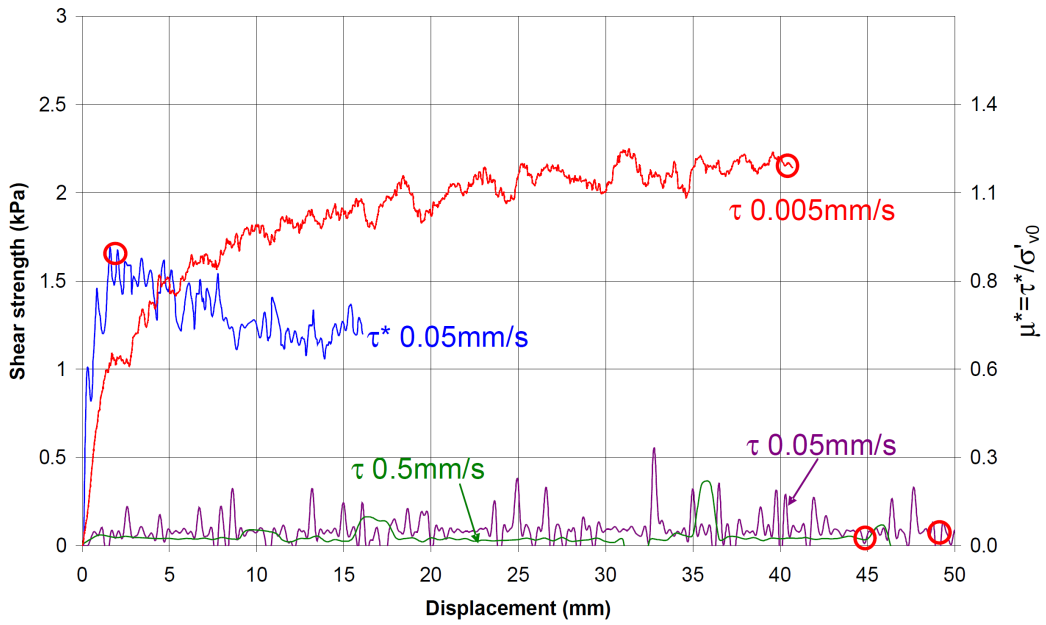
Fig. A.13 F 0.09m rough
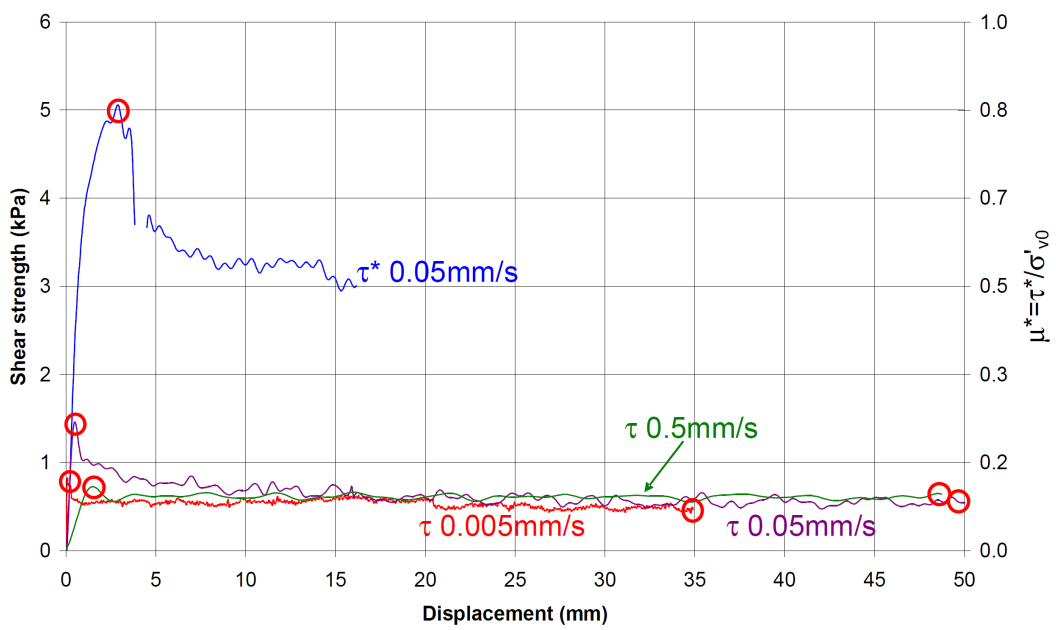
Fig. A.14 F 0.2m rough

A. CAM-SHEAR TEST SUMMARY AND SHEAR STRESS - DISPLACEMENT PLOTS

Fig. A.15 F 0.3m rough
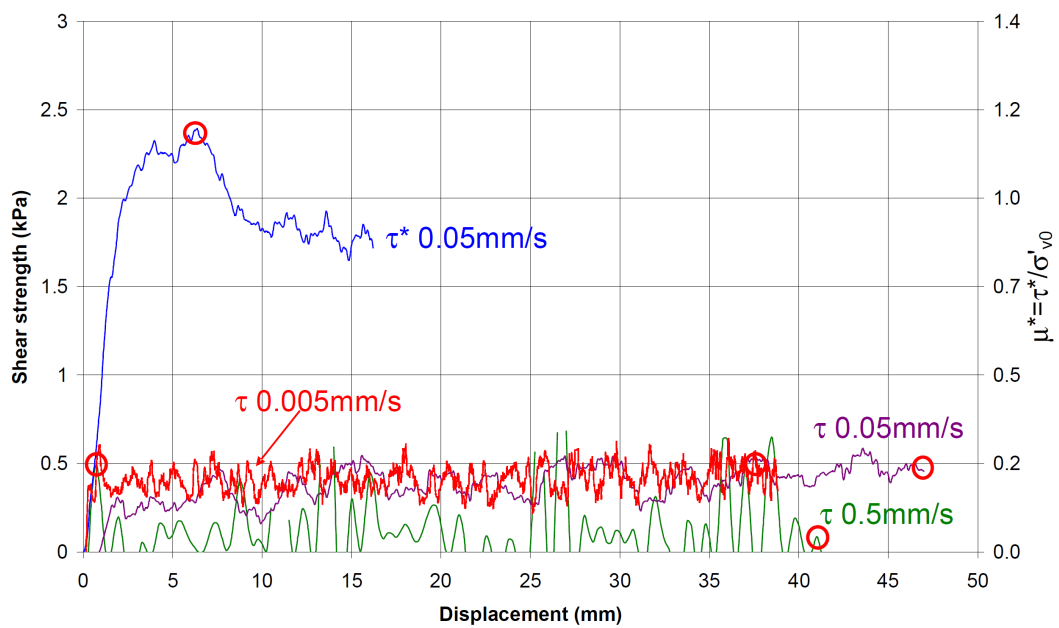
Fig. A.16 G 0.1m rough
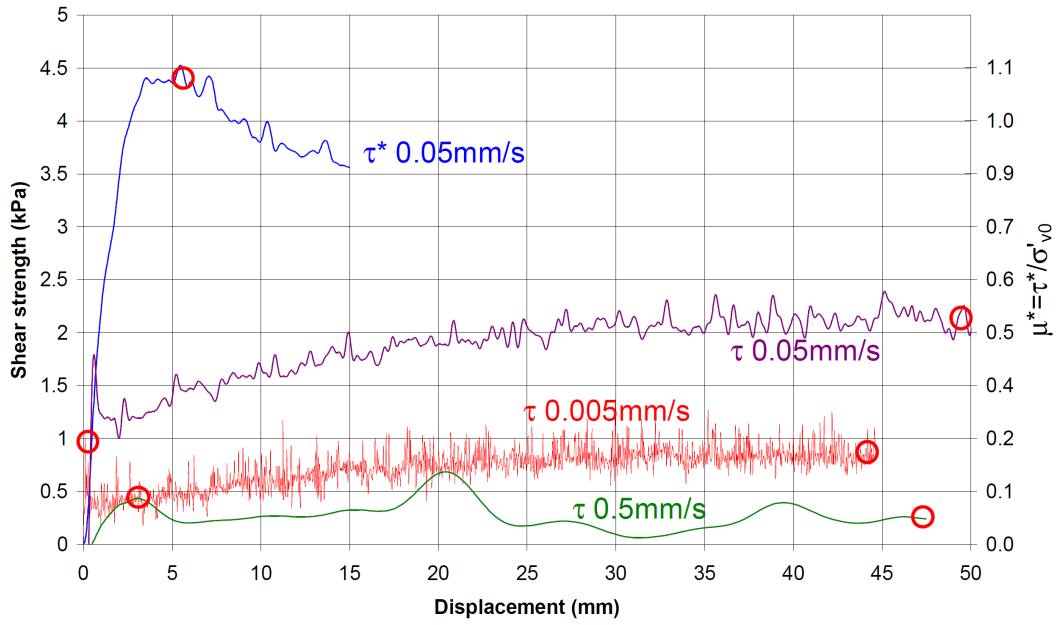
Fig. A.17 G 0.2m rough
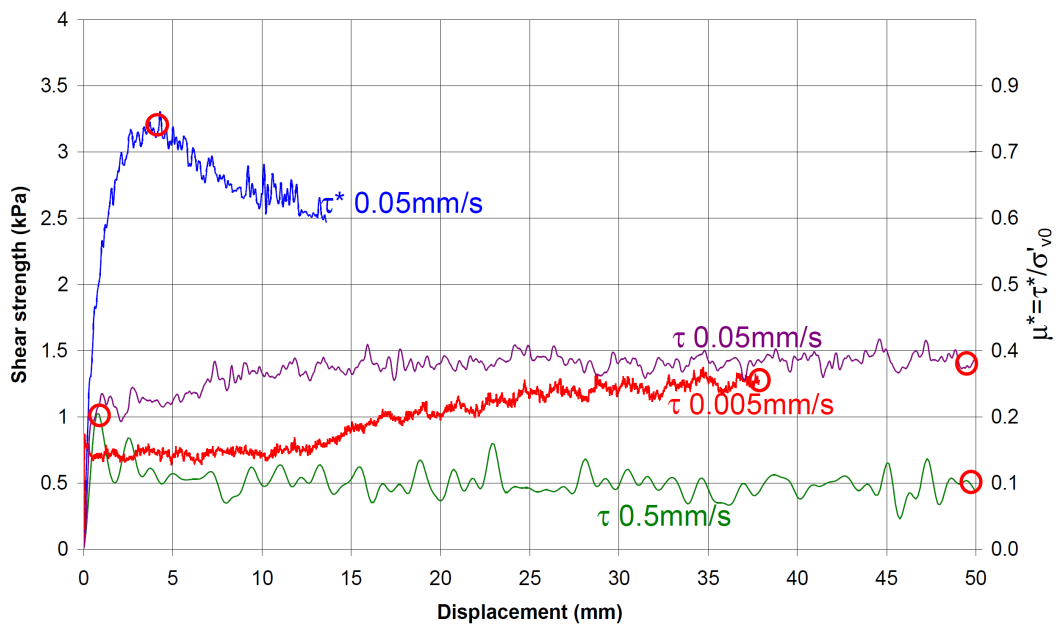
Fig. A.18 H 0.2m smooth

Appendix B

Design Calculations and Drawings for Mini Ball Penetrometer

B. DESIGN CALCULATIONS AND DRAWINGS FOR MINI BALL PENETROMETER

Calculation of strain level for design of proving-ring for mini ball penetrometer

W =	50	N	force
a =	8	mm	outer radius
t =	1	mm	thickness
b =	6	mm	inner radius
R =	7	mm	radius to centroid
E =	7.30E+04	N/mm^2	modulys of elasticity
ν =	3.00E-01		Poisson's ratio
L =	8.00E+00	mm	length
I =	7.33E-01	mm^4	moment of inertia
D_H =	1.02E-01	mm	change in diametral length

strain = 1.04E+03
Moment$_V$ = 1.11E+02 Nmm
Moment$_H$ = -6.36E+01 Nmm

$$\text{Micro-Strain}_H = (WRt)/(2\pi EI) \times 10^6$$
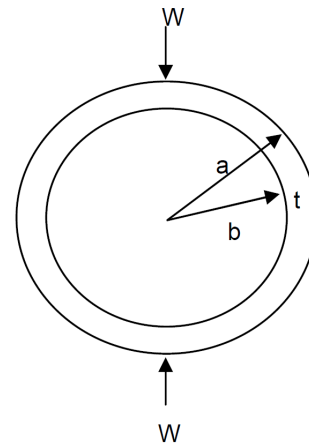
t = 1.00E+00
I = 7.33E-01

W (N)	t=1mm Micro-Strain$_H$
1	20.8
2	41.7
3	62.5
4	83.3
5	104.2
6	125.0
7	145.8
8	166.6
9	187.5
10	208.3
15	312.5
20	416.6
25	520.8
30	624.9
30	624.9
40	833.2
45	937.4
50	1041.6

Fig. B.1 Strain calculations for mini ball penetrometer proving-ring.
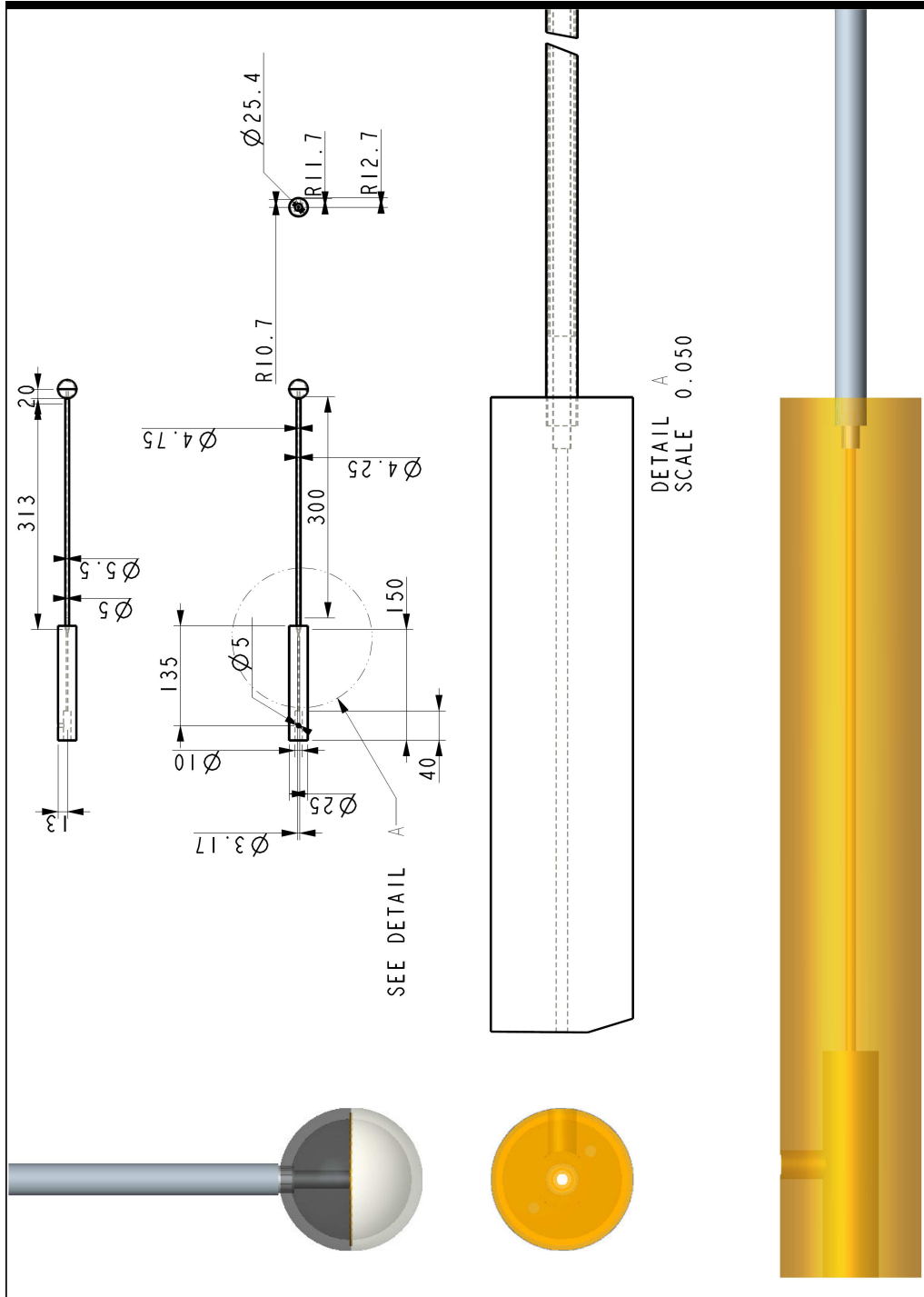
Fig. B.2 Overview dimensions of mini ball penetrometer.

Fig. B.3 Dimensions of lower half of ball, proving-ring load cell and inner shaft.

Fig. B.4 Dimensions of full ball.
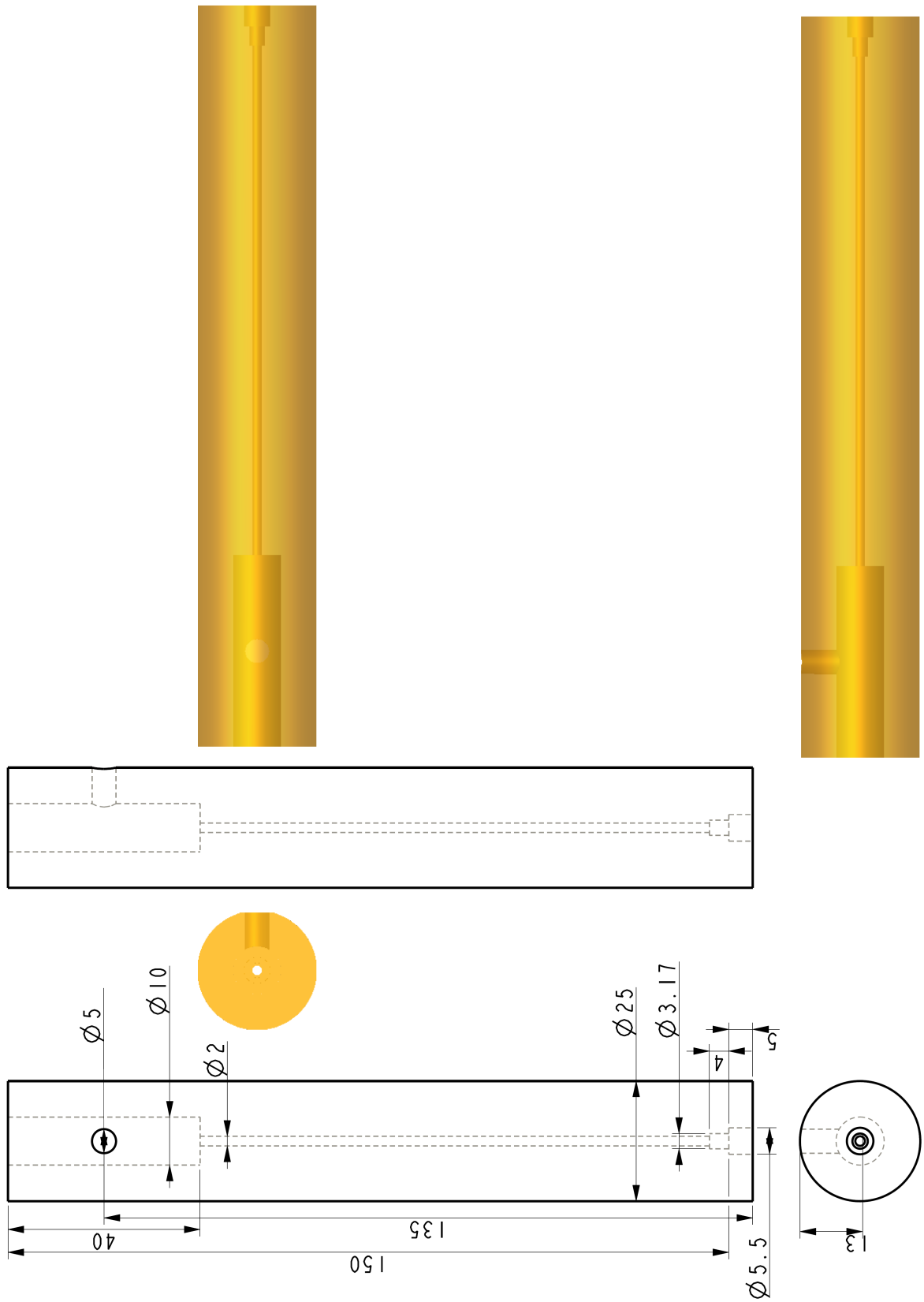
Fig. B.5 Detail of brass connection to actuator.
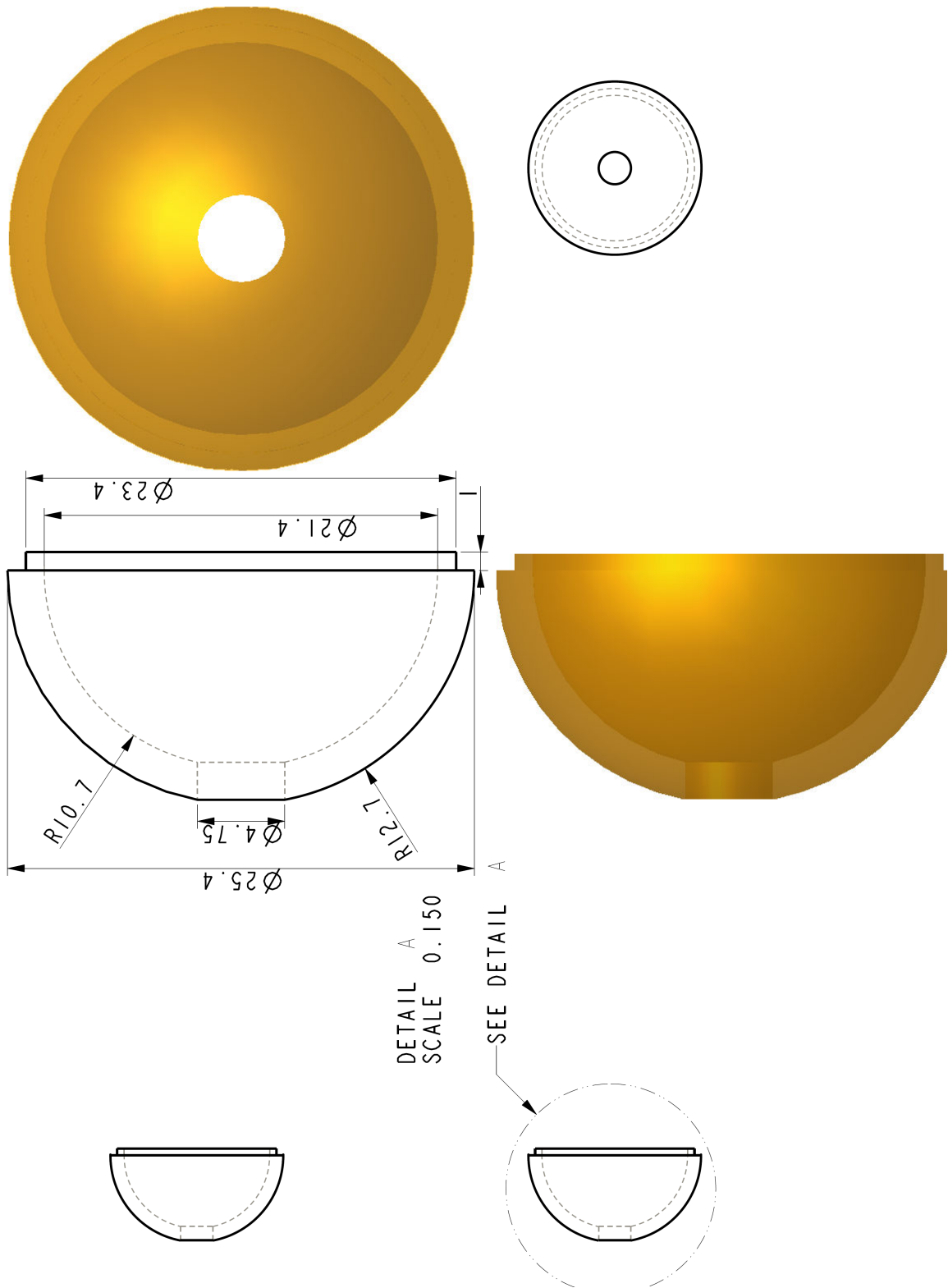
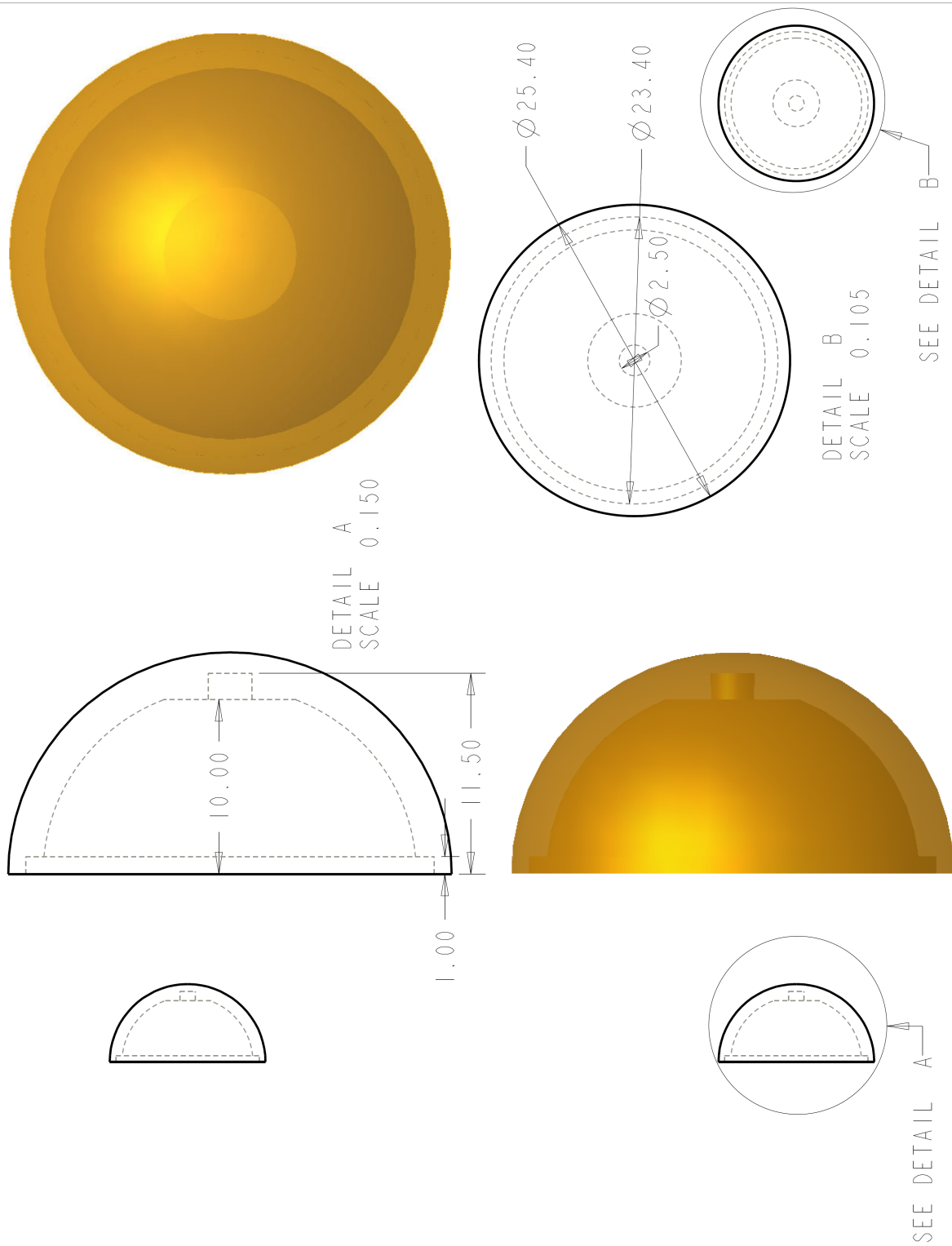Fig. B.6 Detail of upper half of ball.

229

Fig. B.7 Detail of lower half of ball.

Appendix C

Lurina Broth Recipe

Modified after Sambrook and Russell (2001) Per liter: To 950ml of deionized H_2O, add:

- 10g bacto-tryptone
- 5g bacto-yeast extract
- 10g NaCl

1. Shake until the solutes have dissolved
2. Adjust the pH to 7.0 with 5 N NaOH ~0.2ml
3. Adjust the volume of the solution to 1 litre with deionized H_2O
4. Sterilize by autoclaving for 20 minutes

Appendix D

Reviving Procedure for *M. aquaeolei*

Source: NCIMB Revival information (NCIMB (2007b))

1. Apply provided ampoule snappers to ampoule and using thick wadding or gloves, physically snap ampoule
2. Discard upper part of ampoule and cotton plug into a disinfectant solution
3. Flame open end of ampoule
4. Add up to 0.5ml of a suitable liquid medium to suspend the culture
5. Sub-culture into suitable soil and liquid media
6. Numbered filter paper strip should be transferred the top of a pipette to the surface of the solid medium with number upwards

Appendix E

Seawater Agar Yeast Peptone Recipe

Source: NCIMB Growth Media Recipes (NCIMB (2007a), p21)

- 3.0g yeast extract
- 5.0g peptone
- 750.0ml filtered, aged sea water
- 250.0ml distilled water

1. Dissolve ingredients, heating if necessary
2. Adjust pH to 7.3
3. Autoclave at 121℃ for 15 minutes

Appendix F

Faecal pellet percentage plots
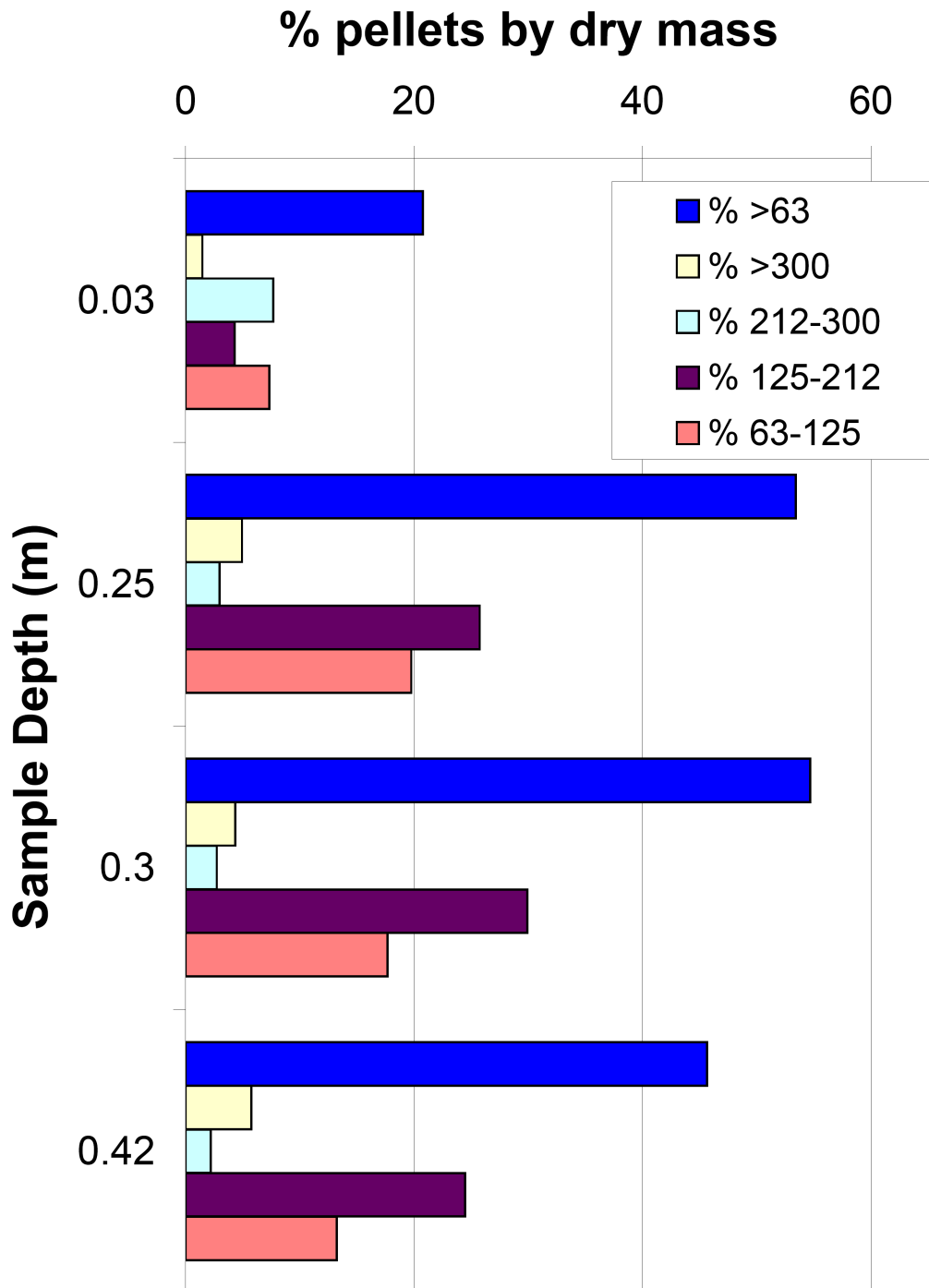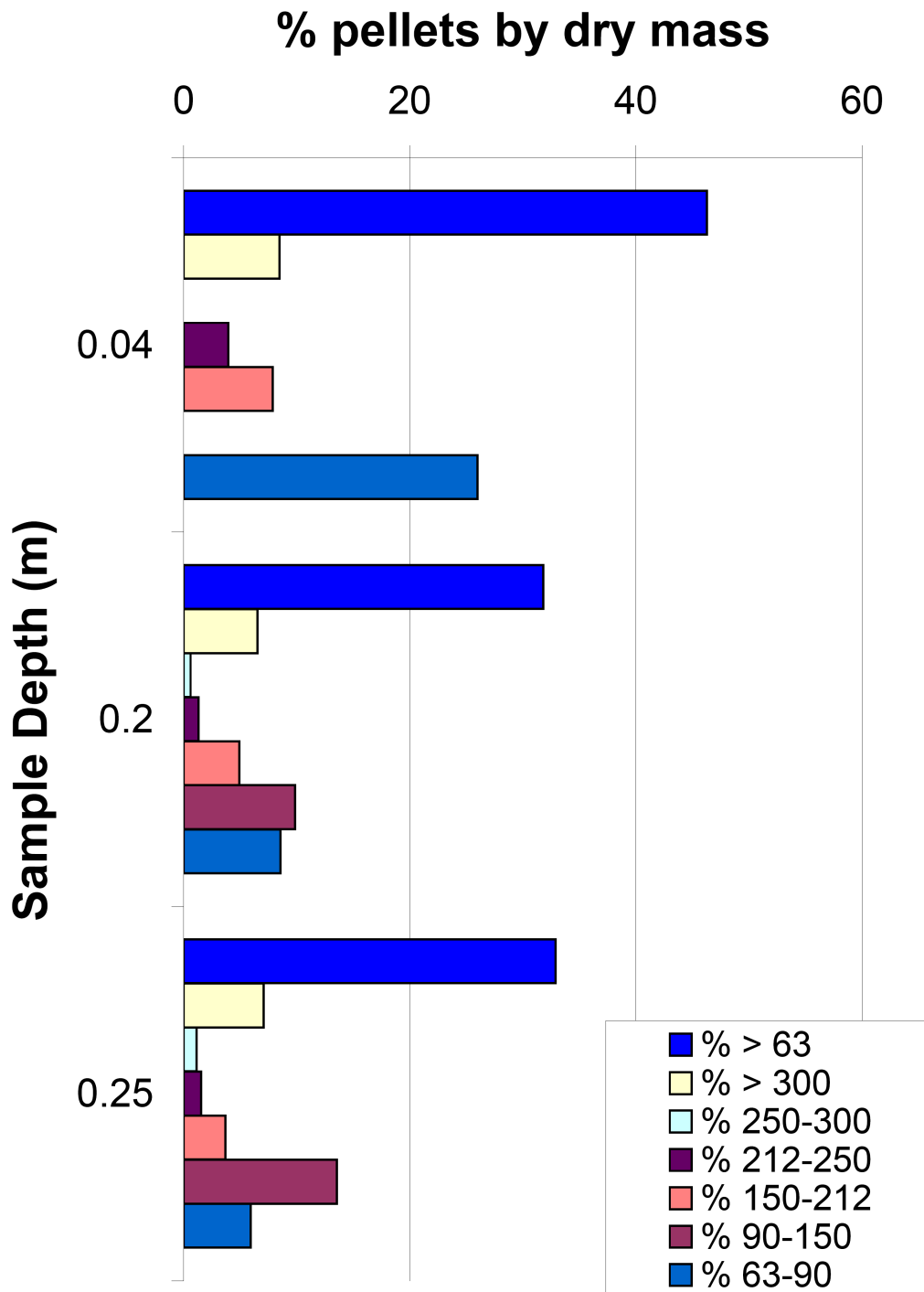
Fig. F.1 Faecal pellet fractions for Core A

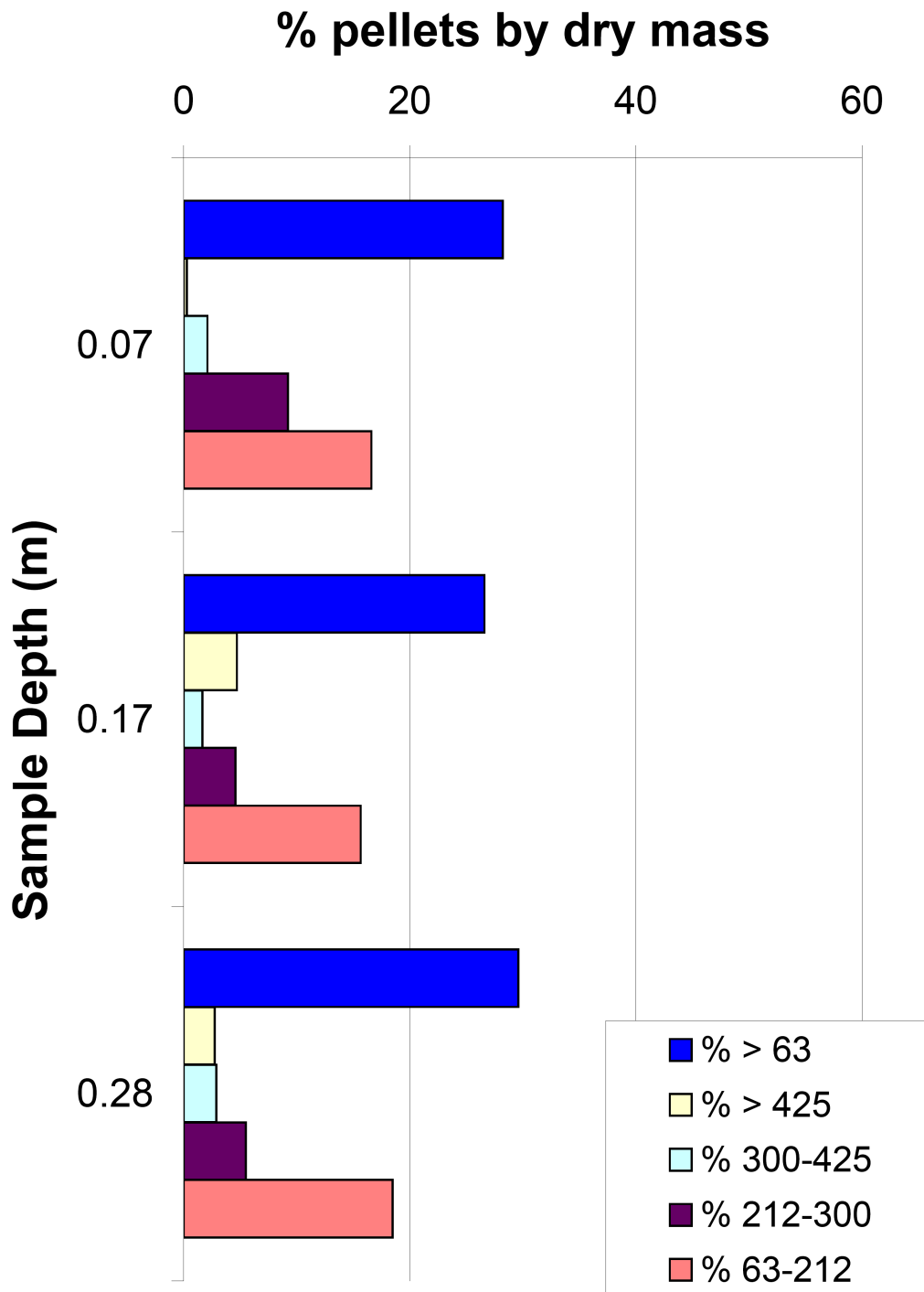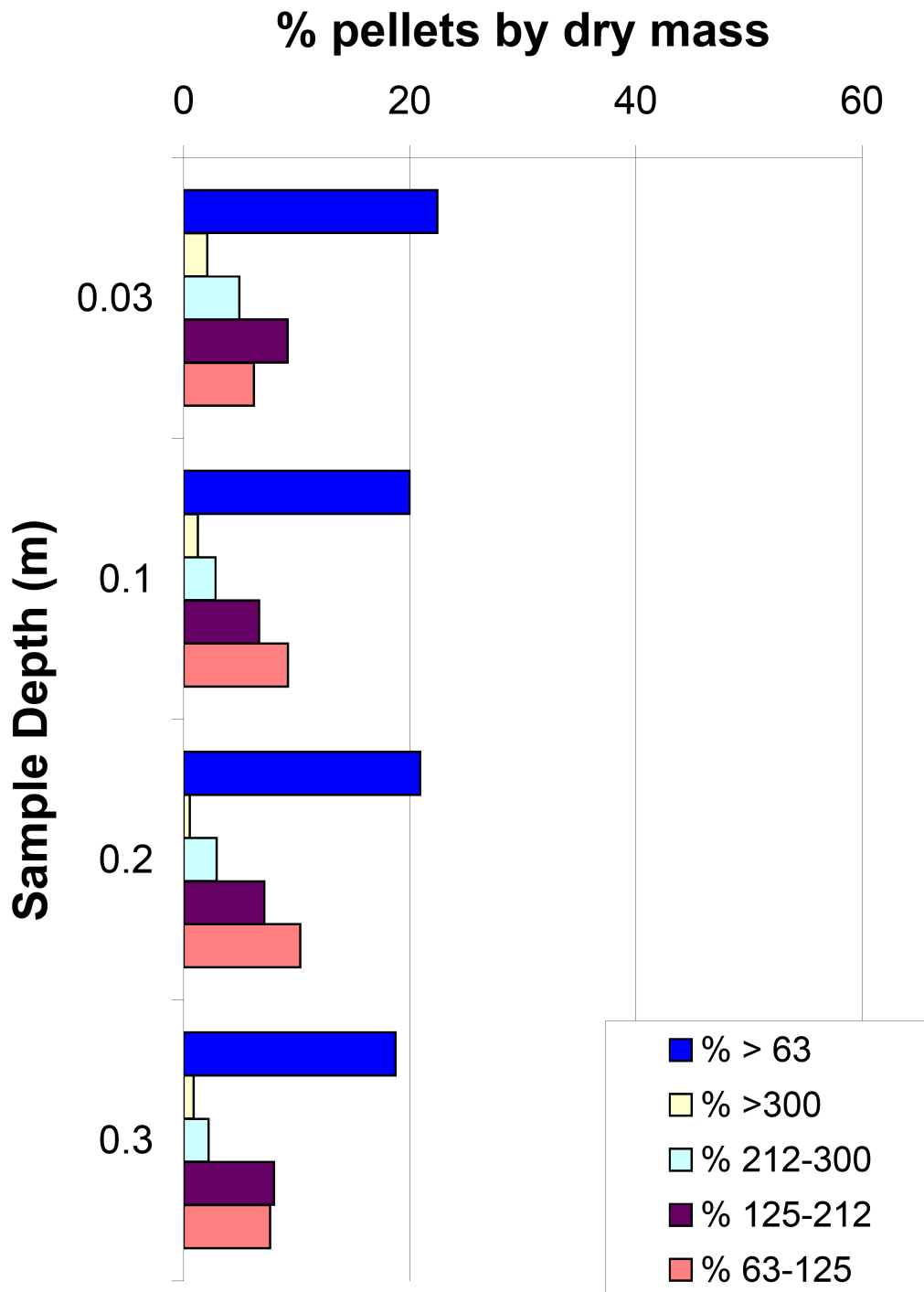Fig. F.2 Faecal pellet fractions for Core C

Fig. F.3 Faecal pellet fractions for Core D

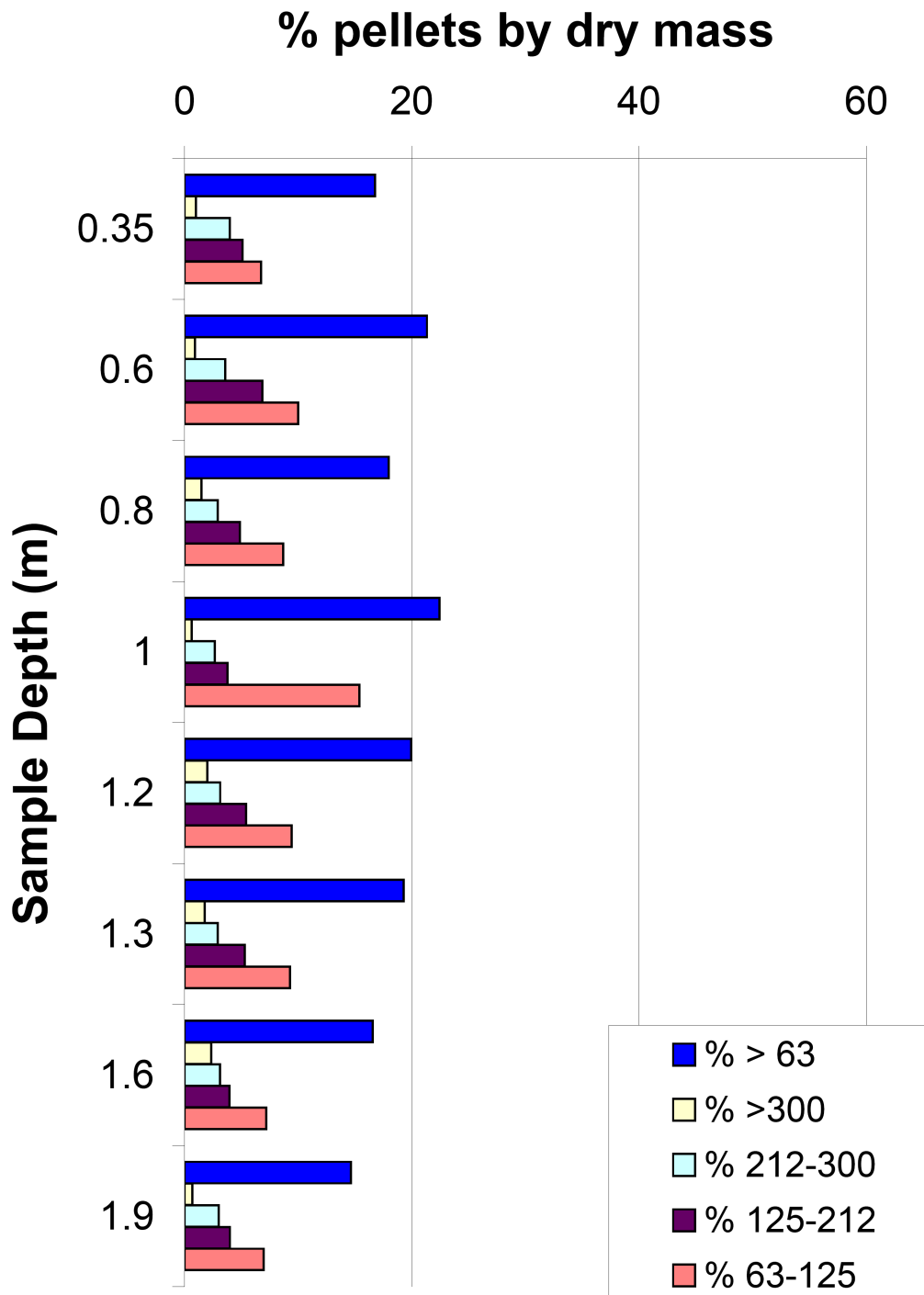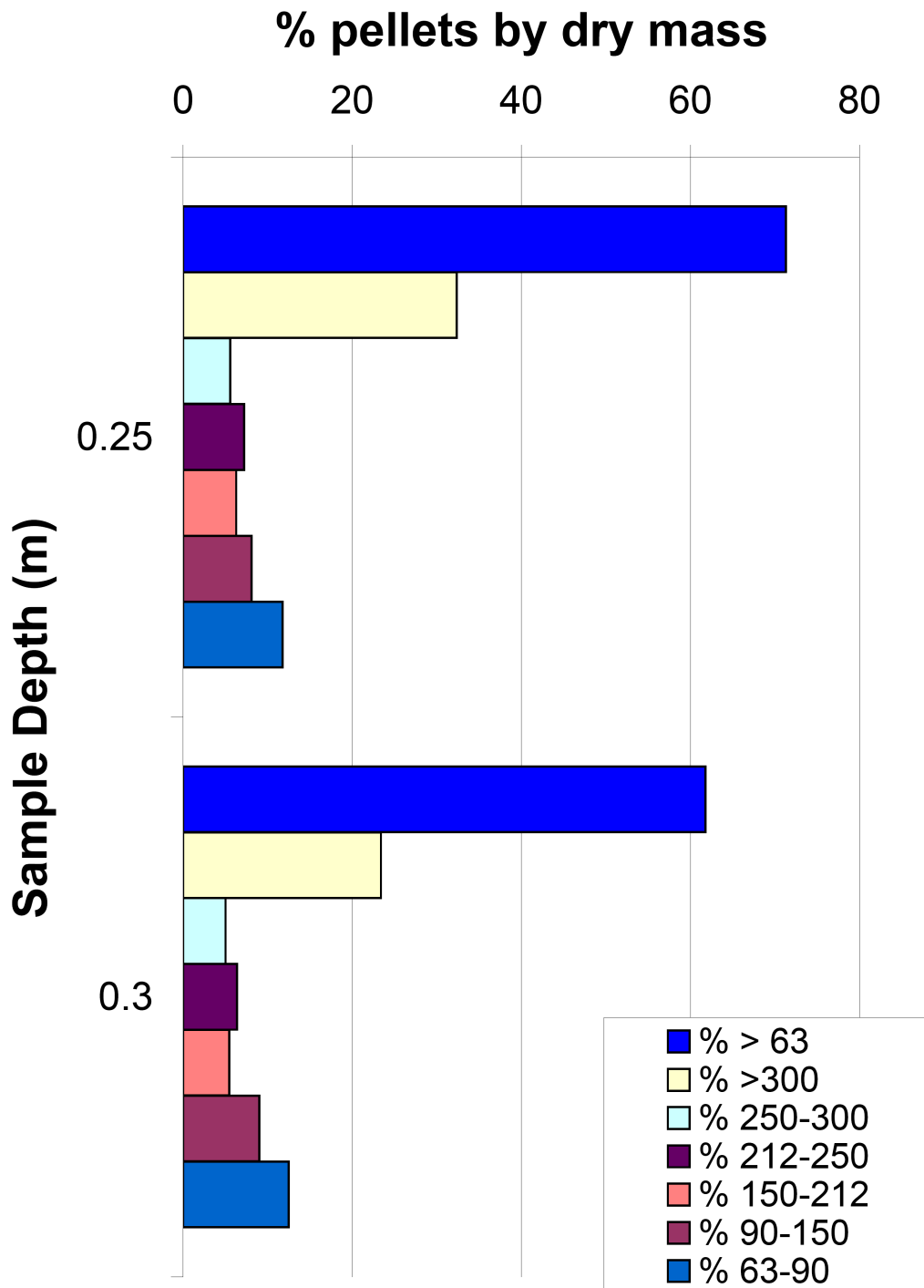Fig. F.4 Faecal pellet fractions for Core E

Fig. F.5 Faecal pellet fractions for Core F

Fig. F.6 Faecal pellet fractions for Core G